

AD

USAAVLABS TECHNICAL REPORT 65-68

GROUND AND FLIGHT TESTS,  
XV-9A HOT CYCLE RESEARCH AIRCRAFT

By

C. W. Pieper

CLEARINGHOUSE FOR FEDERAL SCIENTIFIC AND TECHNICAL INFORMATION			
Hardcopy	Microfiche	156	2
\$17.20	\$1.00	pp	2
ARCHIVE COPY			

March 1966

*Co-cc-1*

U. S. ARMY AVIATION MATERIEL LABORATORIES  
FORT EUSTIS, VIRGINIA

CONTRACT DA 44-177-AMC-877(T)  
HUGHES TOOL COMPANY  
AIRCRAFT DIVISION  
CULVER CITY, CALIFORNIA



Distribution of this  
document is unlimited.

### Disclaimers

The findings in this report are not to be construed as an official Department of the Army position, unless so designated by other authorized documents.

When Government drawings, specifications, or other data are used for any purpose other than in connection with a definitely related Government procurement operation, the United States Government thereby incurs no responsibility nor any obligation whatsoever; and the fact that the Government may have formulated, furnished, or in any way supplied the said drawings, specifications, or other data is not to be regarded by implication or otherwise as in any manner licensing the holder or any other person or corporation, or conveying any rights or permission, to manufacture, use, or sell any patented invention that may in any way be related thereto.

Trade names cited in this report do not constitute an official endorsement or approval of the use of such commercial hardware or software.

### Disposition Instructions

Destroy this report when no longer needed. Do not return it to the originator.



DEPARTMENT OF THE ARMY  
U S ARMY AVIATION MATERIEL LABORATORIES  
FORT EUSTIS VIRGINIA 23604

This report has been reviewed by USAAVLABS and is considered to be technically sound. The work was performed under Contract DA 44-177-AMC-877(T). The program was undertaken to evaluate the feasibility and potential of a hot cycle rotor propulsion system.

Further flight testing of the concept has been undertaken as part of a program to establish the basic hot cycle technology required for future designs employing the hot cycle concept.

Task 1M121401D14403  
Contract DA 44-177-AMC-877(T)  
USAAVLABS Technical Report 65-68  
March 1966

GROUND AND FLIGHT TESTS,  
XV-9A HOT CYCLE RESEARCH AIRCRAFT

SUMMARY REPORT  
HTC-AD 65-13

by

C. W. Pieper  
Project Engineer - Test

Prepared by

Hughes Tool Company, Aircraft Division  
Culver City, California

for

U. S. ARMY AVIATION MATERIEL LABORATORIES  
FORT EUSTIS, VIRGINIA

*Distribution of this  
document is unlimited.*

### ABSTRACT

Under the terms of Contract DA 44-177-AMC-877(T), Hughes Tool Company, Aircraft Division has conducted a ground and flight test program on the XV-9A Hot Cycle Research Aircraft to demonstrate the flight feasibility of the Hot Cycle Rotor System.

During the tests, performed from 10 August 1964 through 5 February 1965, the performance, structural qualities, and feasibility of the Hot Cycle rotor and propulsion system were successfully verified for all normal helicopter flight modes. Ground tests consisted of pre-flight and tie-down tests, which provided a functional checkout of the aircraft systems and test instrumentation and a final checkout of the completed aircraft prior to start of flight tests. The 15 hours of flight testing included evaluation of aircraft and rotor system performance, flight loads, cooling, and flying qualities in various flight modes.

## CONTENTS

	<u>Page</u>
ABSTRACT . . . . .	iii
LIST OF ILLUSTRATIONS . . . . .	vi
LIST OF TABLES . . . . .	ix
LIST OF SYMBOLS . . . . .	x
INTRODUCTION . . . . .	1
CONCLUSIONS . . . . .	3
RECOMMENDATIONS . . . . .	4
SUMMARY . . . . .	5
GROUND TESTS . . . . .	6
GENERAL . . . . .	6
PREFLIGHT TEST RESULTS . . . . .	9
TIE-DOWN TEST RESULTS . . . . .	20
FLIGHT TESTS . . . . .	27
GENERAL . . . . .	27
FLIGHT TEST PROCEDURES . . . . .	27
FLIGHT TEST EVALUATION . . . . .	33
FLIGHT TEST RESULTS . . . . .	37
DESCRIPTION OF TEST AIRCRAFT . . . . .	101
REFERENCES . . . . .	106
DISTRIBUTION . . . . .	108
APPENDIXES	
I. Description of Test Instrumentation . . . . .	109
II. Configuration and Change Log . . . . .	131
III. Pilot Comments and Qualitative Evaluation . . . . .	137
IV. Propulsion System Performance Test Data and Corrections . . . . .	142

## ILLUSTRATIONS

<u>Figure</u>		<u>Page</u>
1	XV-9A Hot Cycle Research Aircraft . . . . .	xiii
2	Pilot Acceleration Due to Force Applied to Main Rotor Shaft at Hub Gimbal Versus Frequency . . . . .	16
3	Normal Acceleration at Tip of Horizontal Stabilizer Due to Force Applied to Main Rotor Shaft at Hub Gimbal Versus Frequency . . . . .	17
4	Fuselage Vertical Bending Versus Fuselage Station . .	18
5	Cyclic Flapwise Blade Bending at Station 75.4 Versus Calibrated Airspeed . . . . .	39
6	Cyclic Spar Axial Load (Chordwise Moment) at Station 90.75 Versus Calibrated Airspeed . . . . .	40
7	Cyclic Chordwise Shear Load at Station 23 Versus Calibrated Airspeed . . . . .	41
8	Cyclic Main Rotor Shaft Bending Versus Calibrated Airspeed . . . . .	42
9	Cyclic Hub Plate Stress Versus Calibrated Airspeed . . . . .	43
10	Cyclic Pitch Arm Load Versus Calibrated Airspeed . .	44
11	Cyclic Flapwise Bending Moment Versus Main Rotor Blade Radius . . . . .	45
12	Cyclic Chordwise Bending Moment Versus Main Rotor Blade Radius . . . . .	46
13	Cycles per Flight Hour Versus Cyclic Spar Axial Load at Station 90.75 . . . . .	47
14	Cycles per Flight Hour Versus Flapwise Blade Bending at Station 75.4 . . . . .	48
15	Summary of Maximum Rotor Temperatures Recorded During Flights 1 Through 21 Inclusive . . . .	51
16	Summary of Maximum Powerplant and Airframe Temperatures Recorded During Flights 1 Through 21 Inclusive . . . . .	53

<u>Figure</u>		<u>Page</u>
17	Propulsion System Station Locations . . . . .	55
18	Rotor Lift Versus Engine Discharge Pressure . . . . .	56
19	Hovering Fuel Flow Versus Gross Weight . . . . .	57
20	T <sub>5</sub> Versus P <sub>5</sub> and P <sub>7</sub> Correlation, Engine 027-1A . . . . .	59
21	T <sub>5</sub> Versus P <sub>5</sub> and P <sub>7</sub> Correlation, Engine 026-1B . . . . .	60
22	Engine Discharge Temperature Versus Pressure . . . . .	62
23	Engine Temperature Relationships . . . . .	63
24	T-64 Engine 027-1A Operating Data . . . . .	65
25	T-64 Engine 026-1B Operating Data . . . . .	66
26	Temperature Rise Versus Fuel Air Ratio . . . . .	67
27	Elements of Power Available and Power Required . . . . .	69
28	Rotor System Pressure Ratio . . . . .	70
29	Rotor Horsepower Available Versus $\bar{P}_5$ (Average Engine Discharge Pressure) . . . . .	72
30	Hover Performance Thrust Coefficient Versus Torque Coefficient . . . . .	73
31	Power Required (Weight = 14,500 Pounds, Sea Level Standard) . . . . .	74
32	Tuft Behavior in Cruise Flight . . . . .	75
33	Predicted Power Required With Drag Cleanup (Weight = 14,500 Pounds, Sea Level Standard) . . . . .	77
34	Tentative Specific Fuel Consumption Correlation . . . . .	78
35	Hot Cycle Rotor Jet Velocity . . . . .	80
36	Level Flight Longitudinal Cyclic-Control Position Versus Airspeed . . . . .	84
37	Full Pedal Deflection Hover Turns . . . . .	88
38	Sideward Flight Control Position Versus Ground Speed . . . . .	89
39	Rearward Flight Longitudinal Cyclic-Control Position Versus Speed . . . . .	90



<u>Figure</u>		<u>Page</u>
40	Maximum Pilot Vertical Acceleration Versus Calibrated Airspeed . . . . .	93
41	Maximum Engine 1 Acceleration Versus Calibrated Airspeed . . . . .	94
42	Maximum Engine 2 Acceleration Versus Calibrated Airspeed . . . . .	95
43	Sound Pressure Level In Hover . . . . .	96
44	Sound Pressure Level In Ground Operation . . . . .	97
45	Sound Pressure Level In Flight . . . . .	98
46	General Arrangement, XV-9A Hot Cycle Research Aircraft . . . . .	103
47	Instrumentation Schematic . . . . .	110
48	Rotor Slip Ring . . . . .	111
49	Oscillograph Installations . . . . .	111
50	View of Oscillographs and Temperature Recorders, Looking Aft . . . . .	112
51	Temperature Recorder Installations . . . . .	112
52	Rotor Thermocouple Switching Boxes . . . . .	114
53	Photopanel Installation . . . . .	114
54	Photopanel Layout . . . . .	115
55	Strain-Gage Bridge Locations, Rotor Blades - Flight Test . . . . .	121
56	Strain Gage, Gyro, Accelerometer, and Transducer Locations . . . . .	123
57	Thermocouple Locations, Rotor Blades and Hub - Flight Test . . . . .	127
58	Thermocouple Location, Hot Gas System . . . . .	129
59	Observed Hovering Fuel Flow Versus Gross Weight . . . . .	145
60	Observed Specific Fuel Consumption Versus Horsepower . . . . .	146

TABLES

<u>Table</u>		<u>Page</u>
I	Preflight and Tie-Down Test Operations Summary . . . .	7
II	Tie-Down Tests - Vibration Level Versus Configuration. . . . .	23
III	Flight Test Operations Summary . . . . .	28
IV	Observed and Corrected Fuel Flow and Rotor and Gas Power . . . . .	143
V	Uncorrected and Corrected Whirl Test Fuel Flow . . . .	144

## SYMBOLS

<u>Symbol</u>	<u>Identity</u>	<u>Units</u>
$A_e$	Nozzle exit area	sq in
$A_{\pi}$	Parasite drag area	sq ft
$C/\Lambda$	Chromel-alumel	
$C_F$	Nozzle thrust coefficient	
$C_P$	Specific heat (constant pressure)	
$C_Q$	Torque coefficient	
$C_T$	Thrust coefficient	
$C_{v_e}$	Nozzle velocity coefficient	
$f$	Blade duct friction coefficient	
$F/A$	Fuel/air ratio	
$F_C$	Coriolis force	lb
$F_j$	Jet thrust	lb
$F_N$	Net thrust (= jet thrust - coriolis force)	
$F/S$	Front spar	
$I/C$	Iron-constantan	
$ICG$	Initial center of gravity	
$i_H$	Incidence of horizontal stabilizer	degrees
$M_e$	Nozzle exit mach number	
$N_f$	Governor shaft rpm	percent
$N_G$	Engine rpm	percent
$N_R$	Main rotor rpm	percent
$P$	Pressure	psia
$P_e$	Nozzle exit static pressure	psia
$PLA$	Power lever angle	degrees
$PPF$	Profile power factor	
$P_T$	Total pressure	psia

<u>Symbol</u>	<u>Identity</u>	<u>Units</u>
$P_{t_e}$	Nozzle exit total pressure	psia
$P_{T_{1,2,3}}$	Pressure at station designations (see Figure 17)	psia
$P_0$	Ambient pressure	psia
QT	Qualification test engines	
R	Universal gas constant	
R/S	Rear spar	
T	Temperature	degrees
TC	Thermocouple	
$T_T$	Total temperature	degrees
$T_{t_e}$	Total temperature, nozzle exit,	deg R
$T_{T_{1,2,3}}$	Temperature at station designations (see Figure 17)	degrees
$V_j$	Jet velocity	fps
$V_T$	Tip speed	fps
W	Mass flow	lb/sec
$W_a$	Air flow	lb/sec
$W_f$	Fuel flow	lb/hr
WL	Waterline	
$W_{1,2,3}$	Mass flow at station designations (see Figure 17)	lb/sec
YT	Preliminary flight rating test engine	
Z/D	Rotor height/diameter	
$\gamma$	Ratio of specific heats	
$\gamma_e$	Ratio of specific heats at nozzle exit	
$\delta$	Relative absolute pressure, $P/P_0$	
$\Delta T$	Ideal temperature drop for given ratio of gas pressure to ambient pressure	
$\theta$	Relative absolute temperature, $T/T_0$	
$\theta_{0.75R}$	Collective-pitch angle at 75-percent blade radius	degrees

<u>Symbol</u>	<u>Identity</u>	<u>Units</u>
$\theta_5$	Average engine discharge temperature/519°R	
$\mu$	Rotor advance ratio, forward speed/tip speed	
$\sigma$	Blade solidity ratio, total blade area/rotor disc area	
$\phi$	Bank angle	degrees

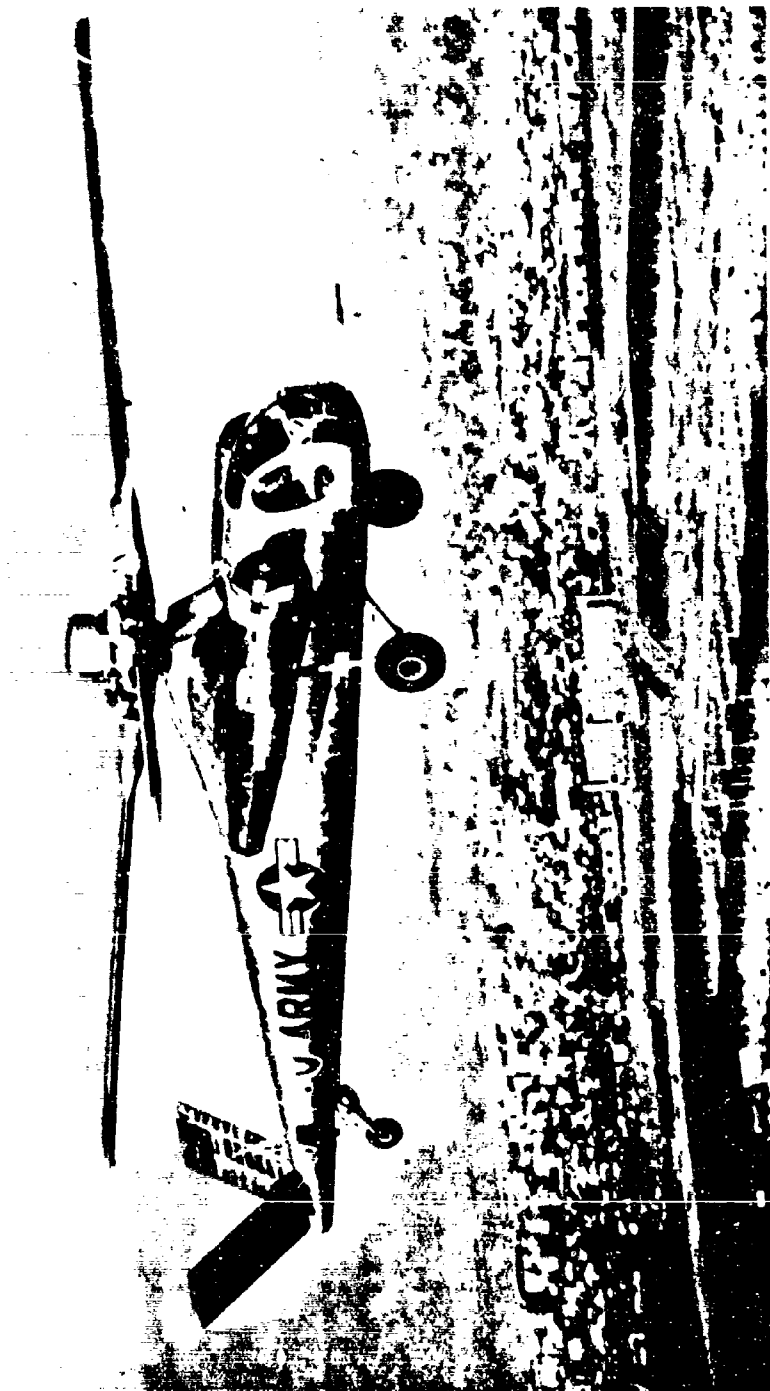


Figure 1. XV-9A Hot Cycle Research Aircraft.

## INTRODUCTION

This report presents the results of ground and flight tests of the U. S. Army XV-9A Hot Cycle Research Aircraft (see Figure 1). The aircraft was designed and constructed by Hughes Tool Company, Aircraft Division, Culver City, California, under contract to the United States Army Aviation Materiel Laboratories (USAAVLABS), Fort Eustis, Virginia.

Testing was accomplished by the contractor at Culver City, California, during the period 10 August 1964 through 5 February 1965. Ground tests consisted of preflight and tie-down tests to provide a functional checkout of the aircraft systems and test instrumentation and a final checkout of the completed aircraft prior to start of flight tests. Flight tests included evaluation of aircraft and rotor system performance, flight loads, component temperatures, and flying qualities in various flight modes.

### GROUND TESTS

Preflight tests consisted of functional checkout of the hydraulic system, flight controls, engine controls, rotor lubrication system, electrical system, and fuel system, and runup of the General Electric YT-64 gas generators to maximum power with diverter valves overboard. In addition, a fuselage shake test was conducted to determine the natural frequencies of the basic airframe components.

Tie-down tests consisted of rotor shakedown and functional checkout of the complete Hot Cycle propulsion system including rotor controls, up to maximum collective-pitch angle at design rotor speed with the aircraft restrained by a cable arrangement. Also accomplished was checkout of the rotor-speed-governing system and single-engine rotor operation. Tie-down tests consisted of 19 runs for a total duration of 13 hours and 20 minutes of rotor operation prior to start of flight test.

### FLIGHT TESTS

The first flight of the XV-9A Hot Cycle Research Aircraft was conducted on 5 November 1964. During the flight test program, 21 flights were conducted for a total duration of 15 hours and 42 minutes of flight time. Flight tests consisted of steady hovering, hovering turns, sideward and rearward flight, transition to forward flight, climb, level flight, descent, approach to hover, and landing. Data were recorded for evaluation of XV-9A performance, stability, controllability,

operating characteristics, flying qualities, structural loads and temperatures, and vibration levels for the various flight conditions. Sound power data, rotor downwash velocity, and static electricity buildup were also recorded.

In general, all test flights were of an exploratory nature, since the XV-9A was the first aircraft to fly with the Hot Cycle propulsion system. The XV-9A was flown by the contractor's chief engineering test pilot during this program. The flight test program was successfully completed on 5 February 1965.



## CONCLUSIONS

The XV-9A Hot Cycle Research Aircraft completed a 15-hour-42-minute flight test program and successfully accomplished the test objectives called for by the Flight Test Program Plan (Reference 1). The test program was accomplished with no major incidents, delays, or failures connected with either the Hot Cycle propulsion system or the associated XV-9A airframe and components.

The performance, structural qualities, and feasibility of the Hot Cycle rotor and propulsion system previously demonstrated during whirl tests were verified during the XV-9A flight test program for all normal helicopter flight modes. The flight test program further verified the feasibility of the Hot Cycle system for integration into a flight qualified aircraft having a high payload to empty weight capability.

The flying qualities of the Hot Cycle rotor system were found to be adequate for this type of research aircraft, and for continued flight envelope expansion after incorporation of the recommendations that follow.

The simplicity and low maintenance characteristics of the Hot Cycle rotor system permitted continued operation during the ground and flight test program, with no repair, replacement, or modification of any major rotor component from aircraft rollout until completion of flight testing.

## RECOMMENDATIONS

The following recommendations are made for further flight testing:

1. Inspect blade spars, retention straps, blade components, rotor hub, and the XV-9A airframe and systems.
2. Investigate means of obtaining increased cyclic and collective-pitch control.
3. Change directional control system to permit full range of yaw control valve opening.
4. Install UHF radio communications system.
5. Remove engine crossflow indicator and warn-divert system.
6. Install a simplified engine low-speed warning indicating system.
7. Recalibrate test instrumentation.
8. Perform additional maintenance items as required, following inspection, to prepare the aircraft and systems for further flight testing.
9. Modify rotor-speed-governing system to minimize tendency to drift.

## SUMMARY

The ground and flight test program of the XV-9A Hot Cycle Research Aircraft was completed on 5 February 1965. The results, together with an analysis of the significant portions of the test data recorded, including qualitative comments and observations, are presented in this report.

The aircraft was extensively instrumented for measurement of structural loads, temperatures, performance, vibration, control positions, rates, and attitudes prior to start of tie-down and flight tests. The instrumentation systems that produced these data were calibrated prior to start of testing and, where appropriate, recalibrated during the course of the test program to ensure maximum accuracy of results. For a description of the test aircraft refer to the section so titled, on page 101. A description of the test instrumentation systems is given in Appendix I.

Flight testing was accomplished within the Hughes Culver City flying area, where restricted air space available was a limiting factor for the maximum flight parameters that could be achieved during this program. Within the allowable air space and flight speed limitations imposed by the FAA for such experimental operations in this area, all normal helicopter flight modes were achieved and evaluated. These included lift-off to hover, steady hovering flight, hovering turns, side-ward and rearward flight, climb, level flight, minimum power descents, approach to hover, and landing.

## GROUND TESTS

### GENERAL

Preflight and tie-down tests were conducted in accordance with Reference 2 during the period 10 August through 4 November 1964. The following preflight tests were accomplished satisfactorily:

- Hydraulic system - functional checkout
- Flight control system - rigging, functional checkout, and proof loading
- Rotor lubrication system - functional checkout
- Electrical system - functional checkout
- Fuselage - shake test
- Engine - runup

Tie-down tests were conducted during the period 17 September through 4 November 1964. A total of 19 runs was accomplished, for a total rotor operating time of 13 hours and 20 minutes. A summary of engine runs and tie-down test runs is shown in Table I. The following tie-down test items were accomplished:

- Rotor and systems shakedown
- Rotor tracking and balance
- Rotor and systems functional checkout
- Rotor-airframe vibration investigation
- Ground instability test
- Engine nacelle and fuselage cooling
- Rotor-speed-governing checkout
- Single-engine rotor operation

The ground tests provided a complete functional checkout of the XV-9A aircraft, including rotor and controls, YT-64 gas generators, diverter valves, hot gas ducts, aircraft systems, yaw control valve, tip cascade nozzles, rotor governing, and test instrumentation, prior to first flight. Tie-down tests were conducted with the aircraft tethered with lesser amounts of restraint during final runs to permit limited aircraft lift-off.

Single-engine capability of the Hot Cycle system was satisfactorily demonstrated by actuating one diverter valve to overboard position and closing the blade-tip cascade nozzles to single-engine position with the rotor operating at normal speed. Single-engine power control and

TABLE I  
PREFLIGHT AND TIE-DOWN TEST OPERATIONS SUMMARY

Run Number	Date	Purpose	Engine 1 (S/N 027-1A)		Engine 2 (S/N 101-3A)	
			Run (Hours)	Run (Hours)	Run (Hours)	Run (Hours)
1	1-9-64	Engine shakedown and operating data systems checkout	00:39	00:53	-	-
2	11-9-64	Engine and nacelle cooling checks; checkout checks; fuel system function test	01:30	00:36	-	-
<u>Tie-down Tests</u>						
1	17-9-64	Rotor shakedown and tracking	00:44	00:46	00:04	00:04
2	21-9-64	Rotor tracking and structural loads	01:01	01:00	00:49	00:49
3	22-9-64	Rotor tracking and structural loads	00:43	00:44	00:28	00:28
4	23-9-64	Rotor balance investigation	00:32	00:40	00:25	00:25
5&5A	23-9-64	Rotor balance investigation; yaw control valve function checkout	01:04	01:02	00:33	00:33
6	24-9-64	Rotor balance; engine acceleration characteristics	00:21	00:24	00:14	00:14
7	25-9-64	Rotor vibration investigation	00:43	00:45	00:34	00:34
8	28-9-64	Rotor vibration investigation; rotor governing checkout	01:34	01:35	01:25	01:25
9&9A	29-9-64	Rotor vibration investigation; rotor governing checkout	01:08	01:06	00:51	00:51
10	30-9-64	Rotor-airframe vibration investigation (tie-down cables slack)	00:37	00:39	00:27	00:27

TABLE I (Continued)

Run Number	Date	Purpose	Engine 1 (S/N 027-1A) Run (Hours)	Engine 2 (S/N 101-3A) Run (Hours)	Rotor Run (Hours)
11	1-10-64	Tip cascade system functional check-out; single-engine operating data to maximum	00:49	00:27	00:36
12	9-10-64	Airframe vibration; engine temperature data; cyclic deflections; generator checkout	00:48	00:48	00:37
13	12-10-64	Airframe vibration; cyclic deflections; diverter valve hydraulic operation; collective-pitch transients	01:15	01:15	01:08
14	13-10-64	Rotor-engine performance; airframe vibration; pitch transients; rotor governing evaluation	01:08	01:10	00:58
15	14-10-64	Ground instability test a/c restrained	00:29	00:29	00:20
16	19-10-64	Engine and nacelle cooling; fuselage cooling	01:45	01:46	00:39
17	2-11-64	Functional checkout of reworked diverter valves; engine and nacelle cooling	00:51	00:48	00:16
18	3-11-64	Rotor governing checkout; rotor overspeed system checkout; emergency rotor tachometer checkout	01:41	01:41	01:28
19&19A	4-11-64	Yaw-control valve checkout; rudder pedal force measurement	02:00	01:58	01:28
TOTAL			21:24	20:32	13:20

governing characteristics were evaluated, and the single-engine rotor power available was determined.

The rotor-governing system, using the  $N_f$  power turbine governing function of the YT-64 fuel controls and a hydraulic rotor-speed feedback system, was tested and adjusted for flight. Rotor governing during collective-pitch transients equivalent to those required for takeoff to hover and hover to landing was successfully demonstrated.

A fuselage shake test was conducted to determine the natural frequencies of the basic airframe structure with engines and equipment installed. The results of these tests were utilized to determine proper location of fuselage ballast to minimize vibration levels in flight.

### PREFLIGHT TEST RESULTS

Preflight tests were conducted after factory completion of the aircraft to accomplish functional checkout of the aircraft systems, rigging and controls checkout, and engine runup. Test instrumentation was installed and calibrated during this period. A fuselage shake test was conducted to determine the structural frequency characteristics of the XV-9A airframe. The following tests were accomplished.

#### 1. Hydraulic System - Functional Checkout

This test was accomplished by means of a ground hydraulic power supply cart connected to each of the XV-9A 3500-psi hydraulic systems. The following items were accomplished:

- Pressure test, each system to 3500 psi
- Bleeding and purging, both systems
- Filling and servicing, both systems
- Diverter valve operational checkout
- Rotor controls operational checkout

Operation of the hydraulic systems, diverter valves, and rotor control servo actuators was normal during these tests.

Additional bleeding of the hydraulic systems was accomplished while motoring the engines by means of the MA-1 GTC starting unit and during initial rotor operation.

The XV-9A hydraulic systems contain closed precharged reservoirs that require filling by means of an external hydraulic cart. The small volume of fluid contained in the system necessitates

thorough bleeding prior to initial operation to eliminate trapped air; however, after this initial bleeding operation, the system maintenance was very low and trouble-free.

The engine-driven pumps developed 3500-psi pressure at all engine speeds from 10-percent  $N_G$  and greater.

## 2. Flight Controls

### a. Rigging and Proof Loads

The flight control pilot linkage rods and the power control linkage were preadjusted prior to final assembly in the aircraft to minimize the system rigging and checkout.

The XV-9A rotor controls were rigged and adjusted with the aircraft jacked into position with the rotor shaft vertical, the swash-plate level, and the hub blocked level. The pitch arm links on the upper torque arm assemblies were adjusted to make the three blade pitch angles equal for all azimuth positions. The three control servo actuator strokes were set prior to assembly.

After initial adjustment, the hub was unblocked and the longitudinal cyclic, lateral cyclic, and collective-pitch throws were checked by measuring the actual blade pitch angle at blade Station 91 by means of a precision inclinometer.

The pilot's cyclic stick stops were fabricated after the initial rigging adjustments were completed. These stops were located in the cockpit on the pilot linkage. Control system interference checks and corrections were made during the course of initial rigging checks.

Initial rotor rigging was adjusted for a collective-pitch angle of  $\theta_{0.75R} = 0$  degrees for full down collective. This was later changed to  $\theta_{0.75R} = -2.0$  degrees during the flight test program to achieve satisfactory rotor speed during minimum power descents.

The rotor control deflections available to the pilot during the final portion of the flight test program were as follows:

Longitudinal cyclic	$\pm 10$ degrees
Lateral cyclic	$\pm 7$ degrees
Collective	-2 degrees to +10 degrees



Rudder and yaw valve rigging were accomplished by initially blocking the yaw pedals neutral and making adjustments in the cable system turnbuckles to rig the yaw valve neutral. Rudder surfaces were rigged to neutral by adjustment of the push-pull tube rod ends.

b. Control System Proof Loading

The pilot's cyclic, collective, and yaw controls were proof-loaded in accordance with Reference 2. No permanent deformation or adverse effect was incurred.

The rotor power linkage was proof-loaded to 3,470 pounds in accordance with Reference 2, except that hydraulic pressure was maintained in the system to prevent possible internal damage to the control servo actuators.

3. Engine Controls - Rigging, and Functional Checkout

The engine power control system was rigged and adjusted by means of protractors temporarily installed on the engine fuel control speed signal shafts. Rigging and adjustment were accomplished in accordance with Reference 2.

a. Power Control Lever Rigging and Clearance Check

The power control levers were rigged at the following positions and power lever angles (PLA) were measured on the fuel control speed signal shaft.

<u>Quadrant Position</u>	<u>PLA (deg)</u>
Off	0
Idle	31.5
Military	71.5
Maximum	121.5

Following completion of rigging adjustments, the power control lever system was actuated and was inspected for proper clearances between moving parts and structure.

Friction check	±2 pounds required at top of power lever
Proof load	25 pounds

b. Collective Coordination and Twist Grip Rigging

The collective-PLA coordination linkage was adjusted for the following positions:

<u>Collective Position</u>	<u>PLA (both) (deg)</u>
Full down	82.5
Full up	112.5

Twist grip rigging was adjusted for 30-degree PLA authority for all positions of the collective-pitch control. Considerable slop was found in the twist grip system, which was partially corrected by replacement of the collective override spring with a stronger spring.

A modification to the power control lever quadrant was accomplished prior to start of flight testing to permit movement of the individual power levers to OFF with collective control full up.

The twist grip authority of 30-degree PLA was found unsatisfactory for some flight conditions, and required pilot manipulation of the individual power levers in flight for large power changes.

c. Friction Checks and Proof Loading

The power control levers were proof-loaded to 25 pounds with the speed signal shafts held fixed. No permanent deformation or damage resulted. The power lever breakout and moving friction were 2.00 and 1.75 pounds, respectively, for all conditions.

4. Rotor Lubrication System

The rotor lubrication system was checked out by means of an auxiliary ground cart to purge air from the pressure lines, adjust the flow control valves, and to verify proper operation of the system.

a. Purging

The auxiliary ground cart was hooked up to the rotor lubrication system by means of jumper lines, and the auxiliary pump was operated at 2150 rpm for 30 minutes, causing MIL-L-6082B Grade 1100 oil to circulate through all pressure and return lines.

The upper radial bearing and lower thrust bearing were jumpered at this time to allow oil to flow from pressure lines directly into return lines.

b. Adjustment of Flow Control Valves

The flow to the upper and lower bearings was measured with a stopwatch, and the valves were adjusted to obtain the following flows:

Upper bearing	2 quarts per minute
Lower bearing	1 quart per minute

c. Functional Checkout of Complete System

The auxiliary ground cart was hooked up to both pressure and scavenge lines and operated at 2150 rpm for 30 minutes. Operation was normal.

During the flight test program it was determined that additional cooling was required for the rotor lube oil, and finned tubing was installed in the return line (preflight 16) and a cooler and 28-volt d-c blower were incorporated (preflight 21). No further cooling problems were then encountered.

5. Electrical System

a. Continuity Checkout

The XV-9A electrical system wiring was continuity-tested to verify proper installation prior to functional checkout.

b. Electrical Functional Checkout

The operational checkout of all electrical equipment was satisfactorily accomplished in accordance with Reference 2, by means of a 28-volt d-c rectifier cart hooked up to the XV-9A system.

c. Fire Detection and Fire Extinguishing Systems

These systems were functionally tested and found satisfactory. In future designs, an improved engine fire warning display is recommended. The engine nacelle fire extinguishing provisions were considered adequate; however, on future aircraft an individual extinguishing agent bottle for each nacelle is recommended.

d. D-C Generator Operation

During initial engine runs and tie-down test runs, the d-c generators would not come on the line when the generator line switches were closed. Investigation by Hughes Tool Company Aircraft Division and by the General Electric Company determined that the commutators had a high-resistance film that prevented voltage buildup. The generators were returned to General Electric Company for rework, and the problem was corrected.

Maximum electrical load during flight with all equipment and test instrumentation operating was approximately 150 amperes. Each generator is rated for continuous operation at 150 amperes. Normally, both generators were kept on the line with approximately balanced electrical load.

6. Fuel System

a. Fuel System Functional Checkout

The XV-9A fuel system was pressure-tested for leaks, and the fuel quantity system and fuel low-level warning system were calibrated and functionally checked out prior to engine runup.

b. Fuel System Pressure Test

An air source and pressure regulator were connected to the fuel supply lines, and all lines and fittings were pressure-tested to 75 psig.

c. Fuel System Filling and Leak Test

The fuel tanks were filled with JP-4 fuel and all fuel tank areas were inspected for fuel leakage. Fuel tank and firewall shutoff valves were opened, and boost pumps were turned on to check for leaks with JP-4 fuel in the system. Proper operation of all shutoff valves and pumps was determined.

d. Fuel Quantity System and Low-Level Warning System Calibration

The fuel quantity system was calibrated for each tank by removing all fuel and filling the tank in 20-gallon increments of JP-4 to maximum capacity. Maximum tank capacity was 245 gallons.

The low-level warning lights were actuated with 50 gallons of fuel remaining. This provides approximately 20-minute hovering flight duration at 15,000-pound gross weight.

The fuel quantity indicating system was fairly linear, but was affected by attitude changes in flight. The dual-needle fuel quantity indicator was difficult to read accurately in flight, and is not recommended for use on future designs.

## 7. Fuselage Shake Test

A shake test of the aircraft was performed with the fuselage suspended from an overhead attach point by rubber shock cords. The aircraft was in a reduced empty weight condition (no fuel or payload, and rotor blades not installed). Accelerometers were located at several positions along the fuselage and engine nacelles, and were oriented to read parallel to the applied shake force at the rotor head (first fore and aft and then lateral).

Figure 2 shows the acceleration at the pilot's seat versus frequency of applied shake force (from 6 to 30 cps) in the vertical (fore and aft force) and lateral (lateral force) directions. The same type of information is shown in Figure 3 for the tip of the horizontal stabilizer. Maximum response in this empty weight condition is seen to occur between 11.5 and 12.2 cycles per second. Since the 3-per-rev forcing frequency of the rotor is 12 cycles per second at 100-percent rotor speed (243 rpm), response of the aircraft is of interest because of the closeness to resonance.

The measured mode shape at empty weight of the lowest fuselage and of the nacelle vertical bending mode is shown in Figure 4 for 11.6 cycles per second shake frequency. Also shown in that figure are the calculated mode shape and frequency of this fundamental mode in the full gross weight condition. It is seen that the frequency of this mode is predicted to drop to 9.4 cps, and that acceleration at the pilot's seat is reduced to approximately 40 percent. During flight tests at near design gross weight (discussed under Flight Test Results), the natural frequency of the lowest mode (detected by engine-located accelerometers) was found to be less than 10 cycles per second. This value was determined by observing engine vibration during flight at reduced rotor speed, where frequency at lowest operating rotor speed (approximately 90-percent rpm) started to approach a resonance, and appreciable engine response was noted. Flight tests at full gross weight therefore confirm the results predicted from

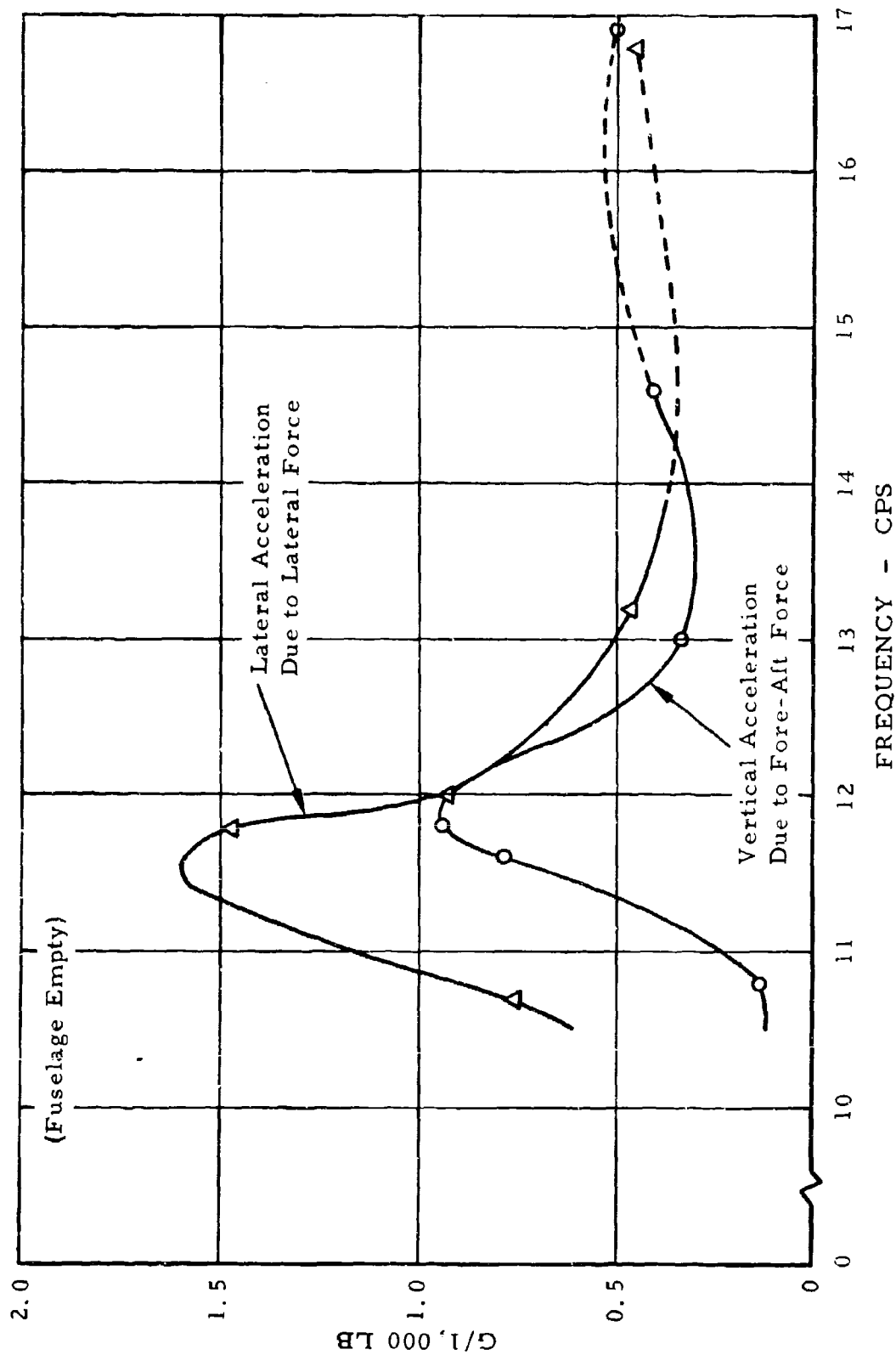


Figure 2. Pilot Acceleration Due to Force Applied to Main Rotor Shaft at Hub Gimbal Versus Frequency.

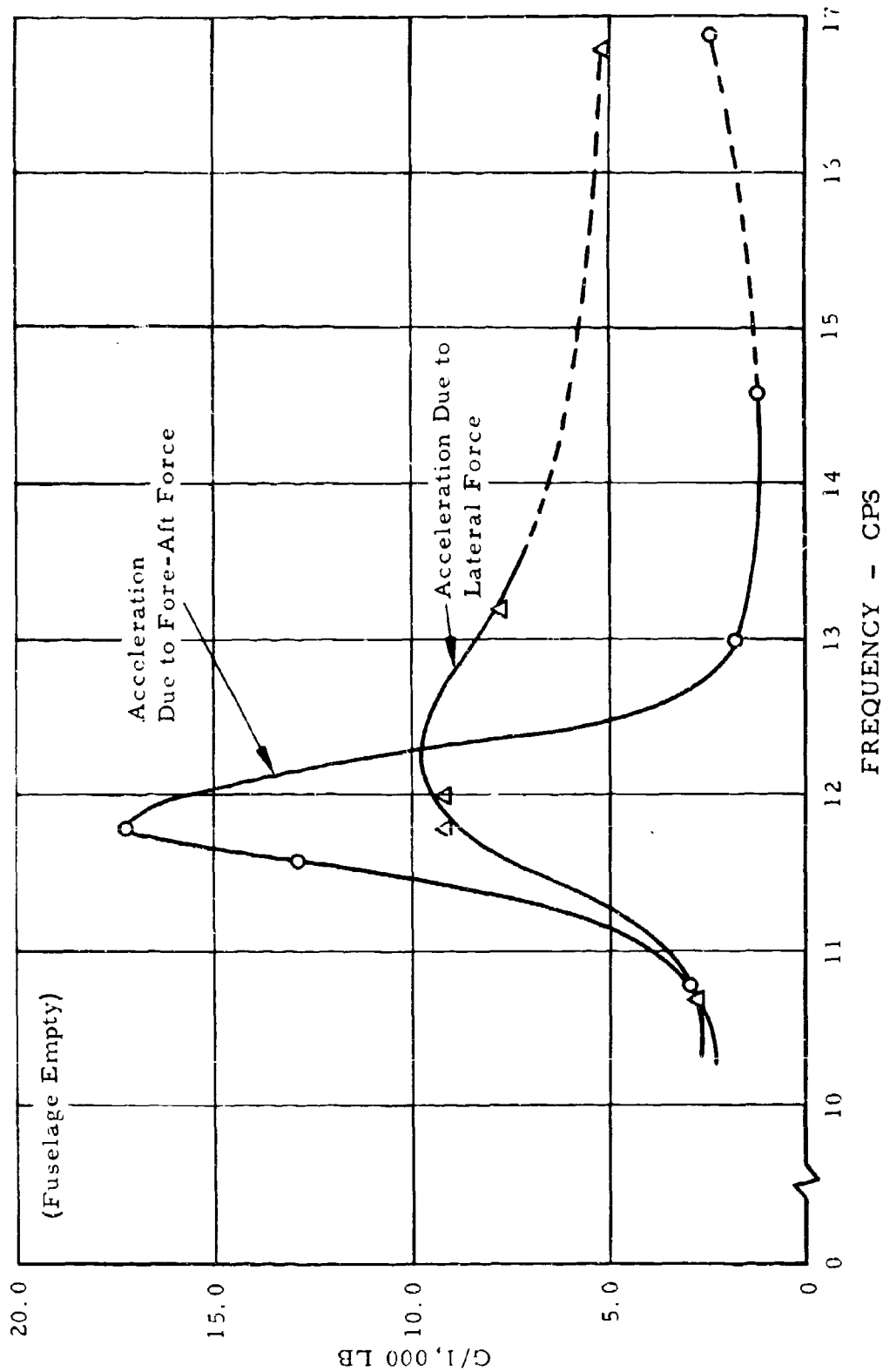


Figure 3. Normal Acceleration at Tip of Horizontal Stabilizer Due to Force Applied to Main Rotor Shaft at Hub Gimbal Versus Frequency.

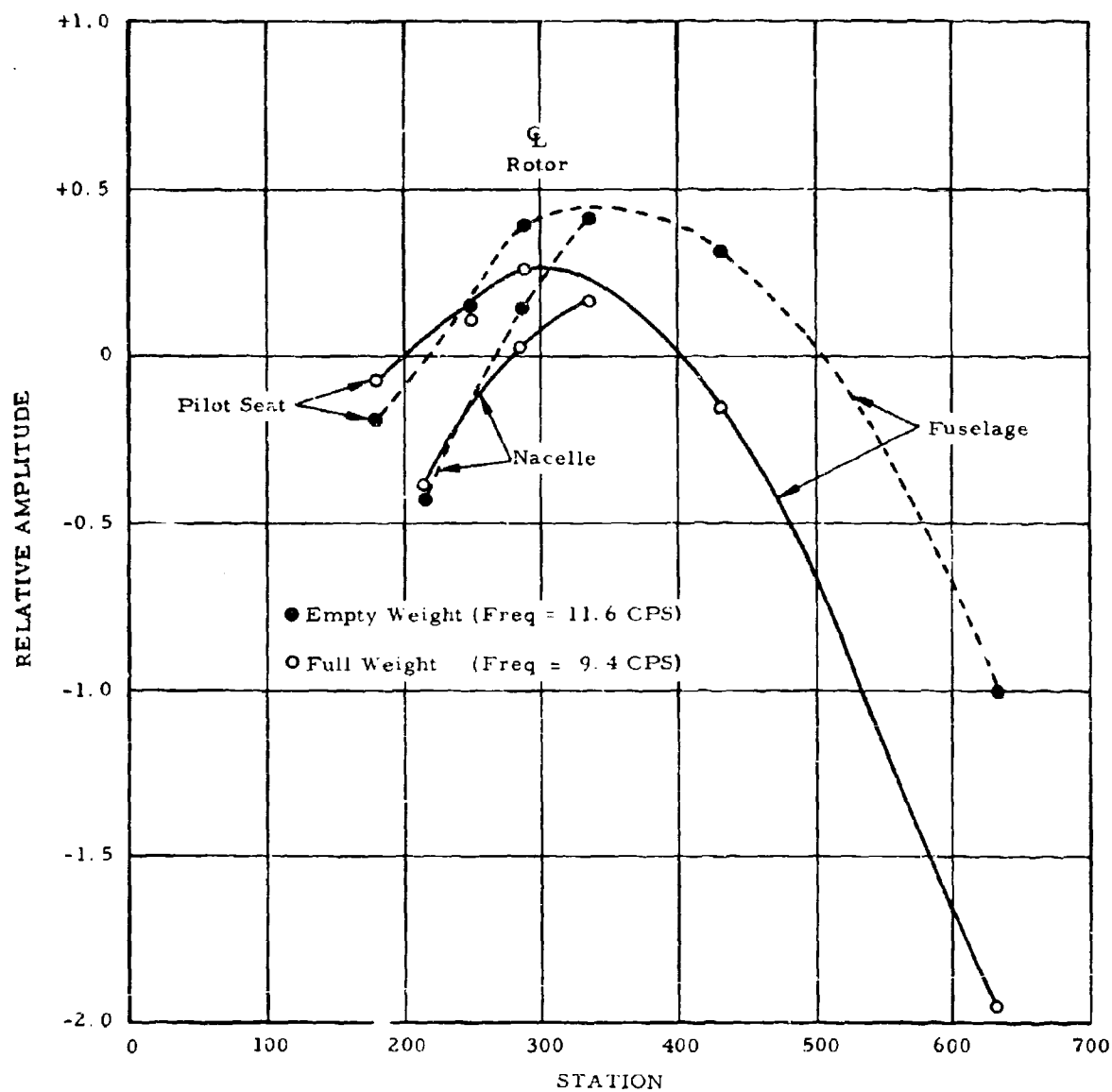


Figure 4. Fuselage Vertical Bending Versus Fuselage Station.



the shake tests at reduced empty weight; that is, the lowest fuselage bending frequency would be below the frequency corresponding to 3 times the lowest operating rotor speed.

## 8. Engine Runup

Engine runup tests were accomplished for functional checkout of the YT-64 gas generators with diverter valves in overboard position, in accordance with Section 9.0 of Reference 2. Two engine runs were made, for a total operating time of 2 hours and 9 minutes on Engine 027-1A and 1 hour and 39 minutes on Engine 101-3A.

The following test items were accomplished during engine runup:

- Engine-start and steady-state operation to 100-percent  $N_G$
- Fuel system functional test
- Hydraulic system checkout
- Electrical system checkout
- Engine and nacelle cooling data
- Cockpit carbon monoxide concentration

### a. Engine Operation

This was the initial YT-64 engine operation in the completed XV-9A aircraft, and the first operation of the flight quality YT-64 gas generators with modified first-stage compressor blading. Data were recorded for starting, acceleration, and steady-state operation up to 100-percent  $N_G$  on both engines.

### b. Fuel System Functional Test

Both engines were operated tank to engine with boost pumps on and off, and on crossfeed with boost pumps on and off, to verify proper fuel system operation up to 100-percent  $N_G$  power setting.

### c. Hydraulic and Electrical System Checkout

Hydraulic system operation was normal, including operation of rotor controls and diverter valves.

The engine-driven 28-volt d-c generators did not function, and the run was made on external power. The generator problem was resolved later by General Electric during tie-down tests.

d. Engine and Nacelle Cooling Data

Structural temperatures, equipment temperatures, and air temperatures were recorded in the engine, nacelle, and pylon structure, and at various points within the nacelle during engine operation up to 100-percent  $N_G$ . Cooling was determined to be adequate for operation of the YT-64 gas generators at maximum power with diverter valves overboard.

e. Cockpit Carbon Monoxide Concentration

Carbon monoxide concentration was measured using an MSA CO detector, and was found to be negligible for all conditions.

TIE-DOWN TEST RESULTS

The completed XV-9A aircraft was tested on a tie-down pad with cable restraints attached to the upper main landing gear strut fittings and the tail gear tie-down fitting for restraint in the vertical, lateral, and longitudinal directions during engine and rotor operation.

A summary of preflight engine runs and tie-down test runs has been shown in Table I. A total of 19 test runs was made, for a total rotor operating time of 13 hours and 20 minutes. Engine operating time at completion of tie-down testing was 21 hours and 24 minutes on Engine 027-1A and 20 hours and 32 minutes on Engine 101-3A. The following tests were accomplished:

- Rotor and system shakedown
- Rotor tracking and balance
- Rotor and systems functional checkout
- Rotor-airframe vibration investigation
- Ground instability test
- Engine nacelle and fuselage cooling verification
- Rotor-speed-governing checkout and adjustment
- Single-engine rotor operation

1. Rotor Tracking and Balance

Rotor blade tracking and balance were accomplished during runs 1 to 6, and satisfactory results were obtained. Rotor track was observed visually, using an engineering transit set up some distance from the aircraft and colored tape strips on the blade tips oriented in a manner to permit blade identification with the rotor

turning. Individual blade adjustments were accomplished by means of the upper control system pitch links.

Rotor balance was accomplished by monitoring the fuselage longeron strain gages on a direct-writing oscillograph and placing small weights near the blade tips according to the rotor unbalance condition indicated by the traces.

After completion of the tracking and balance adjustments, the 1-per-rev vibration was negligible, and no further adjustments were required during tie-down testing.

## 2. Rotor and Systems Functional Checkout

The complete aircraft, including rotor controls, power controls, yaw control, electrical system, hydraulic system, diverter valves, rotor governing, tip cascades, instruments, communications, and test instrumentation, was operated and functionally checked out for flight during tie-down tests. The following items were accomplished:

- a. Stabilized engine and rotor operation for  $\theta = 0, 2, 5, 6, 7, 8, 9$ , and 10 degrees at  $N_R = 100$  percent
- b. Collective pitch-power transients from  $\theta = 2$  degrees  $\rightarrow 9$  degrees  $\rightarrow 2$  degrees
- c. Cyclic control deflections,  $\pm 10$  degrees longitudinal and  $\pm 5$  degrees lateral
- d. Rotor structural loads and temperatures up to  $\theta = 10$  degrees at  $N_R = 100$  percent
- e. Control system checkout on single hydraulic system
- f. Yaw valve operational checkout
- g. Rotor start-up, acceleration to 100-percent  $N_R$ , and shutdown
- h. Rotor-governing setup and  $N_f$  adjustment
- i. Engine nacelle and fuselage cooling verification

## 3. Airframe Vibration Investigation

During initial tie-down tests with restraint cables tight, vertical vibration at the cockpit and at the engine nacelles was encountered at a frequency of 10 to 12 cycles per second. This vibration increased in amplitude with increased collective pitch, and became objectionable to the pilot at collective-pitch angles of more than 5 degrees. The initial tie-down tests were conducted without the fuselage ballast installed, and the starting gross weight with full fuel was approximately 13,700 pounds. This vibratory

mode of the fuselage and engine nacelles was previously observed during fuselage shake tests (see Figure 4) where the natural frequency of the fuselage and engine nacelles was close to 3 per rev (12 cps).

Weights were installed on the forward engine mount truss on each nacelle, to reduce the natural bending frequency of the nacelle structure and reduce the vibration level near 3 per rev. A weight was also installed on the tail landing gear, to reduce fuselage bending frequency.

Test runs were also made with the tie-down cables slackened to evaluate the effect of increased damping provided by the oleo struts and tires. The effect of slackening the cables was to reduce vibration levels.

The description of the configurations tested and tabulation of the vibration levels measured by accelerometers located at various positions are shown in Table II. Configuration C, which had 300 pounds of ballast installed on each engine nacelle, produced the best results.

The fuselage ballast, approximately 1,600 pounds, was installed in the aircraft prior to tie-down run 12 and remained for subsequent runs. The engine nacelle weights were removed to permit installation of nacelle cowling for cooling data.

As pointed out previously, analysis of empty weight fuselage shake test data, Figure 4, indicated that the fuselage natural bending frequency would be appreciably reduced at the design gross weight of 15,300 pounds. Inspection of the mode shape for design gross weight indicates that vibration would be further reduced by installing additional ballast in the cockpit area. (The cockpit is one of the antinodes and one of the most efficient locations for ballast weights.) Cockpit ballast (345 pounds) was installed prior to tie-down run 14.

These changes produced a satisfactory reduction of vibration levels for flight operation of the XV-9A as a research aircraft for Hot Cycle system test and evaluation, but the installations were not optimized because of the short duration of the program.

For flight test, the cockpit ballast was reduced to 250 pounds and the nacelle weights reduced to 200 pounds, because of space

TABLE II  
TIE-DOWN TESTS - VIBRATION LEVEL VERSUS CONFIGURATION

Configu- ration	Run Number	Counter Number	Collective rpm (deg)	Engine 1 Vert Accel (# g)	Engine 1 Lat Accel (# g)	Engine 2 Vert Accel (# g)	Engine 2 Lat Accel (# g)	Channel		Upper Bearing Lat Accel (# g)	Upper Bearing Long Accel (# g)	19 and 20 Chordwise Moment Sta 90 (# in-lb)
								27	34			
A	6	433	2	100.0	0.16	0.12	0.17	0.17	0.20	0.10	0.11	465
B	8	348	2	100.0	0.19	0.12	0.09	0.09	0.16	0.09	0.09	235
C	9	508	2	100.0	0.14	0.12	0.08	0.08	0.22	0.13	0.09	410
D	9A	1,865	2	100.0	0.24	0.10	0.14	0.14	0.22	0.12	0.09	470
E	10	438	2	96.4	0.24	0.07	0.07	0.07	0.33	0.12	0.06	420
A	6	537	5.2	100.0	0.32	0.21	0.19	0.19	0.27	0.24	0.15	1,170
B	8	430	5	99.5	0.13	0.19	0.18	0.18	0.33	0.21	0.20	1,780
C	9	638	5	100.0	0.22	0.11	0.15	0.15	0.22	0.09	0.06	880
D	9A	2,092	5	100.0	0.54	0.21	0.21	0.21	0.50	0.21	0.13	1,250
E	10	581	5	98.0	0.32	0.15	0.09	0.09	0.61	0.20	0.11	1,190
A	6	654	*	11.0	0.10	0.03	0.19	0.19	0.16	0.22	0.04	117
E	10	234	*	0.0	0.32	0.09	0.10	0.10	0.22	0.20	0.05	0
E	10	890	8**	97.5	0.49	0.17	0.16	0.16	0.45	0.24	0.15	2,460

Configuration

- A Tight tie-down cables
- B Tight tie-down cables plus 300 pounds at engine
- C Slack tie-down cables plus 300 pounds at engine
- D Slack tie-down cables, no weight at engine
- E Slack tie-down cables plus 600 pounds at engine plus 100 pounds at tail

\*Engines overboard, at high power

\*\*Lift-off

limitations. The in-flight vibration characteristics are discussed under Flight Test Results.

#### 4. Ground Instability Test

Ground instability tests were accomplished during run 15 in accordance with Section 12.0 of Reference 2.

Cyclic excitation was applied by the pilot by moving the cyclic stick in a circular motion at various frequencies from 0 to 5 cps for approximately 1-degree amplitude with collective-pitch settings of 2 degrees and 5 degrees at 90-, 95-, and 100-percent  $N_R$ .

Analysis of oscillograph records showed no evidence of mechanical instability. Chordwise blade loads were near or exceeded the maximum allowable, where stick motion was near 0.4 per rev (1.6 cps). Stick motion at 0.4 per rev excites a frequency of 1.4 per rev in the rotating system. Since the blade chordwise natural frequency is 1.4 per rev, high chordwise moments are encountered during this type of excitation.

#### 5. Rotor Governing

Rotor-speed governing for the XV-9A was accomplished using the standard fuel control mechanism on the YT-64 engines with an input from collective position to compensate for governor droop. It was not feasible to introduce a measure of rotor speed to the fuel control with a short flexible cable (31 inches long on a standard installation) because a cable length of 17 feet would be required, from the rotor to the front face of each fuel control. A hydraulic feedback link was used, which included a hydraulic pump at the rotor, a hydraulic motor at the fuel control, lines between the pump and motor, and a bypass line with a needle valve, to obtain the desired fuel control input speed at 100-percent rotor speed.

Initial tie-down tests were performed without rotor-speed governing. The pilot was required to synchronize rotor blade pitch and engine power lever to maintain rotor speed, and he reported some difficulty in controlling rotor speed. When governing utilizing the rotor-speed signal (hydraulic link) was used, the pilot reported rotor-speed control as satisfactory during transient collective pitch changes. Rotor-speed governing utilizing the hydraulic speed signal was then used for the balance of the tie-down tests and for all flight tests.

The governing system was not entirely satisfactory, however, because over the duration of a flight some drift of speed signal to each engine would occur (almost always engine 1), and the pilot was required to adjust power levers (speed-selector levers) individually to keep gas generator speeds reasonably matched (within 3 percent of each other). The feedback link to engine 2 was stable and repeatable within the accuracy of instrumentation (less than  $\pm 1$  percent variation of speed signal/rotor speed) and performed in accordance with the system design requirements. The no. 1 feedback link/fuel control system contained some element causing drift that has not yet been identified and will require further testing or modification to obtain drift-free operation. The pilot was, however, always able to make a suitable correction, although he reported that the frequency of power lever adjustment required to balance engine speeds increased as the program continued.

#### 6. Single-Engine Operation

The XV-9A propulsion system has a common ducting system for the two engines, and tip nozzles sized for the two-engine case. If an engine fails, or if the pilot chooses to practice one-engine operation, it is necessary to reduce tip nozzle area to one-half to keep the remaining engine on a proper operating line. Each blade tip is equipped with a two-position cascade, and these are closed to the half-area position after the engine diverter valve is actuated to the overboard position. Power is then increased on the remaining engine to maintain rotor speed and thrust.

Mechanical tests were performed on the tip cascade system, including a warning system that indicates when one engine is performing poorly compared with the other. The tests showed that all mechanical components (valves, switches, and so forth) involved in actuation performed properly, but the warn-divert system, which depended on a small vane in the Y-duct junction to deflect toward a "bad" engine, was not performing satisfactorily. Sufficient engine instrumentation is available to permit the pilot to identify a failing (or failed) engine, but the semiautomatic warning system required adjustment or modification that could not be performed during the present program because of the inaccessible location of the deflecting vane with the power module fully assembled and mounted on the aircraft.

As part of the mechanical checkout of the propulsion system, tests were made during which the pilot switched from two engines to one engine and back to two engines. Stabilized data were taken at topping

engine speed while a single engine was powering the rotor. The following results were obtained, using procedures for calculation of power discussed later:

<u>Engine</u>	<u>Engine RPM (percent)</u>	<u>Rotor RPM</u>	<u>T<sub>5</sub> (deg F)</u>	<u>Calculated Rotor Horsepower</u>
026	102.4*	96.9	1,026	985
027	102.8*	97.3	1,015	1,036

\*Note: These values of gas generator speed are less than the maximum steady-state value of 104 percent allowed by General Electric in order to permit margin for speed increase at topping when the yaw valve is opened and the engine operates along a droop line as a result of the increase in nozzle area. It should be noted that the rotor powers given here are subject to correction for an unknown amount of leakage through the diverted engine diverter valve.

These values differ by  $\pm 1\frac{1}{2}$  percent from their average value, which is within the accuracy of the procedures used here. The average 1,020 horsepower achieved in the test was obtained with tip nozzles that are large enough to bring the engine near to operating speed limit before they reach their turbine temperature limit. By reducing the tip nozzle area, and retopping the engines to suit the changed nozzle, the engines can be brought to exhaust temperatures (T<sub>5</sub>) of 1,130 degrees F, which represents a sufficient increase to achieve an expected 1,200 horsepower per engine.

Rotor-speed-governing was used during these single-engine tests, and was satisfactory except for some of the drift mentioned above.



## FLIGHT TESTS

### GENERAL

The flight test program was conducted during the period 5 November 1964 through 5 February 1965. It consisted of 21 flights, for a total flight time of 15 hours and 42 minutes. All flight test objectives outlined in the flight test program plan, Reference 1, were achieved. The entire ground test and flight test program was completed satisfactorily. The flight and operational characteristics of the XV-9A aircraft and Hot Cycle propulsion system were found to be satisfactory, after incorporation of minor system modifications, for continued research flight testing and Hot Cycle system research.

A summary of flight test operations is shown on Table III. A description of the test aircraft is given in the section following, and a description of the test instrumentation system is presented in Appendix I. A configuration and change log, showing the major items of rework, change, or replacement during the flight test program, is presented in Appendix II.

Maintenance of the Hot Cycle rotor system during the ground and flight test program was minimal, and the basic components (including blades, hub, rotating and stationary ducting, seals, bearings, rotor shaft, tip cascades, and rotating controls) were unchanged and required only routine inspection during the program. Because of the concurrent fatigue testing of the blade root-end structure, the leading and trailing edge sections of the rotor blades were removed after each five hours of flight for inspection of the blade spars and attachment bolts. No discrepancies were found. The blade spar inspection was required as a result of fatigue cracks that occurred during the blade root-end fatigue tests (see Reference 3).

### FLIGHT TEST PROCEDURES

All flight test operations were preceded by a standard preflight inspection of the airframe, rotor, gas generators, and systems, to ensure safety of flight and proper operation of the aircraft. A preflight inspection and functional checkout of the test instrumentation system was conducted prior to each flight to ensure proper data acquisition.

Flight plans were prepared in accordance with the flight test program plan and as determined by analysis of the data from previous flights and qualitative pilot evaluation.

TABLE III  
FLIGHT TEST OPERATIONS SUMMARY  
(U.S. Army 15107)

Flight Number	Date	Purpose	Engine 1		Engine 2		Rotor Run (Hours)	Flight Time (Hours)
			(S/N 027-1A)	Run (Hours)	(S/N 101-3A)	Run (Hours)		
1	5-11-64	Taxi and ground handling evaluation; hovering evaluation	01:02	01:03	00:58	00:13		
2	6-11-64	Rotor-speed-governor ground checkout; hovering evaluation; transition to forward flight and flare	02:02	02:03	01:42	00:30		
3	12-11-64	Hovering evaluation; forward flight to 20 and 30 knots; sideward flight	01:25	01:25	01:13	00:59		
4	16-11-64	Hovering evaluation; forward flight to 30 and 40 knots; sideward flight	00:58	01:02	00:39	00:28		
5	19-11-64	Hovering evaluation; forward flight to 40 and 50 knots; rudder system force measurement	01:43	01:43	01:26	00:37		
6	20-11-64	Hovering; normal and single hydraulic systems; landing evaluation; manual rotor-speed-governing evaluation	01:32	01:32	01:04	00:33		
							Total 31:38*	

TABLE III (Continued)

Flight Number	Date	Purpose	Engine 1 (S/N 027-1A) Run (Hours)	Engine 2 (S/N 026-1B) Run (Hours)	Rotor Run (Hours)	Flight Time (Hours)
7	8-12-64	Hovering evaluation; structural loads and con- trol; forward flight to 70- knot CAS; pacer airspeed calibration (ground run included)	01:56	01:59	01:23	00:23
8	9-12-64	Hovering evaluation; structural loads and con- trol; normal flight pattern; ground run rotor govern- ing checkout	01:41	01:45	01:31	00:31
9	11-12-64	Hovering evaluation; per- formance; level flight to 85-knot CAS; pacer air- speed calibration	01:03	01:04	00:57	00:43
10	18-12-64	Hovering evaluation with servo dither; level flight to 95 knots; 200-lb weights on engines; airspeed cali- bration, ground speed course	01:43	01:43	01:36	01:17
11	22-12-64	Hovering evaluation; 90° turns left and right; for- ward flight to 100-knot CAS; sideward flight; descents at 50- and 60-knot IAS	01:14	01:14	01:03	00:49

TABLE III (Continued)

Flight Number	Date	Purpose	Engine 1 (S/N 027-1A) Run (Hours)	Engine 2 (S/N 026-1B) Run (Hours)	Rotor Run (Hours)	Flight Time (Hours)
12	29-12-64	Hovering evaluation; sound measurement; level flight data at 50-, 60-, 70-, 80-, and 90-knot IAS; climbs at 102 and 103% $N_G$ ; descents at 50-knot IAS	01:31	01:44	01:17	01:10
13	6-1-65	Hovering evaluation; dither on and off; climbs at 40- and 50-knot IAS; level flight turns, $\phi = 20^\circ$ 80- and 90-knot IAS	01:28	01:32	01:13	00:57
14	11-1-65	Airspeed calibration; ground course, 80- and 90- knot IAS; climbs at max coll; level flight turns, $\phi = 30^\circ$ ; descents $\theta = -2^\circ$	01:26	01:28	01:10	00:56
15	14-1-65	Reset engine idle to 75% NG; reset governing; hovering performance $N_R = 100\%$ and 95%; hover turns, $90^\circ$ left and right; sideward flight, 20 mph right and left	02:12	02:31	00:42	00:28

TABLE III (Continued)

Flight Number	Date	Purpose	Engine 1 (S/N 027-1A) Run (Hours)	Engine 2 (S/N 026-1B) Run (Hours)	Rotor Run (Hours)	Flight Time (Hours)
16	20-1-65	Engine operating data; cleaned compressors; engine-rotor power transients; climb, 50-knot IAS; level flight turns, $\phi = 30^\circ$ ; 60-, 70-, and 80-knot IAS	01:28	01:24	01:02	00:29
17	21-1-65	Hovering performance, $N_R = 93.5\%$ , $100\%$ , $103\%$ ; level flight; speed-power 58-, 71-, 80-, 87-, and 95-knot IAS; rotor downwash; ground run; reset overspeed switch	02:01	02:08	01:55	01:13
18	26-1-65	Hovering performance at 95% and 100% $N_R$ ; rotor downwash and sound data; climb, descents, rearward flight; run-on landings	01:48	01:50	01:41	01:10
19	26-1-65	Hovering turns, $180^\circ$ and $360^\circ$ ; descents at 90% $N_R$ ; level flight, 70-knot IAS; tuft photos	01:51	01:57	01:41	01:04

TABLE III (Continued)

Flight Number	Date	Purpose	Engine 1		Engine 2		Flight Time (Hours)
			(S/N 027-1A) Run (Hours)	(S/N 026-1B) Run (Hours)	(S/N 026-1B) Run (Hours)	(S/N 026-1B) Run (Hours)	
20	28-1-65	Hover performance point, 101% $N_R$ ; hover turns, 180° and 360°; sideward and backward flight; level flight speed-power, 90-knot IAS	00:53	00:59	00:47	00:33	
Ground Run	3-2-65	Engine operating and acceleration data; engine-rotor acceleration data with $N_G$ mismatch; rotor speed vs PLA and rotor speed vs yaw valve characteristics	01:24	01:31	00:52	-	
Ground Run	4-2-65	Engine rotor acceleration data with mismatch; rotor-engine sound data at 50 ft; single-engine rotor operation and topping; rotor governing with $N_f$ bypass closed	01:58	02:02	01:52	-	
21	5-2-65	Electrostatic voltage measurement	01:35	01:45	01:28	00:39	
TOTAL			62:06	31:26*	45:22	15:42	

\*Engine S/N 101-3A removed prior to flight 7; engine S/N 026-1B installed for flight 7 and on.

Two-way radio communication between the XV-9A and ground personnel was maintained during all flight operations, for monitoring and coordinating test operations. A flight test log was kept for each flight test operation, to document operating time and pilot observations and to facilitate data reduction.

### FLIGHT TEST EVALUATION

The XV-9A aircraft was evaluated and test data were recorded for evaluation of Hot Cycle performance, structural loads and temperature, stability and control characteristics, vibration levels, and aircraft performance for the following flight conditions:

- Engine and rotor start
- Rotor acceleration
- Taxi and ground handling
- Hovering
  - Steady hover
  - Hover turns of 90, 180, and 360 degrees
- Transition to forward flight
- Approach to hover
- Climb
- Level flight
- Level flight turns at 20- and 30-degree bank angles
- Sideward flight to right and left
- Rearward flight
- Progressive 360-degree turns
- Descents, normal and minimum-power
- Landing

The flight test results are summarized in the following paragraphs under the headings listed below and are presented in greater detail in the Flight Test Results section. Because of the large volume of flight test data recorded, only the significant portions are presented in this report. All other flight test data are on file at the contractor's facility.

1. Structural loads
2. Structural and equipment operating temperature
3. Performance
4. Flying qualities
5. Miscellaneous hovering tests

## 1. Structural Loads

Structural loads data were reviewed carefully after each flight, to ensure that excessive loads were not developed in critical components or that a structural failure had not occurred.

Data are presented for level flight at various airspeeds up to the maximum flown. In general, the cyclic loads recorded in critical components were below design levels. High chordwise blade loads resulting from 0.4 per rev (1.6 cps) pilot-induced cyclic stick movements were reduced by control system modifications to decrease servo valve friction and provide centering forces on the cyclic control stick. Cyclic loads data are shown for blade spar flapwise and chordwise bending, blade chordwise shear load, rotor shaft bending, hub plate stress, and pitch arm load. Flapwise and chordwise bending data versus blade radius are shown to agree well with the design blade radius moment curves.

Frequency spectrums are shown for blade flapwise bending and cyclic spar axial load, for use in determination of calculated blade life (see Reference 4).

Visual inspection of all primary structural components, including the critical blade spar area at Station 91, was accomplished after each flight. Prior to aircraft roll-out, the rotor blade spars were modified at this station to alleviate a stress concentration at the most outboard attachment of the laminated spar to the spar-root fitting. The modification consisted of reducing the fitting thickness at this location and adding another bolt just inboard. The modification was necessitated by the occurrence of a fatigue crack in the spars at this location on the blade root-end fatigue test specimen (see Reference 3). Complete blade spar inspection was accomplished each five flight hours by removal of leading and trailing edge sections. No structural problems were encountered.

## 2. Structural and Equipment Operating Temperatures

Extensive temperature measurements were recorded in the engine nacelles, rotor hub-pylon area, and fuselage, to verify adequate cooling of structure and equipment. A total of 129 thermocouple outputs was recorded for these areas. Satisfactory cooling was obtained for all engine nacelle, rotor hub-pylon, and fuselage structure.



High rotor lubrication oil temperatures (215-degree F maximum) occurred during hover on flight 15. Provisions for additional rotor lube oil cooling were incorporated in the system, and rotor oil temperatures remained below 200 degrees F on subsequent flights.

Rotor structural temperatures were recorded during all flights, and were checked after each flight to determine that the various rotor components were well within operating limits.

Charts showing the location of thermocouples and the maximum temperatures recorded during the flight test program are presented on pages 51 and 53, under Flight Test Results.

### 3. Performance

Performance data are presented and discussed in the categories of overall performance, engine performance, and individual component performance. The rotor lift obtained during hovering agrees closely with previous whirl test data where fixed tip cascade nozzles were used, and with earlier predictions. Flight test fuel consumption (corrected as described in Appendix IV) was found to be 5 to 8 percent higher than predicted. This difference is possibly related to having a lower nozzle velocity coefficient, higher duct friction coefficient, or higher profile drag coefficient in the flight tests compared with original performance predictions.

### 4. Flying Qualities

The XV-9A flying qualities were qualitatively evaluated for all normal helicopter flight conditions within the restricted flight envelope that was possible within the Culver City flying area. Data are presented to show longitudinal control positions in level flight, yaw valve effectiveness during hover, and control positions during sideward and rearward flights.

Evaluation of the aircraft's handling characteristics for pull and hold and pulse-type control displacement maneuvers was not performed, because of the restricted flight area. Thus, no attempt is made to compare the predicted handling characteristics (control power and damping) presented in Reference 5 with flight test data.

It is anticipated that during the 20-hour follow-on test program, maneuver-type stability and control tests will provide sufficient data to more fully evaluate the flying qualities of the aircraft.

5. Vibration

The three-bladed XV-9A rotor transmits vibration to the fuselage predominantly at 3 per rev, which corresponds to 12 cps at full rotor speed. Because the fuselage first natural bending frequency is close to this value (9.4 - 11.6 cps), a certain amplification of response takes place. Vibration levels at cockpit were lowest during hover and increased during level flight, with the maximum recorded during transition to forward flight and approach to hover. Vibration data are presented for pilot's vertical acceleration and engine nacelle vertical and lateral acceleration for various air-speeds. Average vertical acceleration at the pilot's position was  $\pm 0.35$  g in level flight and  $\pm 0.13$  g during hover.

6. Pilot Comments and Qualitative Evaluation

A summary of pilot's comments and qualitative evaluation of the XV-9A flying qualities, systems operation, and functional characteristics is presented in Appendix III.

7. Miscellaneous Hovering Tests

Sound power levels, rotor downwash velocity, and static electricity buildup were measured during hovering flights. Sound power level was also measured during a 90-knot flyover at 50-foot altitude.

a. Sound Power Levels

The overall sound level of the XV-9A during hover was not objectionable to nearby observers. Sound power level measured in the cockpit during flight was 109 decibels. This was not objectionable to the pilot, and radio communications were satisfactory. Sound data were recorded from 50- to 400-foot distance from the aircraft at 100-foot intervals for four azimuth positions. Sound power level measured at 200 feet in hover was 103 decibels.

b. Rotor Downwash

Rotor downwash velocity was measured during hover at approximately 20-foot wheel height. The maximum velocity measured was 73 feet per second at approximately 70-percent blade radius. The aircraft was hovered over unprepared surfaces with no deterioration of the surface and no engine ingestion problem.

c. Static Electricity Buildup

The electrostatic voltage buildup and charging current were measured during hover at 20-foot wheel height. The electrostatic charge was low (7 to 9 kilovolts) in comparison with measurements taken on a large shaft-driven helicopter (H-37), which were 50 kilovolts or greater (see Reference 6).

## FLIGHT TEST RESULTS

1. Structural Data

XV-9A rotor blade moments experienced during flight were fairly typical of those experienced on other helicopters. Blade moments were low during hover, fairly high when accelerating or decelerating through the transition region, low at the minimum power speed, and increased thereafter with speed.

In addition to the typical response to aerodynamic excitation, a type of excitation and response was encountered that is typical of chordwise unarticulated blades. The XV-9A rotor blades have a chordwise natural frequency of 1.4 per rev. Motion of the cyclic stick at 0.4 per rev in the nonrotating system will excite 1.4 per rev in the rotating system; 0.4 per rev is 1.6 cps, which is a frequency at which pilots occasionally move the cyclic stick. Only a small content of 0.4 per rev in the stick input waveform is sufficient to excite chordwise bending. The XV-9A pilot inputs at this frequency were reduced by installing cyclic stick centering springs and by reducing servo-valve friction as much as possible, both of which improved the "feel".

Presented as Figures 5 through 10 are plots of the significant structural loads from flight 17. Stabilized data were obtained on this flight for five airspeeds up to 108-knot calibrated airspeed (CAS). Bending moments versus rotor blade radius are shown in Figures 11 and 12.

- Figure 5. Cyclic Flapwise Blade Bending at Station 75.4 Versus Calibrated Airspeed.
- Figure 6. Cyclic Spar Axial Load (Chordwise Moment) at Station 90.75 Versus Calibrated Airspeed.
- Figure 7. Cyclic Chordwise Shear Load at Station 23 Versus Calibrated Airspeed.
- Figure 8. Cyclic Main Rotor Shaft Bending Versus Calibrated Airspeed.
- Figure 9. Cyclic Hub Plate Stress Versus Calibrated Airspeed.
- Figure 10. Cyclic Pitch Arm Load Versus Calibrated Airspeed.
- Figure 11. Cyclic Flapwise Bending Moment Versus Main Rotor Blade Radius.
- Figure 12. Cyclic Chordwise Bending Moment Versus Main Rotor Blade Radius.

During the course of the flight program, various maneuvers were performed, including turns, climbs, descents, sideward and rearward flight, and flares. Only limited maneuvers could be performed, because of the airspace and airspeed limits imposed over the Hughes Airport. As an indication of the range and distribution of blade fatigue moments during flight, a spectrum of chordwise bending at Station 90.75 is presented as Figure 13. Figure 14 is a spectrum of flapwise bending at Station 75.4. These spectra were obtained from a typical flight (flight 13) that included speeds to 103-knot calibrated airspeed, turns, descents, climbs, and hovering turns.

## 2. Structural and Operating Temperatures

### a. Rotor Temperatures

Temperatures of the rotor and associated components were recorded on a Brown recorder. Inputs from thermocouples located in various parts of the blades were channeled to three switching boxes, then to a hot reference junction box, through the main rotor slip ring, finally terminating at the Brown recorder.

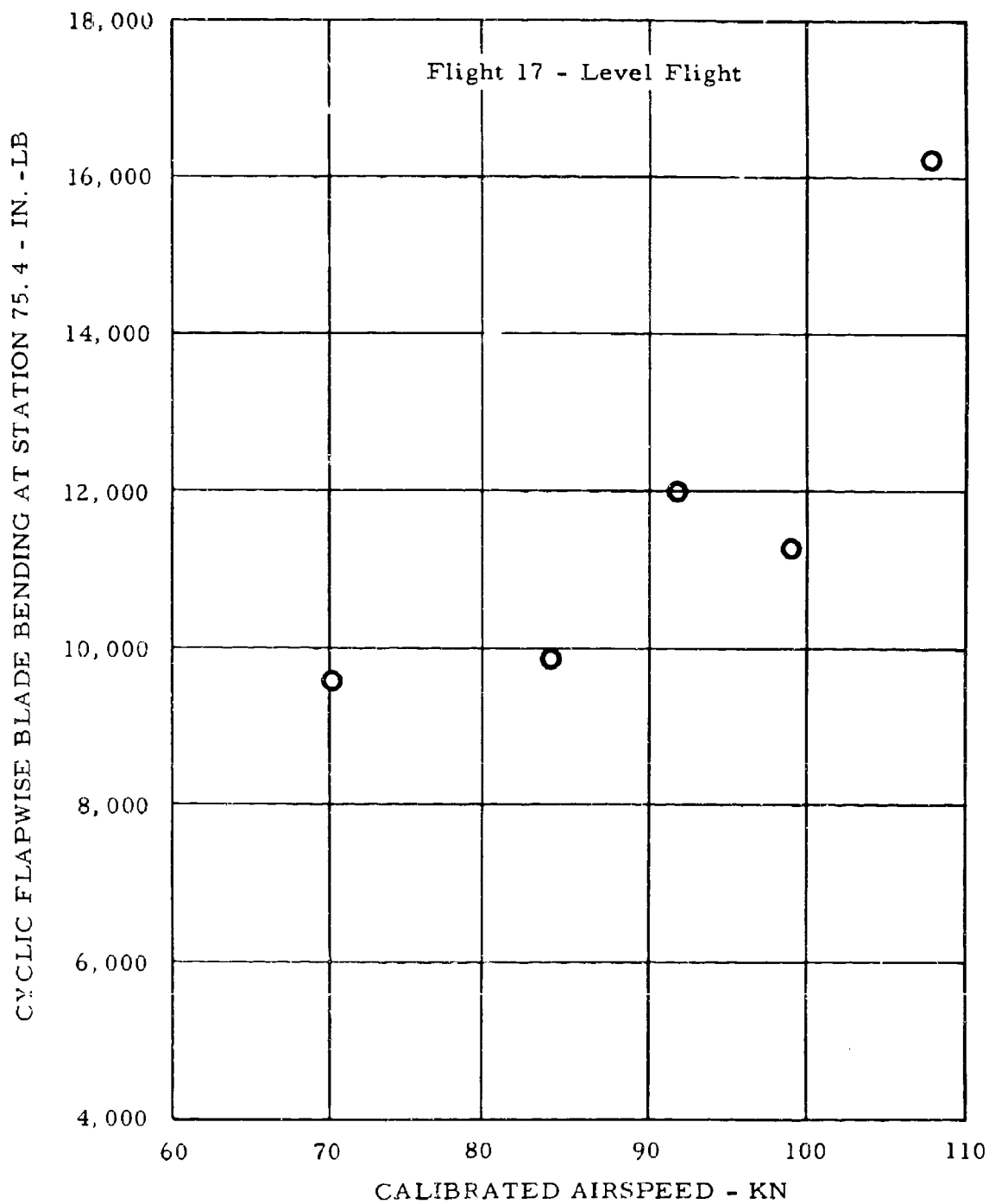


Figure 5. Cyclic Flapwise Blade Bending at Station 75.4 Versus Calibrated Airspeed.

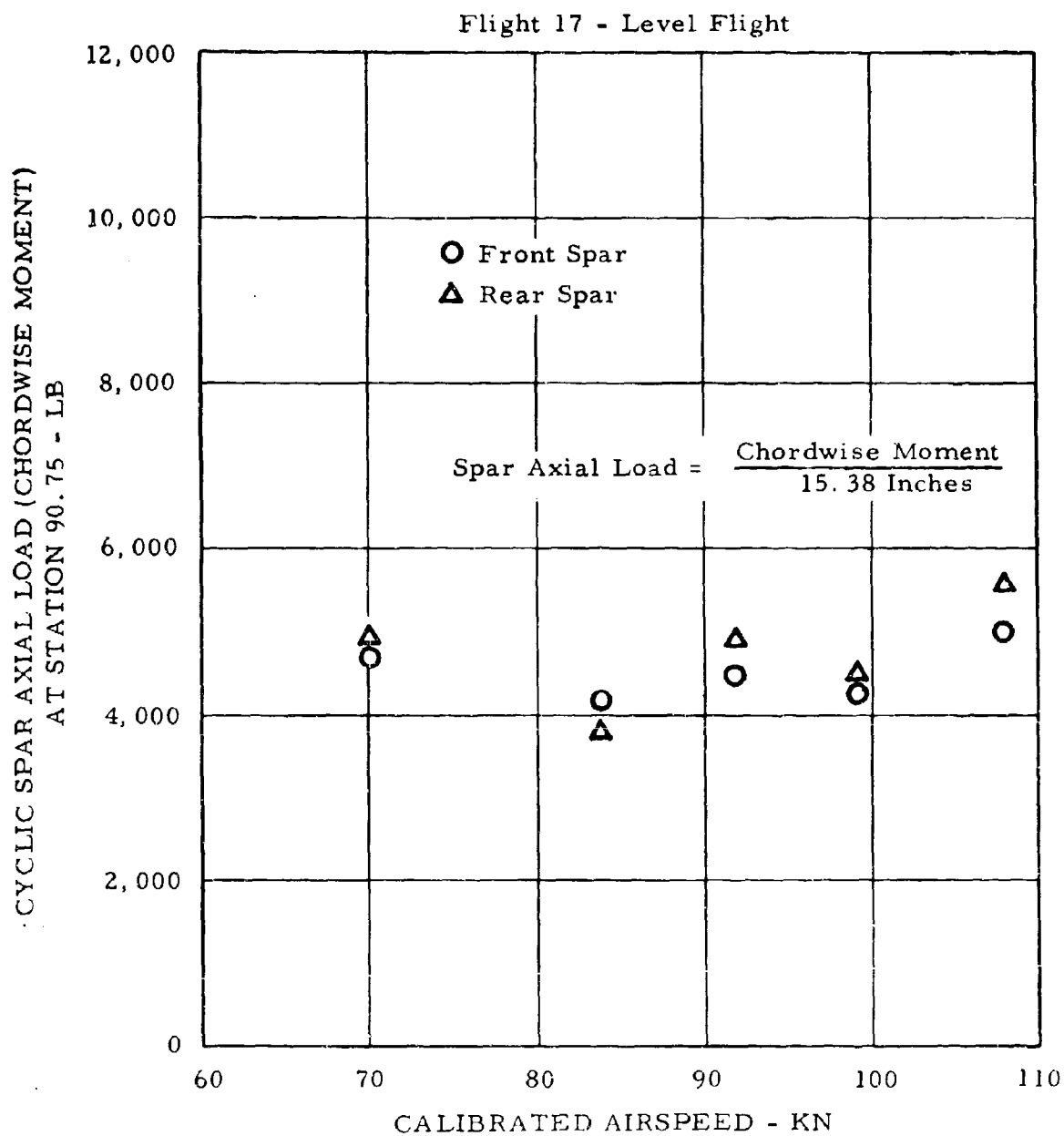


Figure 6. Cyclic Spar Axial Load (Chordwise Moment) at Station 90.75 Versus Calibrated Airspeed.

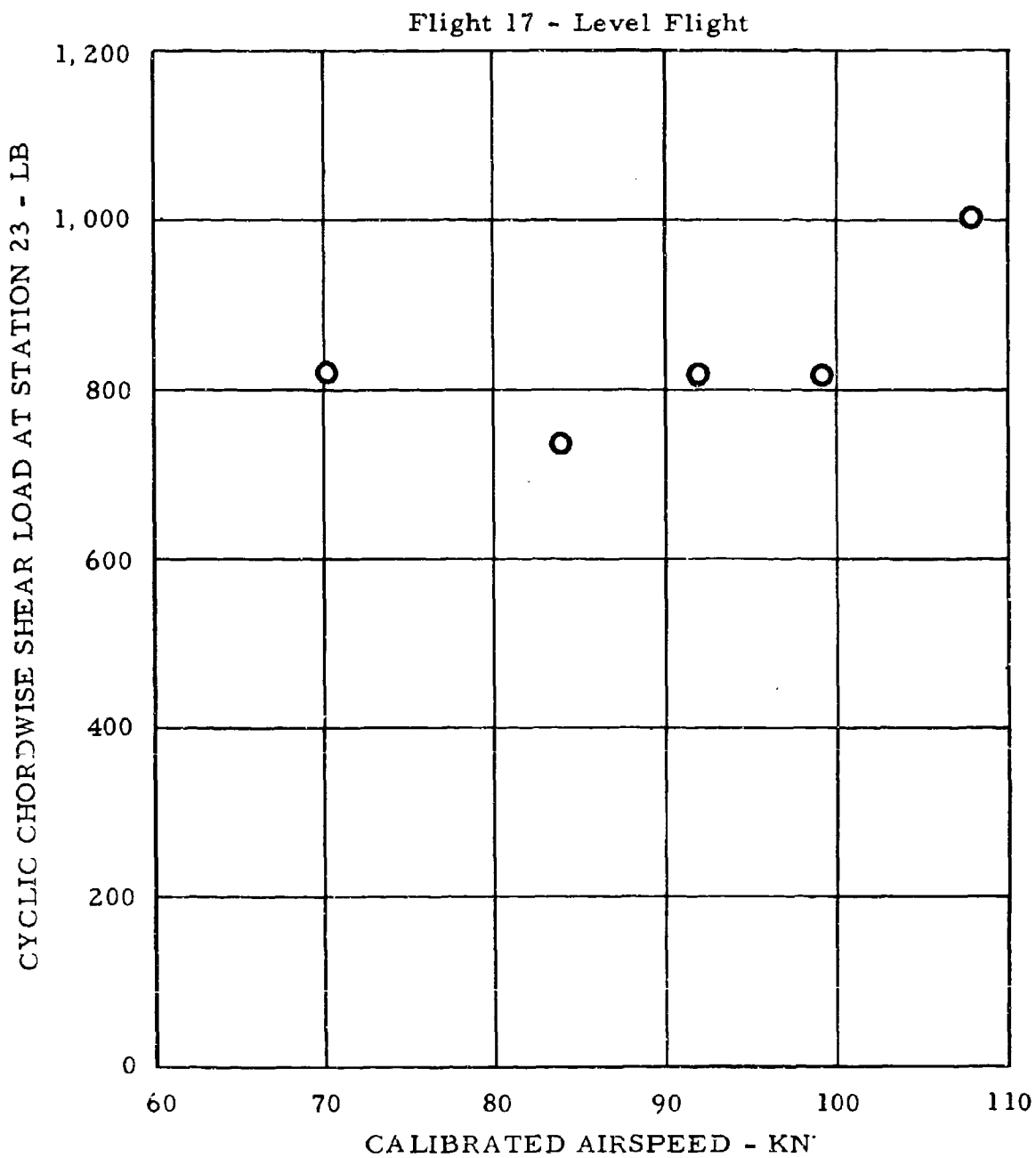


Figure 7. Cyclic Chordwise Shear Load at Station 23 Versus Calibrated Airspeed.

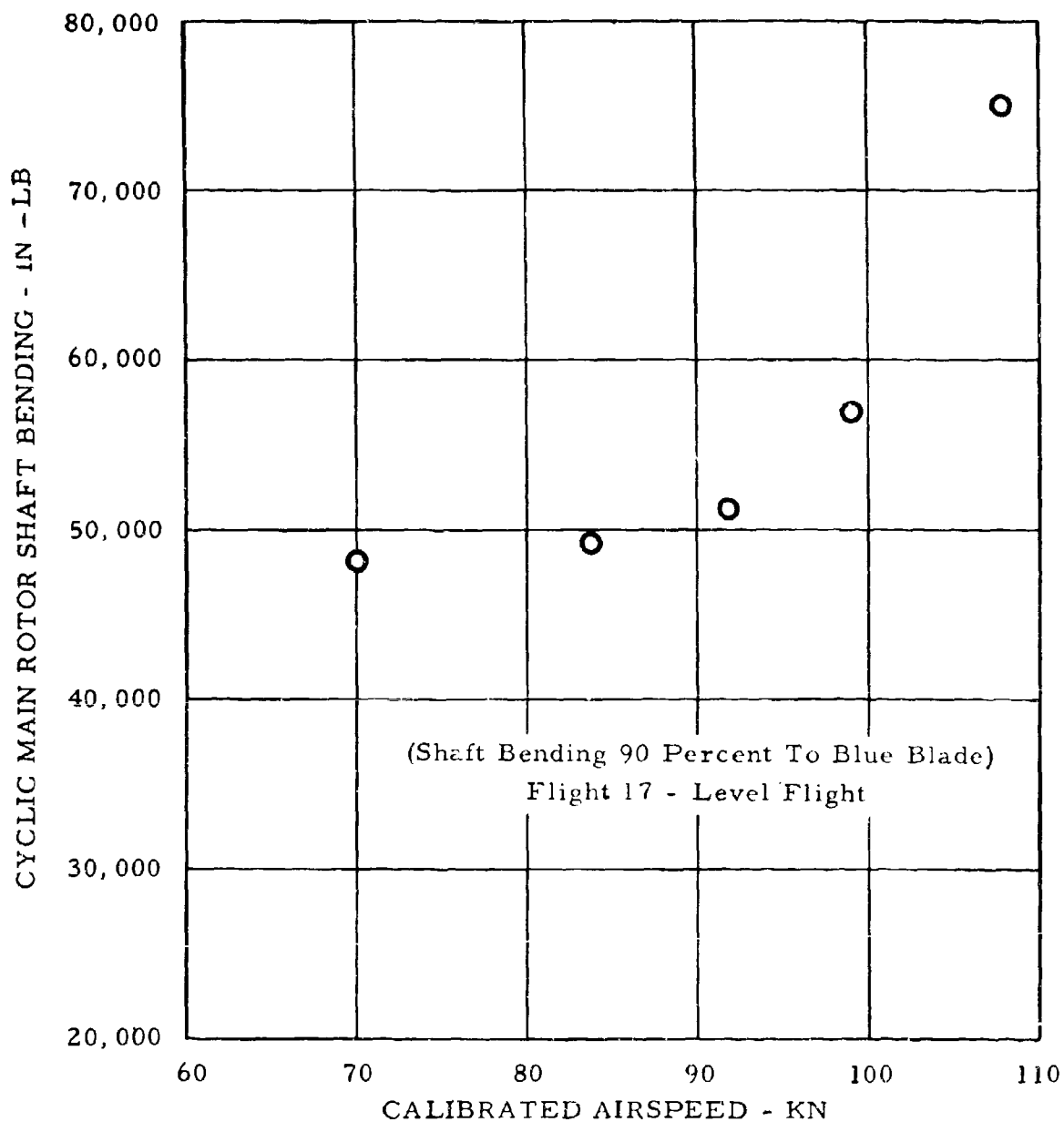


Figure 8. Cyclic Main Rotor Shaft Bending Versus Calibrated Airspeed.



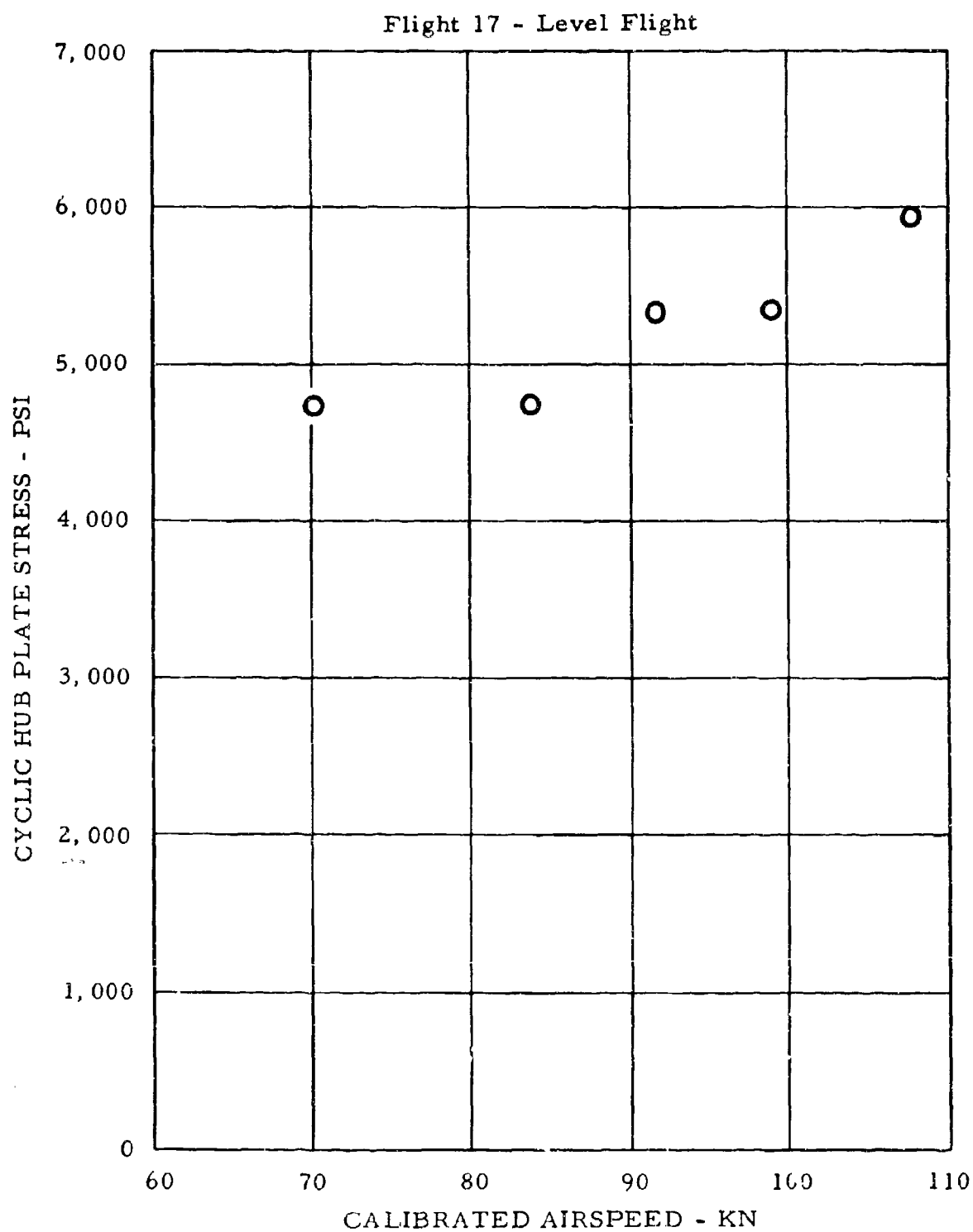


Figure 9. Cyclic Hub Plate Stress Versus Calibrated Airspeed.

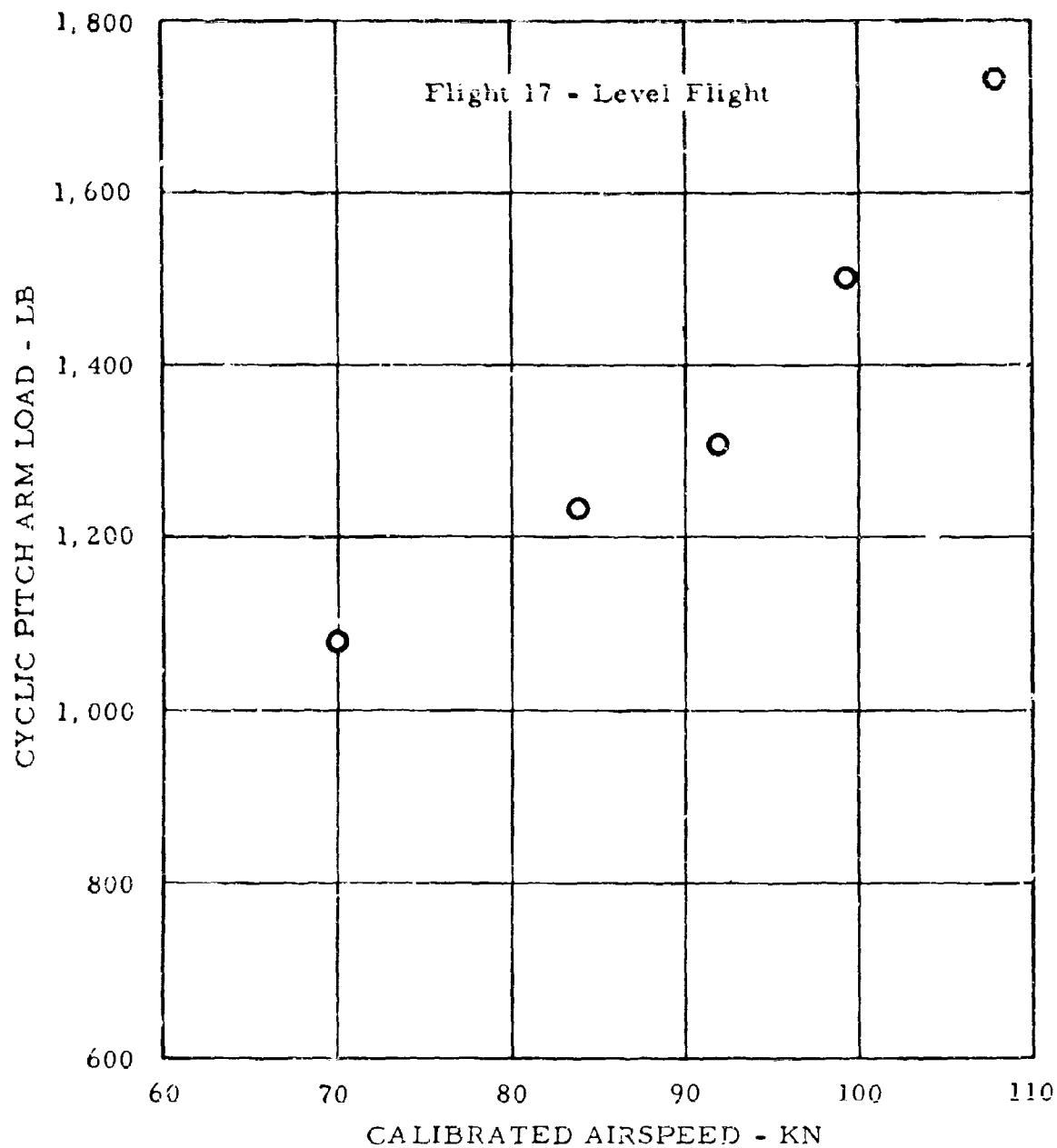


Figure 10. Cyclic Pitch Arm Load Versus Calibrated Airspeed.

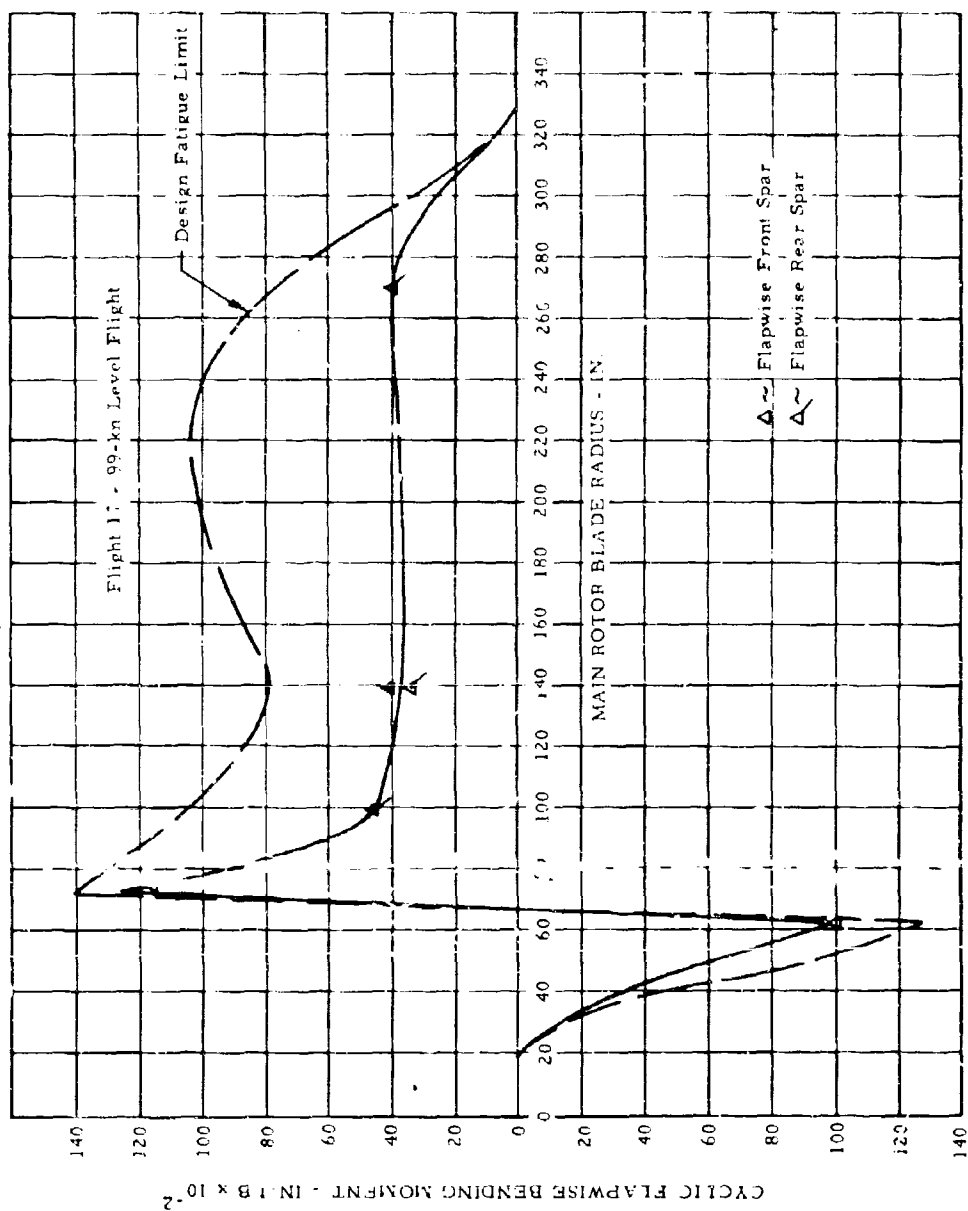


Figure 11. Cyclic Flapwise Bending Moment Versus Main Rotor Blade Radius.

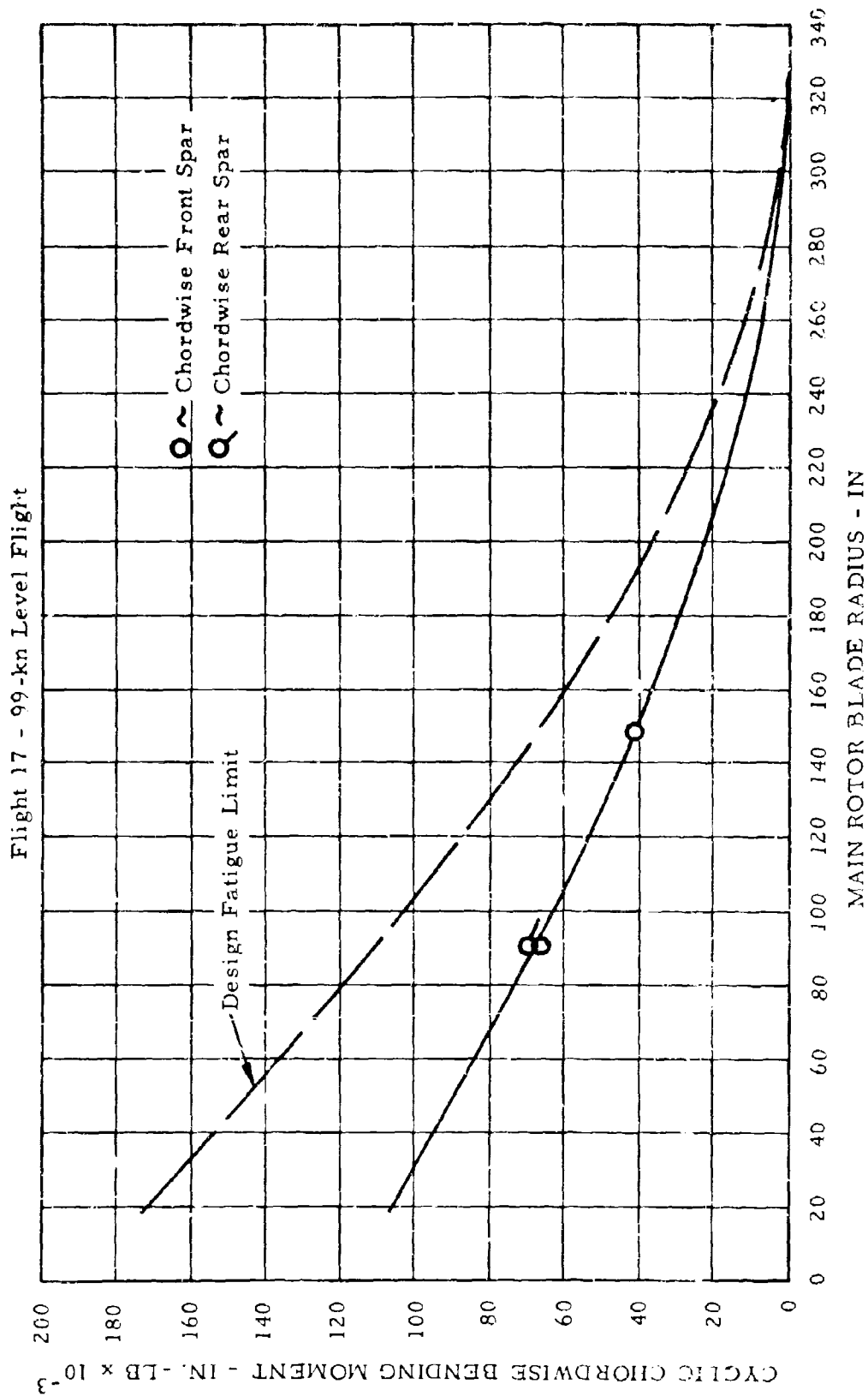


Figure 12. Cyclic Chordwise Bending Moment Versus Main Rotor Blade Radius.

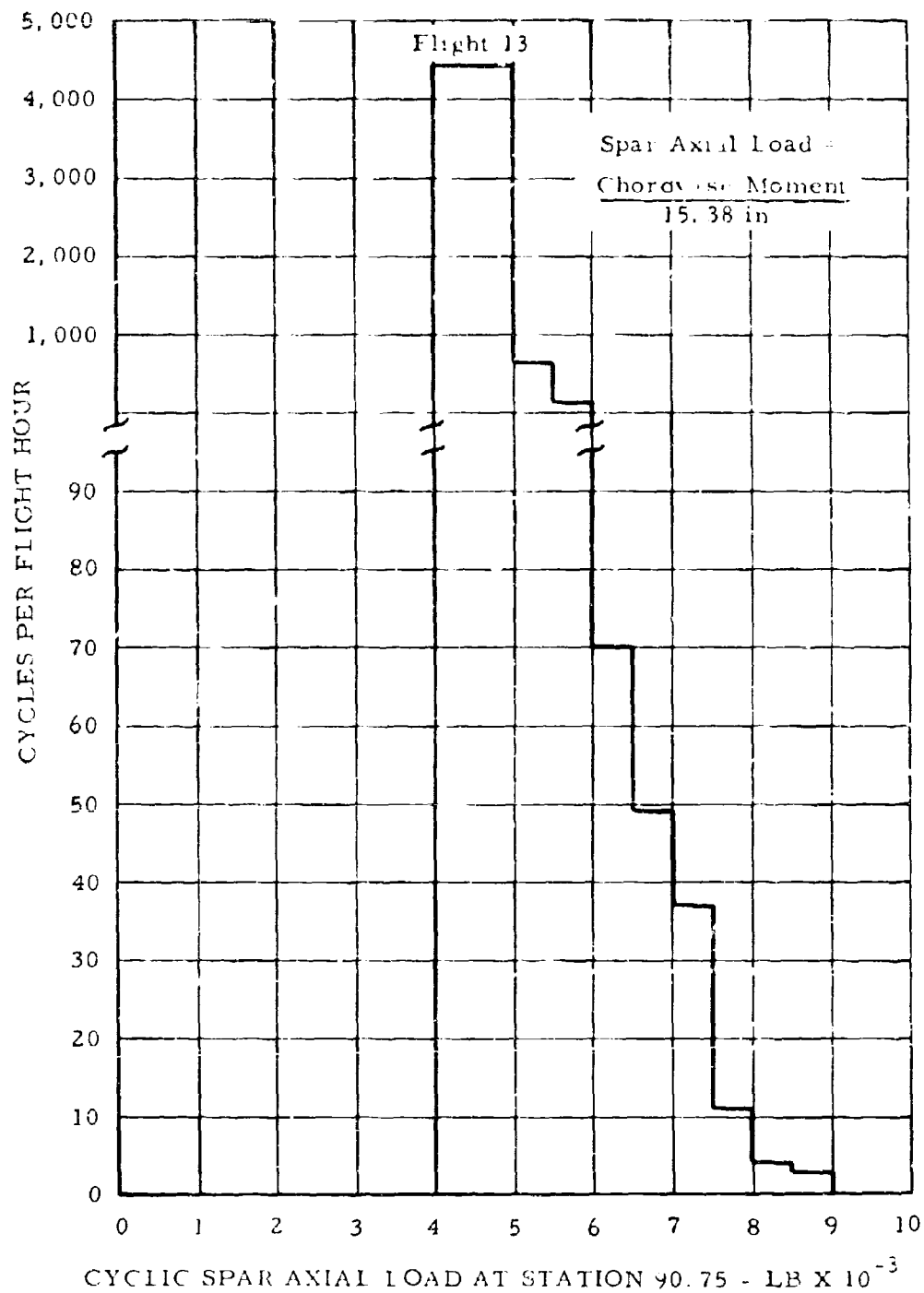


Figure 13. Cycles per Flight Hour Versus Cyclic Spar Axial Load at Station 90.75.

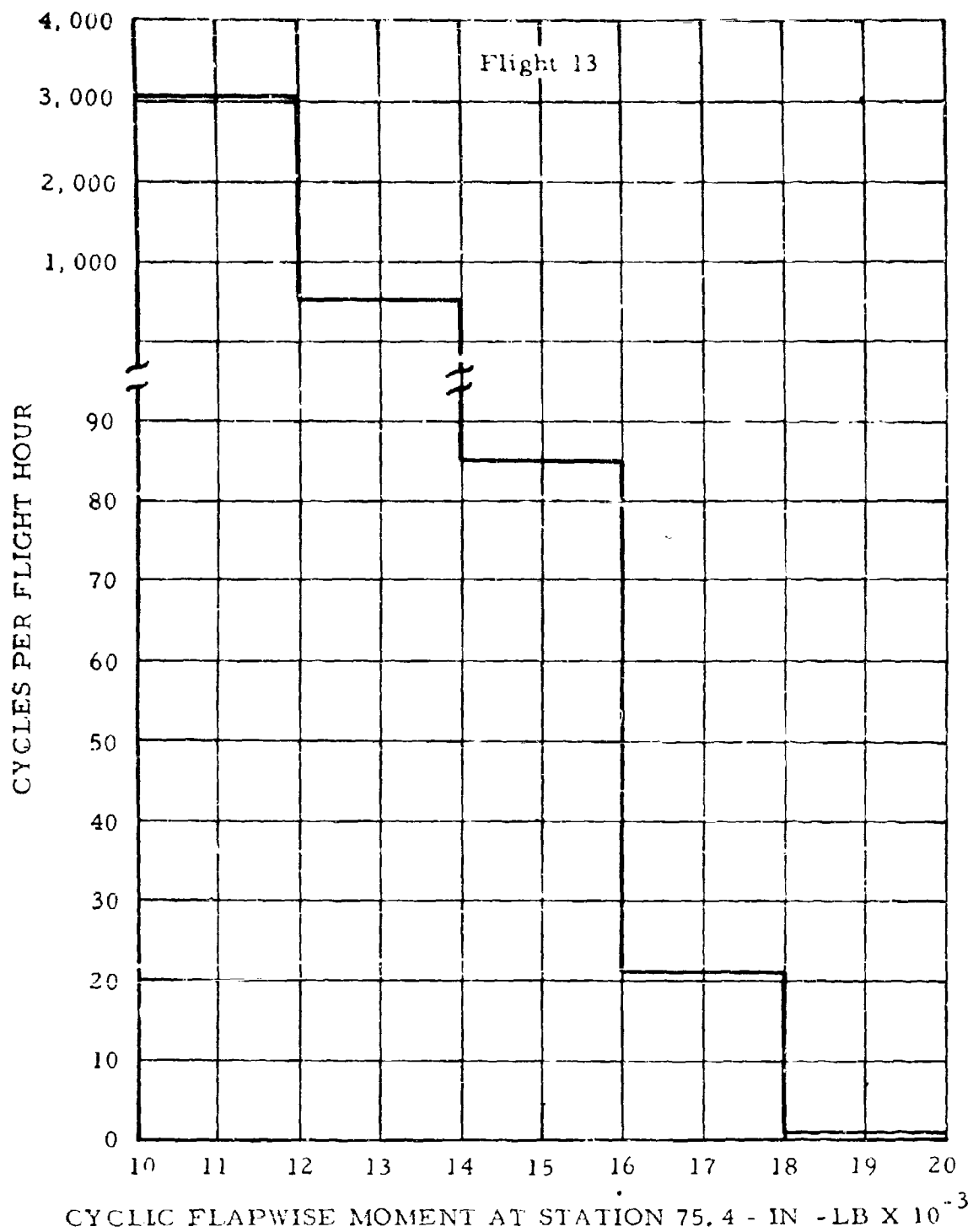


Figure 14. Cycles Per Flight Hour Versus Flapwise Blade Bending at Station 75.4.

Data from the Brown recorder were read and analyzed, and produced operating temperatures of the following rotor components and systems: (1) blade-tip gas, (2) front and rear spars, (3) flexures, (4) ribs, (5) spar cooling air, (6) outer skins, (7) gas duct walls, (8) rotor shaft, (9) tip transducer housing, (10) root cooling air, (11) rotor spokes, (12) ball joint inner surface, (13) upper and lower bearings, and (14) inboard articulate duct seals.

Figure 15 shows the location of the thermocouples along the rotor, and its accompanying tabulation summarizes the maximum temperatures recorded during the flight test program (flights 1 through 21), together with the estimated limit temperatures associated with that section of the rotor. Maximum power from the engines occurred on flight 14, and, as can be seen from the tabulation, none of the rotor temperatures recorded exceeded the estimated limit temperatures.

#### b. Powerplant and Airframe Temperatures

Temperatures of the powerplant and airframe components were recorded in a manner similar to that for the rotor temperatures, except that no hot reference junction box was used, inasmuch as a slip ring was not needed. Operating temperatures of the following powerplant and airframe components were read and analyzed from the Brown recorder: (1) engine and engine accessories, (2) engine and diverter valve bay, (3) lateral pylons and nacelles, (4) radial and thrust bearing housings, (5) aft fuselage and yaw valve compartment, (6) yaw duct and Y-duct blankets, (7) yaw duct and Y-duct bays, and (8) yaw valve outlet.

Figure 16 shows the location of the thermocouples throughout the powerplant and airframe of the XV-9A. The tabulation included in this figure summarizes the maximum temperatures recorded during the flight test program, together with the estimated limit temperature associated with that section of the airframe and powerplant. None of the temperatures recorded exceeded the estimated limit temperatures for the powerplant and airframe of the XV-9A.

### 3. Performance Tests

The total performance of a Hot Cycle helicopter can be divided into engine performance and rotor performance, with the division taking place at the gas generator exit, Station 5 of Figure 17.

In the discussion that follows, overall rotor performance is treated first, followed by fuel consumption, engine performance, and rotor system component performance.

a. Overall Rotor Performance

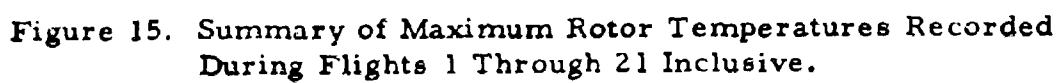
On the basis of the relationship of rotor lift to engine pressure ratio, the overall hover performance of the Hot Cycle rotor with two-position tip nozzles used in flight tests agrees very well with earlier whirl tower tests using fixed nozzles (as seen in Figure 18). The test data also show good agreement with previously predicted performance of the rotor. The capability of the rotor to convert engine discharge pressure into rotor lift is directly dependent upon rotor parameters such as blade duct pressure loss, tip cascade area and performance, and external blade aerodynamics, but is virtually independent of engine parameters such as compressor bleed and exhaust gas temperature. The data of Figure 18 are plotted without any corrections other than instrument calibrations. The excellent agreement between the test data and the predicted line confirms the overall validity of the performance predictions made for the Hot Cycle rotor system. Exact definition of the rotor system component performance values and effective cascade area has not been entirely achieved to date, and there is reason to believe that certain components are not operating precisely as assumed in the rotor performance calculations. This matter will be discussed further in succeeding paragraphs; however, it is important to recognize that the overall rotor system does produce lift in nearly exact agreement with predictions, including agreement of the predicted maximum lift.

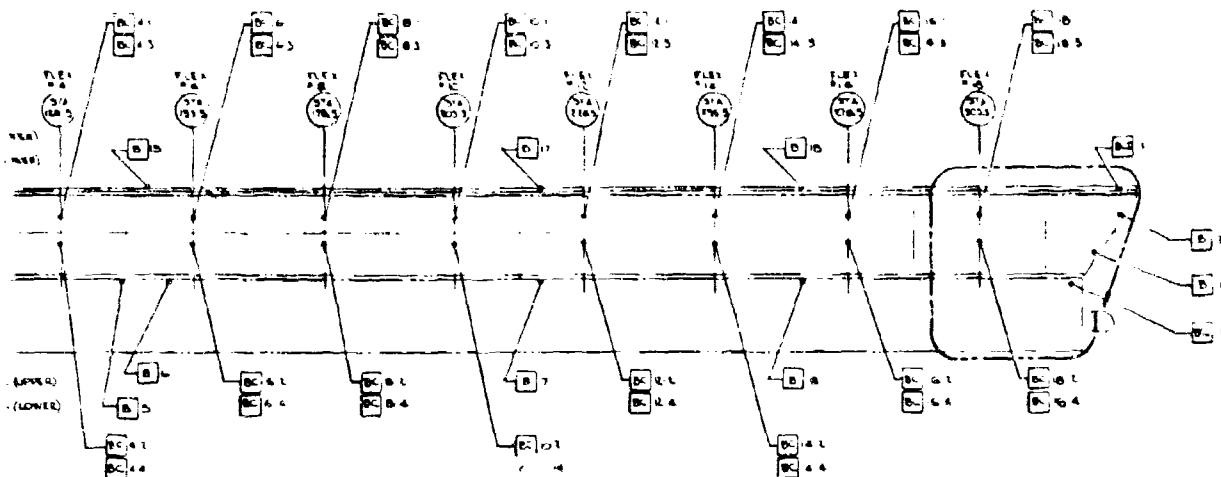
b. Fuel Consumption

Fuel consumption characteristics of the XV-9A are presented in Figure 19, corrected for engine operating conditions consistent with original performance predictions. Appendix IV presents the actual measured data on fuel flow, together with a discussion of corrections.

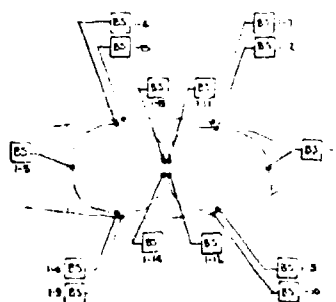
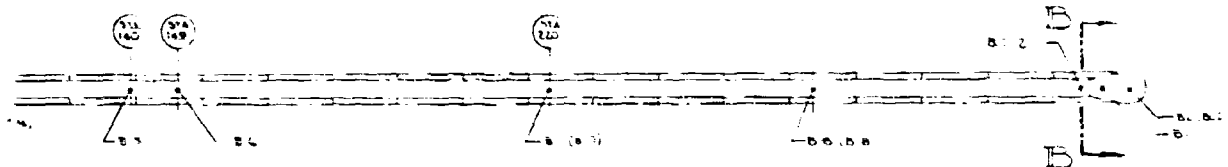
As corrected, both flight and whirl test fuel flows are in excellent agreement with predictions at low rotor lift and tend to be 8 or 10 percent higher than predicted at high lift. This discrepancy is presumed to be the result of component performance irregularities. Since the various detail performance factors have a different relationship for fuel flow as compared with rotor lift, it is possible



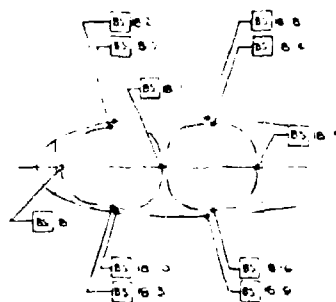




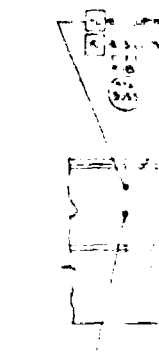
PLAN VIEW OF BLUE BLADE



SECTION A-A  
SEGMENT 1



SECTION B-B  
SEGMENT 2



VIEW C  
END OF LEG  
BLADE AT 2.0



VIEW D  
END OF LEG  
BLADE AT 2.0

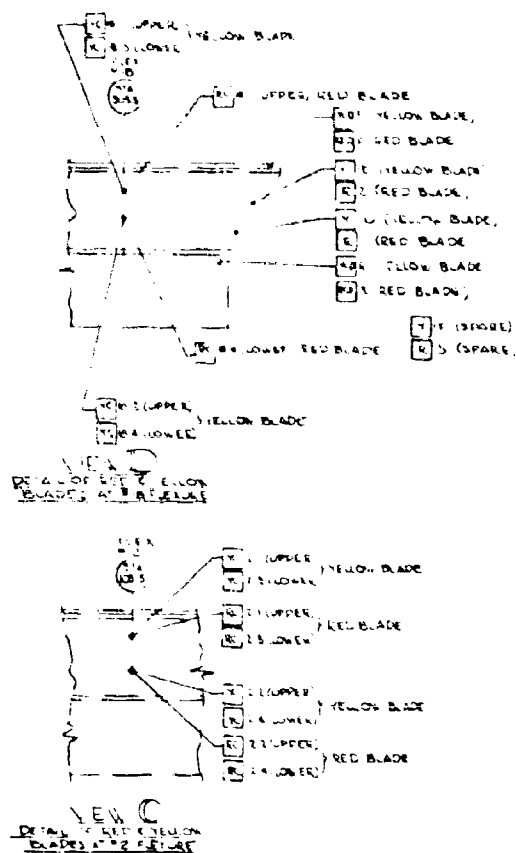
3 SET SEPARATE DATA SHEETS FOR THERMOCOUPLE LISTINGS & RECORDED TEMPERATURES

4 THERMOCOUPLE SHEETS FOR BLADE & HUB (SEPARATE FOR 1) ONLY SEE SHEET FOR OTHER THERMOCOUPLES

5 UNLESS OTHERWISE SPECIFIED, THE LETTER "A" DENOTES BLADE

NOTE

atures Recorded  
ve.



# Thermocouple

Number	Location
BC 2-1	Station 103.5 Flexure 2 Upper
BC 2-2	Station 103.5 Flexure 2 Upper
BC 2-3	Station 103.5 Flexure 2 Lower
BC 2-4	Station 103.5 Flexure 2 Lower
BC 4-1	Station 128.5 Flexure 4 Upper
BC 4-2	Station 128.5 Flexure 4 Upper
BC 4-3	Station 128.5 Flexure 4 Lower
BC 4-4	Station 128.5 Flexure 4 Lower
BC 6-1	Station 153.5 Flexure 6 Upper
BC 6-2	Station 153.5 Flexure 6 Upper
BC 6-4	Station 153.5 Flexure 6 Lower
BC 8-1	Station 178.5 Flexure 8 Upper
BC 8-2	Station 178.5 Flexure 8 Upper
BC 8-3	Station 178.5 Flexure 8 Lower
BC 8-4	Station 178.5 Flexure 8 Lower
BC 10-1	Station 203.5 Flexure 10 Upper
BC 10-2	Station 203.5 Flexure 10 Upper
BC 10-3	Station 203.5 Flexure 10 Lower
BC 10-4	Station 203.5 Flexure 10 Lower
BC 12-4	Station 228.5 Flexure 12 Lower
BC 14-1	Station 253.5 Flexure 14 Upper
BC 14-3	Station 253.5 Flexure 14 Lower
BC 14-4	Station 253.5 Flexure 14 Lower
BC 16-3	Station 278.5 Flexure 16 Lower
BC 16-4	Station 278.5 Flexure 16 Lower
BC 18-1	Station 303.5 Flexure 18 Upper
BC 18-2	Station 303.5 Flexure 18 Upper
BC 18-3	Station 303.5 Flexure 18 Lower
BC 18-4	Station 303.5 Flexure 18 Lower
BS 1-8	Station 97 Blade Skin Upper Aft
BS 1-9	Station 97 Blade Skin Lower Aft
BS 1-10	Station 97 Blade Skin Lower Fwd
BS 18-7	Station 310 Blade Skin Upper Fwd
BS 18-8	Station 310 Blade Skin Upper Aft
BS 18-9	Station 310 Blade Skin Lower Aft
BS 18-10	Station 310 Blade Skin Lower Fwd
BS 1-1	Station 96 Fwd Duct Fwd Wall
BS 1-4	Station 96 Aft Duct Upper Wall
BS 1-5	Station 96 Aft Duct Aft Wall
BS 18-1	Station 309 Fwd Duct Fwd Wall
BS 18-2	Station 309 Fwd Duct Upper Wall
BS 18-4	Station 309 Aft Duct Upper Wall
BS 1-11	Station 96 Fwd Duct Aft Wall
BS 1-12	Station 96 Fwd Duct Aft Wall
BS 1-13	Station 96 Aft Duct Fwd Wall
BS 1-14	Station 96 Aft Duct Fwd Wall
BS 18-5	Station 309 Aft Duct Aft Wall
BS 18-6	Station 309 Aft Duct Lower Wall
BS 18-11	Station 309 Fwd Duct Aft Wall
BS-1	Blue Blade Aft Duct Gas

Location	Maximum Temperature Recorded	Estimated Limit Temperature	Thermocouple Number	Location
Station 103.5 Flexure 2 Upper Fwd	482	600	B-2	Blue Blade Fwd Duct
Station 103.5 Flexure 2 Upper Aft	510		BCDR	Station 321 Cooling
Station 103.5 Flexure 2 Lower Fwd	530		BCDF	Station 330 Cooling
Station 103.5 Flexure 2 Lower Aft	480		B 57	Station 57 Cooling
Station 128.5 Flexure 4 Upper Fwd	125		B1A	Station 63 Aft Spar
Station 128.5 Flexure 4 Upper Aft	320		B2A	Station 63 Aft Spar
Station 128.5 Flexure 4 Lower Fwd	515		B1B	Station 75.4 Aft Spar
Station 128.5 Flexure 4 Lower Aft	530		B2B	Station 75.4 Aft Spar
Station 153.5 Flexure 6 Upper Fwd	485		B3C	Station 91 Aft Spar
Station 153.5 Flexure 6 Upper Aft	537		B 4	Station 100 Aft Spar
Station 153.5 Flexure 6 Lower Aft	575		B 5	Station 140 Aft Spar
Station 178.5 Flexure 8 Upper Fwd	520		B 7	Station 220 Aft Spar
Station 178.5 Flexure 8 Upper Aft	526		B 8	Station 270 Aft Spar
Station 178.5 Flexure 8 Lower Fwd	463		B 12A	Station 75.4 Aft Spar
Station 178.5 Flexure 3 Lower Aft	500		B 13	Station 91 Aft Spar
Station 203.5 Flexure 10 Upper Fwd	533		B 14	Station 100 Aft Spar
Station 203.5 Flexure 10 Upper Aft	445		B 15	Station 145 Aft Spar
Station 203.5 Flexure 10 Lower Fwd	201		B 17	Station 220 Aft Spar
Station 203.5 Flexure 10 Lower Aft	295		B 18	Station 270 Aft Spar
Station 228.5 Flexure 12 Lower Aft	510		BR-1	Station 45 Flexure
Station 253.5 Flexure 14 Upper Fwd	280		BR-2	Station 63 Inner Surface
Station 253.5 Flexure 14 Lower Fwd	640		BR-3	Station 73 Inner Surface
Station 253.5 Flexure 14 Lower Aft	485		BBJ-1	Station 19 Inner Surface
Station 278.5 Flexure 16 Lower Fwd	322		YC 2-1	Station 103.5 Flexure
Station 278.5 Flexure 16 Lower Aft	358		YC 2-2	Station 103.5 Flexure
Station 303.5 Flexure 18 Upper Fwd	419		YC 2-3	Station 103.5 Flexure
Station 303.5 Flexure 18 Upper Aft	391		YC 2-4	Station 103.5 Flexure
Station 303.5 Flexure 18 Lower Fwd	410		YC 18-1	Station 303.5 Flexure
Station 303.5 Flexure 18 Lower Aft	450		YC 18-2	Station 303.5 Flexure
Station 97 Blade Skin Upper Aft	292		YC 18-3	Station 303.5 Flexure
Station 97 Blade Skin Lower Aft	248		RC 2-1	Station 103.5 Flexure
Station 97 Blade Skin Lower Fwd	225		RC 2-2	Station 103.5 Flexure
Station 310 Blade Skin Upper Fwd	241		RC 2-3	Station 103.5 Flexure
Station 310 Blade Skin Upper Aft	185		RC 2-4	Station 103.5 Flexure
Station 310 Blade Skin Lower Aft	500		RC 18-1	Station 303.5 Flexure
Station 310 Blade Skin Lower Fwd	473	600	Y 57	Yellow Blade Sta 57
Station 96 Fwd Duct Fwd Wall	615	1000	Y 73	Yellow Blade Sta 85
Station 96 Aft Duct Upper Wall	690	1000	YCDR	Yellow Blade Sta 321
Station 96 Aft Duct Aft Wall	550	1000	YCDF	Yellow Blade Sta 330
Station 309 Fwd Duct Fwd Wall	850	950	R 57	Red Blade Sta 57 Cooling
Station 309 Fwd Duct Upper Wall	851	950	R 73	Red Blade Sta 85 Cooling
Station 309 Aft Duct Upper Wall	885	950	RCDF	Red Blade Sta 330 Spoke
Station 96 Fwd Duct Aft Wall	905	1150	RCDR	Red Blade Sta 321 Spoke
Station 96 Aft Duct Fwd Wall	910		HUB 2	Shaft 1 In. Below Seal
Station 96 Aft Duct Fwd Wall	600		HUB 3	Shaft Below Spoke
Station 96 Aft Duct Fwd Wall	905		HUB 5	Spoke Centerline
Station 309 Aft Duct Aft Wall	910		HUB 6	Spoke Halfway to Bearing
Station 309 Aft Duct Lower Wall	885		HUB 7	Spoke Over Upper Bearing
Station 309 Fwd Duct Aft Wall	862		YC 18-4	Sta 303.5 Flexure 18
Blue Blade Aft Duct Gas	1042	1150		

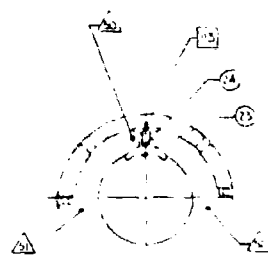
Temperature in degrees Fahrenheit.

D

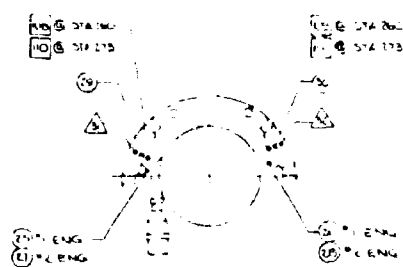
Thermocouple Number	Location	Maximum Temperature Recorded	Estimated Limit Temperature
1	Blue Blade Fwd Duct Gas	1038	1150
DR	Station 321 Cooling Air Aft Spar	183	250
DF	Station 330 Cooling Air Fwd Spar	195	250
57	Station 57 Cooling Air Hub and Blade	170	250
A	Station 63 Aft Spar Upper	97	350
A	Station 63 Aft Spar Lower	101	
3	Station 75.4 Aft Spar Lower	99	
3	Station 75.4 Aft Spar Upper	165	
3	Station 91 Aft Spar Center	105	
	Station 100 Aft Spar Center	150	
	Station 140 Aft Spar Center	164	
	Station 220 Aft Spar Center	213	
	Station 270 Aft Spar Center	215	
2A	Station 75.4 Aft Spar Upper	135	
3	Station 91 Aft Spar Center	134	
4	Station 100 Aft Spar Center	130	
5	Station 145 Aft Spar Center	179	
7	Station 220 Aft Spar Center	180	
8	Station 270 Aft Spar Center	227	350
-1	Station 45 Flexure Bottom	130	300
-2	Station 63 Inner Surface Rib	170	300
-3	Station 73 Inner Surface Rib	145	300
1-1	Station 19 Inner Surface Tube	260	300
2-1	Station 103.5 Flexure 2 Upper Fwd	465	600
2-2	Station 103.5 Flexure 2 Upper Aft	506	
2-3	Station 103.5 Flexure 2 Lower Fwd	278	
2-4	Station 103.5 Flexure 2 Lower Aft	153	
18-1	Station 303.5 Flexure 18 Upper Fwd	352	
18-2	Station 303.5 Flexure 18 Upper Aft	335	
18-3	Station 303.5 Flexure 18 Lower Fwd	385	
2-1	Station 103.5 Flexure 2 Upper Fwd	440	
2-2	Station 103.5 Flexure 2 Upper Aft	415	
2-3	Station 103.5 Flexure 2 Lower Fwd	470	
2-4	Station 103.5 Flexure 2 Lower Aft	448	
18-1	Station 303.5 Flexure 18 Upper Fwd	361	600
7	Yellow Blade Sta 57 Cooling Air	143	250
	Yellow Blade Sta 85 Cooling Air	155	
DR	Yellow Blade Sta 321 Spar Cooling Air	173	
DF	Yellow Blade Sta 330 Spar Cooling Air	169	
7	Red Blade Sta 57 Cooling Air	165	
	Red Blade Sta 85 Cooling Air	226	
DF	Red Blade Sta 330 Spar Cooling Air	178	
DR	Red Blade Sta 321 Spar Cooling Air	178	250
2	Shaft 1 In. Below Seal	168	500
3	Shaft Below Spoke	201	500
5	Spoke Centerline	131	400
6	Spoke Halfway to Bearing	188	600
7	Spoke Over Upper Bearing	160	400
18-4	Sta 303.5 Flexure 18 Lower Aft	322	600

E

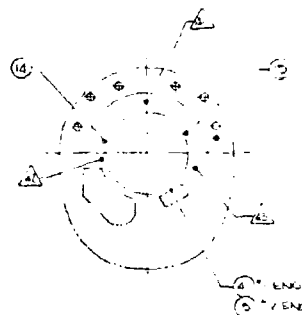




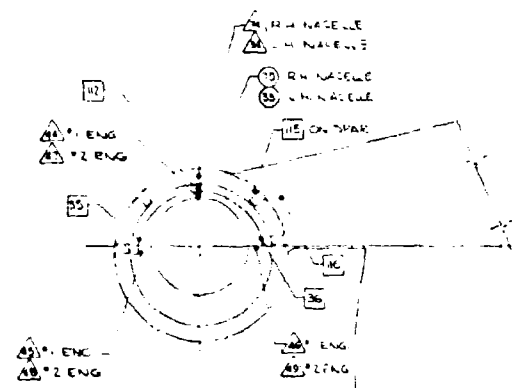
SECTION B-B  
DIA 450 (REF)



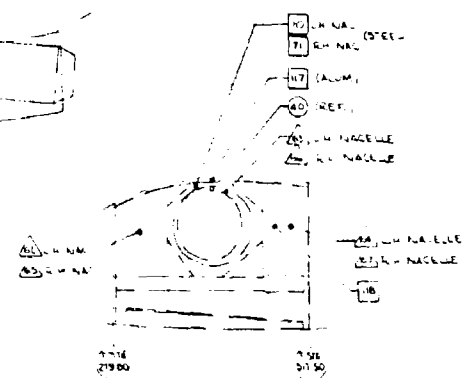
SECTION C-C  
DIA 250 (REF)



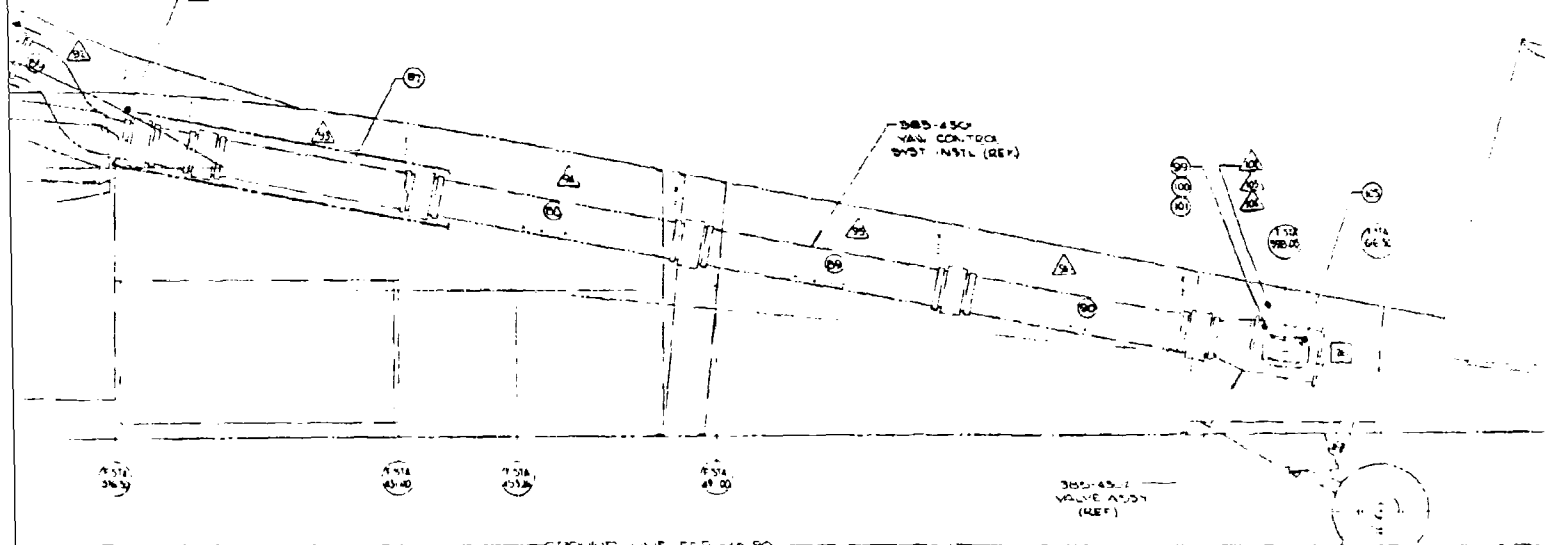
SECTION A-A



SECTION D-D  
FRONT SPAR APPROX



SECTION E-E  
BL 22 (REF)



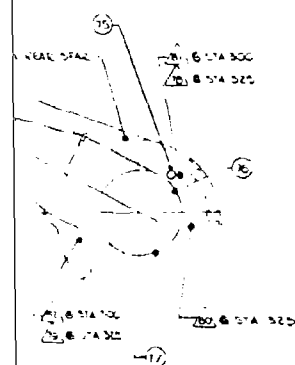
GROUND LINE FEB 48 90





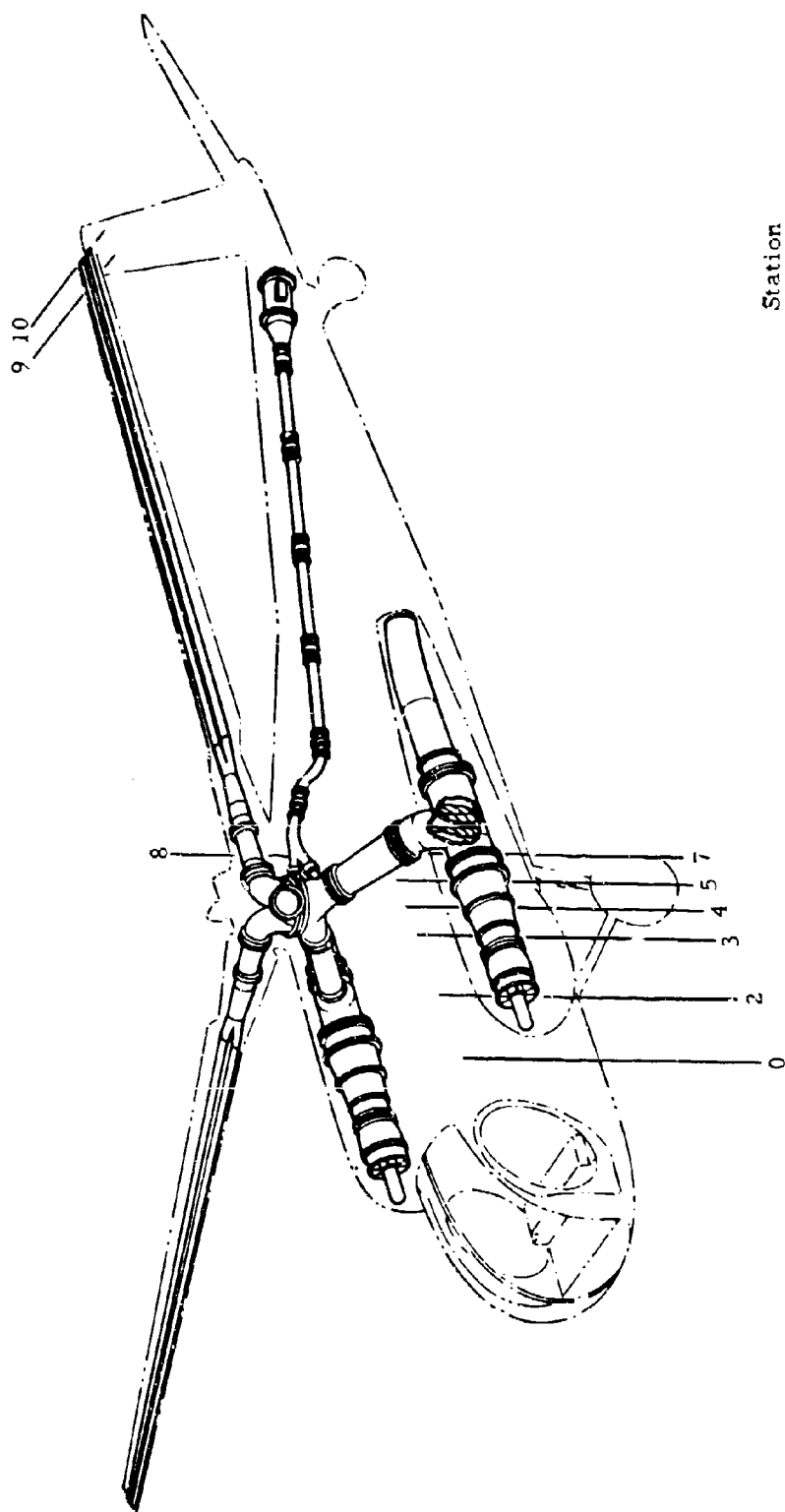
Thermocouple Number	Type	Location	Maximum Temperature Recorded	Estimated Limit Temperature	Thermocouple Number
1	Case	Generator Engine 1	219	220	70
2		Generator Engine 2	210	220	71
3		Fuel Control Engine 1	124	220	72
4		Ignition Box Engine 1	210	250	73
5		Ignition Box Engine 2	232	250	74
6		Stator Vane Actuator Engine 1 LH	265	250	75
7		Stator Vane Actuator Engine 1 RH	198	250	76
8		Fuel Nozzle Inlet - Top Engine 1	633	800	77
9		Hydraulic Pump Engine 1	172	275	78
10		Engine Oil Pump Engine 1	189	300	80
11		Engine Oil Pump Engine 2	150	300	81
12		Accessory Drive Gearbox Engine 1	158	250	82
13		Front Frame Engine 1	100	200	83
14		Engine Compressor Engine 1 LH	632	800	84
15		Engine Compressor Engine 1 RH	644	800	85
16		Engine Combustor	685	850	86
18		Engine Turbine	977	1150	87
20		Engine Exhaust Frame	923	1100	88
22		Engine Exhaust Clamp	732	1100	89
23		Aft Engine Mount Flange	457	800	90
24		Aft Engine Mount Brace	397	800	91
25		Wire Temp Engine 1 Tunnel LH	351	500	92
26		Wire Temp Engine 1 Tunnel RH	325	500	93
27		Wire Temp Engine 2 Tunnel LH	374	500	94
28		Wire Temp Engine 2 Tunnel RH	345	500	95
29		Insulation Blanket Sta 260 Tunnel RH	302	400	96
30	Case	Insulation Blanket Sta 260 Tunnel LH	327	400	97
31	Air	Engine 1 Tunnel LH	207	300	98
32	Air	Engine 1 Tunnel RH	248	300	99
33	Case	Crossover Shroud Engine 1 Insulation	342	350	100
34	Air	Crossover Shroud Engine 1 Insulation	306	350	101
35	Struct	Crossover Shroud Engine 1 LH	383	700	102
36	Struct	Crossover Shroud Engine 1 RH	653	700	103
37		Canted Rib (Lower) Engine 1 Nacelle	312	400	104
38	Comp	High Pressure Fuel Line Engine 1	111	150	105
39	Case	Generator Case (Bottom) Engine 2	235	220	107
40	Case	Diverter Valve Transition Duct Eng 1	342	400	108
41	Air	LH Nacelle Sta 220 Top	205	250	109
42		LH Nacelle Sta 220 LH	142	250	110
43		LH Nacelle Sta 220 RH	129	250	111
44		LH Nacelle Sta 275 Top	359	475	112
45		LH Nacelle Sta 275 LH	352	475	113
46	Air	LH Nacelle Sta 275 RH	471	475	114
47	Comp	High Pressure Fuel Line Engine	124	150	115
48	Struct	Aluminum Skin Over Canted Rib RH	172	250	116
49	Struct	Aluminum Skin Over B/L 22 RH	176	250	117
50	Air	LH Nacelle Sta 245 Top	378	400	118
51		LH Nacelle Sta 245 LH	298	400	119
52		LH Nacelle Sta 245 RH	295	400	120
53		LH Nacelle Sta 300 Top	351	400	121
55		LH Nacelle Sta 300 RH	342	400	122
56		LH Nacelle Sta 325 Top (Approx)	338	400	123
59		LH Nacelle Sta 344 Top (Approx)	342	450	124
60		LH Nacelle Sta 344 90° (Approx)	334	450	125
61		LH Nacelle Sta 344 120° (Approx)	363	450	127
62		Lateral Pylon LH Nacelle Fwd	217	350	128
63		Lateral Pylon LH Nacelle Center	334	350	130
64		Lateral Pylon LH Nacelle Aft	231	350	131
65		Lateral Pylon RH Nacelle Fwd	268	350	132
66		Lateral Pylon RH Nacelle Center	268	350	134
67	Air	Lateral Pylon RH Nacelle Aft	241	350	135
68	Struct	LH Nacelle Canted Rib Web	203	300	136
69	Struct	RH Nacelle Canted Rib Web	219	300	138
					141

NOTE: Temperature in degrees Fahrenheit.



Q. WITHIN THE GEOMETRIC FORMS  
A. INDICATE THE THERMOCOUPLE  
ID. IN TABLE  
P. IS AN AIR THERMOCOUPLE,  
S. IS A STRUCTURE THERMOCOUPLE,  
C. IS A CASE THERMOCOUPLE.

	Maximum Temperature Recorded	Estimated Limit Temperature	Thermocouple Number	Type	Location	Maximum Temperature Recorded	Estimated Limit Temperature
	219	220	70	Struct	LH Nacelle - Bl 22 Top Flange	225	350
	210	220	71	Struct	RH Nacelle - Bl 22 Top Flange	259	350
	124	220	72	Case	Y Duct Flange - Yaw Control	766	900
	210	250	73	Case	Crossover Shroud Engine 2 Insul	349	350
	232	250	74	Air	Crossover Shroud Engine 2	349	350
1 LH	205	250	75	Case	Diverter Valve Actuator Engine 2	205	275
1 RH	198	250	76	Case	Nacelle Skin at 90° RH Sta 300	243	400
Line 1	633	800	77	Case	Generator Case (Bottom) Engine 2	217	200
	112	275	78	Air	RH Nacelle Sta 325 Top	354	400
	189	300	80		RH Nacelle Sta 325 RH	289	400
Engine 1	180	300	81		RH Nacelle Sta 300 Top	351	400
	158	250	82	Air	RH Nacelle Sta 300 LH	347	400
	100	200	83	Struct	Alum Skin at Canted Rib Attach	201	250
1 LH	633	800	84	Case	Accessory Gearbox	174	250
1 RH	644	800	85		Insulation Blanket Yaw Duct	82	450
	685	850	86		Insulation Blanket Yaw Duct	476	450
	977	1150	87		Insulation Blanket Yaw Duct	400	450
	923	1100	88		Insulation Blanket Yaw Duct	388	450
	732	1100	89		Insulation Blanket Yaw Duct	392	450
	457	800	90	Case	Insulation Blanket Yaw Duct	183	450
	397	800	91	Air	Aft Fuselage	262	300
LH	351	500	92		Aft Fuselage	255	300
RH	325	500	93		Aft Fuselage	176	300
LH	374	500	94		Aft Fuselage	165	300
RH	385	500	95		Aft Fuselage	185	300
unnel RH	302	400	96	Air	Aft Fuselage	88	300
unnel LH	327	400	97	Case	Bellows Insulation Blanket	442	450
	207	300	98		Marmion Clamp	786	800
	248	300	99		Yaw Valve Insulation Blanket	295	500
Insulation	342	350	100		Yaw Valve Insulation Blanket	304	500
Insulation	306	350	101	Case	Yaw Valve Insulation Blanket	331	500
LH	383	700	102	Air	Yaw Valve Compartment	122	350
RH	653	700	103	Air	Yaw Valve Compartment	126	350
Nacelle	312	400	104	Air	Yaw Valve Compartment	140	350
Engine 1	111	150	105	Case	Yaw Valve Outlet Flange	622	900
Engine 2	205	220	107	Struct	Frame Fus Sta 376.50	214	350
uct Eng 1	342	400	108		Engine 1 Tunnel Sta 260 LH	464	700
	205	250	109		Engine 1 Tunnel Sta 260 RH	527	700
	142	250	110		Engine 1 Tunnel Sta 273 LH	426	700
	129	250	111		Engine 1 Tunnel Sta 273 RH	496	700
	369	475	112		Engine 1 Crossover Shroud G. Sta 275.11	140	700
	352	475	113		Engine 1 Aft Engine Mount	324	600
	471	475	114		Engine 1 Diagonal Tube	496	600
Engine	124	150	115		Engine 1 Front Spar at 145°	322	600
Rib RH	172	250	116		LH Nacelle Outbd On Al Spar Web	248	250
RH	176	250	117		Aluminum Skin on Lateral Pylon	187	250
	378	400	118		B L 22.00 Bulkhead	190	250
	298	400	119		Canted Rib Cap	550	550
	295	400	120		Upper Pylon Tube	122	500
	351	400	121		Diverter Valve Mounting Link	397	500
	342	400	122		LH Nacelle Sta 300 Top (Approx)	302	400
rox)	338	400	123		LH Nacelle Sta 300 at 45°	241	400
rox)	342	450	124		LH Nacelle Sta 300 at 90°	273	400
rox)	334	450	125	Struct	LH Nacelle Sta 300 at 120° (Approx)	293	400
prox)	363	450	127	Case	Stationary Swashplate Bearing	97	175
wd	217	350	128	Case	Crossflow Indicator	93	400
enter	334	350	130	Air	Y-Duct Bay	225	250
it	201	350	131	Air	Y-Duct Bay	86	250
ed	268	350	132	Air	Y-Duct Bay	243	250
enter	268	350	134	Case	Y-Duct Insulation Blanket	403	450
it	241	350	135	Case	Y-Duct Insulation Blanket	356	450
	203	300	136	Case	Y-Duct Insulation Blanket	428	450
	219	300	138		Oil in No. 2 Cooler	187	275
			141		Oil in No. 1 Cooler	171	275
				Case	Lower Bearing Case	147	212
				Case	Upper Bearing Case	189	212



Station	
0	Ambient
2	Compressor Inlet
3	Compressor Discharge
4	Turbine Inlet
5	Turbine Discharge
7	Engine Exhaust
8	Blade Root
9	Blade Tip Cascade Inlet
10	Cascade Exit

Figure 17. Propulsion System Station Locations.

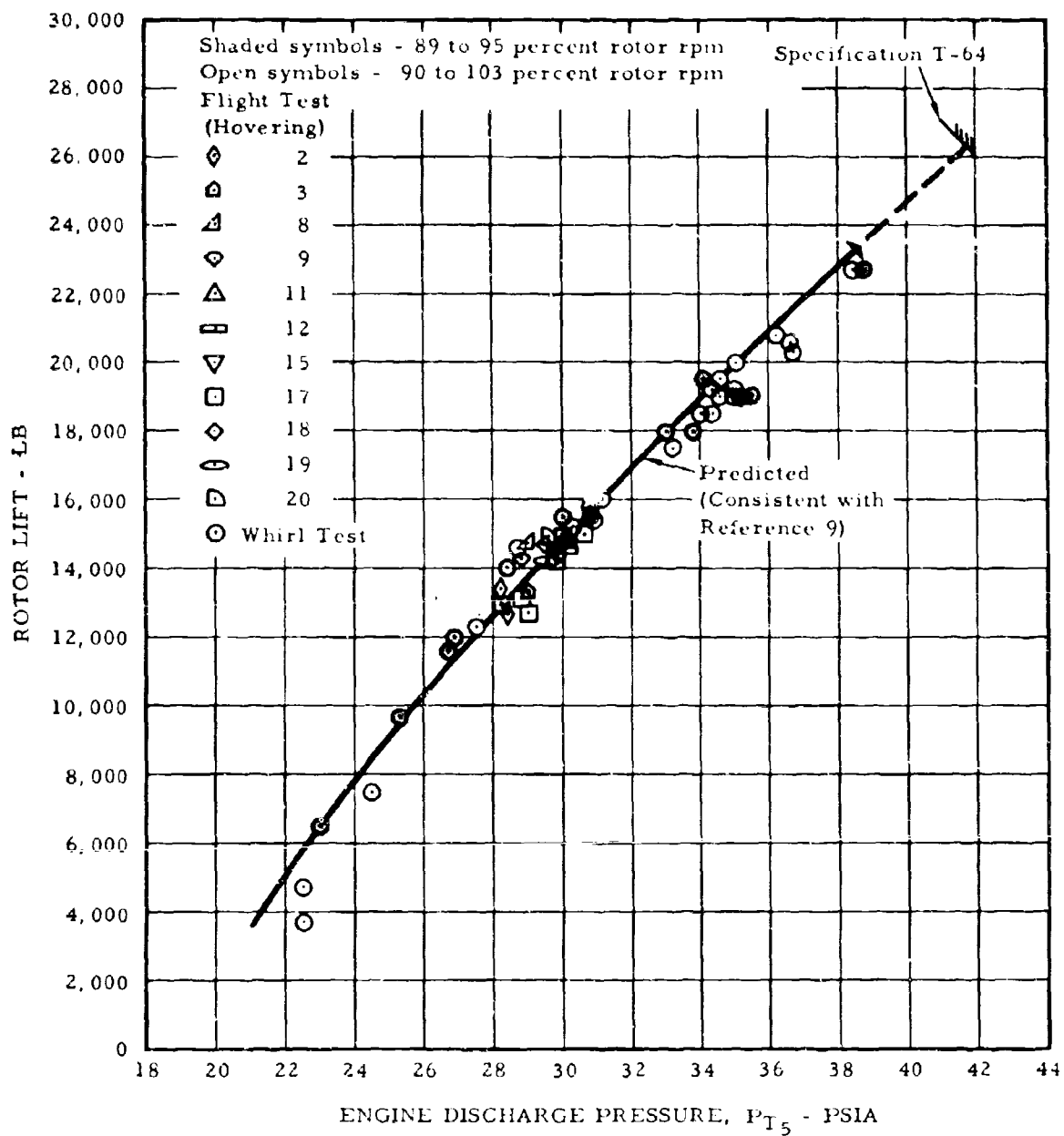


Figure 18. Rotor Lift Versus Engine Discharge Pressure.

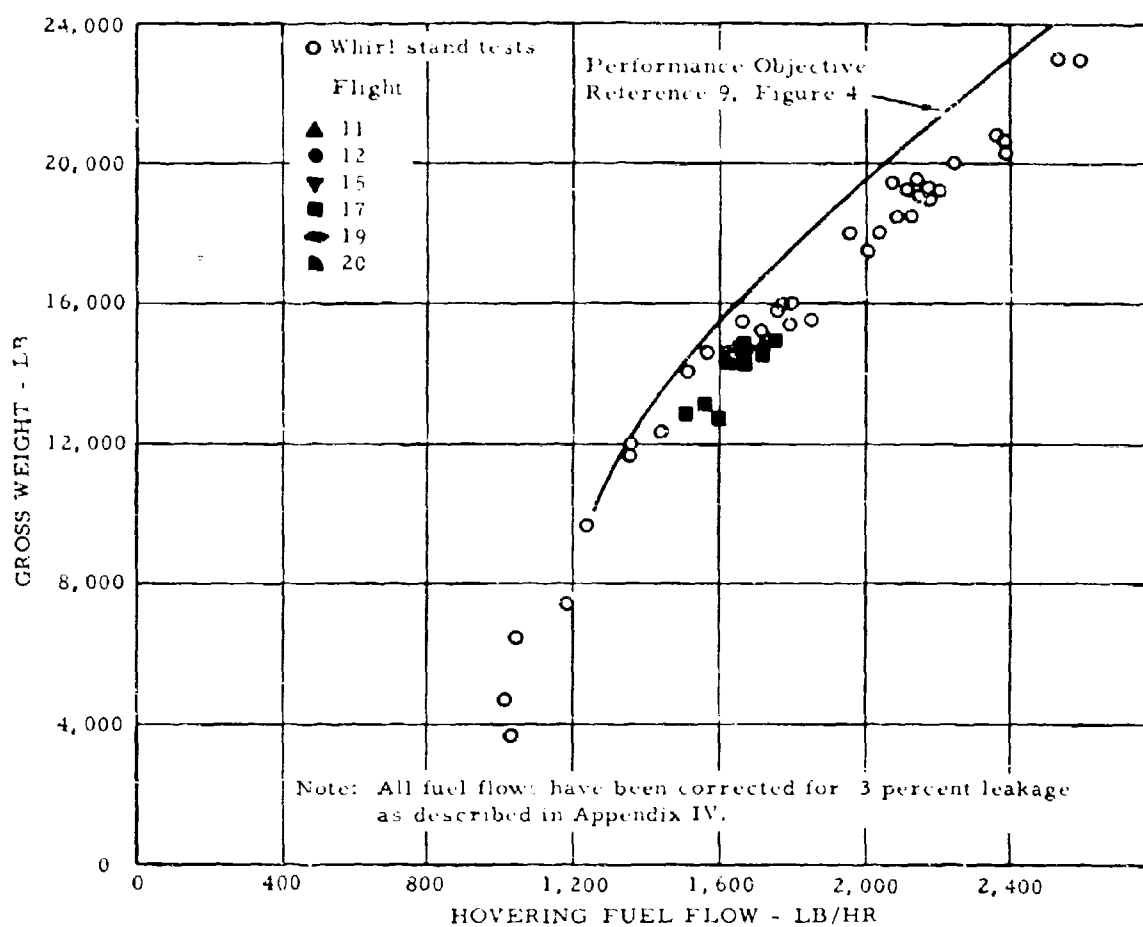


Figure 19. Hovering Fuel Flow Versus Gross Weight.

for excellent overall agreement to exist on lift while a noticeable discrepancy exists in fuel consumption.

The flight fuel flows of Figure 19 may be marginally higher than the whirl tower flows, although the effect -- if present -- is largely obscured by data scatter. If there is indeed such a difference, it is most probably the result of increased leakage during flight.

#### c. Engine Performance

The Hot Cycle airframe and its gas generator engine share an interface at the engine tailpipe, Station 5. At this interface, the airframe sees the engine as a gas source, with pressure and temperature being the most important parameters. As discussed earlier, the rotor lift depends primarily upon  $P_5$ , while rotor fuel consumption increases with increasing  $T_5$  for constant lift (constant  $P_5$ ). Also at the interface, the engine sees the rotor system only as an effective tailpipe discharge area. It should be noted that there is a preferred choice of tailpipe area, depending on two different criteria; namely, the rotor specific fuel consumption (SFC) and the maximum rotor horsepower. For best SFC, the rotor requires a minimum  $T_5$  for a given  $P_5$ . The engine has a preferred tailpipe area at which it will deliver the lowest  $T_5$  for a given  $P_5$ . As the tailpipe departs from this preferred area,  $T_5$  increases, very slowly at first then more rapidly as the mismatch becomes larger.

An indication that the XV-9A duct system presents a desirable apparent tailpipe area to its two T-64 engines is graphically displayed in Figures 20 and 21. Although there are known changes in flow area within the flight test data (due to yaw valve opening, in particular), there is remarkably little scatter in the  $T_5$  versus  $P_5$  data for either engine. Furthermore, the absolute level of flight test  $T_5$ 's is at the extreme lower limit of the General Electric predelivery calibration test results for each engine.

For maximum power, the engine must reach maximum allowable turbine inlet temperature and maximum allowable rpm simultaneously. The two sets of cascades used to date have bracketed the proper area for maximum power and any necessary final adjustments will not penalize fuel consumption.

Having established that the engines are operating with their preferred tailpipe areas, it is logical to compare the whirl and flight  $T_5$ 's with those provided by General Electric for the fully qualified

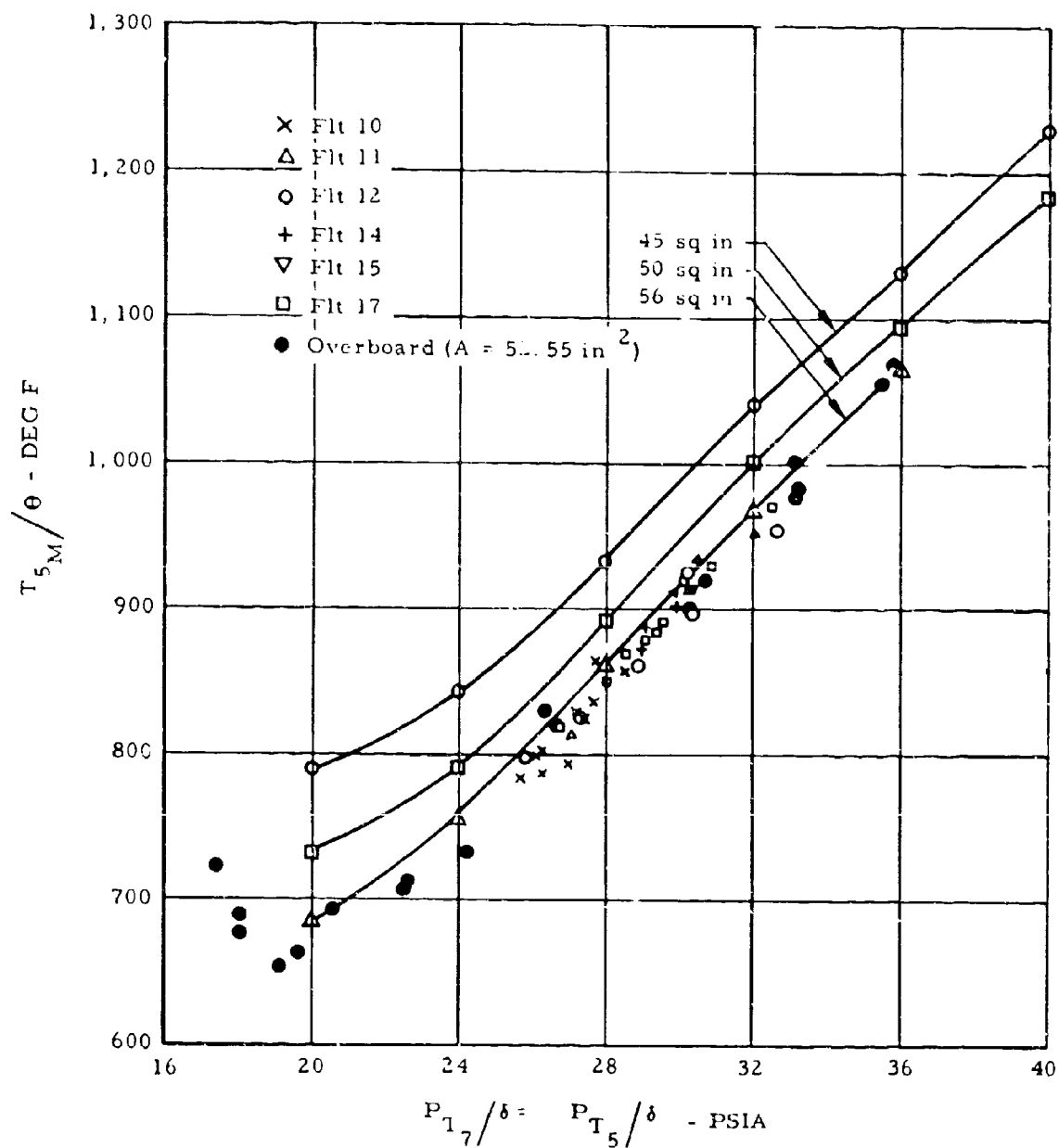


Figure 20.  $T_5$  Versus  $T_5$  and  $P_7$  Correlation, Engine 027-1A.

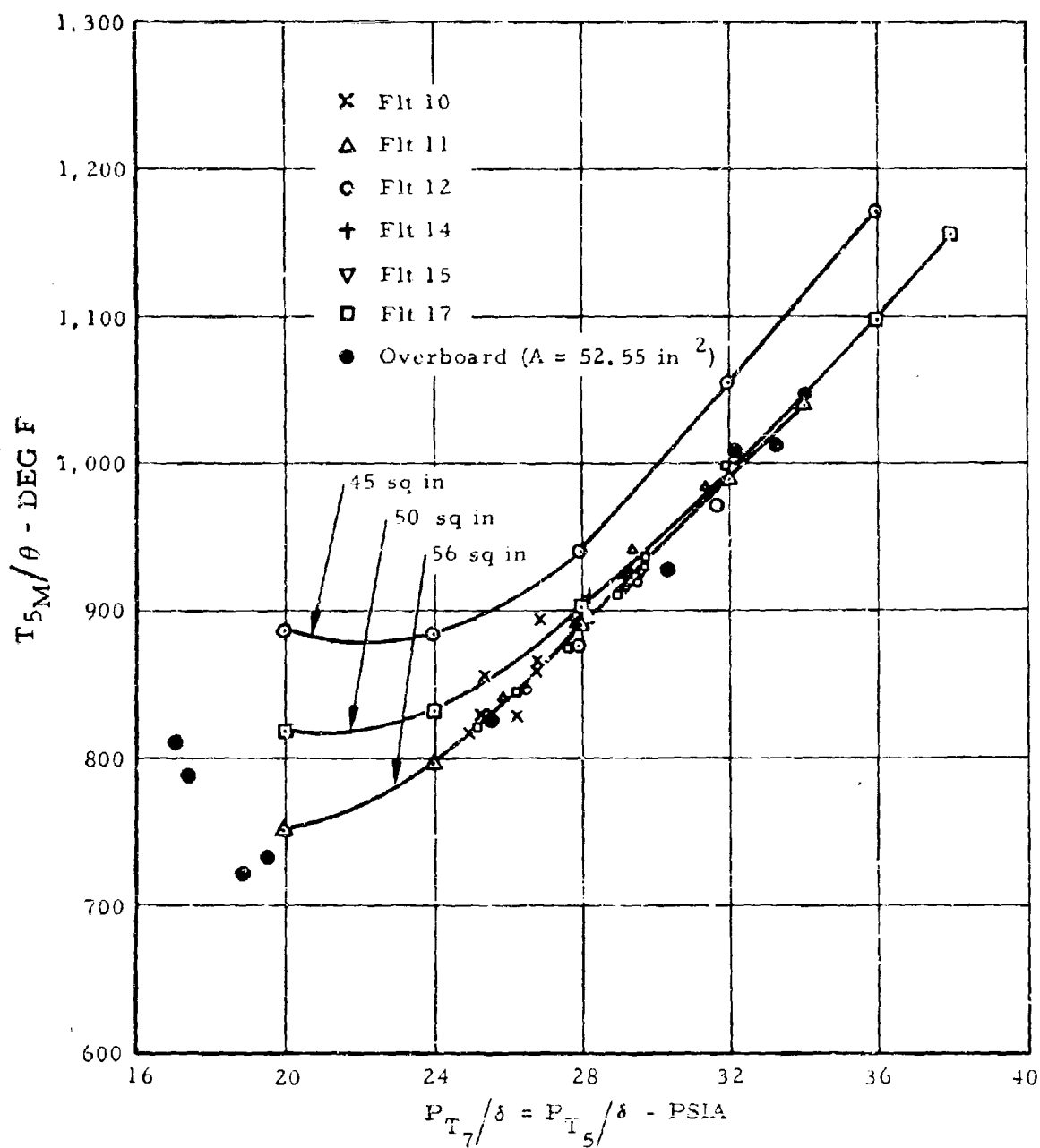


Figure 21.  $T_5$  Versus  $P_5$  and  $P_7$  Correlation, Engine 026-1B.



T-64 engine. This comparison is made in Figure 22, with  $T_5$ 's and  $P_5$ 's averaged for two engines at each test point. The consistency of both whirl and flight results is encouraging.

Engine deterioration during operation would show up immediately on a  $T_5$  versus  $P_5$  plot as an increase in  $T_5$  for a given  $P_5$ . No such trend is visible within the flight test results. There are a few questionable  $T_5$  points within the whirl test results.

This company has developed a rather unusual technique for determining engine mass flow through the use of flow conditions at the turbine nozzle diaphragm station. This technique avoids uncertainties due to compressor inlet flow profiles and variable guide vane hysteresis that limit the accuracy of the ordinary compressor flow calibration technique. This new technique was first used in connection with the whirl test, Reference 7, and has been refined and simplified during the present flight program. Engine temperature maps relating turbine inlet temperature,  $T_4$  (which is not measured directly), to the measured temperatures,  $T_2$ ,  $T_3$ , and  $T_5$ , have been constructed by correlating data from General Electric predelivery calibrations of all T-64 engines used to date in the XV-9A programs. A family of these maps for various  $T_2$ 's has been prepared with direct-reading temperatures for use in engine topping. On these maps,  $T_4$  can be compared directly against  $T_{4\max}$  without the necessity for intermediate slide rule manipulations. Airflow is readily calculated from this  $T_4$  and measured  $P_3$  by the equation:

$$W_a = 6.06 P_3 / \sqrt{T_4}$$

where:

$$W_a \approx \text{lb/sec}$$

$$P_3 \approx \text{psia}$$

$$T_4 \approx ^\circ\text{R}$$

The map for standard  $T_2$  is presented in Figure 23 as an example of the family used in data reduction.

In addition to its usefulness in establishing proper engine topping and in calculating airflow, the engine temperature map offers one of several alternative indications of the apparent tailpipe area seen by the engine. The tailpipe area lines on Figure 23 are drawn from General Electric predelivery calibrations of the two

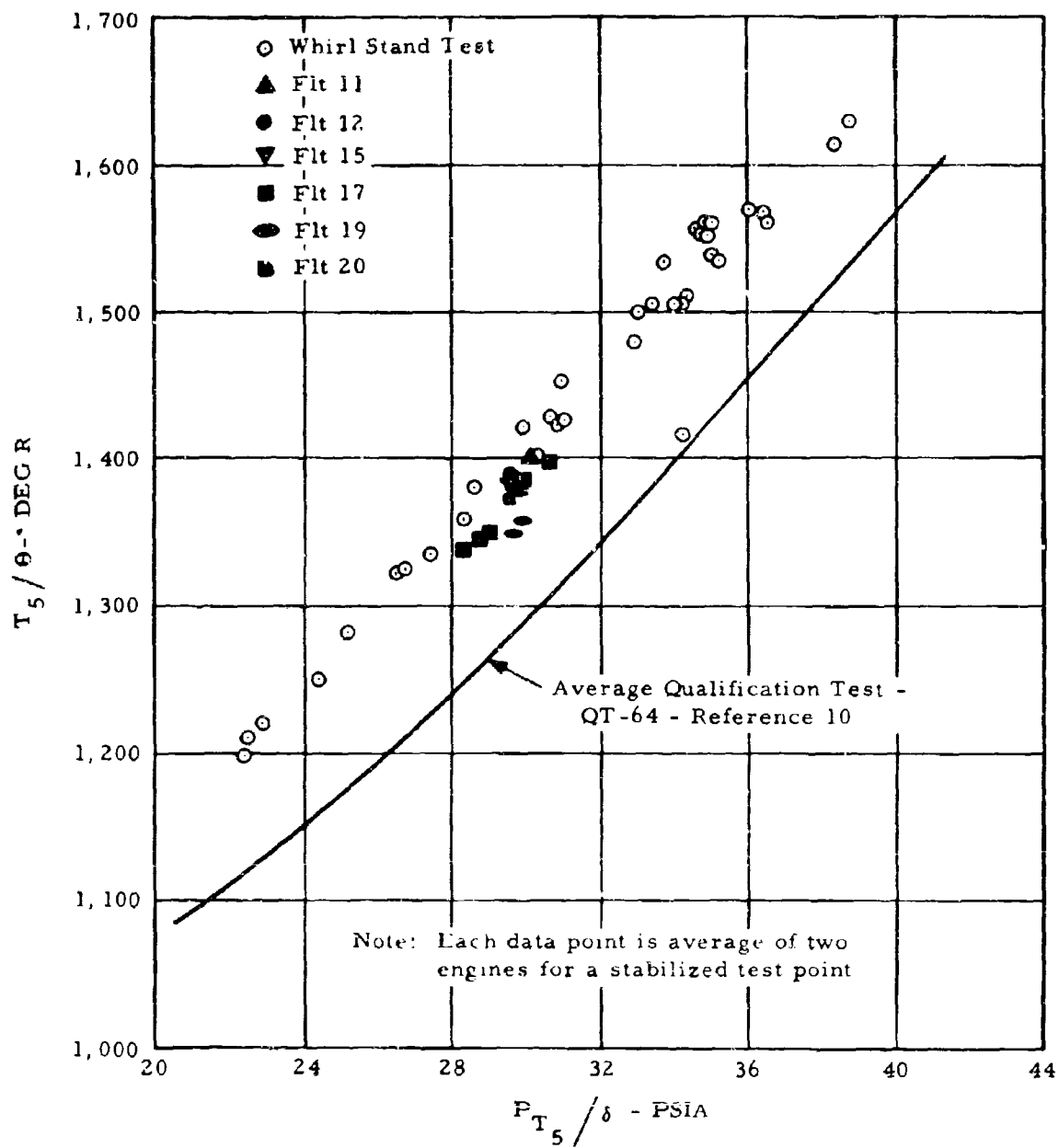


Figure 22. Engine Discharge Temperature Versus Pressure.

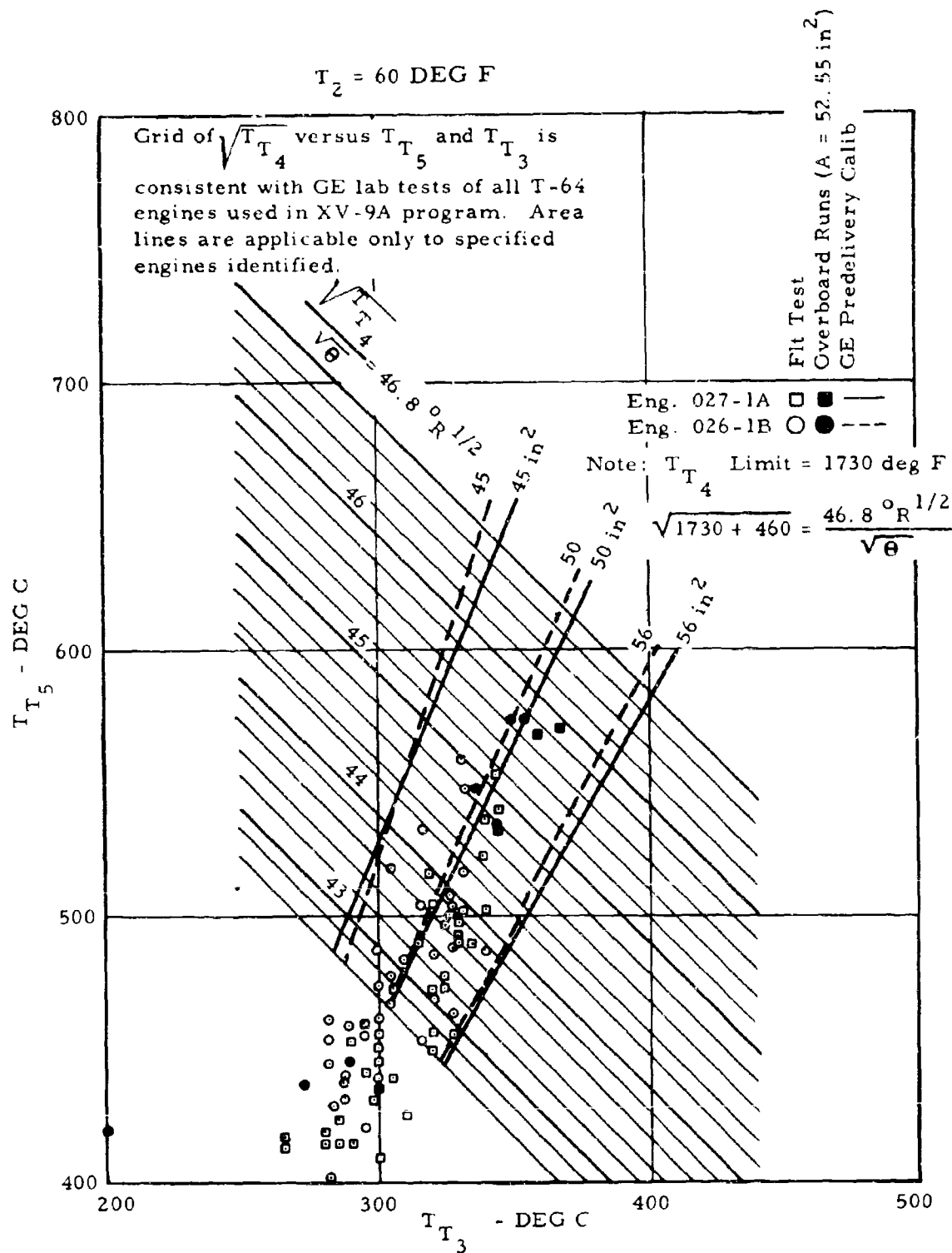


Figure 23. Engine Temperature Relationships.

YT-64's used in the flight test program. The tailpipe area presented by the XV-9A rotor system appears to be the same as the nacelle tailpipe area, 52.5 square inches per engine, for a total of 105 square inches. (Note that the nacelle exit points are generally compatible with the General Electric area lines on Figure 23.) The considerable scatter of points -- particularly for engine 026 -- is perplexing in view of the excellent correlations obtained in Figures 20, 21, and 26. It is possible that the  $T_3$  probe in engine 026 was intermittently malfunctioning during the testing.

Another indication of effective tailpipe area can be obtained from engine rpm versus temperature maps such as Figures 24 and 25. Movement of the variable guide vanes used in the T-64 compressor can affect compressor performance much in the manner of changes in mechanical rpm. Changes in the guide vane schedule thus introduce errors in any correlation using rpm as a parameter. Total effective tailpipe area as read from Figures 24 and 25 would be approximately 115 square inches. However, the nacelle overboard runs still agree with the engine-to-rotor runs, strongly suggesting that the rotor flow area is still  $2 \times 52.5 = 105$  square inches. In view of the known weakness of compressor speed ( $N_G$ ) as a correlating parameter for engines having variable compressor geometry, there is little doubt that engine maps such as Figures 20 through 23 offer the most reliable indications of deduced parameters such as  $T_4$ ,  $W_a$ , and tailpipe area.

A final viewpoint on engine performance is offered in Figure 26. Here, engine fuel/air ratio is plotted against measured engine temperature rise. The solid line represents General Electric's prediction for the T-64 engine as well as their predelivery calibration of the YT-64's used in the XV-9A. This line is also consistent with the theoretical heating value of typical jet fuel, Reference 8. The flight points for both engines are remarkably consistent -- speaking well for all the temperature and flow rate measurements that are involved. The offset of the flight test fuel/air ratios to higher values for a given temperature rise is believed to be due to compressor bleed flow used to drive the oil cooler aspirator. As pointed out in Appendix IV, the correction of hovering fuel flow for compressor bleed, Figure 19, amounts to moving the fuel/air ratio points from their observed location to the General Electric calibration line. Shaft power extraction for hydraulic pump and generator drive also contributes to the increase in fuel/air ratio, but the magnitude of this effect would be less than 1/4 of 1 percent for the 6 to 7 horsepower extracted per engine during the flight tests.

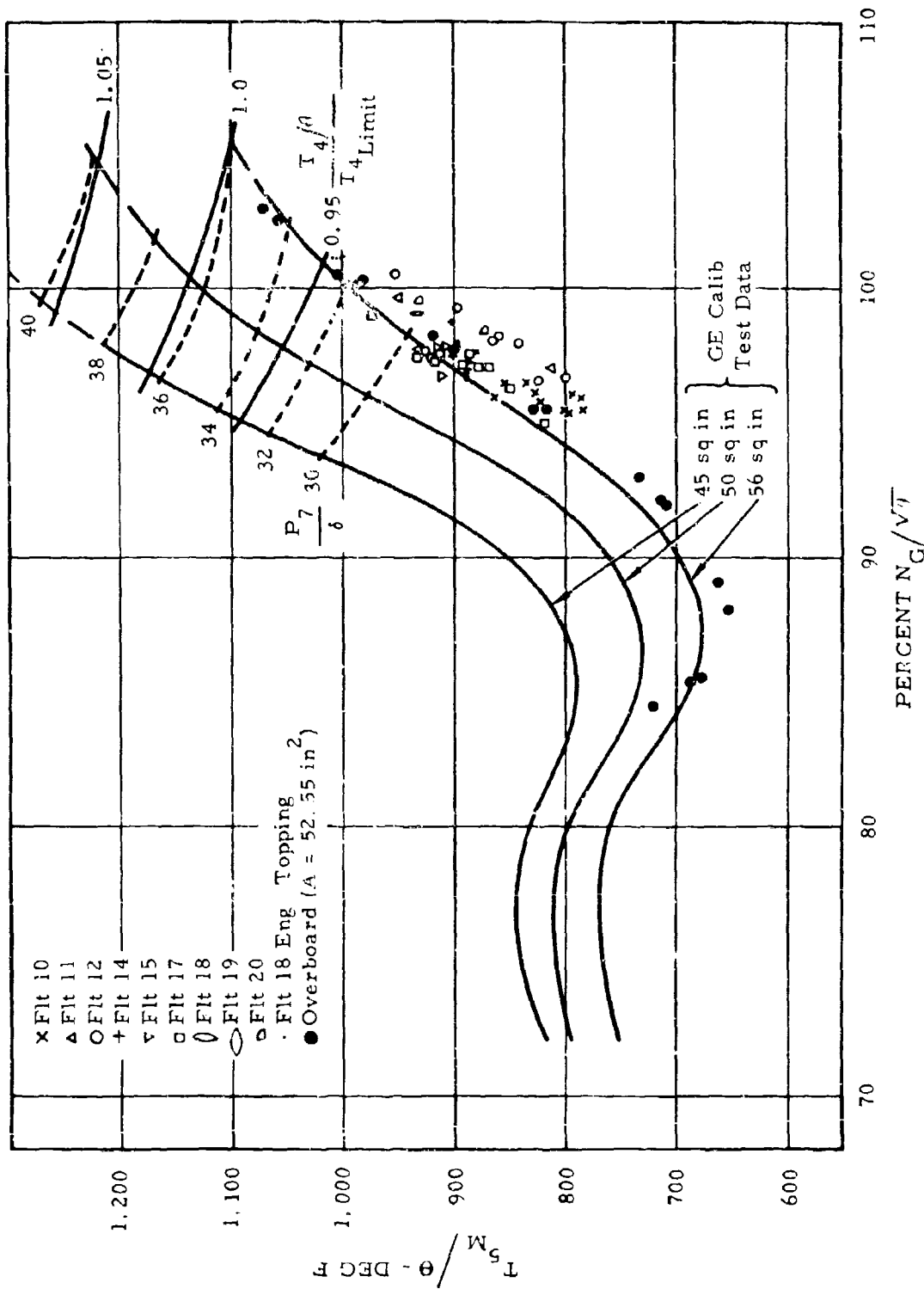


Figure 24. T-64 Engine 027-1A Operating Data.

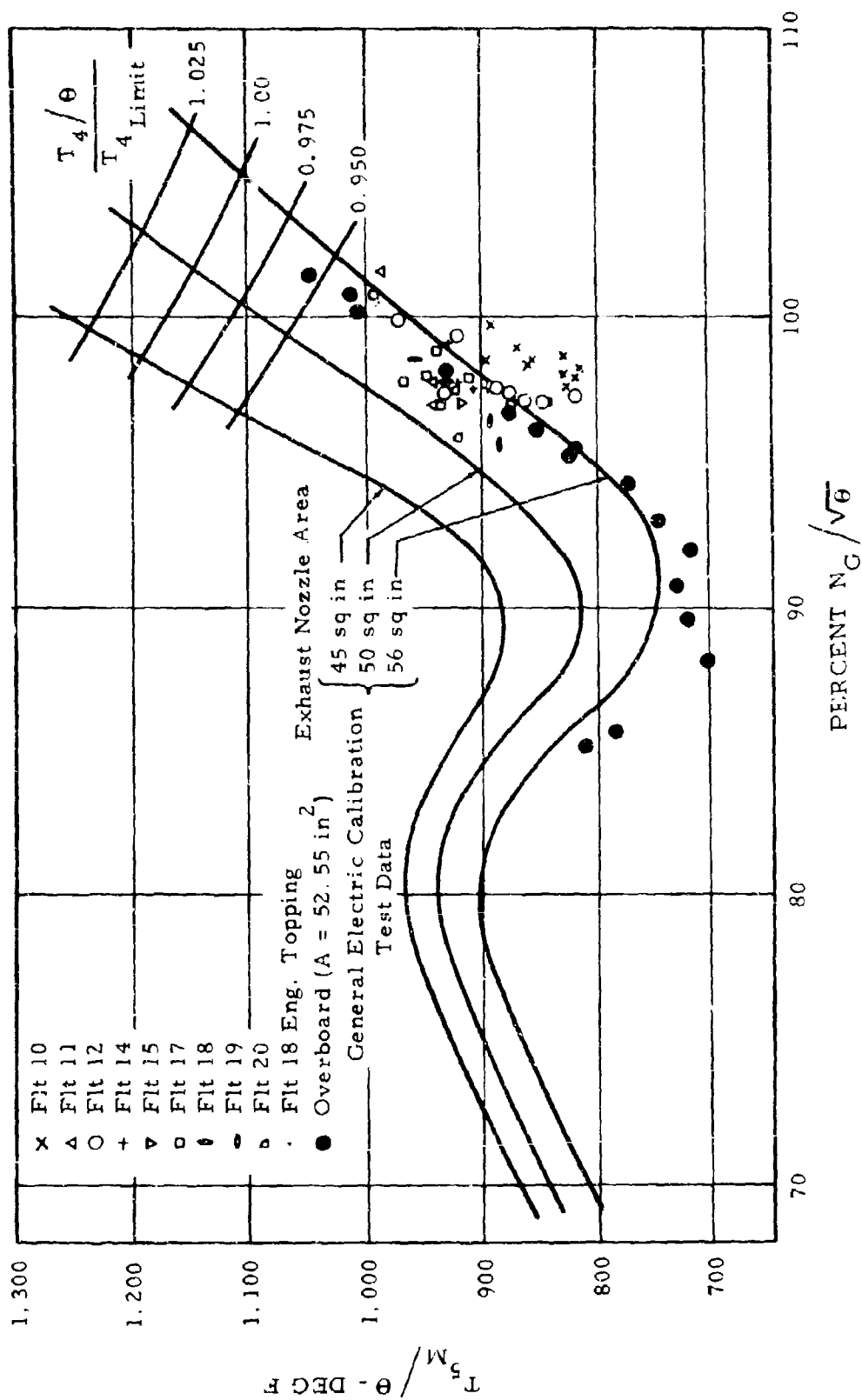


Figure 25. T-64 Engine 026-1B Operating Data.

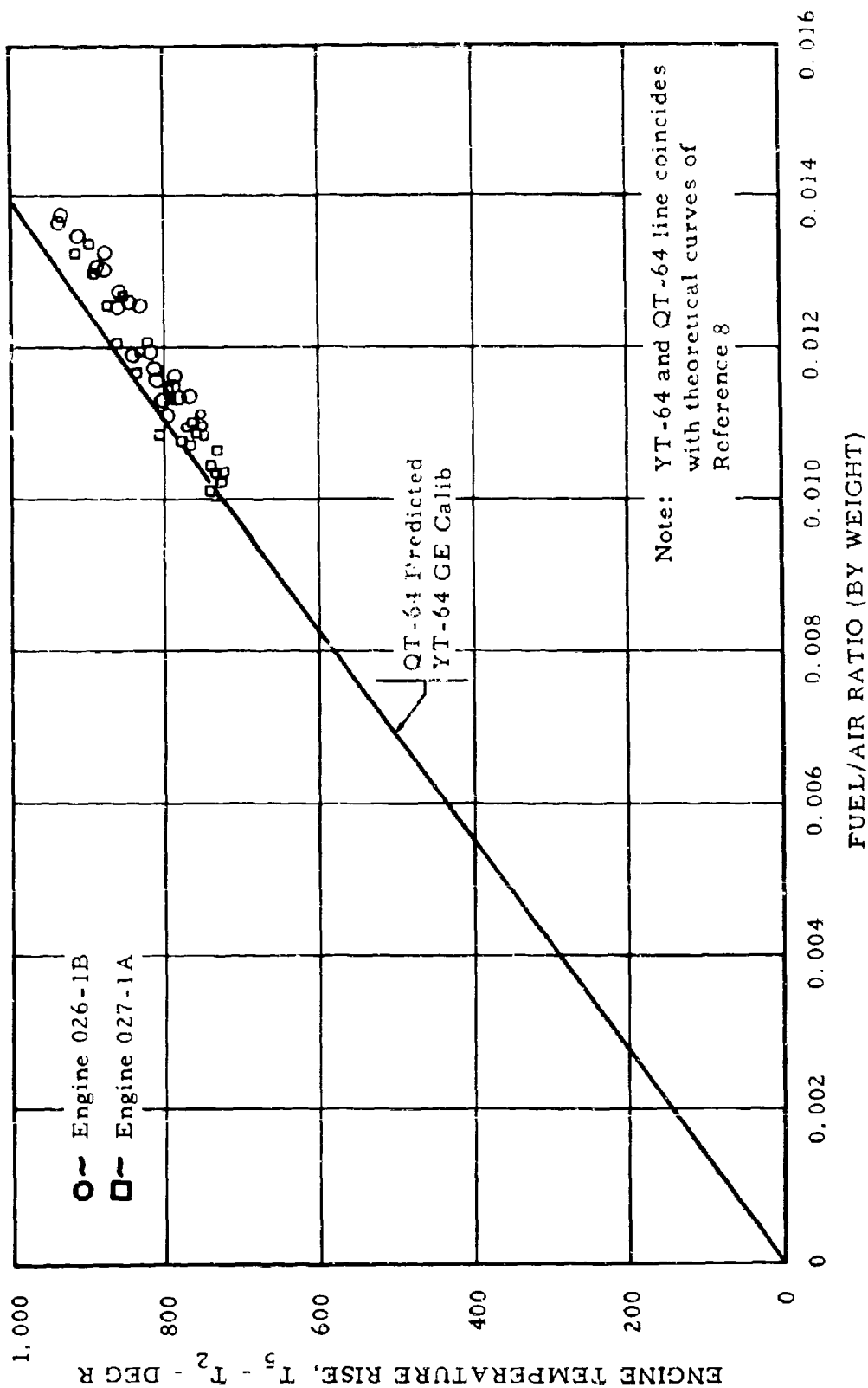


Figure 26. Temperature Rise Versus Fuel Air Ratio.

#### d. Rotor System Component Performance

Just as the engine and airframe performance can be separated at Station 5, the rotor system internal and external aerothermodynamic performance can be divided at the rotor tip. The internal flow system produces net tip thrust, or rotor power. The rotor exterior flow field converts rotor power into lift. The major components that interact to establish total system performance are listed and categorized in Figure 27, which will serve as an introduction and guide to the following comments. Without exception, each of these component performance items has a precedent within the body of previous experience. The value that has been assigned to each item as a part of Hot Cycle performance calculations is, therefore, almost certain to be within a few percent of the true value. The problem of refining these estimates is not an easy one, since the accuracy available from flight test instrumentation is sometimes only marginally better than the accuracy of the original assumptions.

The most critical quantity in the rotor performance breakdown is the duct average total pressure at the tip, yet this is a most difficult measurement to take in view of the temperatures and acceleration g loads prevailing at that point. Six of the best commercially available transducers have been installed during whirl stand and flight tests, and considerable effort has been expended on calibration procedures. To date, however, full confidence cannot be placed in these readings. Calibration under full temperature, pressure, and g load is an absolute requirement in order to establish this confidence, and attempts to obtain such a calibration are being continued as part of the follow-on flight test program.

As matters now stand, the measured tip pressures cannot be reconciled with other data on mass flow, leakage, tip cascade area, and cascade discharge coefficient. If the measured pressures were some 5 percent higher, they could be reconciled with those factors, and, in addition, would become more consistent with pressures calculated from classic duct friction coefficients. Figure 28 presents a representative sampling of flight test tip pressure data, along with an indication of whirl stand results and the originally estimated performance.

Pending justification for revising the tip pressures, the measured pressures have been taken at face value in studying the probable performance of other rotor components. Obviously, a series of



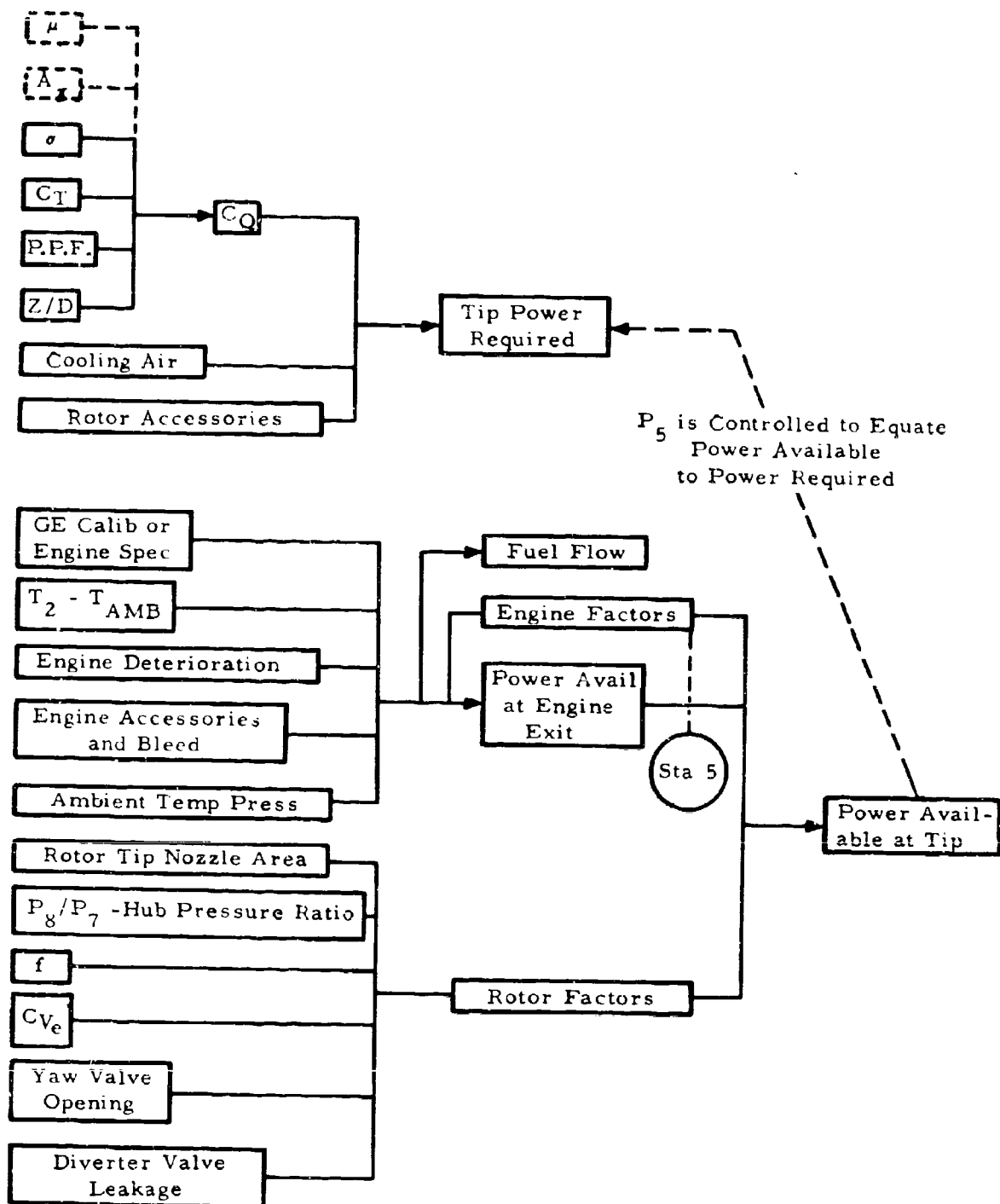


Figure 27. Elements of Power Available and Power Required.

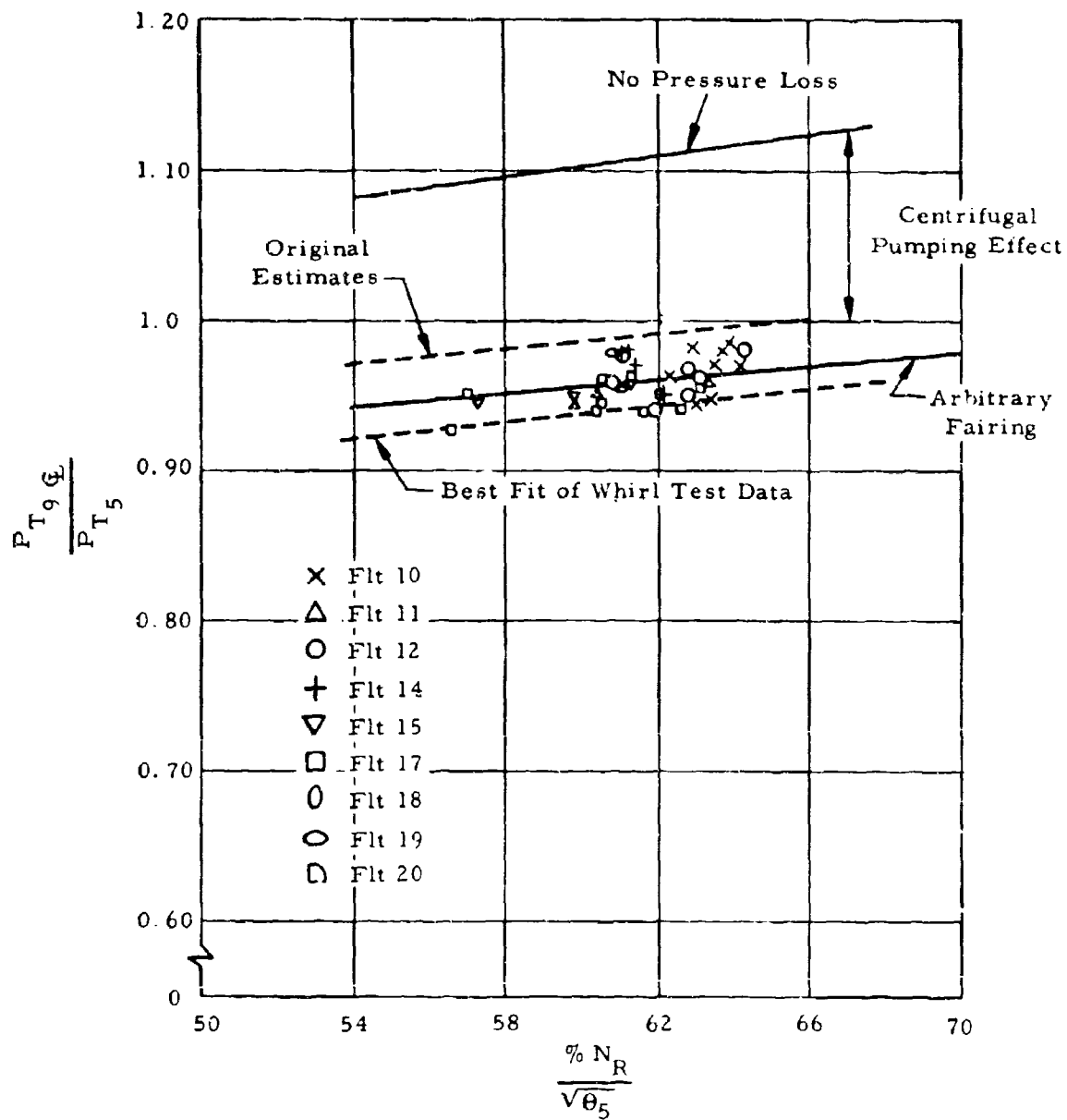


Figure 28. Rotor System Pressure Ratio.

minor adjustments may be necessary when the tip pressure-mass flow contradiction is finally resolved.

Rotor horsepower available versus engine discharge pressure, Figure 29, represents the first step in establishing a component performance breakdown based insofar as possible on measured parameters. Since rotor horsepower is not measured directly but is calculated from many input quantities and the line shown is based on similar calculations, no valid comparisons can be drawn in Figure 29. However, this tentative assessment of rotor power input leads to external aerodynamic performance comparisons as follows.

The basic gas conditions that were used to calculate the rotor horsepower given in Figure 29 (used in conjunction with Figures 30, 31, and 32) and the equivalent values of engine gas power based on those gas conditions are given in Appendix IV.

In Figure 30, rotor torque coefficient is plotted against rotor thrust coefficient, with the resulting correlation suggesting that the blade profile power factor may be 1.25 rather than 1.0 as could be expected for a helicopter rotor of normal construction. The XV-9A rotor does have surface irregularities at the leading edge segment joints that could no doubt cause a drag increase of this magnitude. Future Hot Cycle rotors will, of course, incorporate additional finesse in fabrication to avoid this roughness. Figure 30 also illustrates the fact that a 25-percent increase in blade profile power factor results in an increase of less than 10 percent in hovering power required.

Figure 31 presents a study of forward flight performance of the XV-9A, based on the tentative horsepower available of Figure 29. In order to deduce the aircraft parasite drag area,  $A_p$ , dummy plots of power required versus true airspeed were prepared for assumed values of parasite area and for the rotor torque coefficient deduced from the hover tests. Three dummy plots were prepared:

Gross weight = 14,500 pounds, sea level standard  
Gross weight = 13,000 pounds, sea level standard  
Gross weight = 14,500 pounds, 2,000-foot standard

This set of plots permitted correction of the level flight points to allow for the effect of density and gross weight variation from point to point. When the corrected points were plotted against a background grid of power required versus true airspeed, it was possible

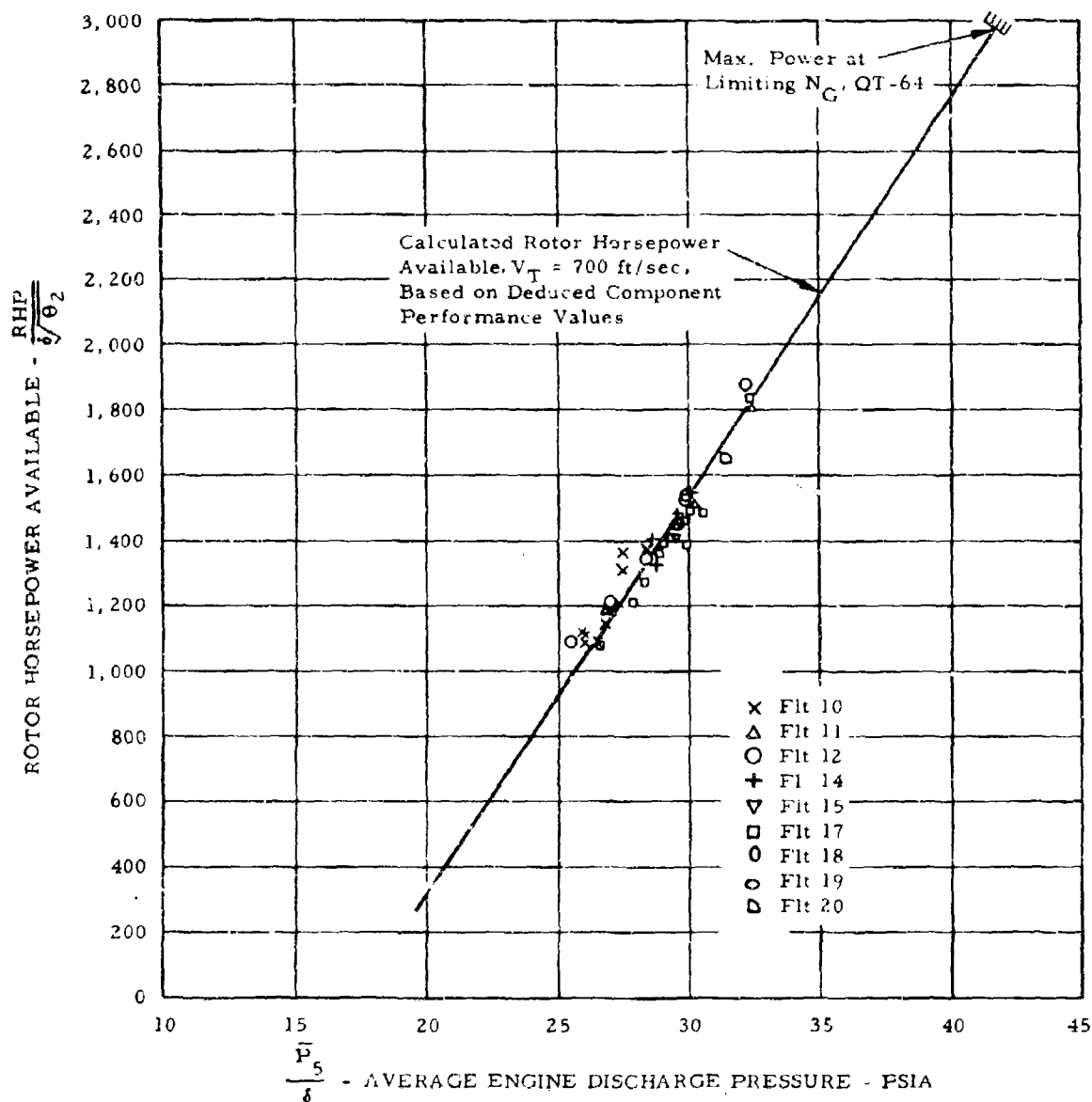


Figure 29. Rotor Horsepower Available Versus  $\bar{P}_5$  (Average Engine Discharge Pressure).

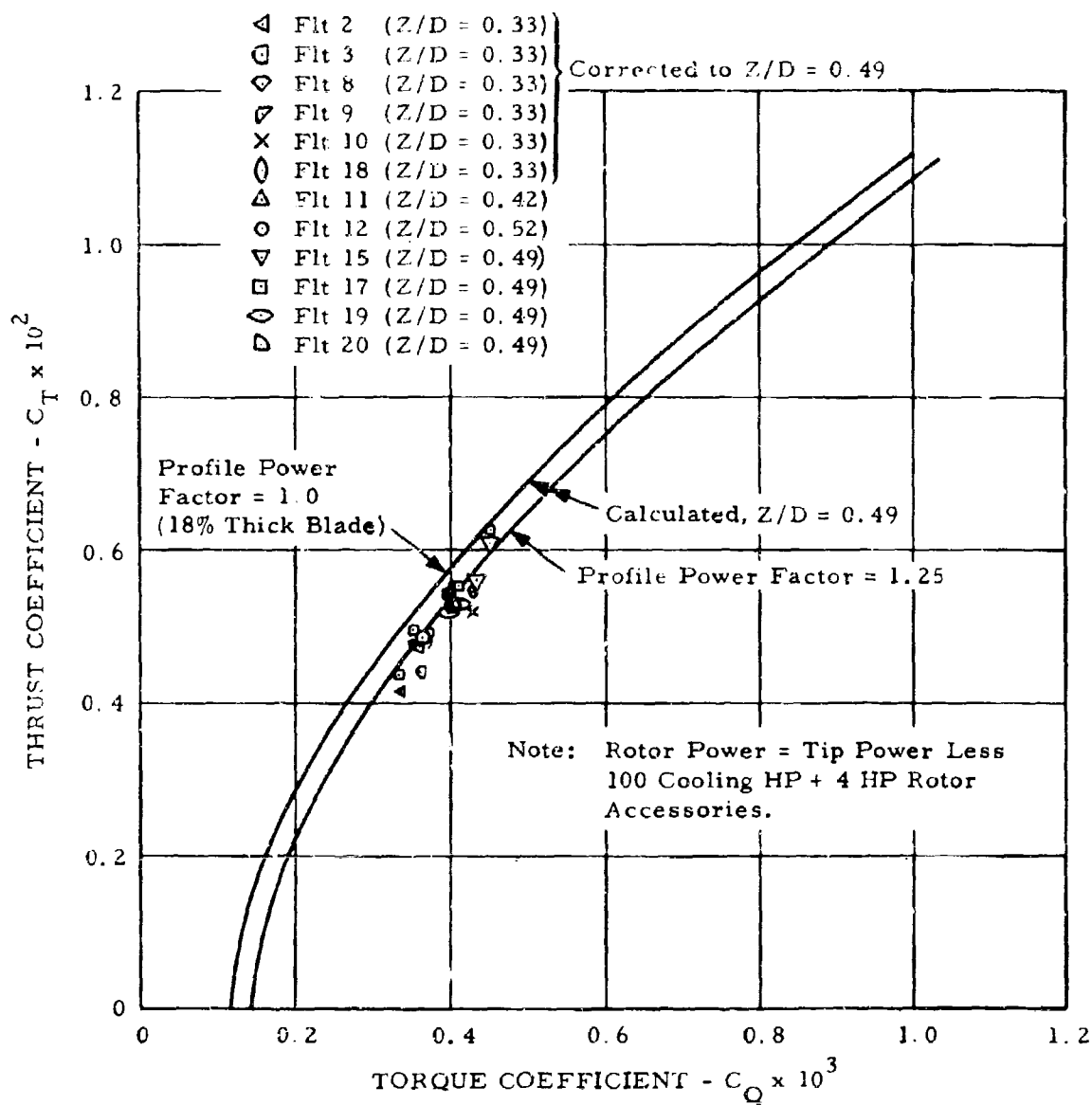


Figure 30. Hover Performance Thrust Coefficient Versus Torque Coefficient.

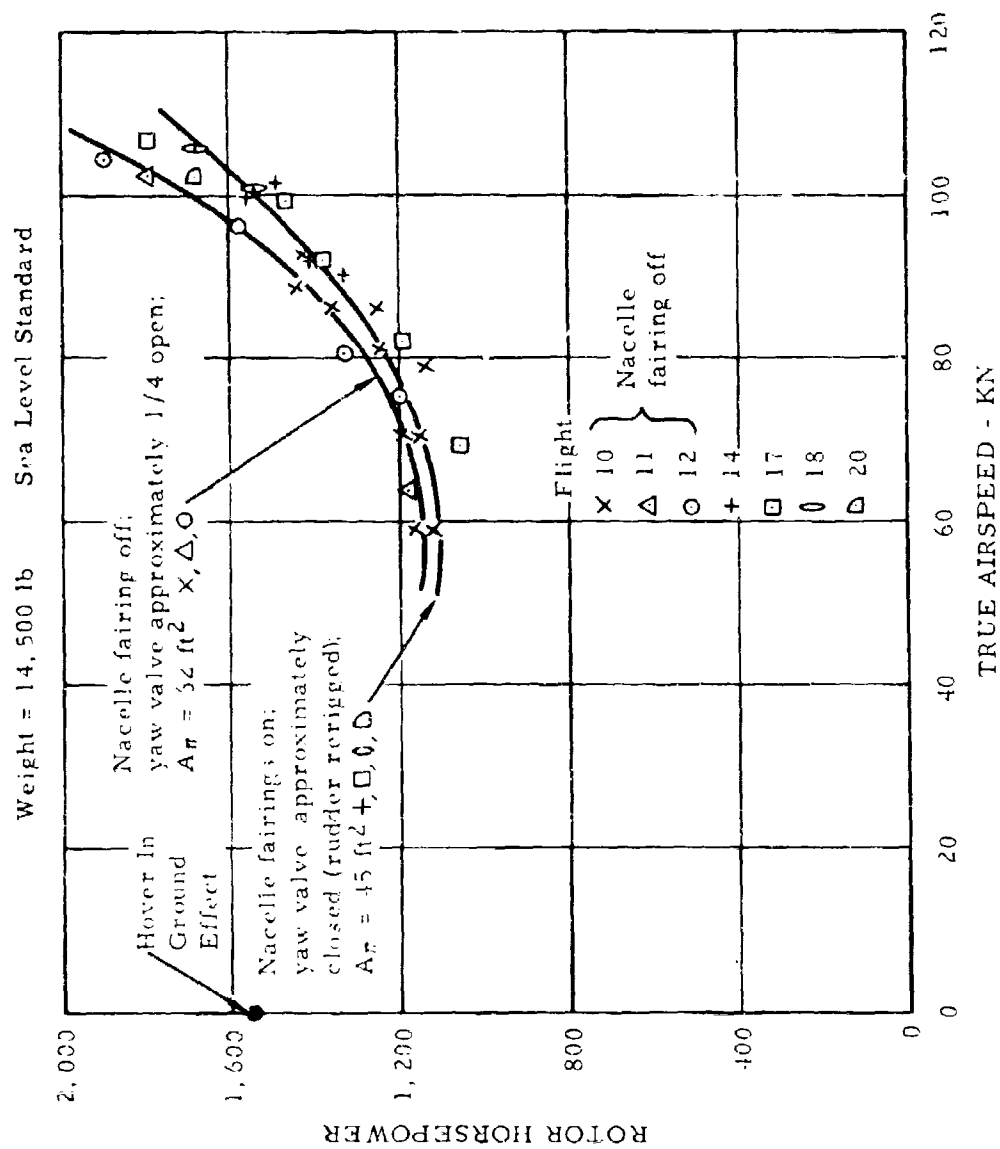


Figure 31. Power Required (Weight = 14,500 Pounds, Sea Level Standard).



Figure 32. Tuft Behavior in Cruise Flight.

to observe the helicopter parasite drag area. Those calculations that best fair the various sets of flight data are reproduced in Figure 31 along with the test points. Data handled in this fashion indicated that the parasite drag area,  $A_p$ , of the helicopter for early flights (up to flight 13) was approximately 62 square feet. During these flights, nacelle fairings were not yet installed and the yaw valve was apparently open approximately 25 percent. The flow coefficient of the yaw valve was not known, but, to be conservative, the entire engine airflow (less 3-percent leakage of the diverter valves) was assumed to go to the rotor tips.

For flights after flight 13, the rudder surfaces were rerigged 5 degrees to the right relative to the yaw valve. Yaw valve position was then measured, and found to be closed in cruising flight, ensuring that a minimum amount of flow bled out the yaw valve. Also, nacelle fairings were installed, producing a drag reduction. Data from flights 13 through 20 were corrected for density and weight variations, and the parasite drag area was found to be 45 square feet.

The helicopter was then tufted on the upper side of the left wing, the left side of the pylon, and the upper left fuselage back to the tail. In-flight motion pictures indicated that a substantial amount of separation existed, causing the high parasite drag area deduced from flight test. Analysis of the configuration, with information gathered from individual pictures of the tufted helicopter (Figure 32), indicated that the separation was caused by flow interference between the rotor hub and the fixed airframe surface. A component drag analysis was made, and it was concluded that with improved fairing of the hub, pylon, wing leading edge, landing gear, and so forth, the helicopter parasite drag could be reduced to 22 square feet.

Theoretical calculation of power required using the reduced parasite drag area of 22 square feet was made, and the result was plotted, in Figure 33, showing the predicted effect of drag cleanup.

A final result of the tentative power available curve is the specific fuel consumption study of Figure 34. Fuel flows used here have been corrected in accordance with the discussion given in Appendix IV. The flight points lie approximately 5 to 8 percent above the predicted levels, which is generally consistent with the direct fuel flow versus lift correlation of Figure 19. This agreement cannot be construed as adding confidence to the fuel flow levels, since the same values are used in each figure, but it does suggest that



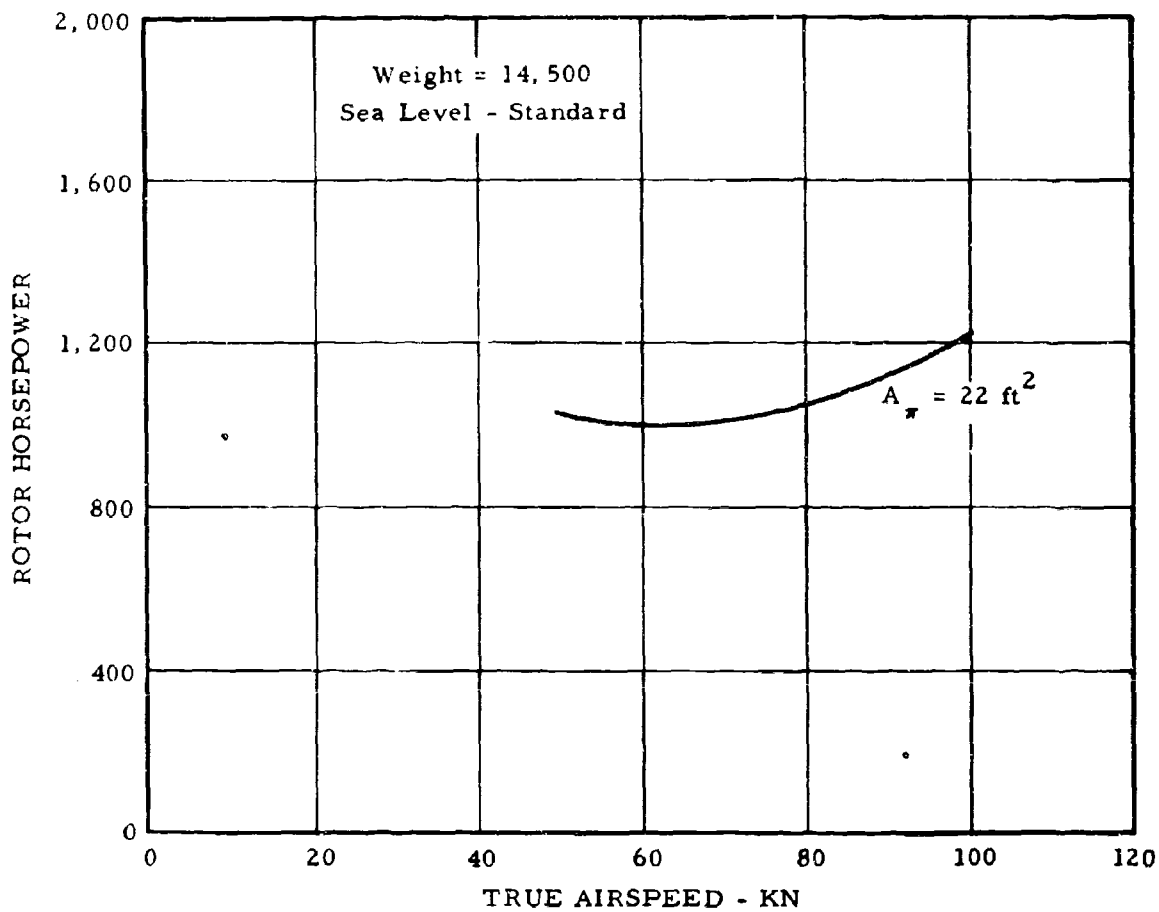


Figure 33. Predicted Power Required With Drag Cleanup  
(Weight = 14,500 Pounds, Sea Level Standard).

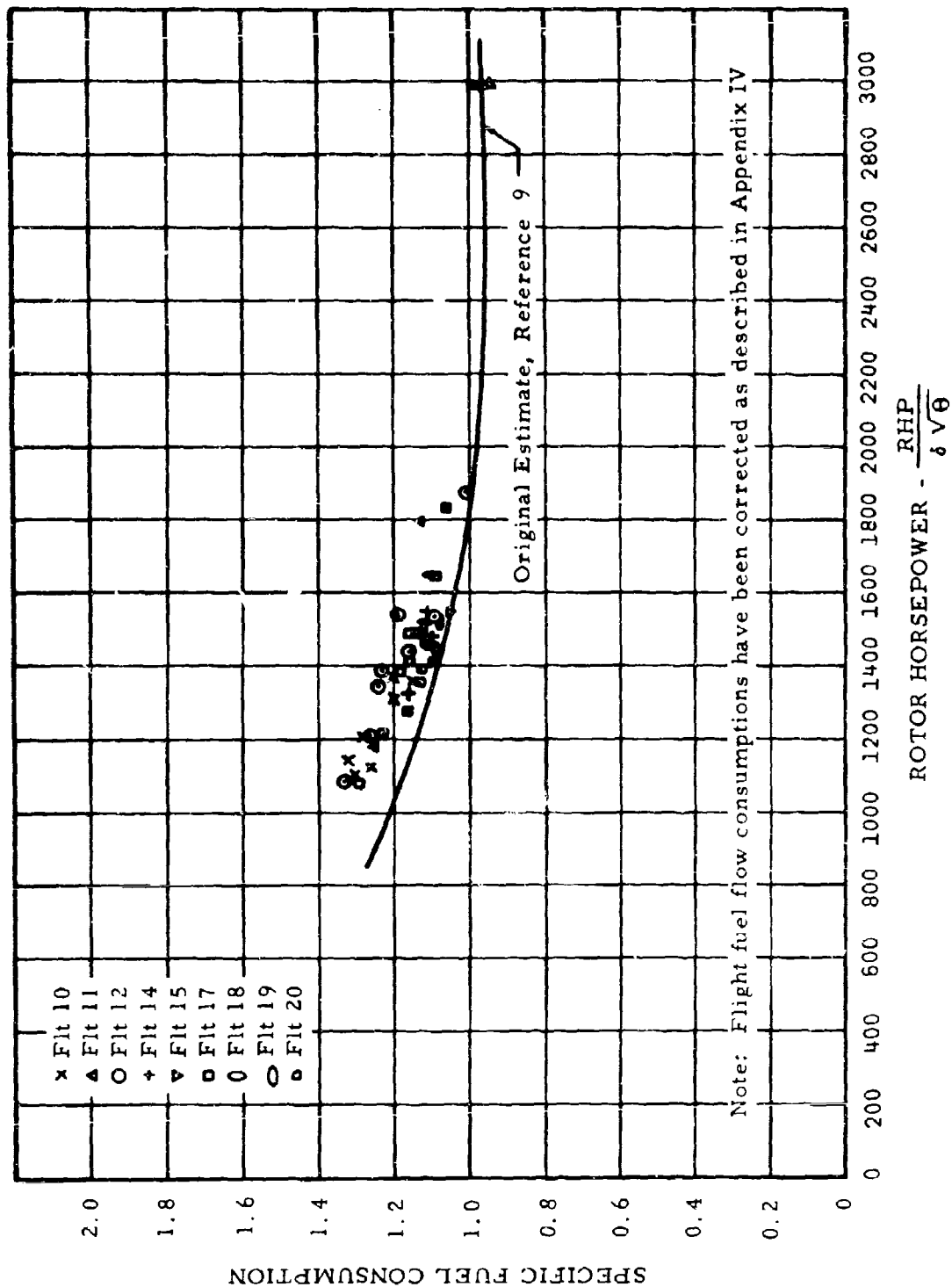


Figure 34. Tentative Specific Fuel Consumption Correlation.

the external aerodynamic assumptions relating rotor power to lift are consistent on an overall basis. The general level of specific fuel consumption deduced in Figure 34 must be taken as highly encouraging, since there are many known areas for future improvement in blade aerodynamic cleanness.

Figure 35 is included herein for convenience of reference. This figure shows ideally expanded jet velocity as a function of duct centerline total pressure for various exhaust gas temperatures. This curve incorporates the effects of real gas thermodynamic properties and also accounts for the ratio of average to centerline total pressure for fully developed turbulent flow at Reynolds and Mach numbers characteristic of the XV-9A rotor ducting.

#### e. Yaw Valve Characteristics

The XV-9A has a reaction-jet-powered rotor that produces no shaft torque except from bearing friction. Directional control in the XV-9A during hover is by means of a reaction-jet yaw valve in the aft fuselage. (Aerodynamic rudder surfaces hinged to the V-tail stabilizers provide the primary directional control in forward flight.)

Results of flight tests indicate that the yaw valve operates successfully in principle, but it has certain deficiencies that limit its usefulness. These are:

1. The gas generator speed will increase when the yaw valve is opened, and an overspeed will result under certain conditions. During yaw valve tests at full power on a single engine, the engine speed increased from 103 to 105 percent and was above the established maximum speed of 104 percent for five seconds. This same type of overspeed could occur in a steady hover turn at full power, if the engines were topped with the yaw valves closed.
2. At full power, a wide open yaw valve can cause a 30-percent reduction of rotor power, even if the engine is initially topped at maximum temperature at a speed (103 percent +) that will allow the engine to reach the maximum speed (104 percent) in steady-state conditions. This results from a combination of the direct loss in power due to mass flow bleed and reduced engine temperature and pressure reached along a fuel control droop line when the yaw valve is opened.

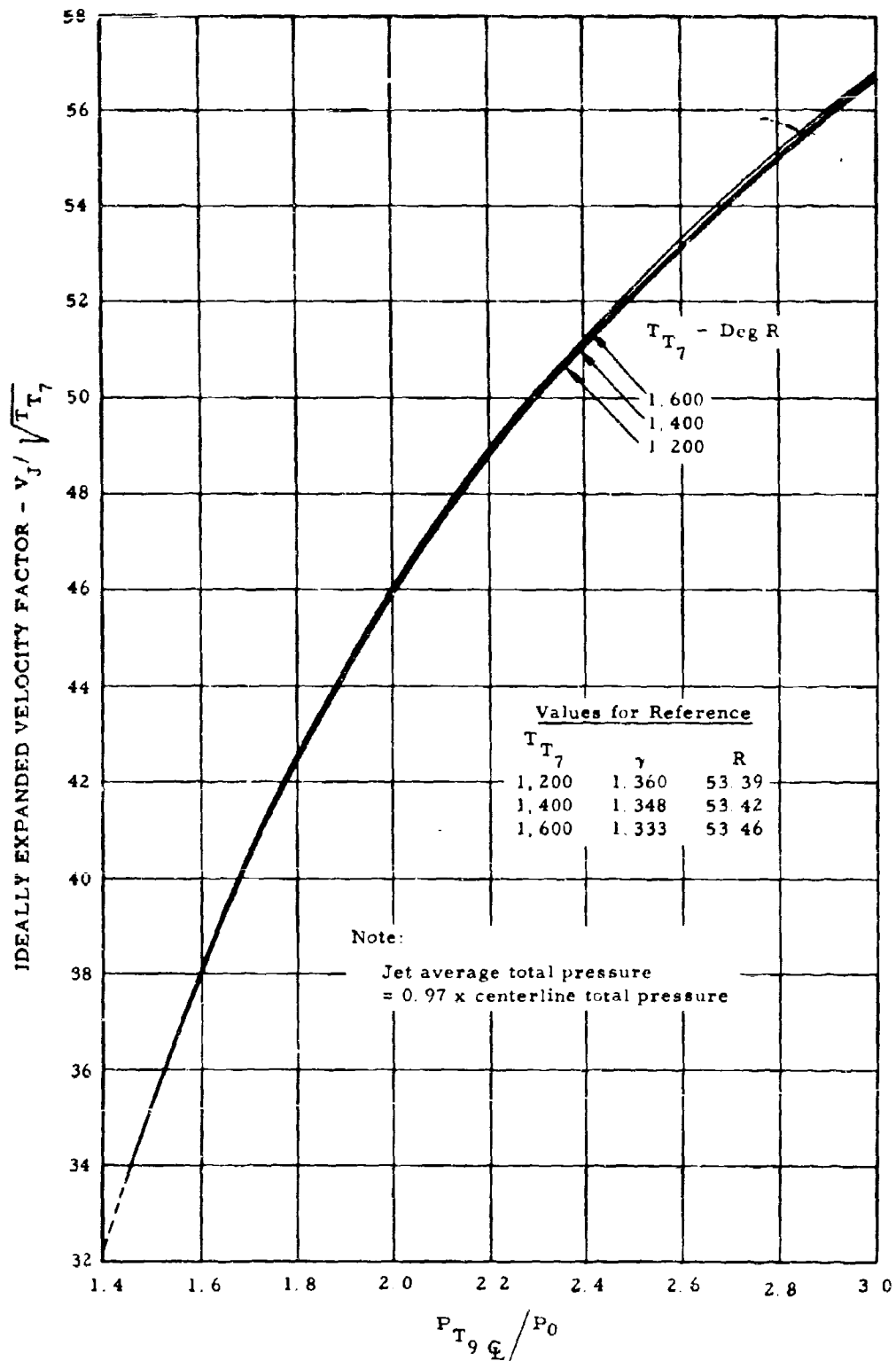


Figure 35. Hot Cycle Rotor Jet Velocity.

3. The direct linking of yaw valve and rudder leads to opening of the yaw valve when the pedals are moved, causing an increase of engine exit area that produces an undesirable change in engine speed during a maneuver.

f. Power Management

The power management system for the gas generators in the XV-9A consists essentially of the same type of pilot-actuated levers and rotor-speed signal input to the fuel control as are found in shaft-driven helicopters. The principal difference in power management for the Hot Cycle results from the interaction effect of one engine on the other, because they share common ducts from the rotor hub to the blade tips.

Normal procedure for power setting is to set collective pitch to obtain the desired flight condition and to use twist-grip control to attain the desired governed rotor speed. Therefore, power lever changes were then made as required during flight to maintain a nearly matched engine speed ( $N_G$ ) condition.

The technique of setting matched engine speed was found to be the most practical means of engine operation, since the YT-64 engine is highly responsive to power lever changes at all speeds above Flight Idle and any change in power lever angle is immediately reflected by change in engine speed. Analysis of engine operating data indicated that with matched  $N_G$  the two engines shared very nearly the same amount of the exit area, which is highly desirable for optimum acceleration characteristics, power output, and assurance of operation within the allowable temperature limits.

During the flight test program, a power recovery from near autorotation was attempted, and the pilot experienced a hangup in which gas generator 2 lagged considerably behind gas generator 1 in speed and compressor discharge pressure. It was determined that the initial difference in gas generator speed was 6.2 percent (78.1 versus 71.9 percent). Later investigation by the engine manufacturer disclosed that inherent differences between engines can lead to a hangup, or even a rollback, if the rotor speed is low (85 percent or less) and gas generator speeds are more than 5 percent apart. With these conditions in mind, the pilot was able to perform the balance of this program with no hangup by keeping the rotor speed above the noted 85-percent lower limit and gas generator speeds more closely matched and always in excess of 88 percent  $N_G$ .

Power control in the XV-9A aircraft was affected by the jet-reaction yaw valve during nonhovering flight. When the yaw valve was opened, the total engine exit area increased, which caused engine speed,  $N_G$ , and temperature,  $T_5$ , to vary.

The rotor-speed-governing system utilized a hydraulic speed servo system to drive the fuel control rotor-speed signal input. Occasional drift of the rotor-governing system would cause a mismatch in power lever angle during normal twin-engine operation. This was objectionable to the pilot, in that power lever position did not consistently reflect a given  $N_G$  or power output. For future designs, the rotor governing system should be modified to minimize this tendency to drift.

#### 4. Flying Qualities

All normal helicopter maneuvers were performed during the 15-hour flight test program within the restricted air space available at the Hughes Culver City plant. All control positions, rates, and attitudes were recorded continuously during flight, and significant quantitative data, corrected to a mid center of gravity and a reference weight, where applicable, are presented herein.

It is anticipated that during the 20-hour follow-on test program additional stability and control tests will provide sufficient data to more fully evaluate the flying qualities of the XV-9A throughout the allowable flight envelope of the aircraft.

The qualitative evaluation of the flying qualities of the current XV-9A, in general, is considered adequate for this type of research aircraft where an existing rotor system (whirl test rotor) is combined into a flight article with minimum modification to the basic rotor system. As stated in Reference 5, future redesign in the area of the hub and control system, to include the use of moderate hub restraint, would provide substantial improvement in the stability and control characteristics of the XV-9A Hot Cycle Research Aircraft.

##### a. Hover

The XV-9A in hover in ground effect at 20-foot wheel height is relatively stable. Qualitative evaluation of the control response in pitch and roll is considered adequate, but somewhat sluggish. Rotor damping in both pitch and roll is considered low. This comment is based on pilot's observations rather than measurements. No

step-type control motion tests were included in this program. It is expected that such tests will be part of the 20-hour follow-on flight test program, at which time a comparison of predicted and actual damping versus control power will be made.

This qualitative evaluation of hover flying qualities of the XV-9A from pilot comments is as predicted in Reference 5, and is directly attributed to the present free-floating hub rotor system of the XV-9A. As mentioned above, by providing a modest amount of hub elastic restraint, a substantial improvement in control response and rotor damping will result from the offset coning hinge acting as an effective offset flapping hinge.

In ground effect, the XV-9A is less stable than it is out of ground effect. As the aircraft approaches the proximity of the ground, the nose of the aircraft tends to pitch down and yaw to the right. The results of the nose-down pitching can be seen in the hover data (0 airspeed) in Figure 36. The longitudinal control position in ground effect is approximately 10 percent more aft (2 degrees cyclic) than it is out of ground effect. Although the aircraft is less stable in ground effect than out of ground effect, the pilot stated that the disturbances experienced while hovering in close proximity to the ground were no more uncomfortable than those experienced in other single-rotor helicopters under similar flight conditions.

During the early flights, the cyclic stick breakout forces were considered objectionable. Investigation indicated this characteristic was caused by the high friction in the hydraulic power-control servo valve O-ring. This friction force caused two objectionable control characteristics: (1) once the controls were displaced by the pilot, the friction force in the servo would cause the control to tend to continue the control motion; (2) to stop the control motion, the pilot would have to apply a reverse control force. The servo valve spools were reworked to reduce friction and a limited reduction was obtained; however, a further reduction in breakout forces was desirable and the use of servo spool dither was investigated.

Reference 11 reported the results of an investigation of the effects of the use of a vibrator to reduce servo valve friction. Results indicated that when the vibrator force is of the same order of magnitude as the valve friction, use of the vibrator overcomes the adverse effects of the valve friction on control characteristics. Based on these results, dither devices (vibrators) were installed

Gross Weight  $\approx 15,300$  lb  
 Sea Level Standard Day  
 $i_H = +3$

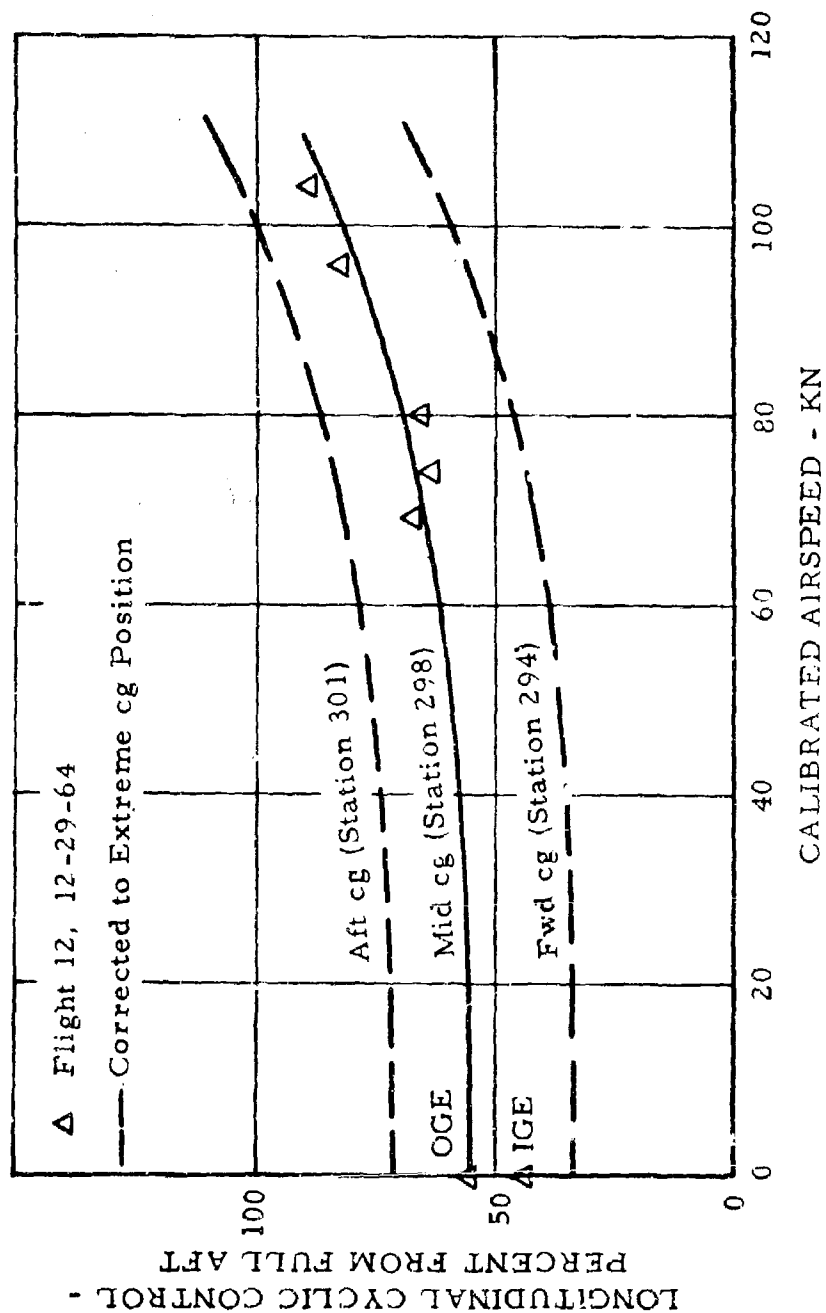


Figure 36. Level Flight Longitudinal Cyclic-Control Position Versus Airspeed.



on the servo valve input rods of the XV-9A. Pilot comments indicated that a measurable improvement was noted in the ease of controlling the cyclic stick.

Later flights also incorporated cyclic stick centering springs and electric trim actuators, which further improved the controllability of the aircraft.

b. Level Flight

Figure 36 presents the longitudinal control positions with speed. The data points are corrected to the typical mid center of gravity position (Station 298). The dash lines represent the control positions corrected to the extreme forward (Station 294) and aft (Station 301) center of gravity locations.

At the forward center of gravity positions, the aircraft can be flown to speeds greater than 120 knots with adequate control margin. At the mid center of gravity position, the maximum speed will be limited to approximately 120 knots, due to the available cyclic control travel.

For the aft center of gravity position, with the current stabilizer incidence fixed at 3-degree nose up, the corrected data indicates that the aircraft forward speed will be limited by the available cyclic travel to approximately 100 knots. If the control travel margin per MIL-H-8501A were required, the maximum speed would be reduced to approximately 90 knots. However, it is anticipated that these speed limits will be increased during the 20-hour follow-on test program by investigating various methods, such as increased stabilizer incidence, increased rotor speed, or increased cyclic control travel from the present limits of 10 degrees forward and 10 degrees aft.

During the early part of the test program, the pilot was required to hold 20- to 30-percent (from neutral) right pedal to maintain a straight heading during forward speeds of 40 knots to maximum speeds tested. The cause was determined by measuring the individual V-tail surface bending loads, and it was established that there existed a differential load between the two surfaces, causing a net yawing moment to the left. This differential tail load is probably caused by small differences in incidence of the two tail surfaces, or possibly by differential angle of attack of the two surfaces caused by the rotor flow field. This problem was corrected

by rerigging the rudder surfaces to permit the use of essentially neutral pedal (and hence zero-yaw valve opening) in cruise flight.

Qualitative evaluation of the dynamic longitudinal and directional stability in forward flight is considered adequate for the current program. However, these characteristics will be evaluated more precisely during the follow-on 20-hour test program by evaluating time histories of displace and hold and control pulse maneuvers.

c. Maneuvers

(1) Hover Turns

The directional control response of the current XV-9A in hover turns is considered adequate. Some of the early problems and fixes are discussed in the following paragraphs. Also discussed is the anticipated improvement in directional control response of the XV-9A for the follow-on 20-hour test program.

The directional control response in hover turns, during the early part of the test program, was considered inadequate. As predicted, the XV-9A (which has a yaw jet but no tail rotor) has low damping in yaw.

Pedal forces were initially high; however, it was found that by exercising the pedals during flight the forces would decrease to a satisfactory level. Investigation indicated that the high pedal forces were caused by high seal friction and by high pressure loads acting on the yaw valve rotor. Cutting back the stiffener lip on the yaw control rotor and modifying the rotor seals relieved the pressure and friction loads and significantly reduced the pedal forces.

There still existed the problem of inadequate yaw control. Investigation indicated a large discrepancy between the measured initial yaw acceleration and the predicted yaw acceleration using the measured thrust from the whirl tower yaw valve tests. Installation of a pressure pickup in the exhaust extension duct, a component not installed on the whirl test configuration, indicated that a negative pressure acting on the exhaust extension duct flange was cancelling approximately 40 percent of the yaw valve thrust. Modification of the exhaust extension duct flange, by adding cutouts around the duct periphery

adjacent to the attach flange, increased the yaw thrust by a substantial amount.

Figure 37 shows the measured yaw rates for full pedal deflection for the original and the modified yaw valves. It can be seen that the initial yaw acceleration (slope of the yaw rate) was more than doubled, from 5 degrees per second<sup>2</sup> for the original yaw valve to 12 degrees per second<sup>2</sup> for the modified yaw valve. However, this increase in yaw acceleration is still below the MIL-H-8501A requirements. The reason for the reduced yaw acceleration over that predicted in Reference 5 stems from two factors: (1) a 25-percent increase in yaw inertia over the original estimate; (2) the present yaw control system limits the yaw valve opening to a maximum of 75 percent for full pedal deflections. It is anticipated that a modified yaw control cable system would allow 100-percent yaw valve opening, and thus increase the yaw thrust output by 35 percent.

## (2) Sideward Flight

Sideward flights were conducted at an average gross weight of 15,300 pounds and corrected to the mid center of gravity location (Station 298). With the modified yaw valves, the XV-9A moves relatively easily into sideward flight. However, pilot comments indicate that the control response of a jet yaw control is somewhat sluggish as compared with a tail rotor control system.

The control positions obtained are presented in Figure 38. As can be seen, during sideward flight the cyclic stick moves aft and in the direction of flight laterally. Aft cyclic movements reach a maximum at approximately 17 knots to the left and somewhat more than 20 knots to the right. The pedal movements reach a maximum at approximately 20 knots in either direction.

## (3) Rearward Flight

The XV-9A moves easily into rearward flight. The nose of the aircraft tends to remain low even at higher rearward speeds. This is probably due to an uplift on the V-tail. The longitudinal cyclic control positions obtained are shown in Figure 39. As can be seen, as rearward speed is increased, the cyclic stick is moved aft from 50 percent to 25 percent

Gross Weight  $\approx$  15,300 lb

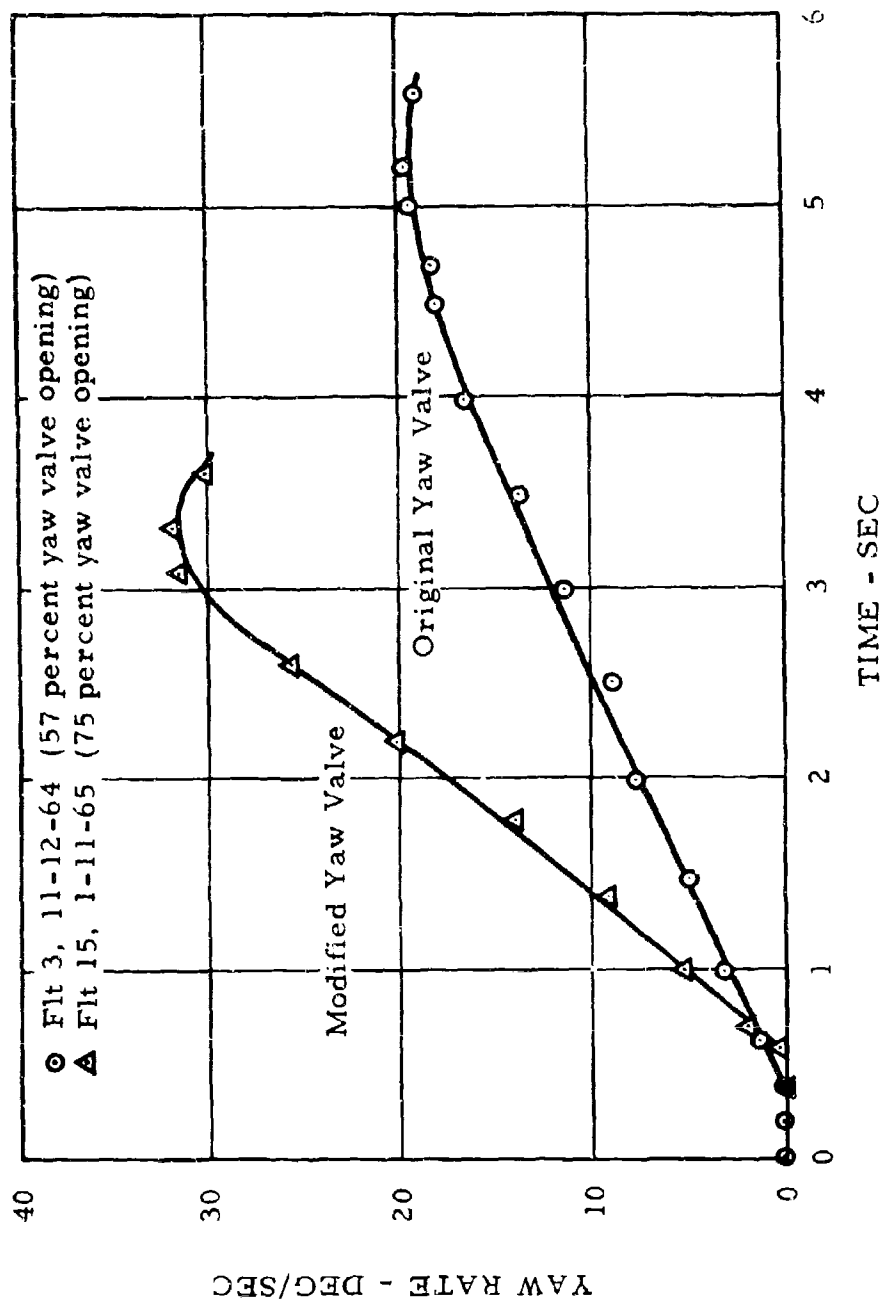
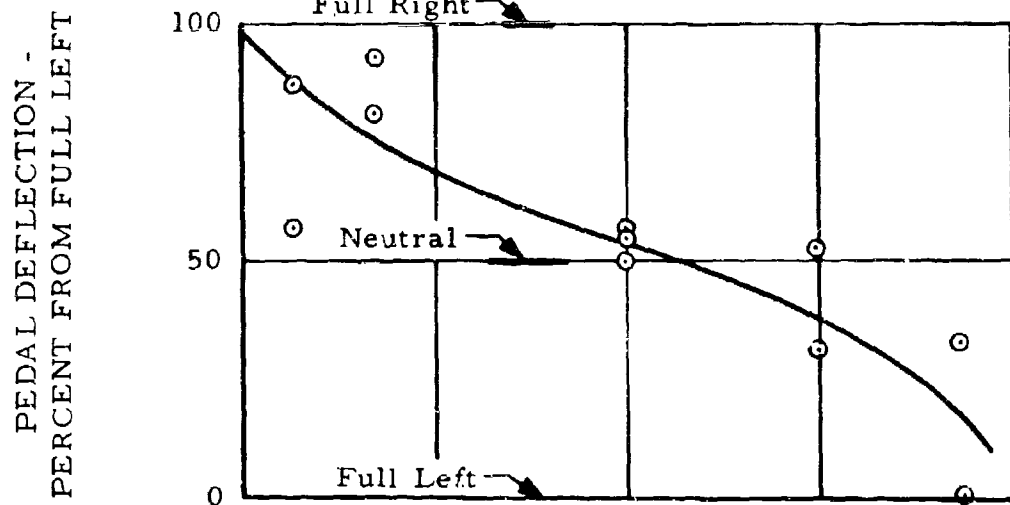


Figure 37. Full Pedal Deflection Hover Turns.

Gross Weight  $\approx 15,300$  lb  
 Lateral cg on Rotor  $\bar{C}_L$   
 Longitudinal cg = Station 298



Flights 11, 15, and 18

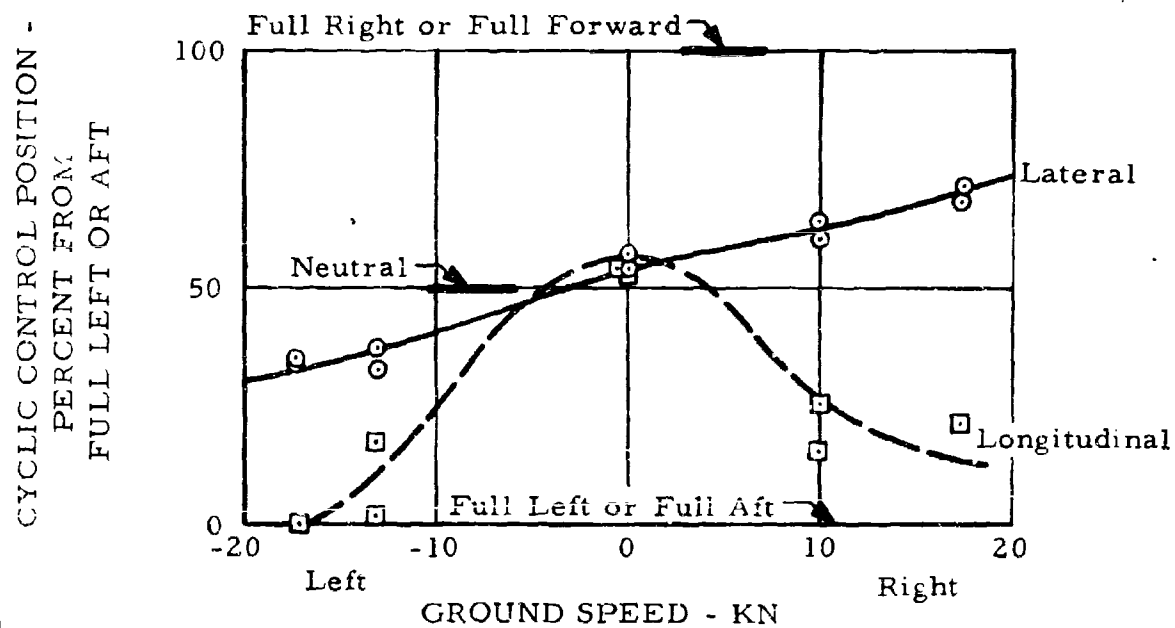


Figure 38. Sideward Flight Control Position Versus Ground Speed.

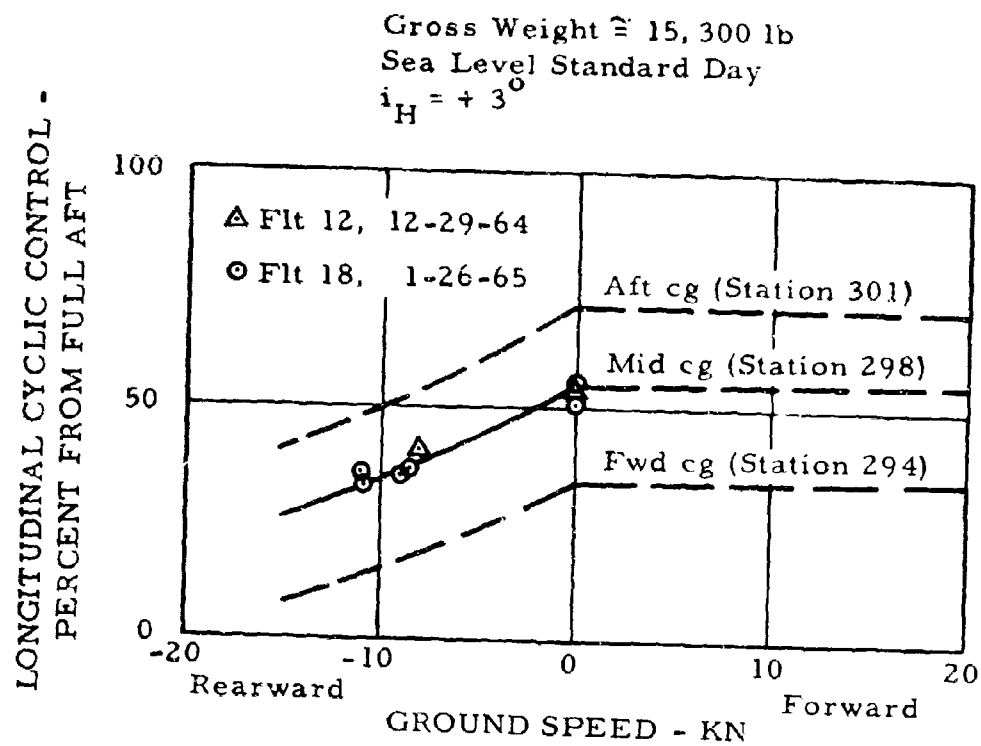


Figure 39. Rearward Flight Longitudinal Cyclic-Control Position Versus Speed.

at approximately 15 knots for the mid center of gravity location. For the critical forward center of gravity location, the maximum aft cyclic will limit the rearward speed to approximately 20 knots.

(4) Climb

The flying qualities during a climb are considered adequate. Vibration levels tended to increase with increasing power.

(5) Turns

The flying qualities during forward flight turns were considered normal. No adverse pilot comments were noted. Vibration levels were substantially the same in normal turns as in level flight at the same speed.

(6) Descents

The handling characteristics during an idle-power descent are considered adequate. However, some adverse comments from the pilot were noted during descents; specifically, that during descents the cyclic stick position was considered too far aft. This will require further investigation during the follow-on test program.

(7) Approach to Land and Touchdown

The handling characteristics during approach to land and touchdown are considered adequate. Flare slows forward speed effectively. Pilot comments indicate that the vibration level during transition and flare is similar to that of large shaft-driven single-rotor helicopters. During the flare, the aircraft has a tendency to yaw nose right, requiring some left pedal input.

5. Vibration

Presented as Figures 40 through 42 are plots of vibratory acceleration versus calibrated airspeed, as follows:

Figure 40. Maximum Pilot Vertical Acceleration Versus Calibrated Airspeed.

Figure 41. Maximum Engine 1 Vertical and Lateral Acceleration Versus Calibrated Airspeed.

Figure 42. Maximum Engine 2 Vertical and Lateral Acceleration Versus Calibrated Airspeed.

The pilot vertical accelerometer was attached to the fuselage structure in the area below the pilot's seat. The engine accelerometers were attached to the forward end of the engine mount structure.

The vibration level shown on Figure 40 is slightly higher than specified in MIL-H-8501A. However, two factors should be taken into account: (1) vibration levels measured on structure are generally higher than those at the pilot's seat; (2) there is a fuselage resonance near 3 per rev (see Fuselage Shake Test, page 15).

Pilot vertical vibration during transition generally peaked at approximately  $\pm 0.34$  g. The peak during a flare was  $\pm 0.56$  g, with the vibration level generally around  $\pm 0.34$  to  $\pm 0.37$  g. A normal turn in the flight pattern resulted in  $\pm 0.32$  g. During hovering the pilot vertical vibration was  $\pm 0.13$  g.

## 6. Miscellaneous Hovering Tests

### a. Sound Power Level

Sound power level data were recorded during hovering flight and during 90-knot flyover at 50-foot altitude. In general, the sound levels agreed with data recorded during previous whirl tests. Sound data were recorded at from 50- to 400-foot distance from the center of the rotor while hovering and with the aircraft on the ground with the rotor turning at 100-percent rotor speed. These data are presented in Figures 43, 44, and 45.

The XV-9A sound level was not objectionable to nearby observers. The ground crew members in close proximity to the aircraft during starting and shutdown used standard jet sound suppressor muffs.

Sound level measured inside the cockpit during flight was 109 decibels. This was not considered objectionable to the pilot when wearing a standard military pilot's protective headgear. Radio communication during all ground and flight conditions was satisfactory with cockpit doors closed.



Flight 17 - Level Flight

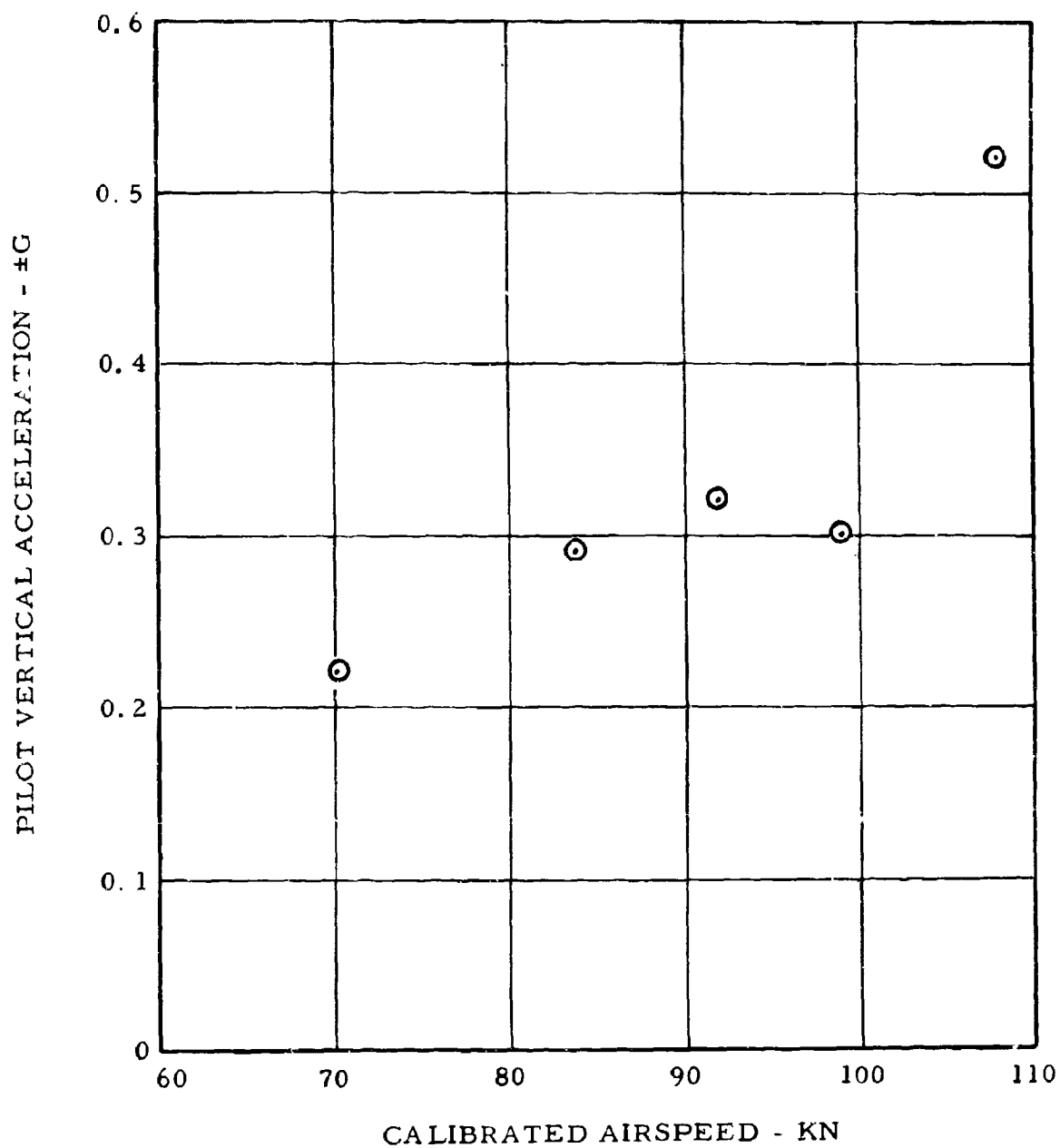


Figure 40. Maximum Pilot Vertical Acceleration Versus Calibrated Airspeed.

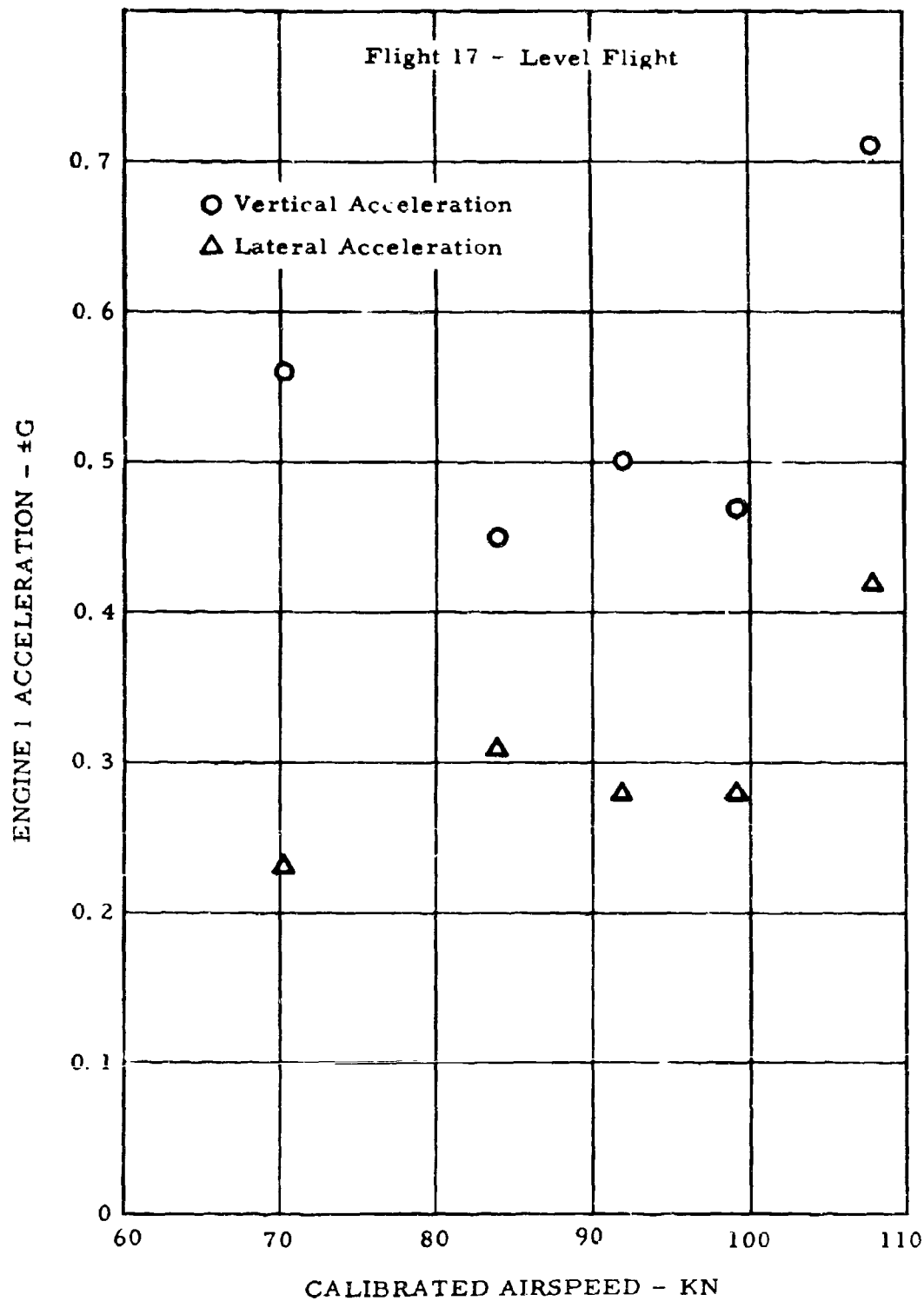


Figure 41. Maximum Engine 1 Acceleration Versus Calibrated Airspeed.

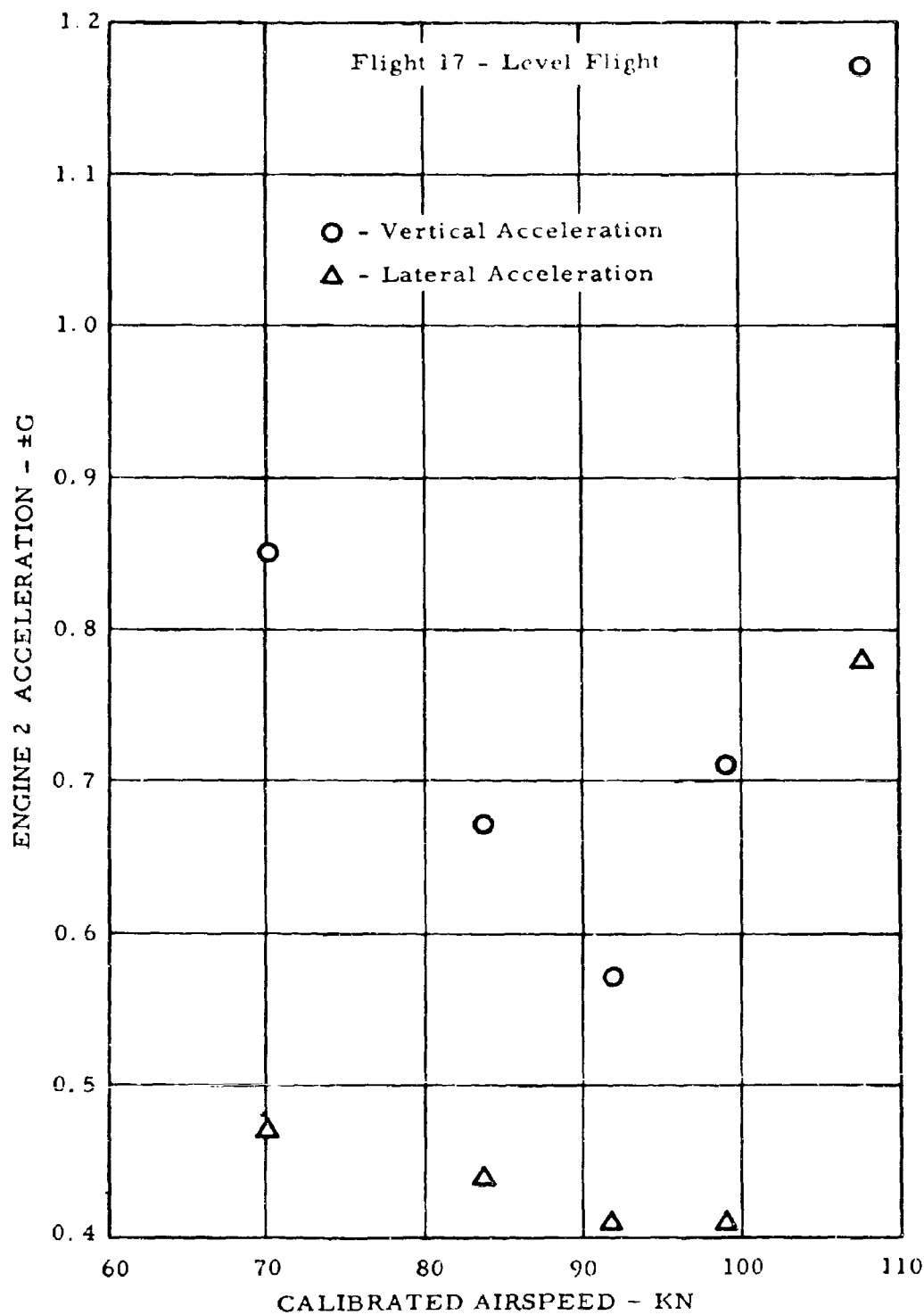
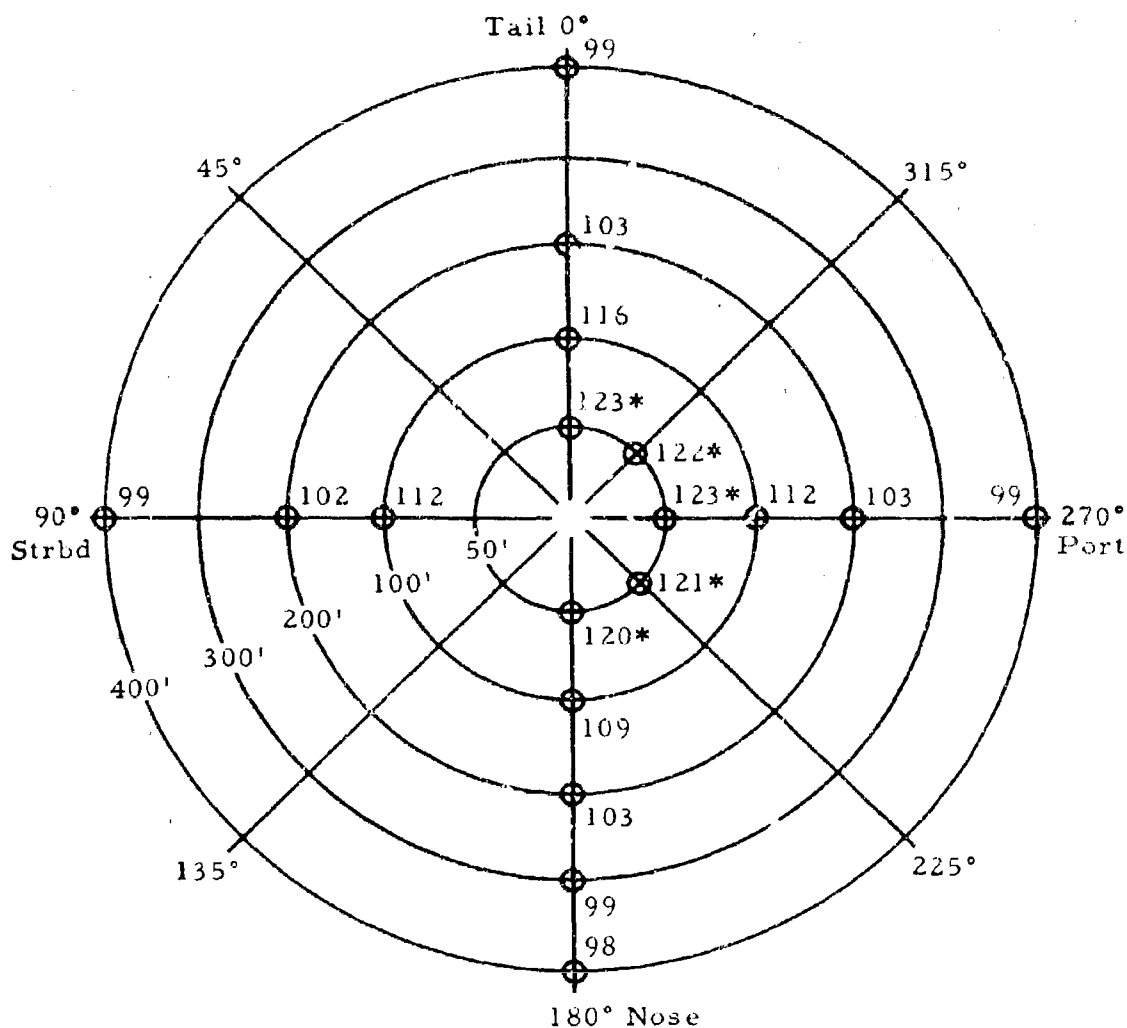


Figure 42. Maximum Engine 2 Acceleration Versus Calibrated Airspeed.

Hover at 15-foot altitude, except \* at 6 feet

Gross weight = 14,000 ± 500 lb



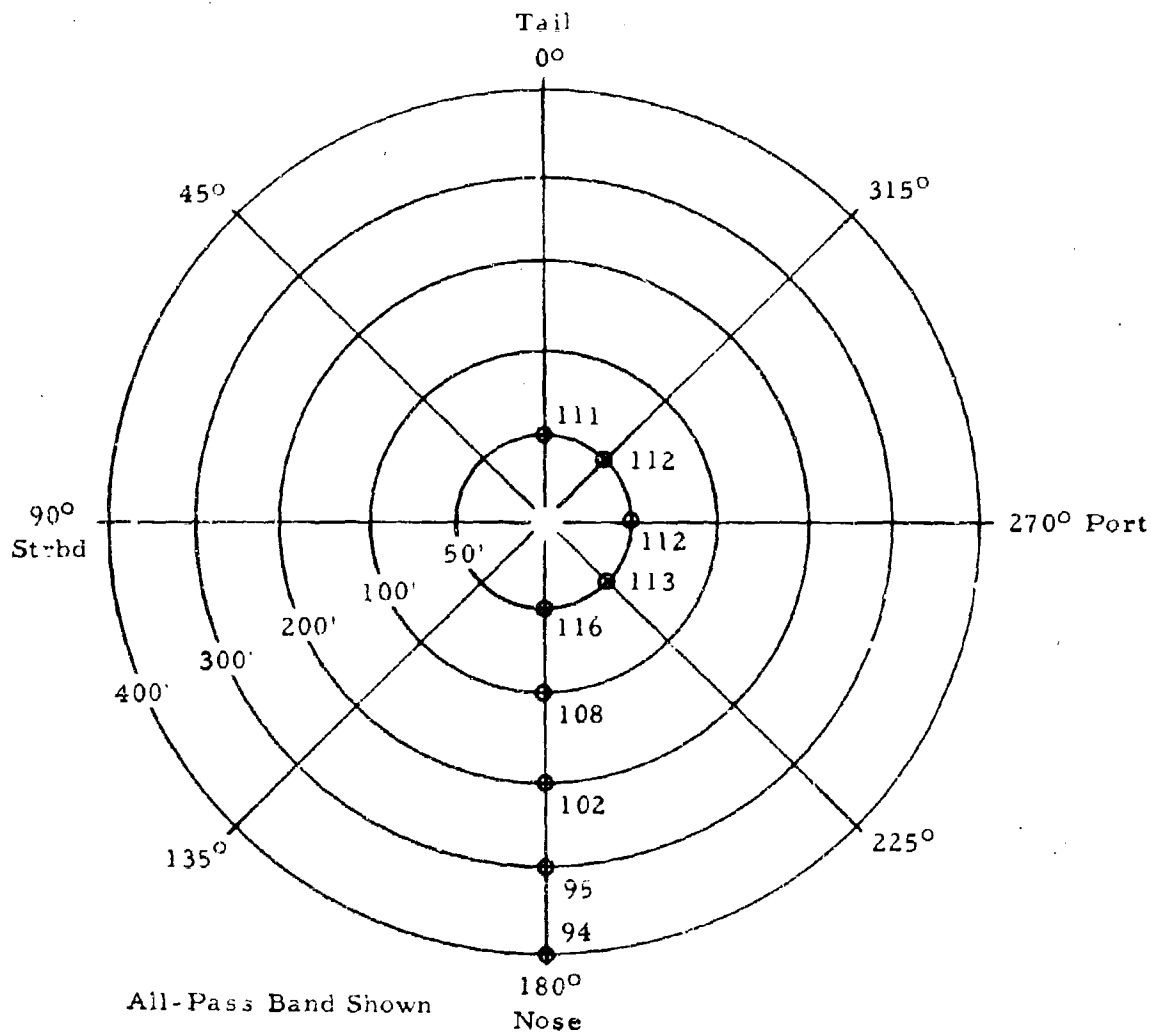
All-pass band shown

Equipment used: General Radio Corporation

1. Octave Band Analyzer
2. Sound Level Meter, Type 1551-C,  
C Weighting
3. Graphic Level Recorder, Type 1521-A
4. Crystal Microphone

Figure 43. Sound Pressure Level In Hover.

Ground operation; rotor at 100-percent rpm, flat pitch



Equipment Used: General Radio Corporation

1. Octave Band Analyzer
2. Sound Level Meter, Type 1551-C,  
C Weighting
3. Graphic Level Recorder, Type 1521-A
4. Crystal Microphone

Figure 44. Sound Pressure Level In Ground Operation.

Flyover at 50-foot altitude, 90 knots

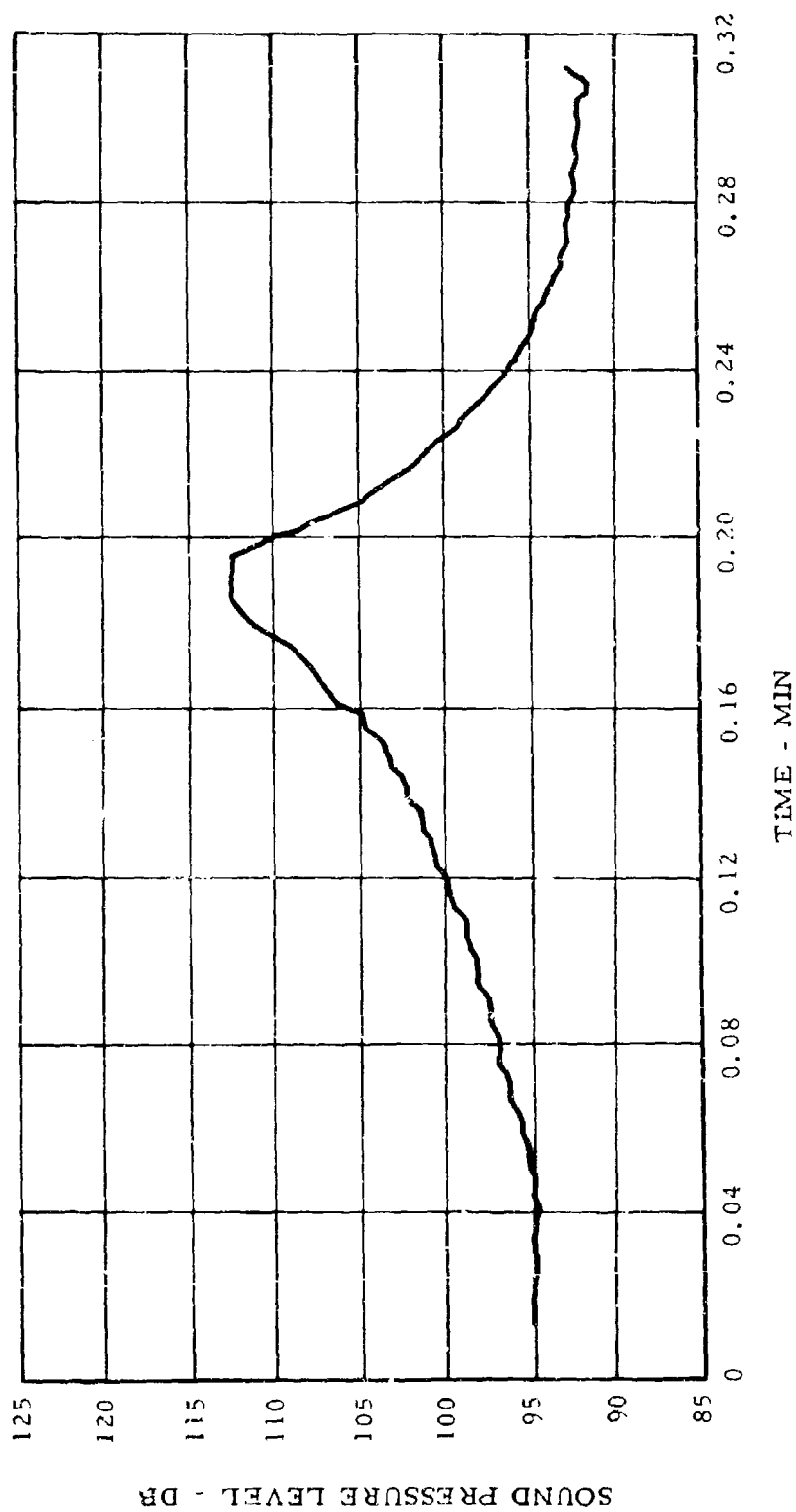


Figure 45. Sound Pressure Level In Flight.

b. Rotor Downwash

Rotor downwash was measured with a hand-held anemometer, while the helicopter hovered at a 27-foot rotor height. The anemometer was held 4 feet above ground level and oriented to measure the downwash vertical flow. Maximum velocity measured was 73 feet per second at approximately 70-percent blade radius and 18 feet per second near the center of the rotor. These data agree closely with downwash data recorded during whirl tests.

The aircraft was hovered at 6-foot wheel height over unprepared sod and dirt surfaces that varied from dead to green grass on the sod surface and from loose dirt to small rocks on the dirt surface. There was no engine foreign object damage (FOD) or rotor blade damage incurred. Recirculation effects during hover were of the magnitude of a 5- to 7-degree F rise in engine inlet temperature when hovering in still air.

c. Static Electricity Buildup

Static electricity buildup was measured during hovering flight by means of a high-voltage cable attached to the nose of the aircraft and instruments located on the ground for measurement of electrostatic voltage and charging current. The cable was kept off the ground by a flexible wooden standard, and a steel grounding stake was imbedded in the ground near the equipment.

The XV-9A was hovered at approximately 20-foot wheel height, and the following average readings were obtained:

Electrostatic voltage	7 to 9 kilovolts
Charging current	2 microamperes
Capacitance	Negligible

Measuring Equipment

Impedance bridge	ESI Model 250-DA
Microammeter	Simpson, 0 to 15 microamperes dc
Electrostatic voltmeter	0 to 30 kilovolts, Scientific Research Corporation Model ESH-NOT

Because of the high humidity (75 percent) at the time of the test, the data obtained may be lower than for conditions in drier air.

However, the reduced electrostatic voltage buildup may be the result of release of hot (ionized) gases ejected from the tip cascade nozzles at the blade tips.



## DESCRIPTION OF TEST AIRCRAFT

The XV-9A Hot Cycle Research Aircraft is a helicopter having a three-bladed Hot Cycle pressure jet rotor driven by high-energy gases produced by two General Electric YT-64 gas generators. The exhaust gas flow produced by the YT-64 gas generators is ducted through J-85 diverter valves, transition ducts, hub, and blade ducts to blade-tip cascade nozzles that produce the rotor driving torque.

A general arrangement drawing of the aircraft follows (Figure 46). A detailed description of the aircraft structure, systems, characteristics, and design criteria is given in Reference 4.

## WEIGHT SUMMARY

	<u>Pounds</u>
Empty weight	8,656
Design minimum gross weight	10,000
Design gross weight	15,300
Design alternate overload gross weight (external load)	25,500
Aircraft weight with zero fuel, crew, and normal instrumentation (actual)	10,645
Fuel (maximum)	3,200
Ballast (internal)	1,455

## PERFORMANCE (Design Objectives)

<u>Condition</u>	<u>Gross Weight (lb)</u>	<u>Altitude and Temperature</u>	<u>Speed (kn)</u>
Maximum Speed	15,300	Sea Level Standard	140
Maximum Speed	10,000	Sea Level Standard	150

## ROTOR CHARACTERISTICS

Number of blades	3
Rotor radius	27.6 feet
Blade area (3 blades)	217.5 square feet
Disc area	2,392.0 square feet
Rotor solidity	0.091
Blade chord	31.5 inches

Blade airfoil  
Blade twist  
Hot gas ducts

NACA 0018  
-8 degrees

Number of ducts per blade  
Total duct area per blade  
Blade-tip cascade area per  
blade (closure valve open)

2  
54.8 square inches  
37.5 square inches

### ROTOR SPEED

	<u>rpm</u>	<u>V<sub>T</sub></u> <u>(fps)</u>
Design operational, power-on or power-off	243	700
Design minimum, power-on	225	(100-percent N <sub>R</sub> ) 648
Design maximum, power-on (red line)	255	734
Design maximum, power-off (red line)	280	807
Rotor speed, limit, power-on or power-off	295	848

### POWERPLANTS

General Electric YT-64 gas  
generators with modified  
first-stage compressor blading

2

### OVERALL DIMENSIONS

	<u>Feet</u>
Aircraft length (rotor turning)	59.70
Fuselage length	44.17
Tread of main wheels	11.00
Height (to top of rotor hub)	12.40
Width (across lateral pylons)	12.20

### EMPENNAGE

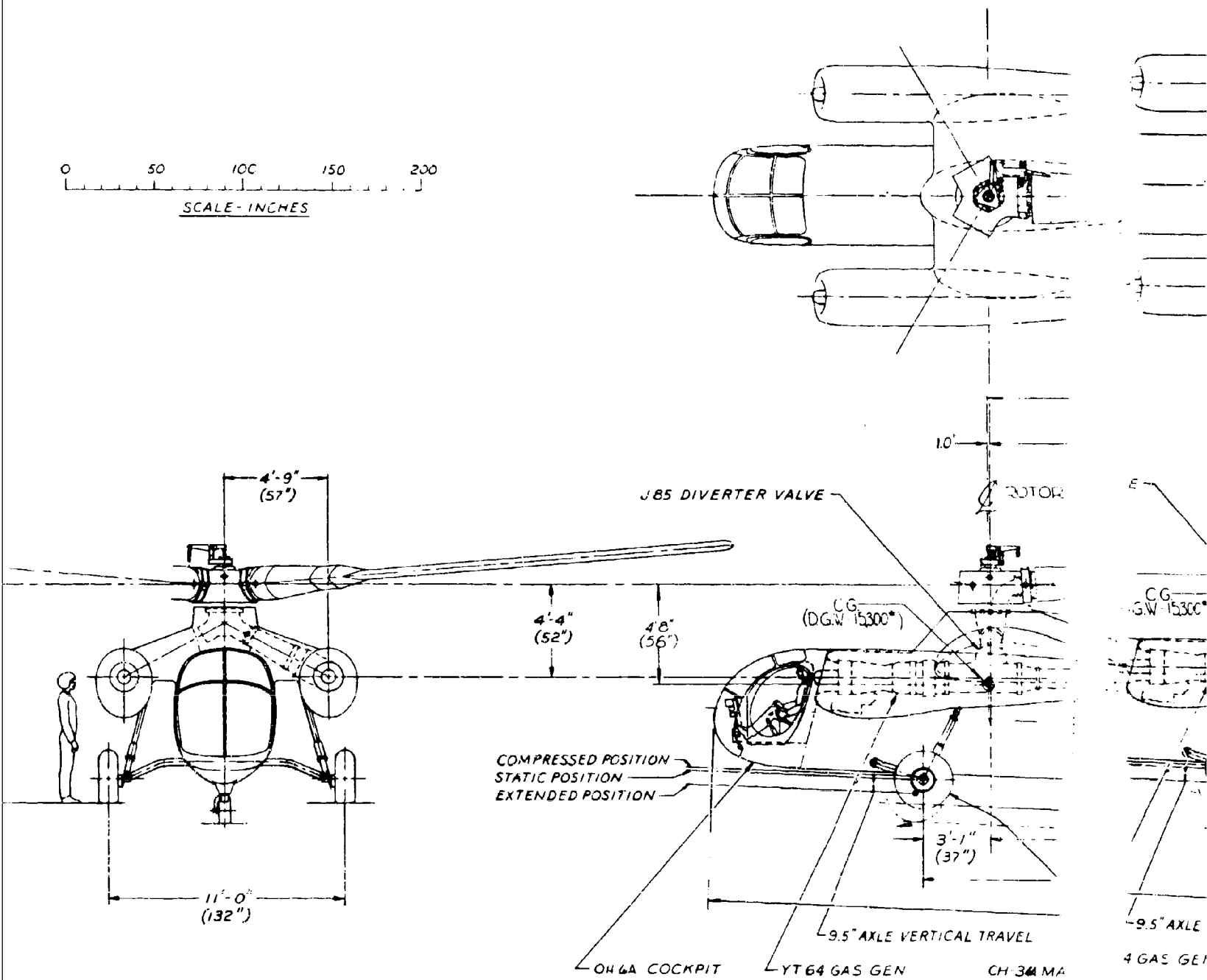
Area (total)	54.00 square feet
Dihedral	45.0 degrees
Sweep	7.5 degrees

10'-4"  
(124")

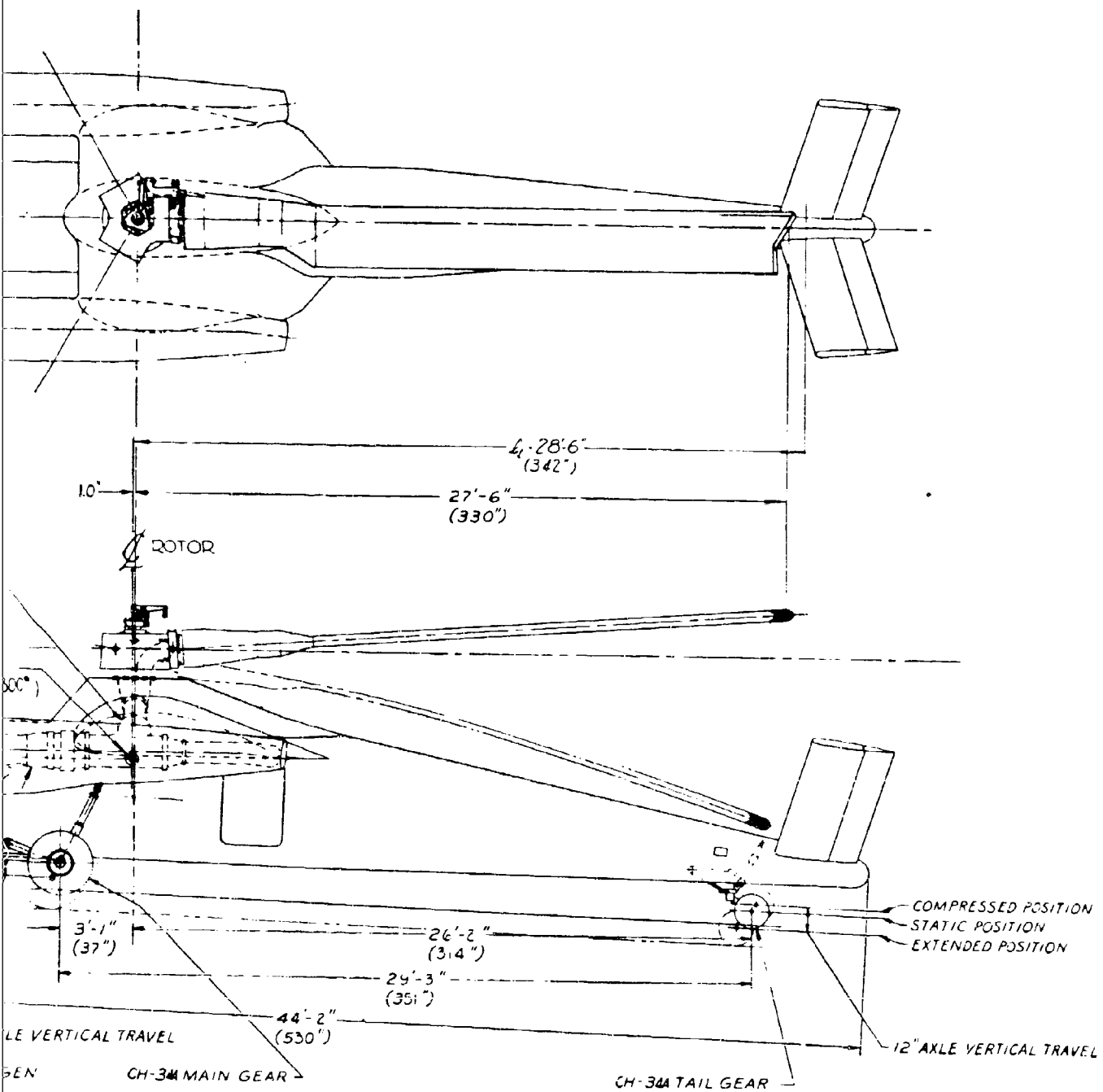


Figure 46

A



16. General Arrangement, XV-9A Hot Cycle Research Aircraft.



Incidence (referenced to rotor shaft)	1.0 degree
Chord	±5 degree adjustment
Span	3.50 feet
Aspect ratio (geometric)	15.40 feet
Airfoil	4.35
Rudder chord (57.5 percent, including overhang)	NACA 0012
Rudder span	1.31 feet
Rudder area	15.40 feet
Rudder deflection	19.90 square feet
	±20.0 degrees

#### MAXIMUM CONTROL DISPLACEMENTS

Cyclic control	
Longitudinal cyclic pitch	10 degrees
Longitudinal cyclic stick travel	11 inches
Lateral cyclic pitch	±7 degrees
Lateral cyclic pitch stick travel	10 inches
Collective	
Collective-pitch travel	12 degrees
Collective-stick travel	7.5 inches
Rudder pedal (from neutral)	
Full left	3.0 inches
Full right	3.0 inches

## REFERENCES

1. Flight Test Program Plan, XV-9A Hot Cycle Research Aircraft, Hughes Tool Company, Aircraft Division Report HTC-AD 64-32 (385-T-18), September 1964.
2. Program Plan, Preflight and Tie-Down Tests, XV-9A Hot Cycle Research Aircraft, Hughes Tool Company, Aircraft Division Report HTC-AD 64-22 (385-T-15), 15 July 1964.
3. Component Testing XV-9A Hot Cycle Research Aircraft Summary Report, Hughes Tool Company, Aircraft Division Report HTC-AD 64-26 (385-T-16), USAAVLABS Technical Report 65-38, December 1965.
4. Aircraft Design, XV-9A Hot Cycle Research Aircraft Summary Report, Hughes Tool Company, Aircraft Division Report HTC-AD 64-11 (385-X-05), USAAVLABS Technical Report 65-29, August 1965.
5. Preliminary Design Study - Hot Cycle Research Aircraft Summary Report, Hughes Tool Company, Aircraft Division Report HTC-AD 62-31 (385-X-02), TCREC\* Technical Report 62-102, March 1963.
6. Helicopter Static Electricity Discharging Device, TCREC Technical Report 62-33, December 1962.
7. Engine and Whirl Tests, XV-9A Hot Cycle Research Aircraft Summary Report, Hughes Tool Company, Aircraft Division Report HTC-AD 64-23, USATRECOM Technical Report 64-67, December 1964.
8. Mulready, R. C., The Ideal Temperature Rise Due to Constant Pressure Combustion of Hydrocarbon Fuels, United Aircraft Corporation Meteor Report UAC-9, July 1947 (See also NACA TN 2357, 1951).
9. Model Specification, XV-9A Hot Cycle Research Aircraft, Rev E, Hughes Tool Company, Aircraft Division Report HTC-AD 62-22 (385-X-01), 15 October 1963.
10. QT Gas Conditions, General Electric Technical Memorandum TM S6-62SE 1570, 1 June 1962.
11. Investigation of Effect of Reduction of Valve Friction in a Power Control System by Use of a Vibrator, NACA RM-L55E18a, July 1955.

\*Now USAAVLABS (U. S. Army Aviation Materiel Laboratories).

## DISTRIBUTION

US Army Materiel Command	6
US Army Mobility Command	5
US Army Aviation Materiel Command	5
Chief of R&D, DA	2
US Army Aviation Materiel Laboratories	17
US Army R&D Group (Europe)	2
US Army Engineer R&D Laboratories	2
US Army Limited War Laboratory	1
US Army Human Engineering Laboratories	1
US Army Research Office-Durham	1
US Army Test and Evaluation Command	1
Plastics Technical Evaluation Center	1
US Army Medical R&D Command	1
US Army Engineer Waterways Experiment Station	1
US Army Combat Developments Command, Fort Belvoir	2
US Army Combat Developments Command Transportation Agency	1
US Army Combat Developments Command Experimentation Command	3
US Army Combat Developments Command Aviation Agency	2
US Army War College	2
US Army Command and General Staff College	1
US Army Transportation School	2
US Army Aviation School	1
US Army Quartermaster School	2
US Army Transportation Center and Fort Eustis	2
US Army Infantry Center	2
US Army Tank-Automotive Center	2
US Army Aviation Maintenance Center	2
US Army Armor and Engineer Board	1
US Army Electronics Command	2
US Army Aviation Test Activity	2
Air Force Flight Test Center, Edwards AFB	2
US Army Field Office, AFSC, Andrews AFB	1
Air Force Systems Command, Wright-Patterson AFB	3
Air Force Flight Dynamics Laboratory, Wright-Patterson AFB	1
Systems Engineering Group (RTD), Wright-Patterson AFB	2
Air Proving Ground Center, Eglin AFB	1
Bureau of Ships, DN	1
Bureau of Naval Weapons, DN	6
Office of Naval Research	4
Chief of Naval Research	1
US Naval Research Laboratory	1
US Naval Air Station, Patuxent River	2
Bureau of Medicine and Surgery, DN	4
US Naval Air Station, Norfolk	1

David Taylor Model Basin	1
Commandant of the Marine Corps	1
Marine Corps Liaison Officer, US Army Transportation School	1
Testing and Development Division, US Coast Guard	1
Ames Research Center, NASA	1
Lewis Research Center, NASA	1
Manned Spacecraft Center, NASA	1
NASA Representative, Scientific and Technical Information Facility	2
Research Analysis Corporation	1
NAFEC Library (FAA)	2
National Tillage Machinery Laboratory	1
US Army Human Research Unit	2
Electronics Research Laboratories, Columbia University	1
US Army Board for Aviation Accident Research	1
Bureau of Safety, Civil Aeronautics Board	2
US Naval Aviation Safety Center	2
Federal Aviation Agency, Washington, D. C.	1
CARI Library, FAA	1
Bureau of Flight Standards, FAA	1
Civil Aeromedical Research Institute, FAA	2
The Surgeon General	1
Armed Forces Institute of Pathology	1
US Department of Health, Education, and Welfare	1
Aviation Safety Engineering and Research	1
Flight Safety Foundation, Inc.	1
Defense Documentation Center	20
US Government Printing Office	2



## APPENDIX I DESCRIPTION OF TEST INSTRUMENTATION

For the 15-hour flight test program, the XV-9A Hot Cycle Research Aircraft was equipped for continuous onboard recording of instrumentation measurements and pilot comments during all flight test operations. The recording equipment provided permanent records that were later analyzed to obtain required test data. Test instrumentation (Figure 47) was used to measure flight parameters, engine and rotor performance, stability and control characteristics, dynamic characteristics, structural loads, and structural temperatures.

### RECORDING EQUIPMENT

#### Oscillographs

Two 50-channel oscillographs were used for recording strain-gage and transducer outputs, as listed on pages 117 through 119. Each oscillograph was equipped with a 400-foot-capacity paper magazine. The oscillographs were set to run at one-inch-per-second paper speed, with provision for a 10-inch-per-second jump speed controlled by a switch on the pilot's cyclic stick for high-speed data acquisition. Ansco color paper was used for all operations. Results were very satisfactory, and data reduction was simplified by having four different color data traces available for trace identification and separation.

The strain-gage bridges on the rotor were plugged into junction boxes on the rotor head that were connected to a 200-track slip ring. The slip ring installation is shown in Figure 48. From the slip ring, the wires ran to bridge balance boxes. These balance boxes had the capability of being used in a common power configuration. The use of common power greatly reduced the number of slip ring tracks required for a given number of bridges. For strain gages and transducers whose outputs did not pass through the slip ring, additional balance boxes were used. These balance boxes employed an individual voltage adjustment on each channel for attenuation. The oscillographs and balance boxes are shown in Figures 49 and 50.

#### Temperature Recorders

Two potentiometer-type 12-point thermocouple temperature recorders (Figures 50 and 51) were used to monitor rotor and fuselage temperatures as listed on pages 119 and 120. Chromel-alumel thermocouples

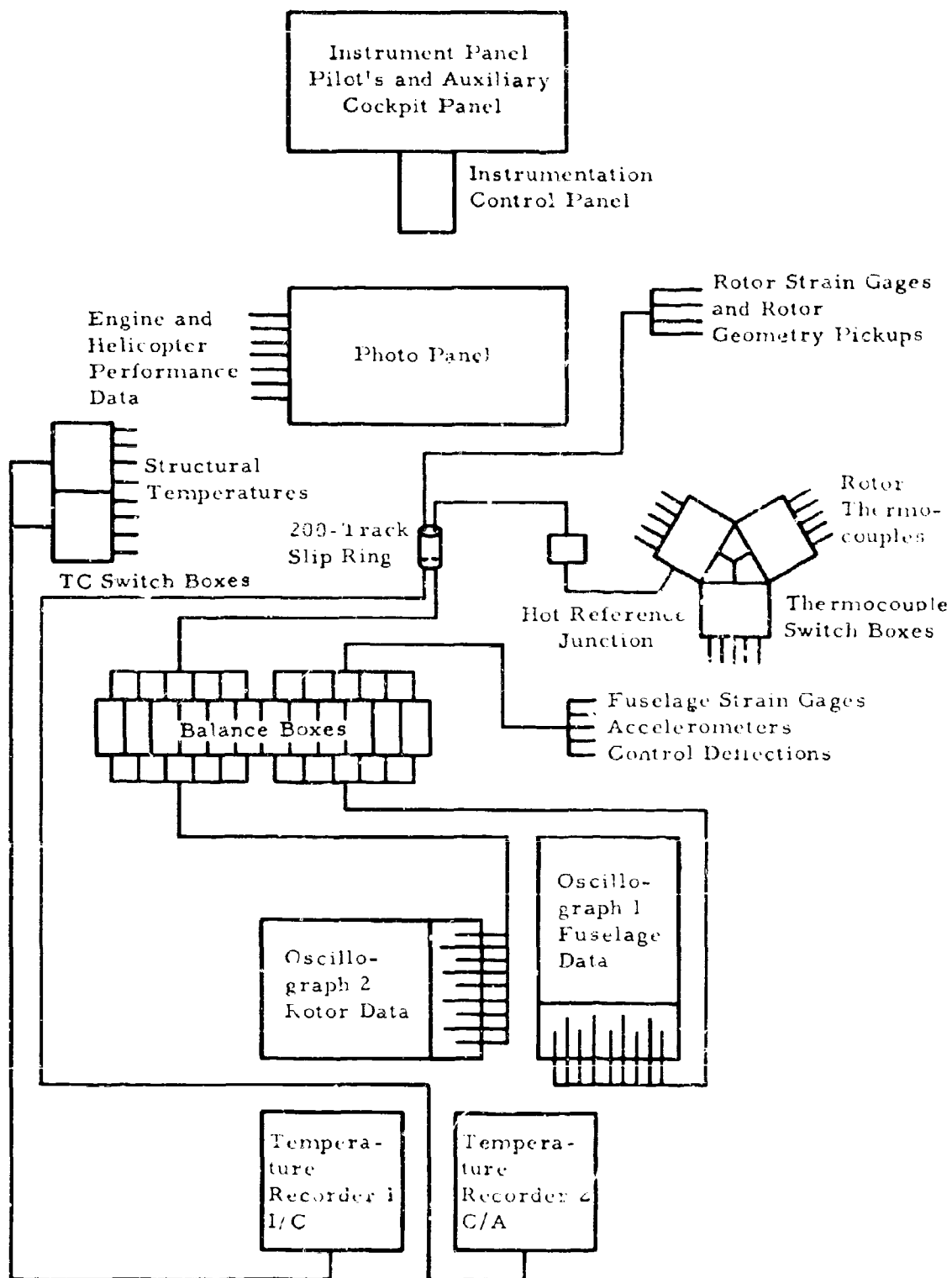


Figure 47. Instrumentation Schematic.

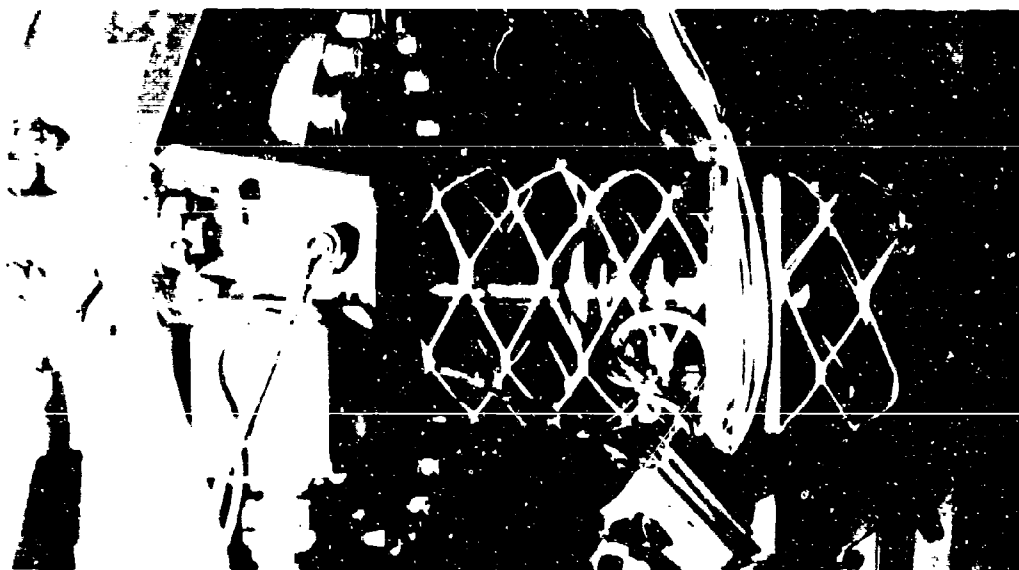


Figure 48. Rotor Slip Ring.

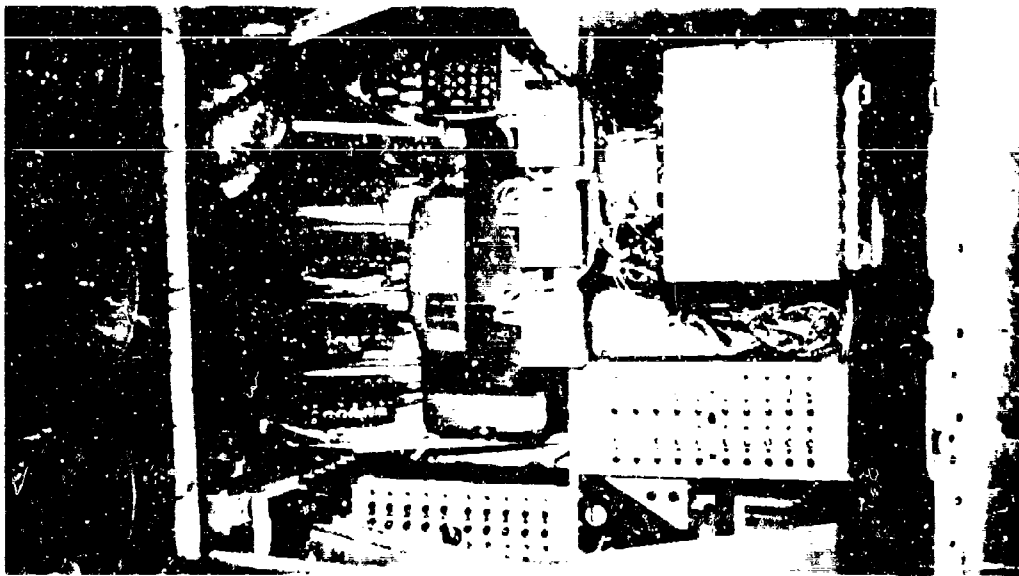


Figure 49. Oscillograph Installations

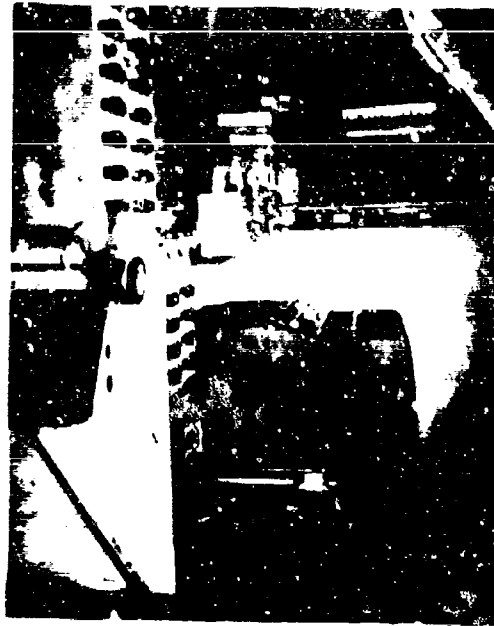


Figure 50. View of Oscillographs and Temperature Recorders, Looking Aft.

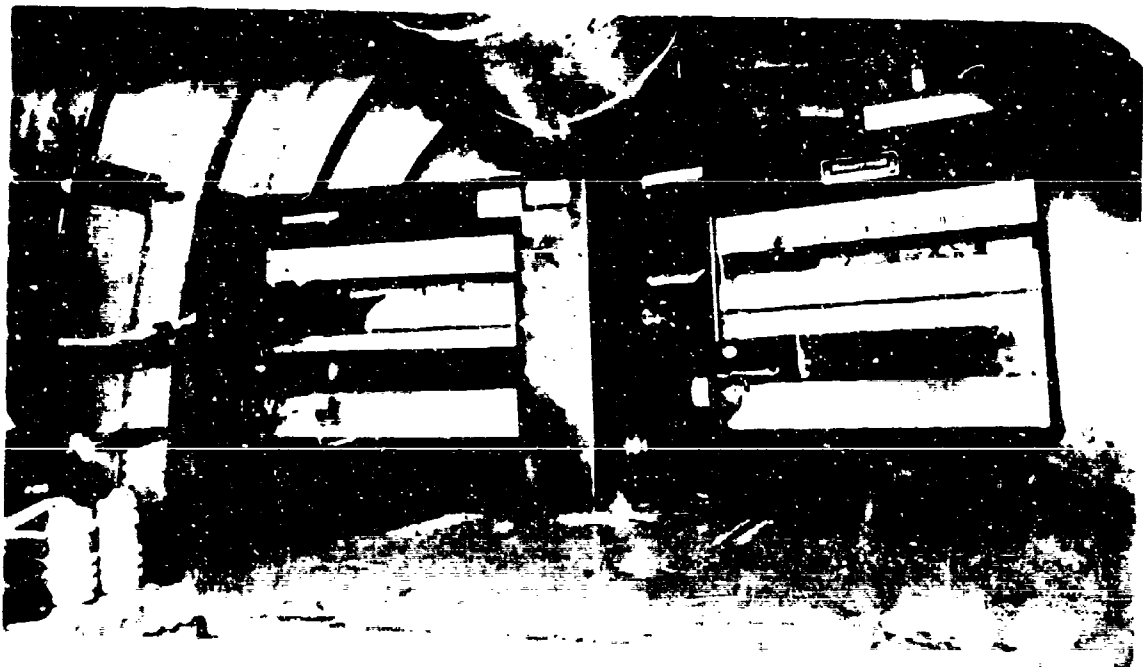


Figure 51. Temperature Recorder Installations.

were used for rotor measurements, and iron-constantan thermocouples were used for fuselage measurements.

Switching boxes were used to provide 120 rotor and 120 fuselage temperature locations. Output from the rotor thermocouple switching boxes (Figure 52) was compared with a hot reference junction before the slip ring to prevent end-junction dissimilar metals from forming a thermocouple that could introduce error into the measurement since the slip ring had gold contacts. A hot reference junction was not used in the fuselage thermocouple circuit, and iron-constantan wires were used all the way to the Brown recorders.

#### Photopanel

The photopanel (Figures 53 and 54) was used to monitor engine performance functions and flight parameters for analysis and evaluation of the Hot Cycle propulsion system. Gages used in the photopanel, as listed on page 117, were standard calibrated instrument-panel-type gages as used in the pilot's panel. A 35mm. sequence camera with a 400-foot film magazine operating at one frame per second was used for recording. A jump-speed switch on the pilot's cyclic stick was used to increase operating speed to 8 frames per second for high-speed data acquisition. Satisfactory results were obtained using panchromatic film and the reflected light of two 32-volt 250-watt lamps operating at 28 volts.

#### Tape Recorder

A battery-powered tape recorder was used to monitor all radio communication between the pilot and the ground observers. Data was read off the instrument panel by the pilot along with a data correlation number to establish flight parameters during a test point. The data correlation system is described below. Tape speed used was 1-7/8 inch per second using a 1,200-foot spool of Mylar tape, which provided two hours of recording.

#### Data Correlation

With flight data being recorded on various different pieces of equipment, it was necessary to incorporate a data correlation system to simplify the task of data reduction after a test flight. The data correlation system provided a timing number on all instrumentation records simultaneously at two-second intervals. This system was activated by an intervalometer that triggered the following: (1) counters on the

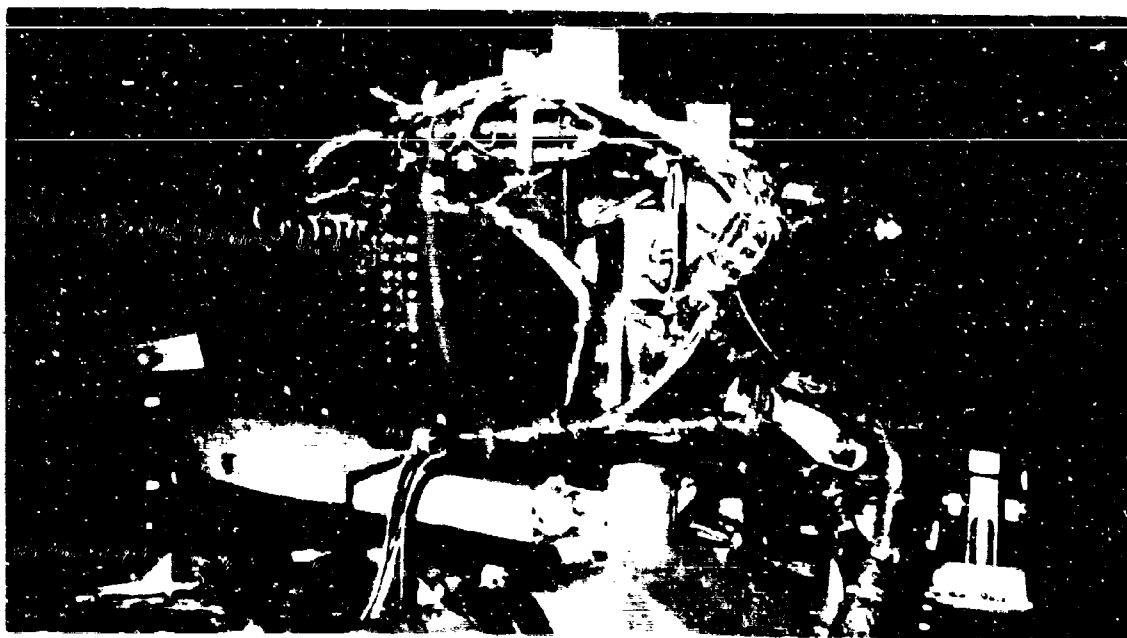


Figure 52. Rotor Thermocouple Switching Boxes.

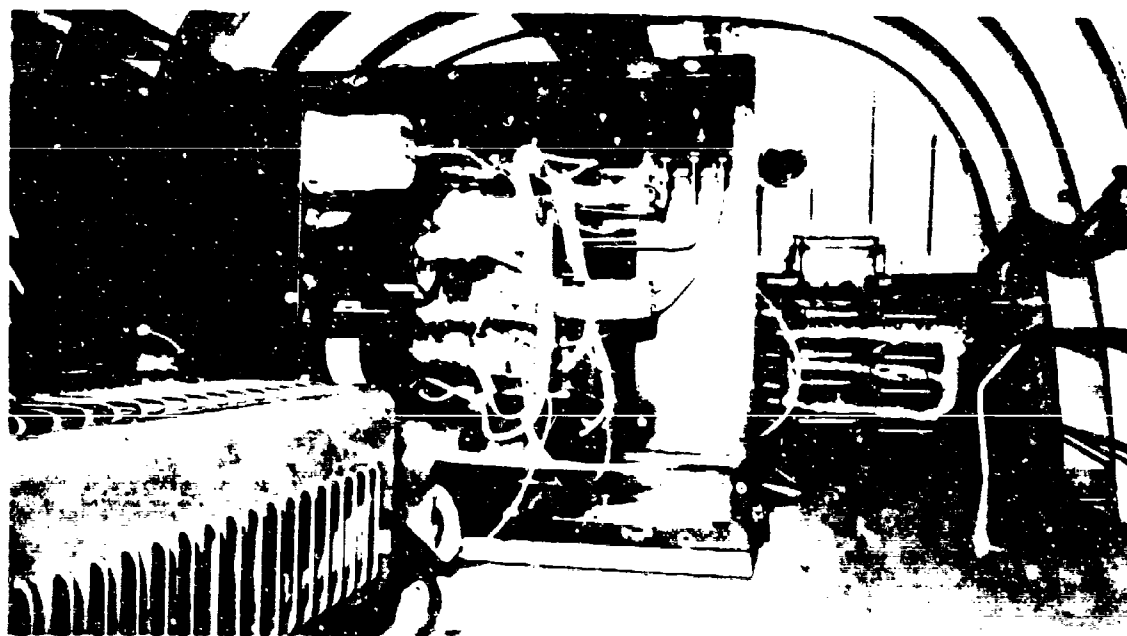


Figure 53. Photopanel Installation.

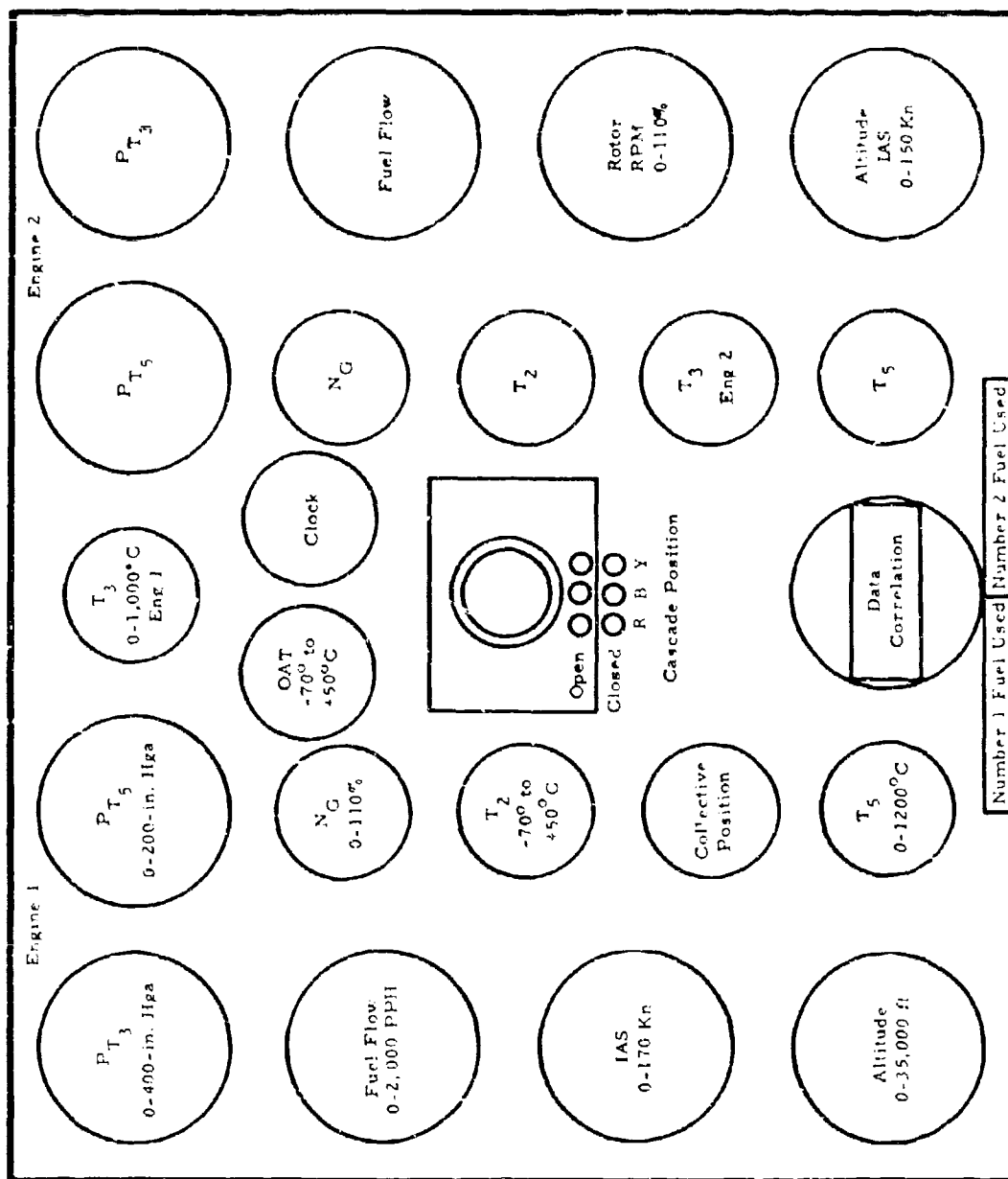


Figure 54. Photopanel Layout.

pilot's panel and photopanel, (2) event counters in each oscillograph, and (3) number-stamping machines attached to each temperature recorder.

#### Cockpit Camera

A 16mm motion picture camera was mounted in the left seat of the helicopter. A 120-degree wide-angle lens provided coverage of the instrument panel, the pilot's hands, and the horizon. A 400-foot magazine provided 12 minutes of film at 24 frames per second.

### LIST OF INSTRUMENTATION MEASUREMENTS

#### Pilot's Panel, Direct Reading Instruments

Air speed indicator  
Pressure altitude indicator  
Rate of climb indicator  
Attitude indicator, pitch and roll  
Turn and bank indicator  
Engine turbine speed indicator, each engine  
Engine discharge pressure indicator, each engine  
Engine exhaust gas temperature indicator, each engine  
Engine fuel flow indicator, each engine  
Engine oil pressure indicator, each engine  
Engine oil temperature indicator, each engine  
Fuel quantity indicator, dual reading, forward and aft tanks  
Hydraulic pressure indicator, dual reading, both systems  
Rotor tachometer  
Rotor oil pressure indicator  
Rotor oil temperature indicator  
Crossflow indicator  
Tilt-stop indicator  
Ammeter (2)  
Voltmeter  
Inverter frequency meter  
Emergency rotor tachometer  
Outside air temperature indicator  
Compass

#### Auxiliary Cockpit Panel, Direct Reading Instruments

Engine vibration amplitude indicator, each engine  
Clock



Collective control position indicator  
Longitudinal cyclic control position indicator  
Lateral cyclic control position indicator  
Rudder pedal position indicator  
Pressure altitude indicator  
Accelerometer, vertical  
Engine discharge pressure indicator (sensitive), each engine  
Data correlation counter  
Oscillograph record counter  
Film footage counter, photopanel

Photopanel (35mm Sequence Camera), Flight Parameters and Engine Performance

Airspeed indicator  
Pressure altitude indicator  
Rotor tachometer  
Collective-pitch position indicator  
Engine turbine discharge pressure indicator, each engine  
Engine turbine discharge temperature indicator, each engine  
Engine compressor discharge pressure indicator, each engine  
Engine compressor discharge temperature indicator, each engine  
Engine turbine speed indicator, each engine  
Engine fuel flow indicator, each engine  
Engine inlet temperature indicator, each engine  
Clock  
Data correlation counter  
Fuel counter, both engines  
Outside air temperature indicator  
Tip cascade position indicator

Oscillograph No. 1, 50 Channel, Performance, Stability and Control, and Structural Load Measurements

Rotor rpm and azimuth  
Collective-pitch position  
Compressor discharge pressure, each engine  
Turbine discharge pressure, each engine  
Power lever angle, each engine  
Compressor variable geometry position, each engine  
Engine rpm, each engine  
Engine mount acceleration, vertical, each engine  
Engine mount acceleration lateral, each engine  
Blade-tip gas pressure, three blades (forward and aft ducts)  
Angle of sideslip

Yaw-control duct pressure  
Yaw-control outlet duct pressure  
Y-duct crossflow vane position  
Longitudinal cyclic-control position  
Lateral cyclic-control position  
Rudder pedal position  
Rudder surface position  
Rate of pitch  
Rate of roll  
 $N_f$  governor shaft rpm, each engine  
Diverter valve position, each valve  
Rate of yaw  
Pitch attitude  
Roll attitude  
Directional heading  
Vertical acceleration at cg  
Lateral acceleration at cg  
Control actuator position, rh  
Control actuator position, lh  
Control actuator position, vertical  
Fuselage-longeron axial strain, Station 321, upper lh  
Fuselage-longeron axial strain, Station 321, lower lh  
Fuselage-longeron axial strain, Station 321, upper rh  
Fuselage-longeron axial strain, Station 321, lower rh  
Stabilizer bending, lh forward spar  
Stabilizer bending, lh rear spar  
Stabilizer bending, rh forward spar  
Stabilizer bending, rh rear spar  
Data correlation

Oscillograph No. 2, 50 Channel, Rotor Geometry, Blade and Hub  
Structural Load Measurements

Rotor rpm and azimuth  
Collective-pitch position  
Strap windup, blue blade  
Blade pitch angle  
Blade flapping angle  
Hub tilt angle  
Flapwise bending, Station 63, front and rear spar, blue blade  
Flapwise bending, Station 75.4, front and rear spar, blue blade  
Flapwise bending, Station 100, front and rear spar, blue blade  
Flapwise bending, Station 140, front and rear spar, blue blade  
Flapwise bending, Station 220, front and rear spar, blue blade  
Flapwise bending, Station 270, front and rear spar, blue blade

Chordwise bending, Station 90.75, front and rear spar, blue blade  
Chordwise bending, Station 149.0, front and rear spar, blue blade  
Chordwise shear, Station 23, feathering ball, blue blade  
Vertical shear, Station 23, feathering ball, blue blade  
Duct torsion, Station 15, inboard articulate duct, yellow blade  
Blade torsion, Station 38, blue blade  
Blade torsion, Station 83, blue blade  
Main shaft bending, WL-12.0 in plane of blue blade  
Main shaft bending, WL-12.0, 90 degrees to blue blade  
Hub gimbal lug bending  
Hub plate strain, forward and aft  
Pitch-arm-link load (3 blades)  
Swashplate drag-link load  
Acceleration, lateral, upper bearing support  
Acceleration, longitudinal, upper bearing support  
Acceleration, vertical, fuselage at horizontal stabilizer  
Acceleration, lateral, fuselage at horizontal stabilizer  
Acceleration, vertical, cockpit  
Acceleration, lateral, cockpit  
Longitudinal cyclic position  
Lateral cyclic position  
Longitudinal stick force  
Lateral stick force  
Cascade valve position  
Landing gear oleo position, both oleos  
Air speed

Temperature Recorder No. 1 (Chromel-Alumel), Rotor Temperatures

Blade-tip gas temperature, blue blade  
Front spar temperatures, blue blade  
Rear spar temperatures, blue blade  
Flexure temperatures, blue blade  
Rib temperatures, blue blade  
Spar cooling-air temperatures (3 blades)  
Outer-skin temperatures, blue blade  
Gas-duct wall temperatures, blue blade  
Rotor shaft temperatures  
Tip transducer housing temperature  
Root cooling-air temperature  
Spar temperatures, forward and aft  
Rotor spoke temperatures  
Ball-joint inner surface temperature  
Lower bearing-housing temperature  
Inboard articulate duct-seal temperature

## Temperature Recorder No. 2 (Iron-Constantan), Structural Temperatures

Engine and engine accessory temperatures  
Engine and diverter valve bay temperatures  
Lateral pylon temperatures  
Radial and thrust bearing housing temperatures  
Aft fuselage and yaw valve compartment temperatures  
Yaw duct and Y-duct blanket temperatures  
Y-duct bay temperatures  
Yaw valve outlet temperatures

## STRAIN GAGE INSTALLATION

Foil strain gages with a high-temperature epoxy backing and attached with a high-temperature cement were used in areas where temperatures above 200 degrees F were expected. For application where the temperature was not expected to exceed 200 degrees F, a room-temperature-curing epoxy was used. Each gage installation was subjected to a short cure at the expected operating temperature, to prevent drift.

All strain-gage bridge installations had four active gages, with the exception of the hub plate strain, which had two active gages. All strain-gage bridges on the blade were waterproofed and protected by silastic-rubber compound. This compound was also used to attach the strain-gage lead wiring to the spar. Information on the location of strain-gage bridges is given in Figures 55 and 56.

## BLADE THERMOCOUPLE INSTALLATION

Chromel-alumel (K calibration) thermocouples were used exclusively on the rotor. These thermocouples were 30-gage wire with double-woven fiber glass insulation. The thermocouples on the blade skins, flexures, and duct walls were attached by spotwelding the thermocouple directly to the part. The spotweld formed the junction at which the temperature was measured. These thermocouples and wiring were installed during the initial fabrication of the blue rotor blade.

The temperature of parts subjected to fatigue loading, such as the spars, was measured by using a thermocouple with a junction fused by use of a mercury arc. These thermocouples were then cemented to the part. The thermocouple wire on the spars was attached directly to the spar with a silastic compound. The lead wire for the thermocouples

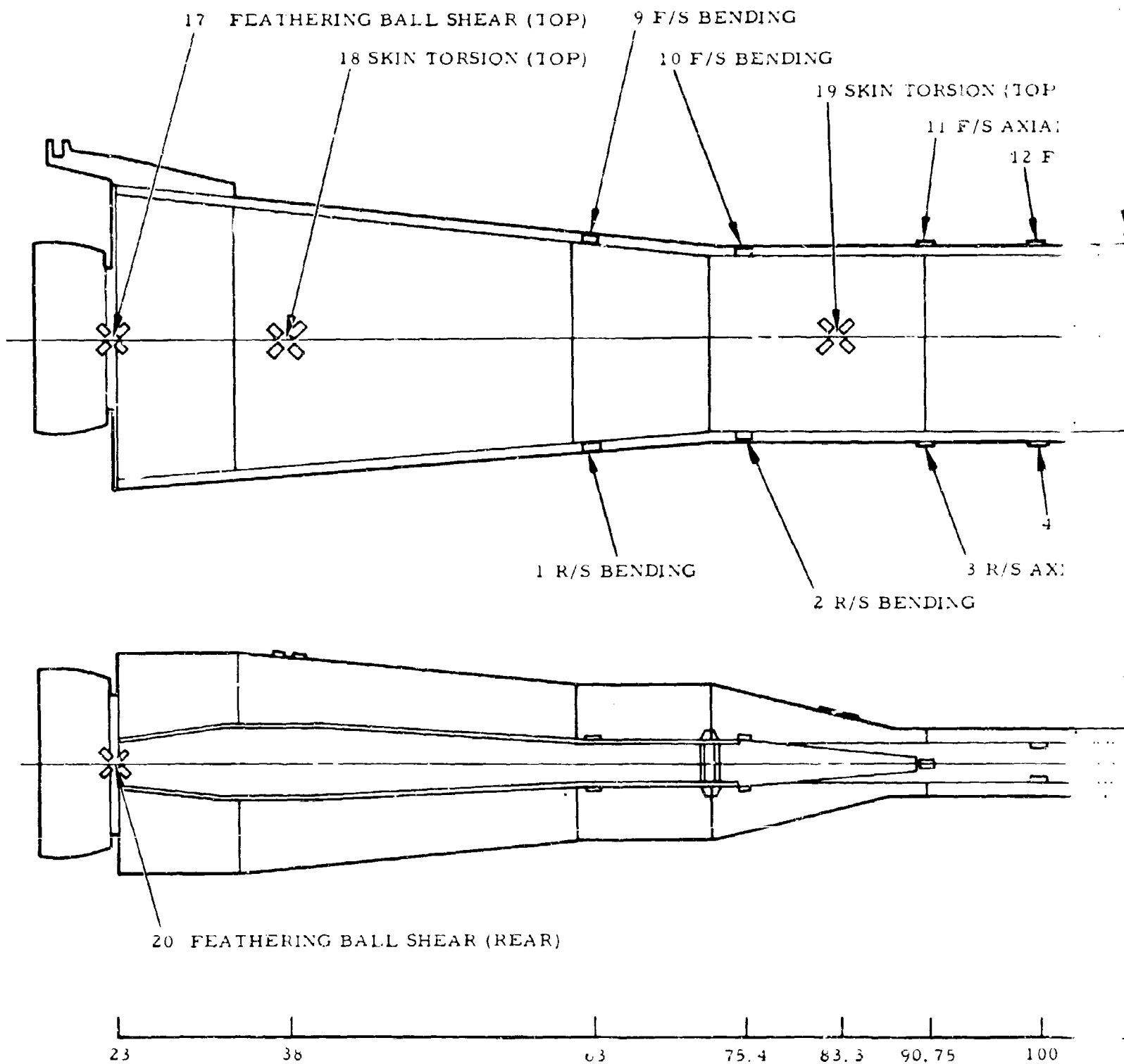
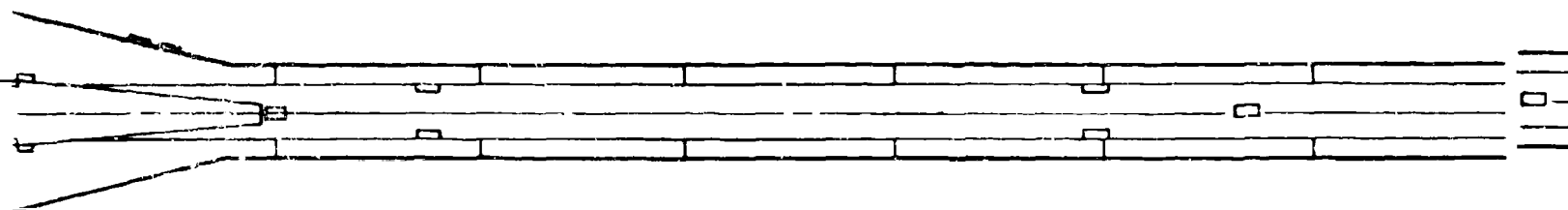
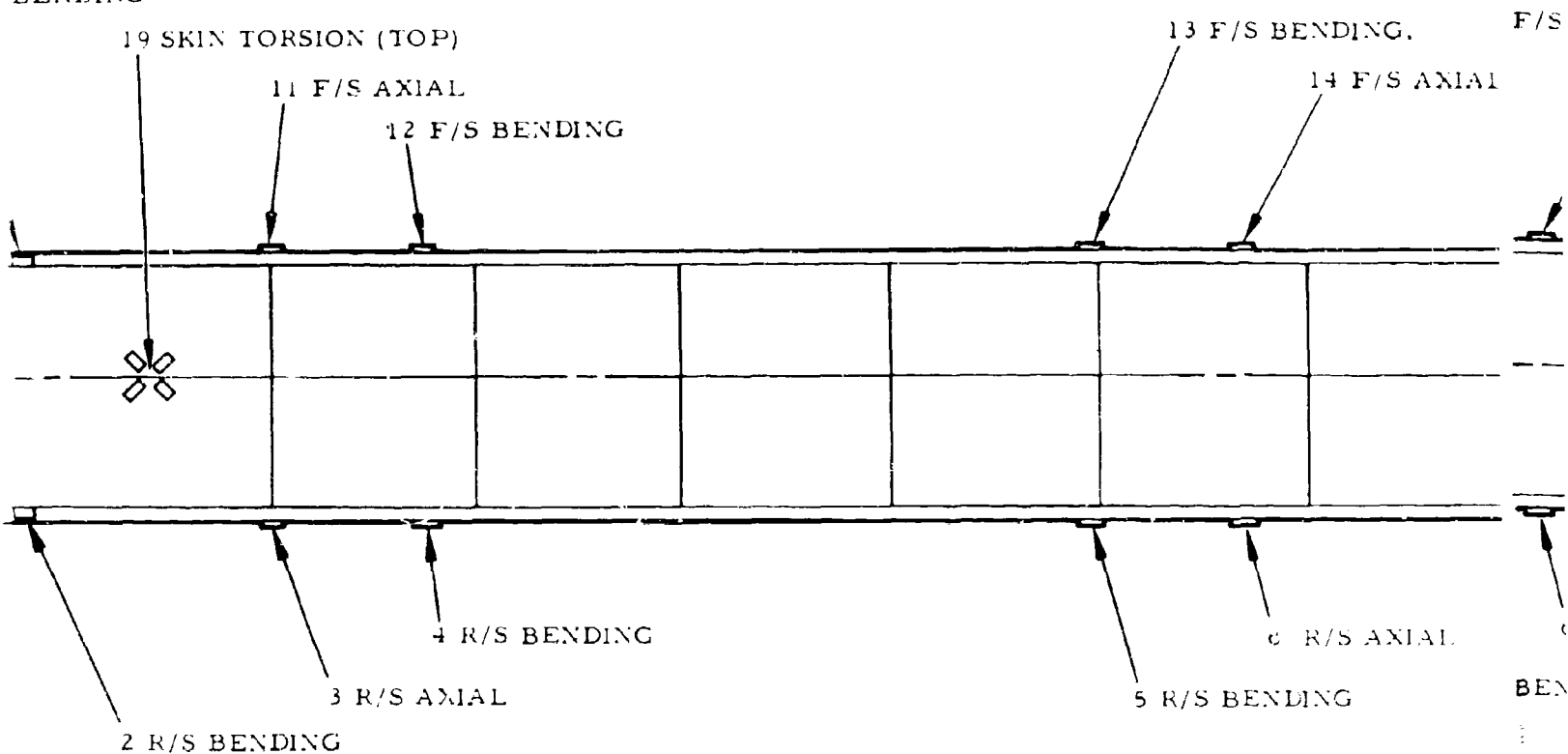


Figure 55. Strain-Gage Bridge Locations, Rotor Blades - Flight Test.

ENDING

BENDING

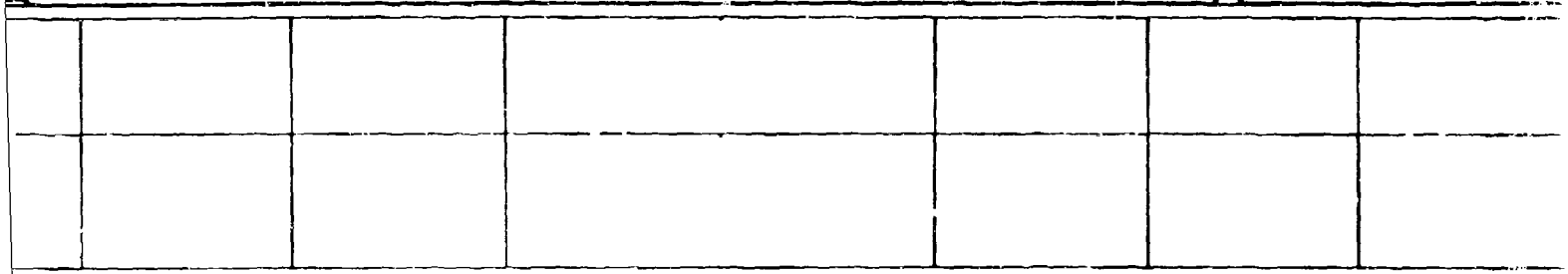


B

/S BENDING.

14 F/S AXIAL

15 F/S BENDING




6 R/S AXIAL

7 R/S BENDING

BENDING




35 180° GIN

15 F/S BENDING

16 F/S BENDING

7 R/S BENDING

8 R/S BENDING

32 0° SHA

33 0° S!

220

270

70

D



34 0° GIMBAL LUG BENDING

35 180° GIMBAL LUG BENDING

16 F/S BENDING

W.L. +4.25

30 90° SHAFT BENDING

31 90° SHAFT BENDING

8 R/S BENDING

32 0° SHAFT BENDING

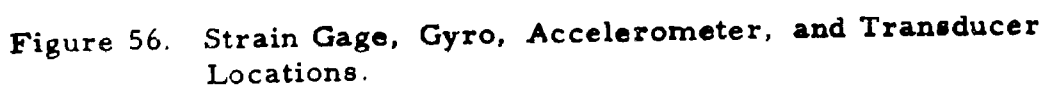
33 0° SHAFT BENDING

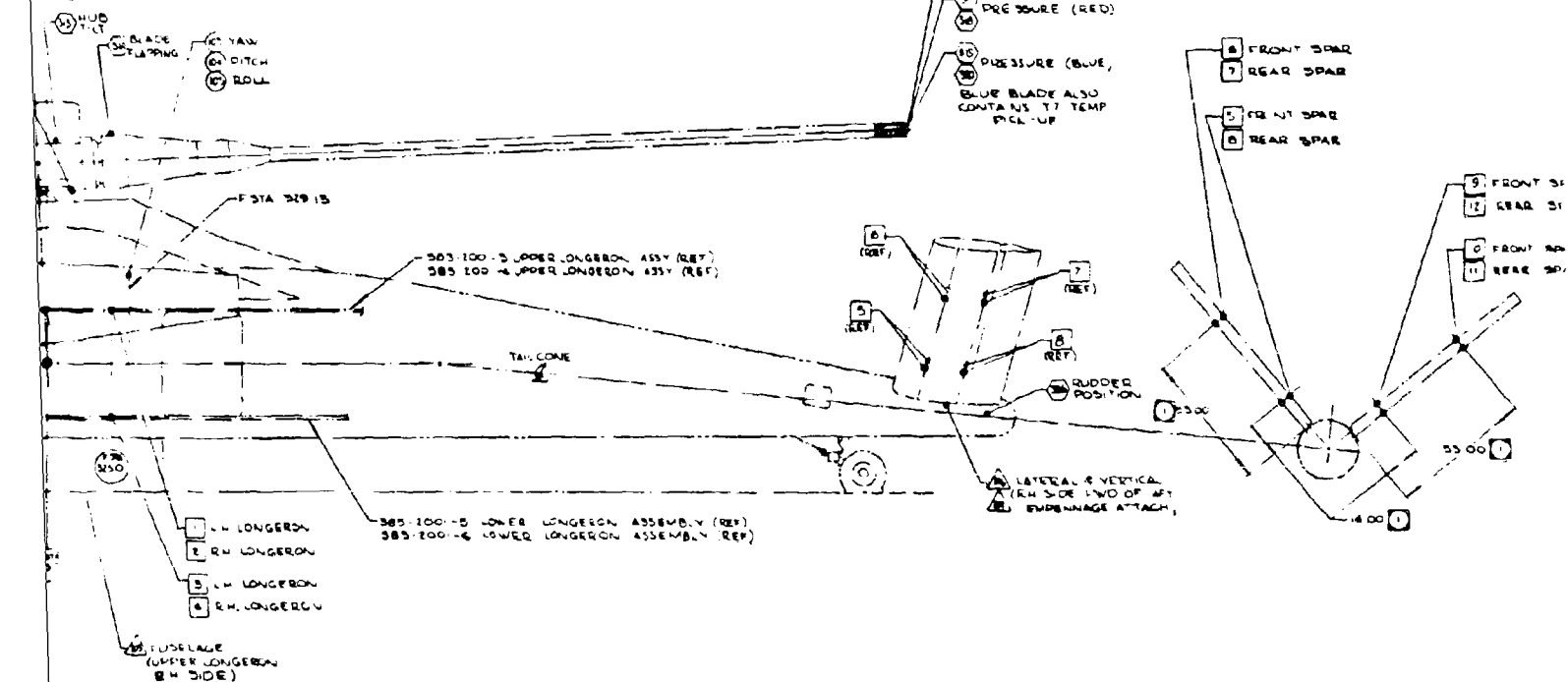
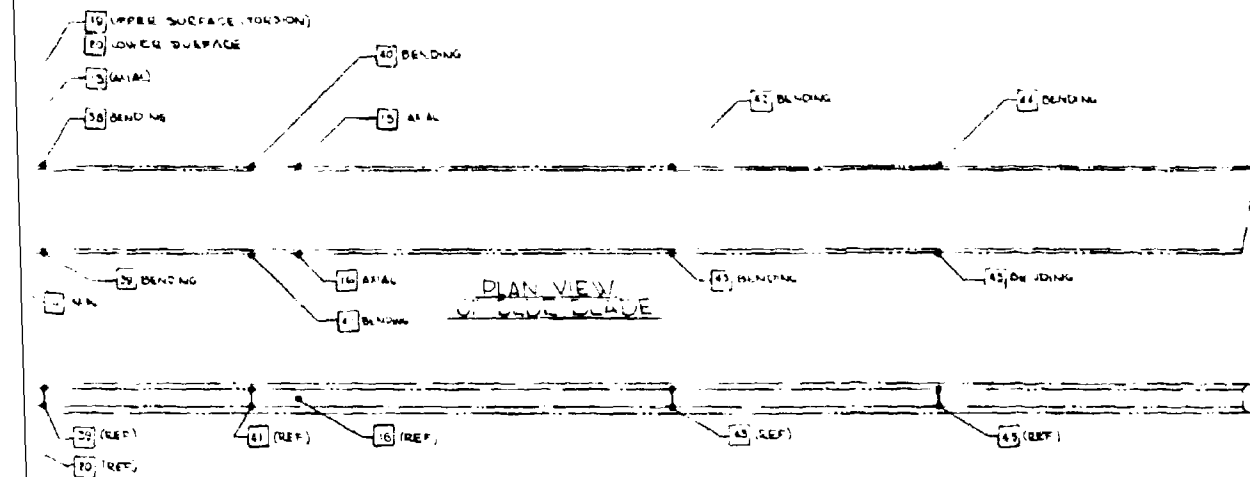
W.L. -9.6

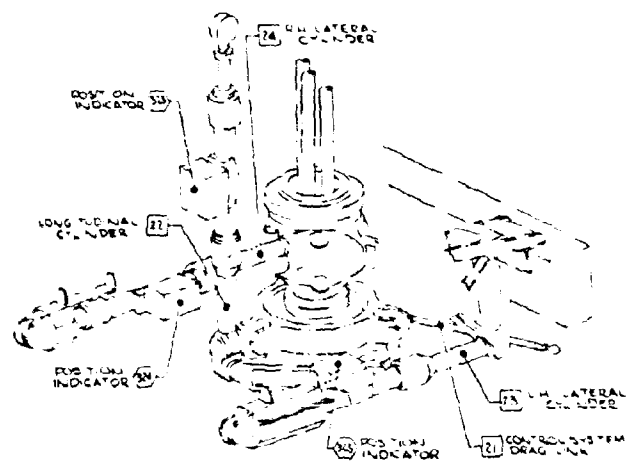
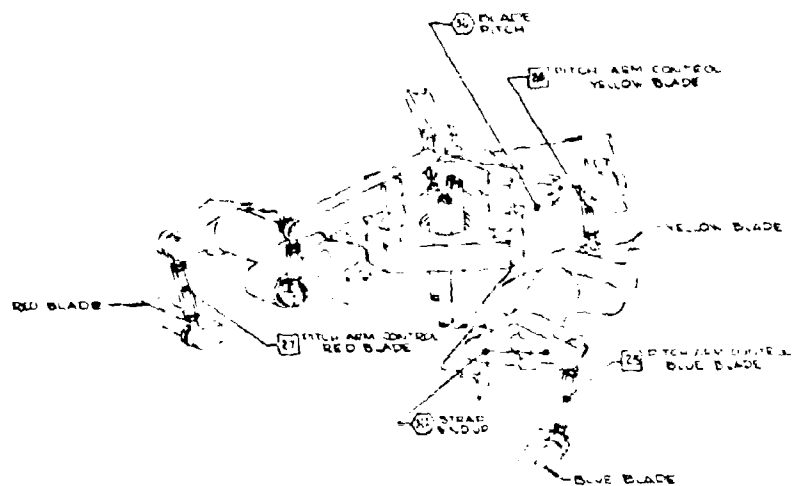
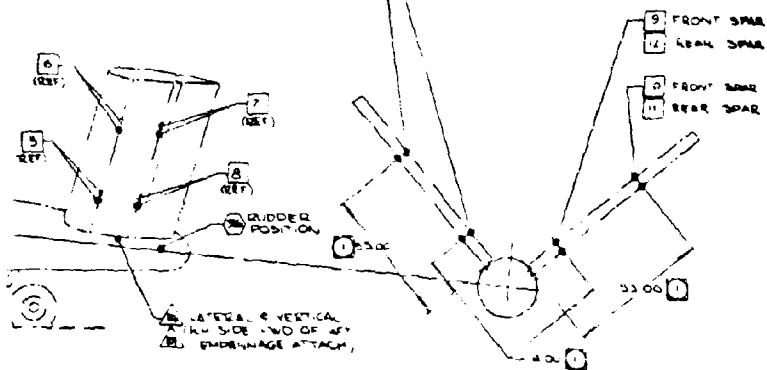
W.L. -10.4

90°

E







STATIONARY SWASHPLATE AREA

ARE

C

Strain Gage Number	Location or Function	Gyro Number	Location
1	(Axial) Sta 325.0 Upper LH Longeron	101	Fwd Fuel Bay F St
2	(Axial) Sta 325.0 Upper RH Longeron	102	Fwd Fuel Bay F St
3	(Axial) Sta 325.0 Lower LH Longeron	103	Sta 329.13 Yaw
4	(Axial) Sta 325.0 Lower RH Longeron	104	Sta 329.13 Pitch
5	LH Stabilizer-Front Spar Bending	105	Sta 329.13 Roll
6	LH Stabilizer-Front Spar Bending		
7	LH Stabilizer-Rear Spar Bending		
8	LH Stabilizer-Rear Spar Bending		
9	RH Stabilizer-Front Spar Bending		
10	RH Stabilizer-Front Spar Bending		
11	RH Stabilizer-Rear Spar Bending		
12	RH Stabilizer-Rear Spar Bending		
13	Blue Blade Axial Sta 90.75 (Fwd)		
14	Blue Blade Axial Sta 90.75 (Aft)		
15	Blue Blade Axial Sta 149.0 (Fwd)		
16	Blue Blade Axial Sta 149.0 (Aft)		
17	Blue Blade Torsion Sta 38 (Upper)		
18	Blue Blade Torsion Sta 38 (Lower)		
19	Blue Blade Torsion Station 83 (Upper)		
20	Blue Blade Torsion Sta 83 (Lower)		
21	Control System Drag Link		
22	Control System Longitudinal Cylinder		
23	Control System LH Lateral Cylinder		
24	Control System RH Lateral Cylinder		
25	Blue Blade Pitch Arm Control Rod		
26	Yellow Blade Pitch Arm Control Rod		
27	Red Blade Pitch Arm Control Rod		
28	Rotor Shaft (Fwd and Aft Bending)		
29	Rotor Shaft (Side to Side Bending)		
30	Gimbal Lug Bending		
31	Gimbal Lug Bending		
32	Blue Blade Horizontal Shear		
33	Blue Blade Vertical Shear		
34	Blue Blade Bending Sta 63 (Front Spar)		
35	Blue Blade Bending Sta 63 (Rear Spar)		
36	Blue Blade Bending Sta 75.4 (Front Spar)		
37	Blue Blade Bending Sta 75.4 (Rear Spar)		
38	Blue Blade Bending Sta 100 (Front Spar)		
39	Blue Blade Bending Sta 100 (Rear Spar)		
40	Blue Blade Bending Sta 140 (Front Spar)		
41	Blue Blade Bending Sta 140 (Rear Spar)		
42	Blue Blade Bending Sta 220 (Front Spar)		
43	Blue Blade Bending Sta 220 (Rear Spar)		
44	Blue Blade Bending Sta 270 (Front Spar)		
45	Blue Blade Bending Sta 270 (Rear Spar)		
46	Hub Plate (Fwd) Blue Blade		
47	Hub Plate (Aft) Blue Blade		

Accelerometer Number	Location
201	Radial Bearing
202	Radial Bearing
203	Pilots Seat Str
204	Pilots Seat Str
205	RH Upper Lo
206	Empennage -
207	Empennage -
208	LH Engine - A
209	RH Engine - A
210	LH Engine - 1
211	RH Engine - 1

Transducer Number	Loca
301	P-5 LH Engin
302	P-5 RH Engin
303	P-3 LH Engin
304	P-3 RH Engin
305	Engine Variat
306	Engine Variat
307	LH Engine - 1
308	RH Engine - 1
309	Collective
310	Rudder Positi
311	Longitudinal C
312	Lateral Cycli
313	Hub Tilt
314	Blade Flappin
315	Yellow Blade
316	Yellow Blade
317	Red Blade - I
318	Red Blade - I
319	Blue Blade -
320	Blue Blade -
321	Blade Pitch
322	Strap Windup
323	Longitudinal C
324	RH Lateral C
325	LH Lateral C
326	Rudder Positi

D

Location or Function	Gyro Number	Location or Function
0 Upper LH Longerons	101	Fwd Fuel Bay F Sta 200 - Pitch-Roll
0 Upper RH Longerons	102	Fwd Fuel Bay F Sta 265 - Yaw Pitch
0 Lower LH Longerons	103	Sta 329.13 Yaw
0 Lower RH Longerons	104	Sta 329.13 Pitch
Front Spar Bending	105	Sta 329.13 Roll
Front Spar Bending		
Rear Spar Bending		
Rear Spar Bending		
Front Spar Bending	Accelerometer	
Front Spar Bending	Number	Location or Function
Rear Spar Bending		
Rear Spar Bending	201	Radial Bearing (Lateral)
al Sta 90.75 (Fwd)	202	Radial Bearing (Longitudinal)
al Sta 90.75 (Aft)	203	Pilots Seat Structure - Vertical
al Sta 149.0 (Fwd)	204	Pilots Seat Structure - Lateral
al Sta 149.0 (Aft)	205	RH Upper Longerons (Approx CG)
sion Sta 38 (Upper)	206	Empennage - Lateral
sion Sta 38 (Lower)	207	Empennage - Vertical
sion Station 83 (Upper)	208	LH Engine - Vertical
sion Sta 83 (Lower)	209	RH Engine - Vertical
Drag Link	210	LH Engine - Lateral
Longitudinal Cylinder	211	RH Engine - Lateral
LH Lateral Cylinder		
RH Lateral Cylinder		
h Arm Control Rod	Transducer	
h Arm Control Rod	Number	Location or Function
h Arm Control Rod		
d and Aft Bending)	301	P-5 LH Engine Pressure
e to Side Bending)	302	P-5 RH Engine
ding	303	P-3 LH Engine
ding	304	P-3 RH Engine
zontal Shear	305	Engine Variable Geometry LH
ical Shear	306	Engine Variable Geometry RH
ing Sta 63 (Front Spar)	307	LH Engine - Power Lever Angle
ing Sta 63 (Rear Spar)	308	RH Engine - Power Lever Angle
ing Sta 75.4 (Front Spar)	309	Collective
ing Sta 75.4 (Rear Spar)	310	Rudder Position
ing Sta 100 (Front Spar)	311	Longitudinal Cyclic
ing Sta 100 (Rear Spar)	312	Lateral Cyclic
ing Sta 140 (Front Spar)	313	Hub Tilt
ing Sta 140 (Rear Spar)	314	Blade Flapping
ing Sta 220 (Front Spar)	315	Yellow Blade - Pressure
ing Sta 220 (Rear Spar)	316	Yellow Blade - Pressure
ing Sta 270 (Front Spar)	317	Red Blade - Pressure
ing Sta 270 (Rear Spar)	318	Red Blade - Pressure
Blue Blade	319	Blue Blade - Pressure
Blue Blade	320	Blue Blade - Pressure
	321	Blade Pitch
	322	Strap Windup
	323	Longitudinal Cylinder Position Indicator
	324	RH Lateral Cylinder Position Indicator
	325	LH Lateral Cylinder Position Indicator
	326	Rudder Position

installed on the blade was attached to the blade by three small sheet-metal clips spotwelded to the blade segment. The wire underneath these clamps was protected by wrapping it with fiber glass tape. Silastic compound was then applied to hold the wire in place. The arrangement worked very well.

The thermocouples installed in the blade-tip cascades were made from inconel-sheathed chromel-alumel wire. Location of thermocouples is given in Figure 57.

### FUSELAGE STRUCTURAL THERMOCOUPLES

Iron-constantan (J calibration) thermocouples were used to monitor the temperatures in the critical areas of the fuselage. These thermocouples were attached directly to the parts by spotwelding. Thirty-gage wire with double fiber glass insulation was used. The location of the various thermocouples is given in Figure 58.

### CALIBRATION PROCEDURE - OSCILLOGRAPHS

#### Strain Gages

All strain-gage bridges except the hub-plate strain and fuselage axial strain bridges were calibrated by applying a known load to the particular part and monitoring the bridge output with a strain analyzer. The strain analyzer reads in microinches of strain. A known accurate resistance was then placed across one leg of the strain-gage bridge, which shifted the strain analyzer reading a certain number of microinches. This shift in strain was equated to the load required to produce the same shift. This procedure produced a value of applied load indication for a given resistance shunt, across one leg of the bridge, called an R-Cal equivalent. This R-Cal resistance was then used to standardize or calibrate the oscillographs by applying the resistance across the bridge leg; the resultant oscillographic trace deflection then equaled the load for that particular R-Cal equivalent. The balance boxes used on the XV-9A were equipped for R-Cal calibration on each oscillographic trace, and this procedure was followed before and after every flight.

#### Pressure Transducers

The pressure transducers used were of the unbonded strain-gage type, and the calibration procedure was similar to that used for strain-gage bridges as described above. Pressure was applied to the transducer

with a dead-weight type of tester and the output measured with a strain analyzer for determining an R-Cal equivalent.

#### Accelerometers

Unbonded strain-gage accelerometers were calibrated by rotating them 90 degrees each way from the center position. This gave a calibration in each direction of the sensitive axis. The output of the accelerometers was recorded by the oscillographs during calibration.

#### Displacement Transducers, Attitude and Rate Gyros

These transducers convert mechanical motion or displacement to a change in electrical resistance by utilizing a potentiometer. Each potentiometer was wired into a wheatstone bridge to condition the electrical signal for use in the bridge balance boxes. The use of the wheatstone bridge and balance box combination allowed these transducers to be calibrated in the same manner used for strain-gage bridges and strain-gage devices.

#### Speed Measuring

The engine speeds, rotor speed, and rotor-driven engine governor speeds were read on the oscillographs as pulse or sine-wave-type signals obtained from magnetic pickups. Speeds were determined by counting the number of pulses or cycles per inch of paper. The oscillograph paper speed was calibrated by applying a signal of known frequency across one of the speed-recording channels and then counting the number of pulses per inch for this known frequency.

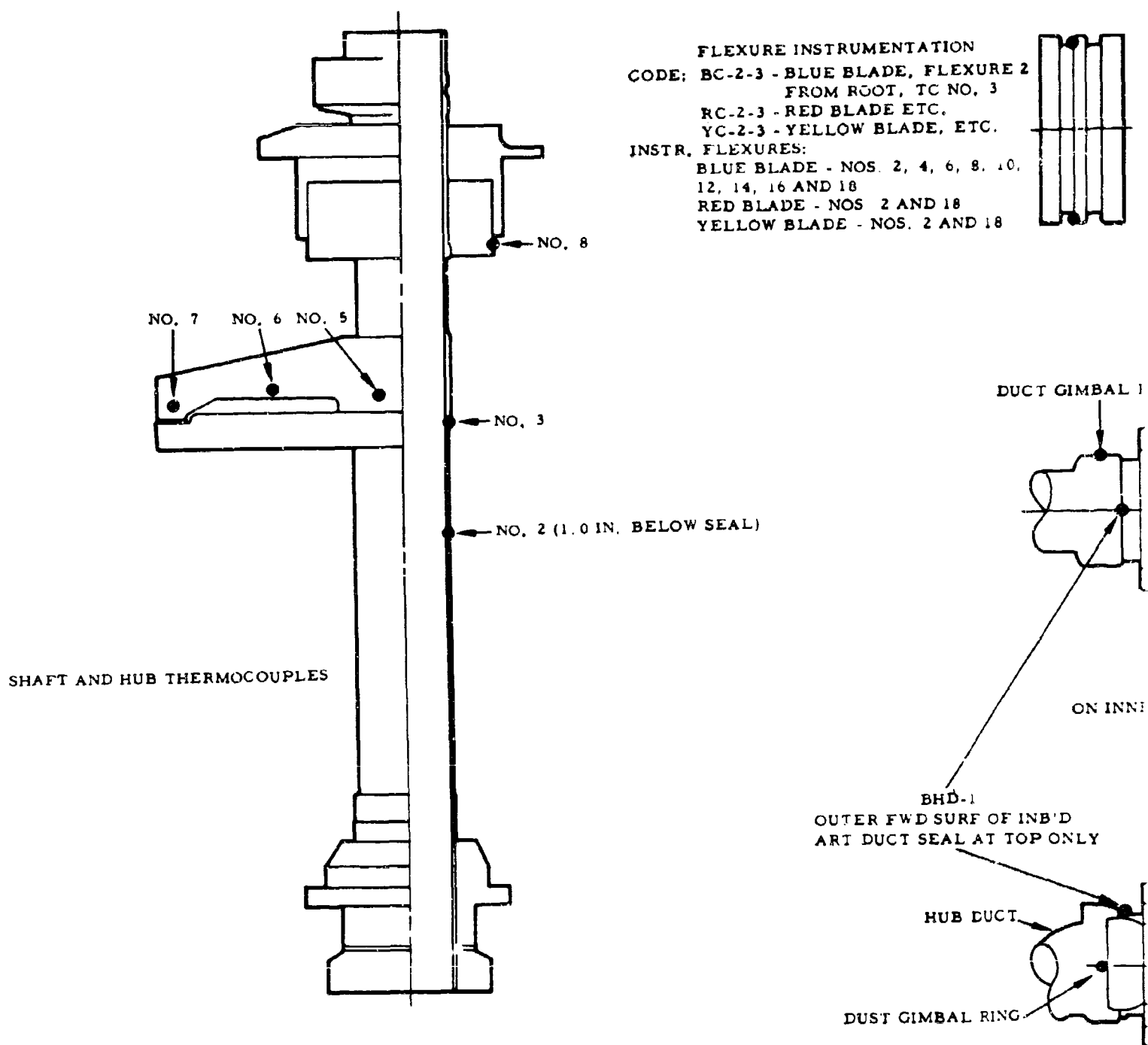
#### Direct-Reading and Photopanel Gages

Direct-reading and photopanel gages were periodically calibrated in the Hughes Aircraft Company Instrumentation Laboratory according to the manufacturer's instructions and specifications. Pressure gages were tested with a dead-weight tester or precision mercury manometer. Engine tachometers and exhaust temperature indicators were checked with a Jet-Cal calibration unit, which is a standard USAF test unit.

#### Thermocouple Calibrations - Temperature Recorders

The thermocouple wire used had standard tolerances of  $\pm 4$  degrees F to 530 degrees F and 3/4 percent from 530 to 1,000 degrees F. The temperature recorders used were calibrated according to the manufacturer's instruction upon installation and at various times throughout the program. The calibrations included both zero setting and span.





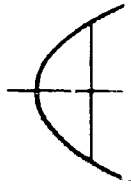
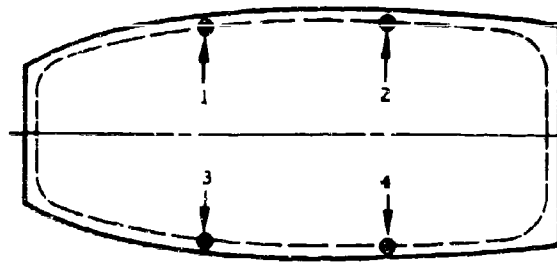
**NOTES:**

1. ALL THERMOCOUPLES CHROMEL ALUMEL
2. REFERENCE DRAWINGS: 285-0937, -0949, -0950, -0951, -1002
3. INSTRUMENTATION INB'D OF STA 91 ON BLUE BLADE ONLY
4. THE COUNTERPART OF BCD-1 ON THE OTHER BLADES IS:  
 RED RCDF, YELLOW YCDF
5. THE COUNTERPART OF BDC-2 ON THE OTHER BLADES IS:  
 RED RCDR, YELLOW YCDR

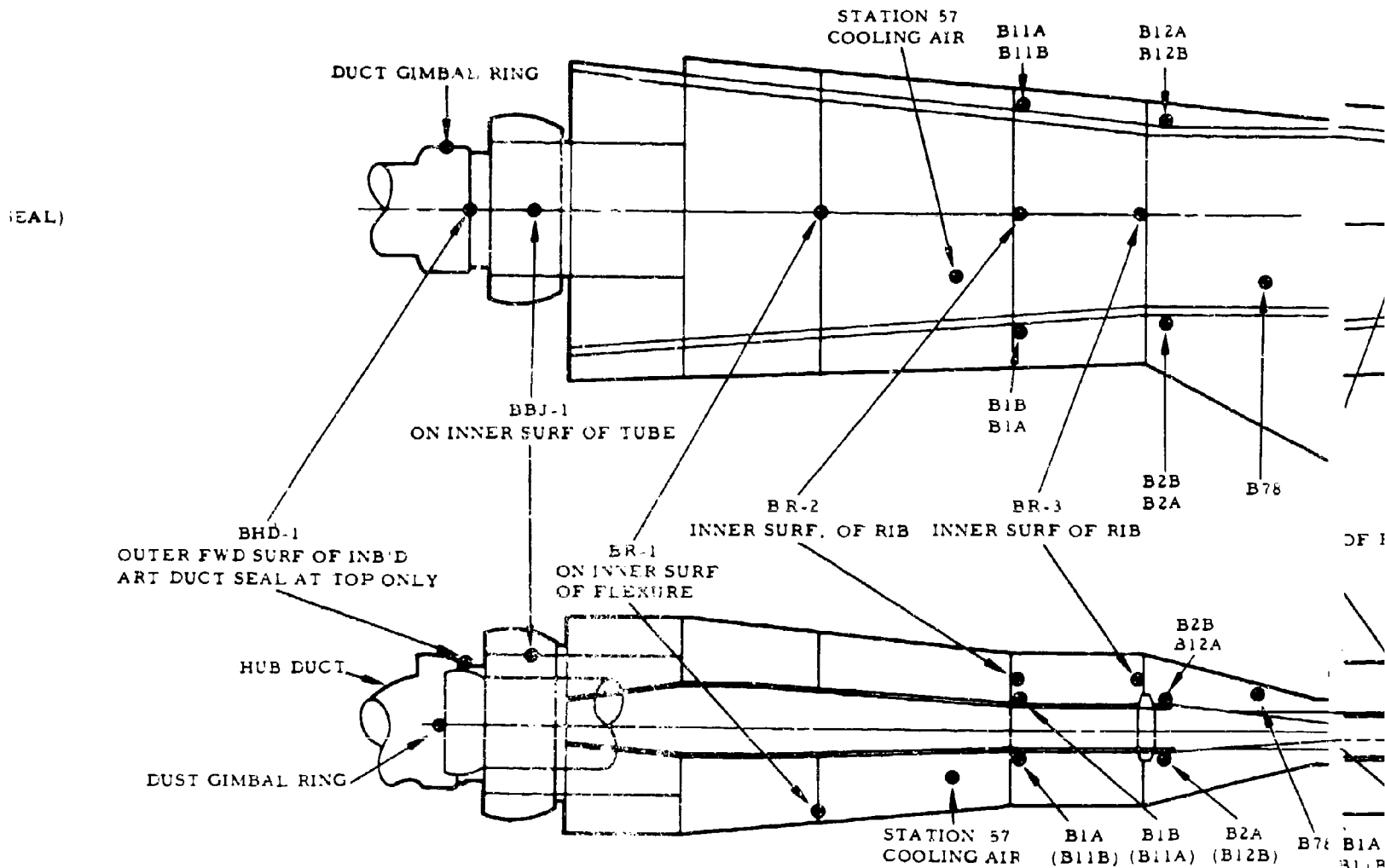
**Figure 57. Thermocouple Locations, Rotor Blades and Hub - Flight Test.**

# FLEXURE THERMOCOUPLES (TYPICAL)

FLEXURE INSTRUMENTATION  
 TC-2-3 - BLUE BLADE, FLEXURE 2  
 FROM ROOT, TC NO. 3  
 TC-2-3 - RED BLADE ETC.  
 TC-2-3 - YELLOW BLADE, ETC.  
 FLEXURES:  
 BLUE BLADE - NOS. 2, 4, 6, 8, 10,  
 12, 14, 16 AND 18  
 RED BLADE - NOS. 2 AND 18  
 YELLOW BLADE - NOS. 2 AND 18



I



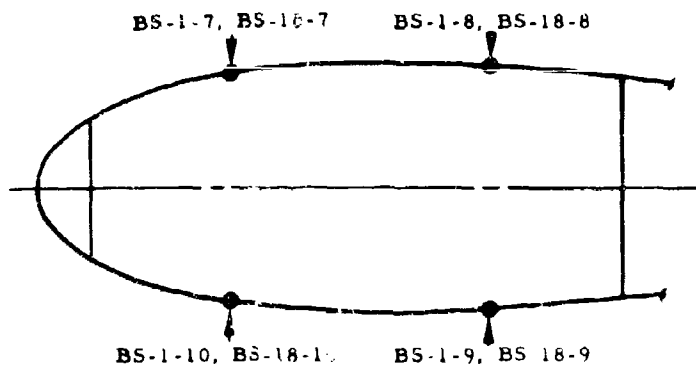
L  
 -0950, -0951, -1002  
 BLUE BLADE ONLY  
 OTHER BLADES IS:

OTHER BLADES IS:

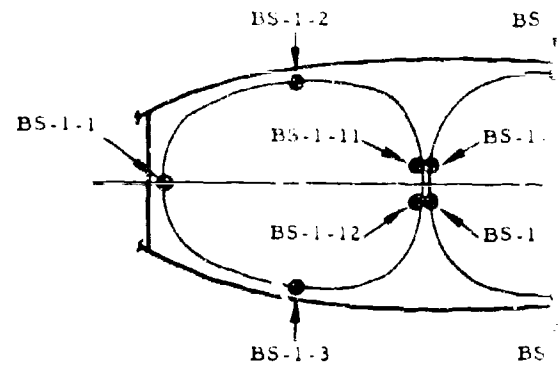
s and Hub -



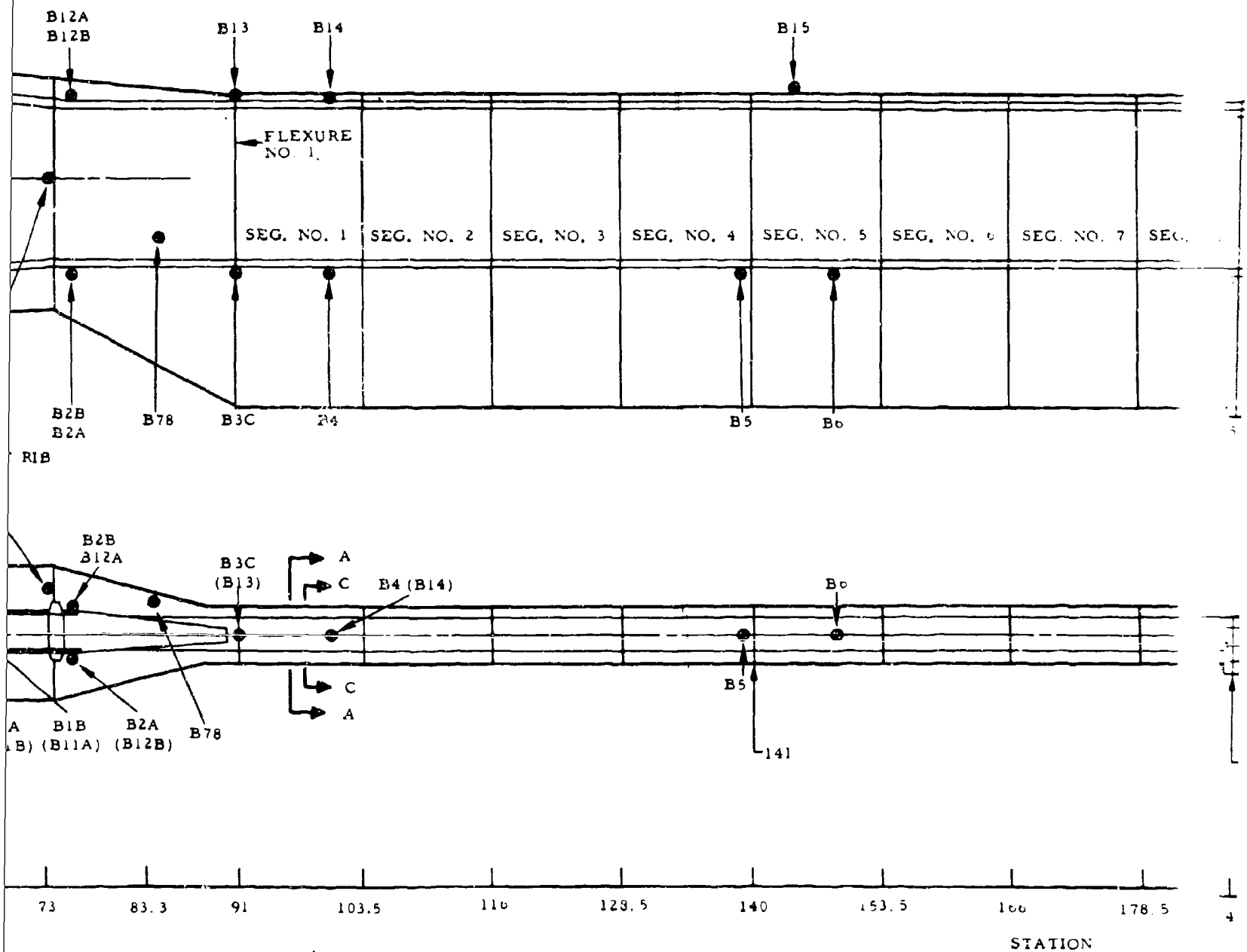
B

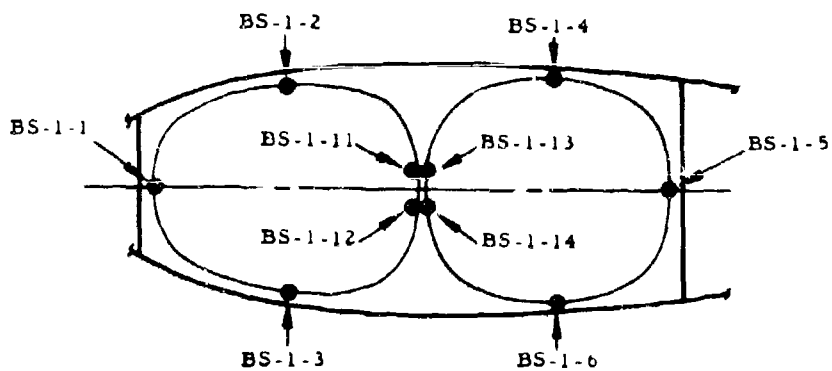


SECTIONS C-C AND D-D  
SKIN THERMOCOUPLES

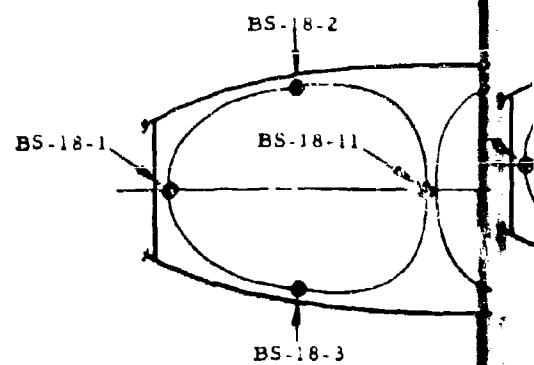


SECTION A-A  
BLADE SEGMENT NO. 1

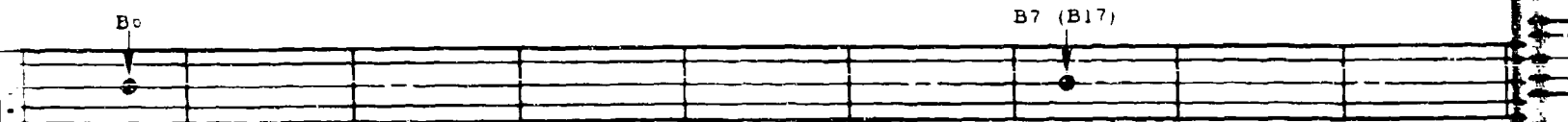
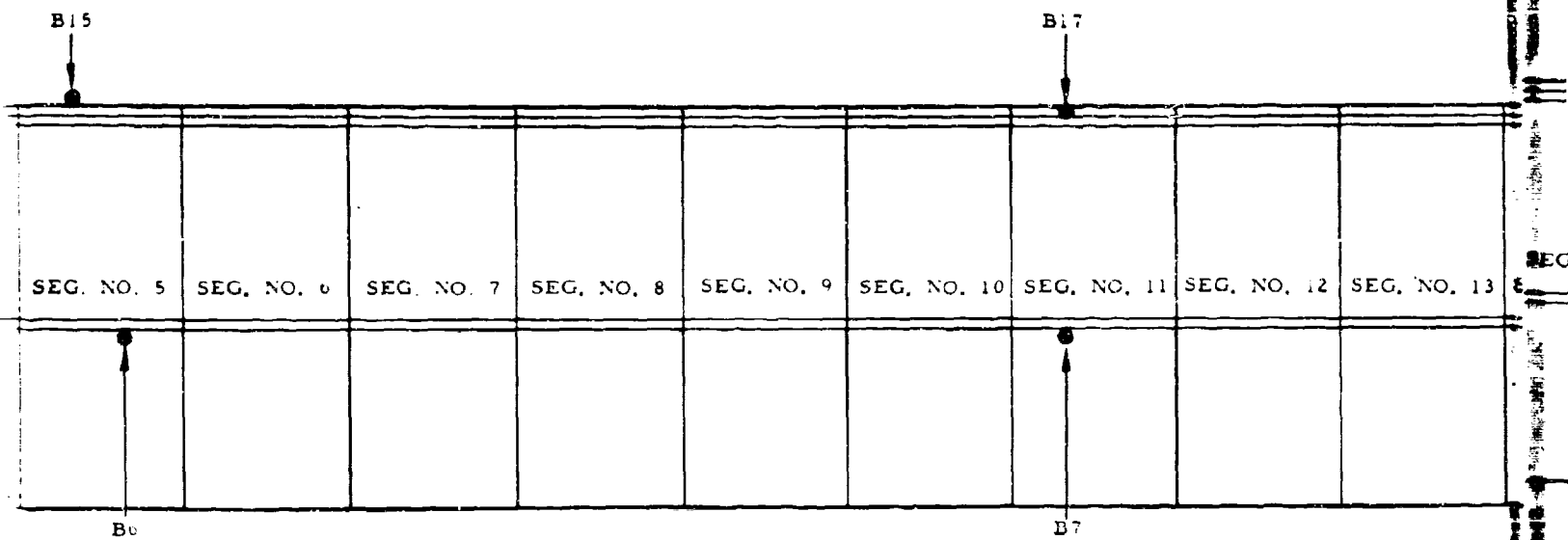




SECTION A-A  
BLADE SEGMENT NO. 1



SECTION  
BLADE SEGMENT

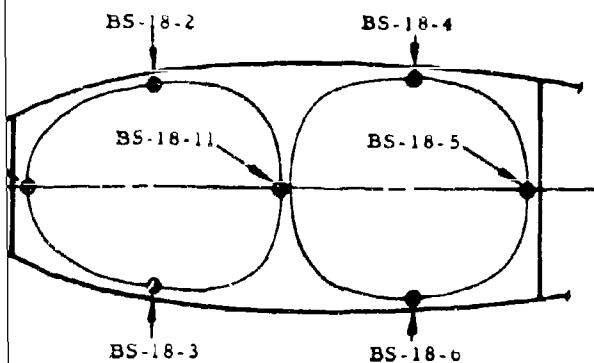


141

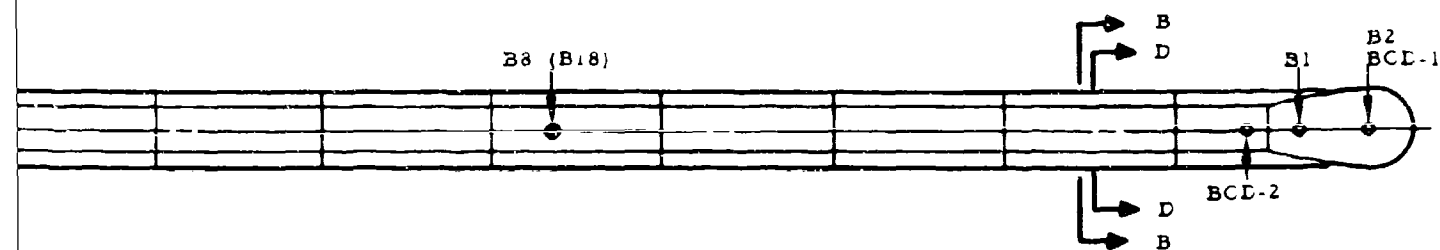
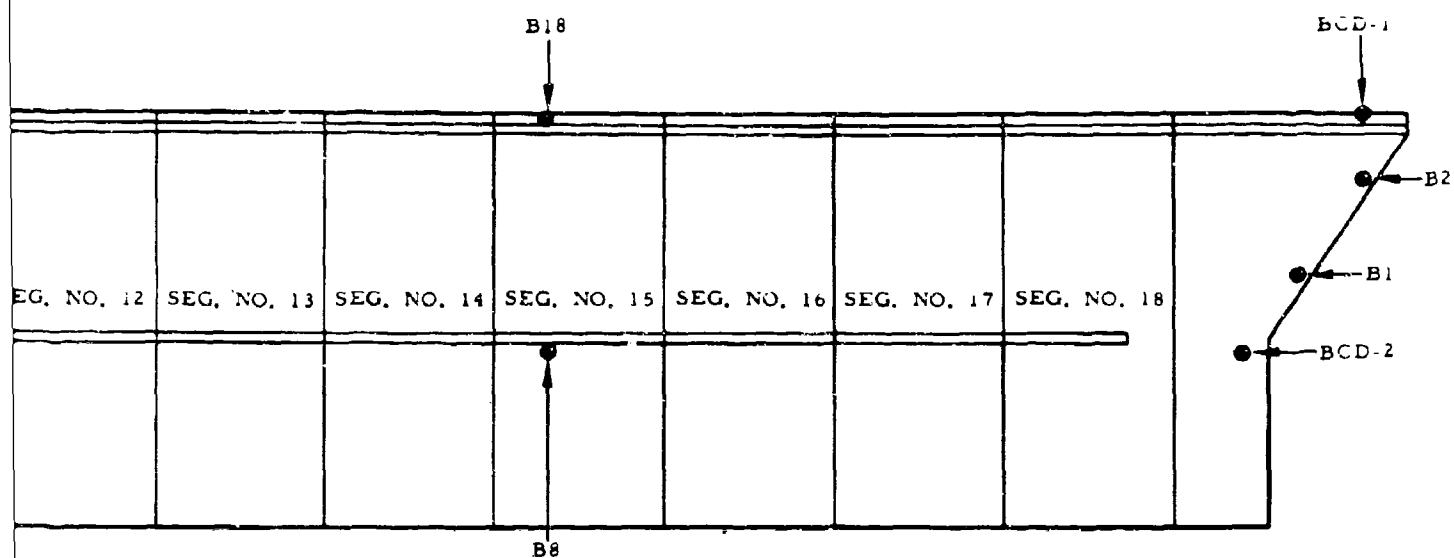
40 153.5 166 178.5 191 203.5 216 220 228.5 241 253

STATION

D



SECTION B-B  
BLADE SEGMENT NO. 18



241

253.5

266 270

278.5

303.5

316

E

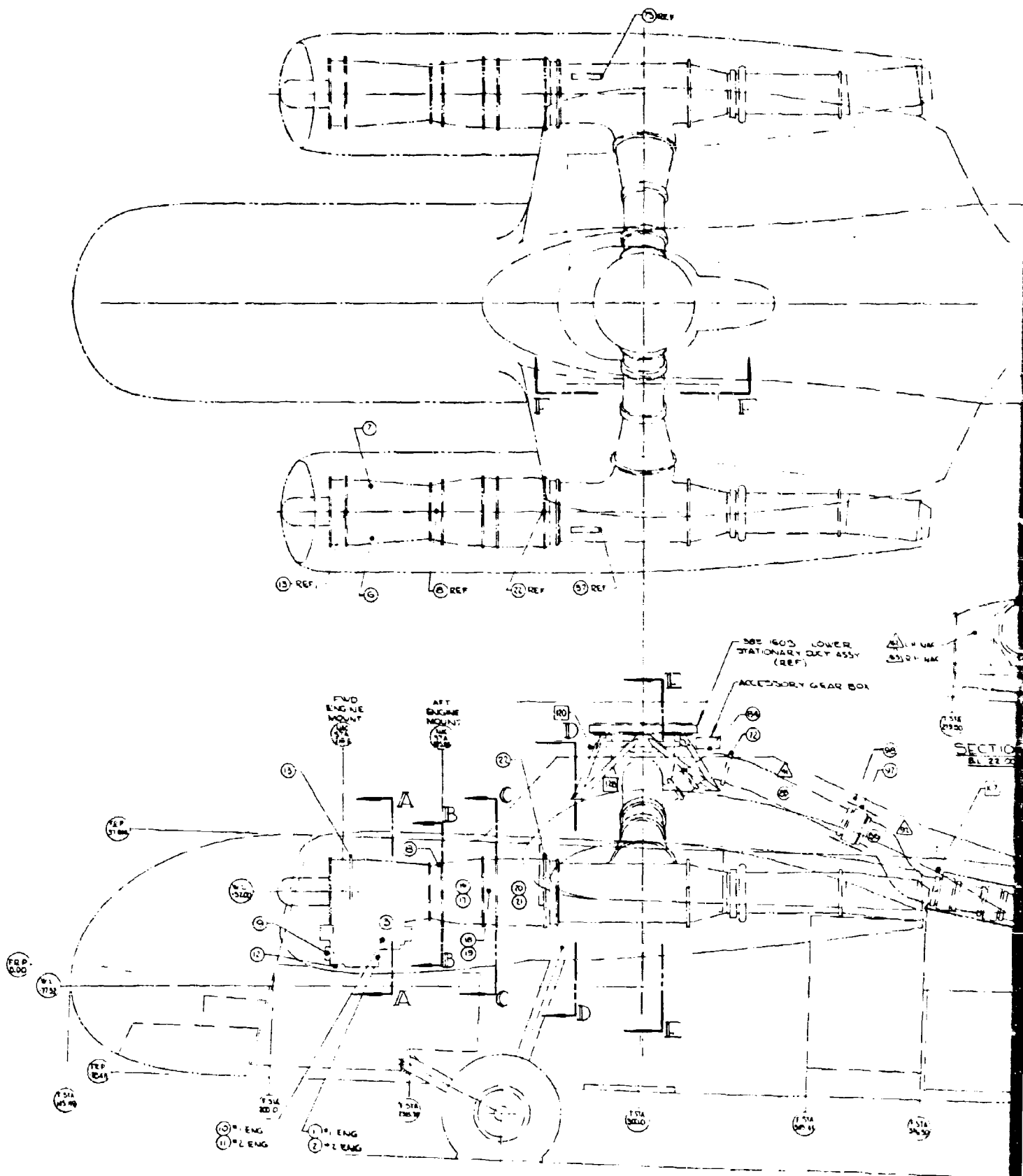
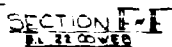
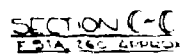
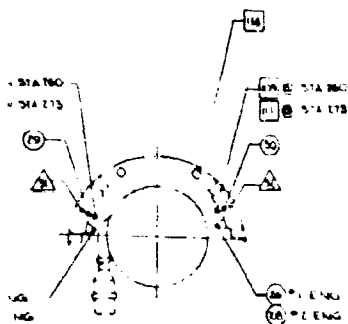


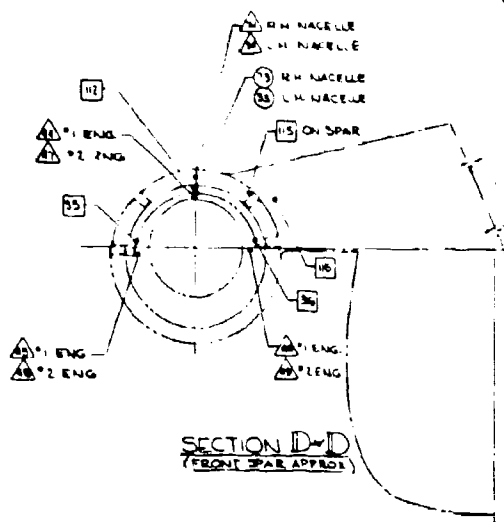
Figure 58. Thermocouple Location, Hot Gas System.

**A**

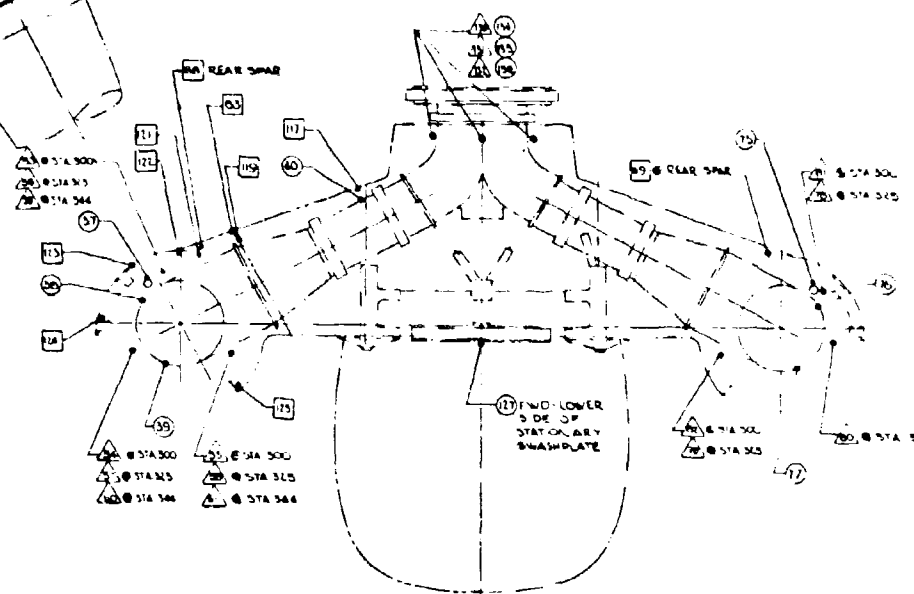
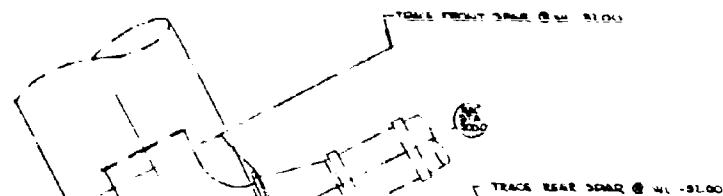




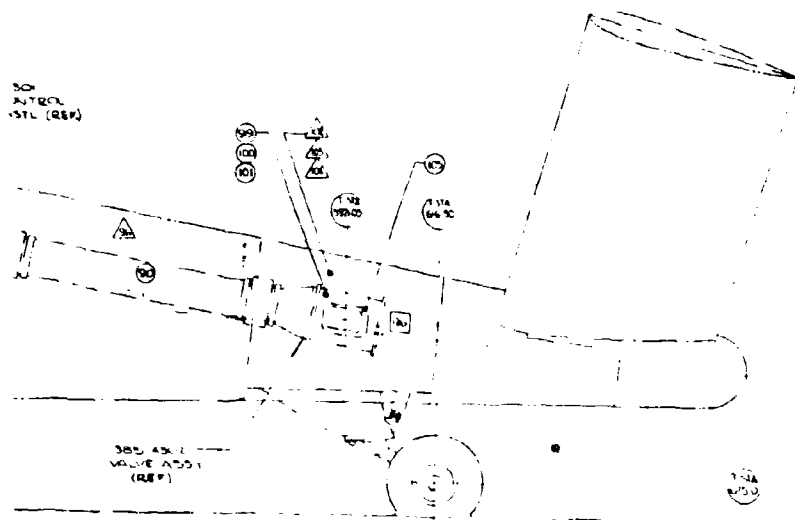
SECTION C-C  
STA 150 APPROX.



SECTION D-D  
FRONT SPAR APPROX.



SECTION E-E  
STA 300 APPROX.





Thermocouple Number	Type	Location
1	Case	Generator Engine 1
2		Generator Engine 2
3		Fuel Control Engine 1
4		Ignition Box Engine 1
5		Ignition Box Engine 2
6		Stator Vane Actuator Engine 1 LH
7		Stator Vane Actuator Engine 1 RH
8		Fuel Nozzle Inlet - Top Engine 1
9		Hydraulic Pump Engine 1
10		Engine Oil Pump Engine 1
11		Engine Oil Pump Engine 2
12		Accessory Drive Gearbox Engine 1
13		Front Frame Engine 1
14		Engine Compressor Engine 1 LH
15		Compressor Engine 1 RH
16		Combustor
17		Combustor
18		Turbine
19		Turbine
20		Exhaust Frame
21		Exhaust Frame
22		Engine Exhaust Clamp
23		Aft Engine Mount Flange
24		Aft Engine Mount Brace
25		Wire Temp Engine 1 Tunnel LH
26		Wire Temp Engine 1 Tunnel RH
27		Wire Temp Engine 2 Tunnel LH
28		Wire Temp Engine 2 Tunnel RH
29		Insulation Blanket Sta 260 Tunnel LH
30	Case	Insulation Blanket Sta 260 Tunnel RH
31	Air	Engine 1 Tunnel LH
32	Air	Engine 1 Tunnel RH
33	Case	Crossover Shroud Engine 1 Insulation
34	Air	Crossover Shroud Engine 1
35	Struct	Crossover Shroud Engine 1 LH
36	Struct	Crossover Shroud Engine 1 RH
37	Case	Diverter Valve Actuator Engine 1
38	Case	Diverter Valve Insulation Engine 1
39	Case	Diverter Valve Insulation Engine 1
40	Case	Diverter Valve Transition Duct Engine 1
41	Air	LH Nacelle Sta 220 Top
42		220 LH
43		220 RH
44		275 Top
45		275 LH
46		LH 275 RH
47		RH 275 Top
48	Air	RH Nacelle Sta 275 LH

Thermocouple Number	Type	Location
49	Air	RH Nacelle
50		LH
51		
52		
53		
54		
55		
56		
57		
58		
59		
60		
61		LH Nacelle
62		Lateral
63		
64		
65		
66		
67	Air	Lateral
68	Struct	LH Nacelle
69	Struct	RH Nacelle
70	Struct	LH Nacelle
71	Struct	RH Nacelle
72	Case	Y-Duct 1
73	Case	Crossover
74	Air	Crossover
75	Case	Diverter
76	Case	Diverter
77	Case	Diverter
78	Air	RH Nacelle
79	Air	RH Nacelle
80	Air	RH Nacelle
81	Air	RH Nacelle
82	Air	RH Nacelle
83	Struct	Alum Sk.
84	Case	Accessories
85	Case	Insulation
86	Case	
87		
88		
89		
90	Case	Insulation
91	Air	Aft Fuselage
92		
93		
94	Air	Aft Fuselage
95		

D

Location	Thermocouple Number	Type	Location
Nacelle Sta 275 RH	96	Air	Aft Fuselage
245 Top	97	Case	Bellows Insulation Blanket
245 LH	98	Case	Marmon Clamp
245 RH	99	Case	Yaw Valve Insulation Blanket
300 Top	100	Case	Yaw Valve Insulation Blanket
300 LH	101	Case	Yaw Valve Insulation Blanket
300 RH	102	Air	Yaw Valve Compartment
325 Top Approx	103	Air	Yaw Valve Compartment
325 90° Approx	104	Air	Yaw Valve Compartment
325 120° Approx	105	Case	Yaw Valve Outlet Flange
344 Top Approx	106	-	
344 90° Approx	107	Struct	Frame Fuselage Sta 376.50
Nacelle Sta 344 120° Approx	108		Engine 1 Tunnel Sta 260 LH
Lateral Pylon LH Nacelle - Fwd	109		260 RH
LH - Center	110		273 LH
LH - Aft	111		Tunnel Sta 273 RH
RH - Fwd	112		Crossover Shroud @ Sta 275.11
RH - Center	113		Aft Engine Mount
Lateral Pylon RH Nacelle - Aft	114		Diagonal Tube
Nacelle - Cant Rib Web	115		Engine 1 Front Spar at 145° Approx
Nacelle - Cant Rib Web	116		LH Nacelle - Outbd on Al Spar Web
Nacelle - Bl 22 Top Flange	117		Aluminum Skin on Lateral Pylon
Nacelle - Bl 22 Top Flange	118		Bl 22.00 Bulkhead
Duct Flange - Yaw Control	119		Canted Rib Cap
Crossover Shroud Engine 2 Insulation	120		Upper Pylon Tube
Crossover Shroud Engine 2	121		Diverter Valve Mounting Link
Diverter Valve Actuator Engine 2	122		LH Nacelle Sta 300 Top (Approx)
Diverter Valve Insulation Engine 2	123		at +5°
Diverter Valve Insulation Engine 2	124		at 90°
Nacelle Sta 325 Top	125		LH Nacelle Sta 300 at 120° (Approx)
Nacelle Sta 325 LH	126	Struct	Yaw Valve Bracket
Nacelle Sta 325 RH	127	Case	Stationary Swashplate Bearing
Nacelle Sta 300 Top	128	Case	Cross Flow Indicator
Nacelle Sta 300 LH	129	-	
Al Skin at Canted Rib Attachment	130	Air	Y-Duct Bay
Accessory Gearbox	131		Y-Duct Bay
Insulation Blanket Yaw Duct	132	Air	Y-Duct Bay
	133	-	
	134	Case	Y-Duct Insulation Blanket
	135	Case	Y-Duct Insulation Blanket
	136	Case	Y-Duct Insulation Blanket
Insulation Blanket Yaw Duct	137		Fuel In - No. 1 Hydraulic Oil Cooler
Aft Fuselage	138		Hydraulic Oil In No. 2 Hydraulic Oil Cooler
	139		Fuel Out No. 1 Hydraulic Oil Cooler
	140		Fuel In No. 2 Hydraulic Oil Cooler
	141		Hydraulic Oil In No. 1 Hydraulic Oil Cooler
Aft Fuselage	142		Fuel Out No. 2 Hydraulic Oil Cooler

APPENDIX II  
CONFIGURATION AND CHANGE LOG

<u>Item Number</u>	<u>Description</u>	<u>Accomplished Preflight Number</u>	<u>Date</u>
1	Weighed aircraft; takeoff gross weight 15,369 pounds; ICG Station 300.2	1	3-11-64
2	Replaced forward fuel filter unit; installed thermal relief valve in fuel system	3	10-11-64
3	Installed flight type Potter fuel flowmeters	3	9-11-64
4	Rerigged yaw valve neutral with pedals and rudder blocked neutral	3	9-11-64
5	Installed 2-pound weights on pilot's cyclic-control stick	3	12-11-64
6	Removed stick weights from pilot's cyclic-control stick	4	13-11-64
7	Change stabilizer incidence angle to 3.5 degrees nose up	5	18-11-64
8	Replaced engine 2 Potter flowmeter	6	20-11-64
9	Removed and reworked yaw valve to reduce operating forces	7	23-11-64
10	Removed diverter valves, S/N 010 lh and S/N 009 rh; installed diverter valves, S/N 012 lh and S/N 011 rh (GE inspection and door rework accomplished at EAFB)	7	23-11-64

<u>Item Number</u>	<u>Description</u>	<u>Accomplished Preflight Number</u>	<u>Date</u>
11	Removed control system servo actuators, S/N 104, 102, 105; installed control system servo actuators, S/N 103, 106, 101, with reworked servo spool assemblies to reduce friction	7	23-11-64
12	Removed engine 2, S/N 101-3A; installed S/N 026-1B	7	23-11-64
13	Installed engine oil header tanks to eliminate venting	7	23-11-64
14	Revised fuselage ballast installation for initial center of gravity at Station 298	7	23-11-64
15	Installed tabs in tip cascades to decrease exit area by a total of 4 square inches (3 blades)	7	23-11-64
16	Installed emergency rotor tachometer indicator and overspeed unit	7	23-11-64
17	Increased stabilizer incidence to 5.0 degrees nose up	7	23-11-64
18	Installed T <sub>3</sub> and T <sub>5</sub> indicators on photopanel	7	23-11-64
19	Modified crossflow indicator and warn-divert unit	7	23-11-64
20	Installed cyclic stick trim actuators	7	23-11-64
21	Reworked diverter valve hydraulic selector valves (Weston) to eliminate intermittent operation	7	30-11-64

<u>Item Number</u>	<u>Description</u>	<u>Accomplished Preflight Number</u>	<u>Date</u>
22	Reworked diverter hydraulic supply valve (Vinson) to eliminate intermittent operation	7	30-11-64
23	Installed accumulator and filters to rotor-speed-governing system	7	30-11-64
24	Relocated MLG ballast to fuselage; installed 250-pound ballast in cockpit	7	2-12-64
25	Rerigged yaw control valve and rudder system, neutral yaw valve, pedal position, and rudder position	7	2-12-64
26	Installed alternate airspeed indicator connected to original pitot and static sources	8	8-12-64
27	Removed both cyclic trim actuator units to rework centering springs	8	8-12-64
28	Changed stabilizer incidence to 4 degrees nose up	8	9-12-64
29	Reduced MLG tire pressure to 45 psi	8	9-12-64
30	Rerigged collective for $\theta = 0$ degree at 0.75 radius on downstop	9	11-12-64
31	Moved fuel totalizer indicators to photopanel	9	10-12-64
32	Changed alternate airspeed indicator to noseboom pitot	9	10-12-64
33	Installed weights on forward engine mounts, 205 pounds each engine; forward cowling removed for flight	10	14-12-64

<u>Item Number</u>	<u>Description</u>	<u>Accomplished Preflight Number</u>	<u>Date</u>
34	Installed dither actuators on control servo actuator spool rod assemblies	10	14-12-64
35	Installed alternate airspeed system indicator on photopanel	10	14-12-64
36	Removed fuselage ballast, 10 pieces, 475 pounds; revised loading, initial gross weight 15,309 pounds, initial center of gravity Station 298.0	10	14-12-64
37	Changed stabilizer incidence to 3.0 degrees nose up	11	22-12-64
38	Moved OAT indicator from left-hand instrument panel to photopanel	12	23-12-64
39	Rerigged rudders to 5 degrees right with pedals and yaw valve neutral	13	30-12-64
40	Installed cyclic control trim actuators and centering springs - final springs	13	4-1-65
41	Rerigged collective for $\theta = -1$ degree at 0.75 radius on downstop	13	4-1-65
42	Conducted weight and balance check; initial gross weight 15,264 pounds, initial center of gravity Station 297.3	14	7-1-65
43	Rerigged collective for $\theta = -2$ degrees at 0.75 radius on downstop	14	8-1-65

<u>Item Number</u>	<u>Description</u>	<u>Accomplished Preflight Number</u>	<u>Date</u>
44	Installed 40-pound ballast at tail landing gear; initial gross weight 15,804 pounds, initial center of gravity 298.0	15	11-1-65
45	Sealed blade leading edge segments from Station 100 outboard to tip with RTV 102 sealer to eliminate cooling air leakage and improve aerodynamic performance	15	11-1-65
46	Replaced rotor hub cooling seal curtain	15	11-1-65
47	Modified yaw-control valve exhaust extensions to provide increased net yaw thrust	15	12-1-65
48	Adjust engine idle $N_G$ to maximum available	15	12-1-65
49	Modified $T_2$ sensor installation in engine inlets to provide improved accuracy	15	15-1-65
50	Installed finned tubing in rotor lube system return lines to provide additional cooling	16	15-1-65
51	Cleaned both engine compressors with Agra-Shell compound per General Electric Instruction SE 1-155	16	15-1-65
52	Installed tufts on engine nacelles and pylon for airflow studies	16	19-1-65
53	Replaced hydraulic pump, engine 1, because of suspected contamination	16	19-1-65

<u>Item Number</u>	<u>Description</u>	<u>Accomplished Preflight Number</u>	<u>Date</u>
54	Replaced hydraulic pressure flex hoses, engines 1 and 2 (engine 1 line failed)	16	19-1-65
55	Adjusted blue blade outer pitch link one-half turn to improve blade tracking	18	22-1-65
56	Reset fuel control overspeed solenoids to limit $N_G$ cutback to 93-percent $N_G$	18	22-1-65
57	Replaced dither actuator on longitudinal control servo actuator	18	22-1-65
58	Replaced torn trailing edge section (transition) inboard of Station 91, yellow blade	20	27-1-65
59	Installed rotor lube oil cooler and 28-volt d-c blower to provide additional rotor lube oil cooling	21	29-1-65
60	Removed and repaired engine oil tank, engine 2 inlet	21	2-2-65
61	Reinstalled modified crossflow indicator and warn-divert unit	21	3-2-65
62	Closed both $N_f$ bypass valves in rotor-governing system and readjusted fuel control $N_f$ setting for 100-percent $N_R$ governed speed at 100-degree PLA	21	4-2-65
63	Revised plumbing for tip pressure transducers, yellow blade and blue blade, for instrument check; yellow blade ported to cooling-air duct; blue blade connected together	21	5-2-65



### APPENDIX III

## PILOT COMMENTS AND QUALITATIVE EVALUATION

### SUMMARY

The flying qualities of the XV-9A were found to be adequate for the mission of Hot Cycle propulsion system research. However, during the course of the evaluation, several limitations were defined, particularly the longitudinal cyclic control and the collective control that are available to the pilot with the present gimbaled hub and control system. It is therefore recommended that in any future Hot Cycle operational aircraft increased control power and increased damping be provided.

Evaluation of control position data and pilot's qualitative comments during initial flights (1 to 11) indicated a horizontal stabilizer incidence of three degrees nose up and rudder setting of five degrees right with pedals and yaw valve neutral as the best configuration for the remaining flights.

All flights were flown with an initial gross weight of approximately 15,300 pounds and mid center of gravity position. Center of gravity position moved forward in flight with equal fuel burnoff from the forward and aft fuel tanks. A fuel management technique was worked out to maintain center of gravity approximately constant by crossfeeding both engines from the forward tank as the flight progressed. This technique will be further refined for the follow-on test program to maintain center of gravity within close limits during flight.

### LONGITUDINAL CONTROL

The pilot's cyclic control system operation was smooth, and the control forces were found satisfactory with either one or both hydraulic systems operating. Increased longitudinal control sensitivity and control power would be desirable.

A considerable amount of aft cyclic stick deflection was required during lift-off to hover for the maximum forward center of gravity location.

During climb, on occasion, the cyclic stick forward stop was reached. The limiting factor in left sideward flight was the cyclic stick aft stop.

Stick position versus airspeed had a stable gradient forward stick deflection for increased airspeed from 70- to 100-knot CAS, and appeared neutral from 40 to 60 knots.

Pitch stability was low for all flight conditions, but appeared to improve with forward flight speed.

During entry to low-power descents, large aft movement of the cyclic stick was required. It is recommended that future autorotational tests be approached cautiously and from airspeeds of less than 90-knot CAS. Emergency autorotation from airspeeds greater than 90-knot CAS will require a programmed collective pitch decrease with airspeed in order to decrease airspeed to 90-knot CAS before full down collective is reached.

Greater pilot attention during minimum or idle-power descents was required because of lack of full twist-grip authority and mismatch of engine power levers.

#### LATERAL CONTROL

Lateral cyclic-control operation was smooth, and the control forces were found satisfactory. Lateral control sensitivity and control power were adequate for the research flight test program; however, improvement in this area would be required for an operational vehicle. Full lateral stick deflection was somewhat difficult to obtain with the stick from three-fourths or further aft, because of interference with the pilot's legs.

Roll stability was also low, but better than pitch stability. The range of lateral cyclic-control appeared adequate, and there were no occurrences of lateral cyclic stick limiting.

#### DIRECTIONAL CONTROL

Since the XV-9A has a reaction-jet-powered rotor, there is no shaft torque produced except from rotor-shaft bearing friction. Directional control in the XV-9A during hover is by means of a reaction-jet yaw valve in the fuselage tail and by means of aerodynamic rudder surfaces hinged to the V-tail stabilizers during forward flight.

The yaw valve, located at the rear of the aircraft, bleeds engine exhaust gases directly for yaw thrust. Opening of the valve adds total exit nozzle area, reducing engine backpressure as well as diverting flow. At any power lever setting of less than full power, the rotor gas generator governing system will accelerate the gas generators to sustain the rotor power at the level required with yaw valve closed. There were no significant power control problems or adverse engine

characteristics encountered during full pedal hover turns or in level flight, climb, or descent.

During initial flights, it was determined that full yaw valve opening was not obtained during hovering turns with full yaw pedal depressed. Modifications are being incorporated in the directional control system to correct this deficiency for the follow-on test program.

During hover in ground effect at 6- to 8-foot wheel height, the XV-9A exhibited a slight right turning tendency, but this characteristic was not always definite.

During hover at 4-foot wheel height and down to touchdown, the aircraft turned to the right, and the pilot held left pedal to hold heading; right cyclic was required to eliminate drift to the left. Aft cyclic was required to hold the hovering attitude, which was characteristically nose-low for this flight condition.

During landing with crosswind from the right, the nose-low attitude and aft stick required were more pronounced.

Directional control sensitivity was adequate, but not as good as that afforded by tail-rotor systems.

Right pedal was required during translational lift and climb. During the course of flight test, it was determined that a 5-degree right rudder deflection was required for trimmed cruise flight, and the rudder surfaces were rigged to 5 degrees right with yaw pedals and yaw valve neutral. Approximately 10-percent right pedal was required during cruise flight with the rudders rigged to 5 degrees right with pedals and yaw valve neutral. During descents, right pedal was required until the flare was begun. Approach to hover required left pedal in varying amounts, depending on the rate of flare. Full left pedal was required during approach to hover at moderate flare rates.

Aircraft turning rates were considered adequate during sustained full pedal hovering turns; however, the low directional control sensitivity required fairly large pedal deflections to establish the initial rate of yaw. Sideward flight to the right was limited by the amount of left yaw valve opening obtainable. Sideward flight to the left was limited by the amount of aft cyclic available.

## VERTICAL CONTROL

Operation of the collective-pitch control was smooth, and sensitivity was satisfactory. After initial adjustments on the collective load balance spring, there was no tendency of the control to creep in either direction.

During lift-off to hover, the aircraft was sensitive to center of gravity position. Forward center of gravity positions caused a pitch-down tendency after lift-off, requiring aft cyclic to correct. Fairly level lift-offs to hover were accomplished with a center of gravity location from mid to aft position.

Slop in the twist-grip control, in addition to the lack of full authority from idle to maximum PLA, made rotor-speed control more difficult for the pilot, particularly during minimum-power descents.

The collective range available was a limiting factor during climb, where insufficient collective pitch was available to absorb maximum engine power at 100-percent  $N_R$ , and during idle power descents, where insufficient down collective was available to maintain better than 91-percent  $N_R$ .

## VIBRATION CHARACTERISTICS

Translational shake was experienced during transition from hover to forward flight and during approach to hover. The vibration level was high during high-power climbs, but reduced considerably during level flight and descents.

## ROTOR-SPEED-GOVERNING

The rotor-speed-governing system, which used a hydraulic rotor-speed feedback link and the  $N_f$  power turbine speed-governing portion of the T-64 fuel controls, was utilized on all flights. The feasibility of governing the Hot Cycle rotor by these means was satisfactorily proven. Additional system development is required to achieve satisfactory results for all flight conditions and to decrease adjustments.

Rotor-speed-governing was stable for all flight conditions, and there were no occurrences of engine surge or rotor overspeed. The rotor-governing system was normally adjusted for a rotor speed of 100 percent at 82.5-degree PLA with matched engine speeds and full down

collective. In flight, the twist-grip control was used to compensate for rotor-speed error above or below 100-percent  $N_R$ , and the individual power levers were used to keep engine speeds,  $N_G$ , matched.

The principal difficulty with rotor-speed-governing was the drift of the  $N_f$  input speed signal, which required the pilot to reset PLA during flight to maintain desired rotor speed. In addition, excessive twist-grip control was necessary during takeoff to hover, descent, and for any large change in collective pitch.

Rotor speed increased from 100- to 102-percent  $N_R$  during lift-off to hover, which was objectionable to the pilot.

APPENDIX IV  
PROPULSION SYSTEM PERFORMANCE TEST DATA  
AND CORRECTIONS

FUEL FLOW

The estimated performance of the XV-9A presented in Reference 5 is based on the expected use of hardware components that are considered typical of production hardware. These items involve the engine, diverter valves, and the method of oil cooling. The actual XV-9A used available components, which resulted in a higher fuel consumption than that predicted using optimum components. The fuel consumption figures in the main body of the report have been corrected where noted. This Appendix presents the observed and corrected data and the method of making these corrections.

Table IV presents observed fuel flow data for all data points taken during testing. It also includes the procedure for determining corrected fuel flow on the basis of original assumptions; namely, with qualification test (QT) rather than preliminary flight rating (PT) engines, and without diverter valve leakage. The gross weights for all hover points are given, and the basic gas conditions that determine rotor power and the equivalent gas power.

Table V presents additional hover fuel data from prior whirl stand tests (Reference 7) for both uncorrected and corrected conditions.

The curve of gross weight versus uncorrected fuel flow (with points taken from Table V) is shown in Figure 59, which is to be compared with Figure 19. The curve of uncorrected specific fuel consumption versus rotor horsepower (with data from Table IV) is shown in Figure 60, which is to be compared with Figure 34.

Both whirl stand and flight fuel flows have been reduced 3 percent to correct for diverter valve (2-1/2 percent), and stationary duct (1/2 percent) leakage, as measured on the whirl stand. This XV-9A hardware is not considered typical of production hardware, so the data have been corrected to reflect the true system performance. There is reason to believe that leakage exceeded 3 percent during flight tests, but since a new measurement was not made, the whirl test value has been used throughout the present analysis.

Fuel flow has been corrected to reflect the better  $T_5$  versus  $P_5$  characteristics of the fully qualified T-64 engines as compared with the

TABLE IV  
OBSERVED AND CORRECTED FUEL FLOW AND ROTOR AND GAS POWER

[illegible]

**TABLE V**  
**UNCORRECTED AND CORRECTED WHIRL TEST FUEL FLOW**

(1)	(2)	(3)	(4)	(5)	(6)	(7)	(8)	(9)	(10)	(11)	(12)	(13)	(14)
Run	Point	Lint (lb)	$W_2$ (lb/sec)	$\frac{P_2}{\delta}$ (psia)	$\frac{T_5}{\theta}$ (deg R)	$\frac{T_5}{\theta} - 519$ (deg R)	Figure 26 $\left(\frac{1_{fuel}}{Air}\right)$	$W_1$ (lb/sec)	$\left(\frac{1_{fuel}}{\theta}\right)_{QT}$ (deg R)	$\left(\frac{1_{fuel}}{\theta}\right)_{QT} - 519$ (deg R)	$\left(\frac{1_{fuel}}{Air}\right)_{QT}$	$(W_2)_{QT}$ (lb/sec)	$0.97 W_1$ (Corrected for leakage)
22	8	16,000	43.50	30.9	1,453	934	0.01300	2,036	1,315	796	0.01110	48.7	1,770
	9	18,000	46.15	33.4	1,505	986	0.01380	2,293	1,382	863	0.01210	48.2	2,035
	10	18,500	46.50	33.7	1,535	1,016	0.01420	2,377	1,432	873	0.01220	48.8	2,080
	11	19,000	46.50	35.2	1,535	1,016	0.01420	2,377	1,433	914	0.01280	48.1	2,150
23	7	17,500	45.80	33.0	1,500	981	0.01370	2,259	1,372	853	0.01200	47.8	2,005
	8	19,200	47.35	34.8	1,561	1,042	0.01460	2,489	1,422	903	0.01270	49.6	2,206
	9	14,000	46.95	34.9	1,551	1,032	0.01440	2,434	1,425	906	0.01270	49.0	2,170
	10	19,000	47.00	34.8	1,551	1,032	0.01450	2,443	1,422	903	0.01270	49.0	2,170
	11	19,300	46.80	35.0	1,561	1,042	0.01460	2,460	1,427	908	0.01270	49.0	2,170
24	9	15,500	42.21	29.9	1,422	903	0.01260	1,915	1,288	769	0.01070	44.4	1,660
	9a	19,500	41.85	34.6	1,555	1,036	0.01450	2,446	1,415	897	0.01250	49.1	2,140
26	10a	4,700	33.80	22.4	1,198	679	0.00940	1,144	1,115	596	0.00826	35.1	1,010
	11a	11,600	38.75	26.5	1,323	809	0.01150	1,604	1,202	683	0.00951	40.7	1,350
	b	14,000	40.90	28.3	1,360	841	0.01170	1,723	1,246	727	0.01010	42.7	1,505
	c	16,000	44.20	31.0	1,426	907	0.01260	2,005	1,317	798	0.01110	46.0	1,785
28	8a	12,000	38.76	26.7	1,325	806	0.01115	1,556	1,207	688	0.00956	40.6	1,355
	b	14,600	41.50	28.6	1,381	862	0.01200	1,793	1,255	736	0.01025	43.6	1,560
	c	15,800	43.82	30.6	1,429	910	0.01270	2,003	1,306	787	0.01096	45.8	1,755
	d	20,000	48.59	35.0	1,540	1,021	0.01410	2,501	1,427	908	0.01270	50.5	2,235
	e	20,800	49.45	36.0	1,570	1,051	0.01470	2,617	1,455	936	0.01311	51.4	2,355
30	14a	15,200	43.62	30.2	1,402	883	0.01230	1,931	1,296	771	0.01075	45.4	1,705
	b	19,250	47.33	34.1	1,505	986	0.01380	2,351	1,402	883	0.01235	49.0	2,110
	c	20,600	49.58	36.4	1,568	1,049	0.01700	2,624	1,467	948	0.01380	51.3	2,380
31	6a	3,700	35.97	22.5	1,210	691	0.00960	1,171	1,117	598	0.00830	35.3	1,024
	b	6,500	33.95	22.9	1,220	701	0.00980	1,198	1,125	606	0.00840	35.4	1,041
	c	7,500	36.73	24.4	1,250	731	0.01010	1,336	1,155	636	0.00880	38.2	1,180
	d	9,700	37.41	25.2	1,282	763	0.01050	1,414	1,172	653	0.00910	39.1	1,240
	e	12,300	40.12	27.4	1,335	816	0.01130	1,628	1,224	705	0.00940	41.9	1,435
	f	15,400	44.29	30.8	1,425	904	0.01260	2,004	1,312	793	0.01110	46.1	1,790
	g	15,500	42.53	34.2	1,416	897	0.01250	1,914	1,405	886	0.01240	42.7	1,850
	h	18,500	47.22	34.3	1,510	991	0.01390	2,363	1,407	888	0.01240	45.9	2,120
	i	18,000	45.20	32.9	1,489	961	0.01340	2,180	1,369	850	0.01190	46.9	1,950
	k	20,300	49.39	36.5	1,561	1,042	0.01460	2,596	1,470	951	0.01340	50.9	2,380
	10a	14,500	46.48	34.0	1,505	986	0.01375	2,301	1,400	881	0.01240	48.2	2,070
	b	23,000	50.53	38.3	1,614	1,095	0.01535	2,792	1,520	1,001	0.01495	51.6	2,530
	c	23,000	59.46	38.7	1,630	1,111	0.01560	2,834	1,532	1,013	0.01425	52.0	2,590

(1) Run number	(8) Fuel flow $W_2 = F/A \times 3,600$ , or (4) $\times$ (8) $\times 3,600$
(2) Test point	(9) Referred temperature for QT engine. Read in Figure 22 at given $P_2/\delta$ , (5)
(3) Lift	(10) As indicated
(4) Engine mass flow, total, lb/sec	(11) Fuel/air (Figure 26) at (10) for QT engine
(5) Referred engine pressure	(12) QT air flow is determined by increasing YT engine air flow (4) by inverse ratio of square root of $T_5$ , that is, $\sqrt{\frac{(1_{fuel}/\theta)}{(1_{fuel}/\theta)_{QT}}}$ or $\sqrt{\frac{(4)}{(12)}}$
(6) Referred engine temperature	
(7) As indicated	
(8) Fuel/air (Figure 26) at (7)	(14) Fuel flow $W_2 = F/A \times 3,600 \times$ leakage factor, or (10) $\times$ (12) $\times 0.97$



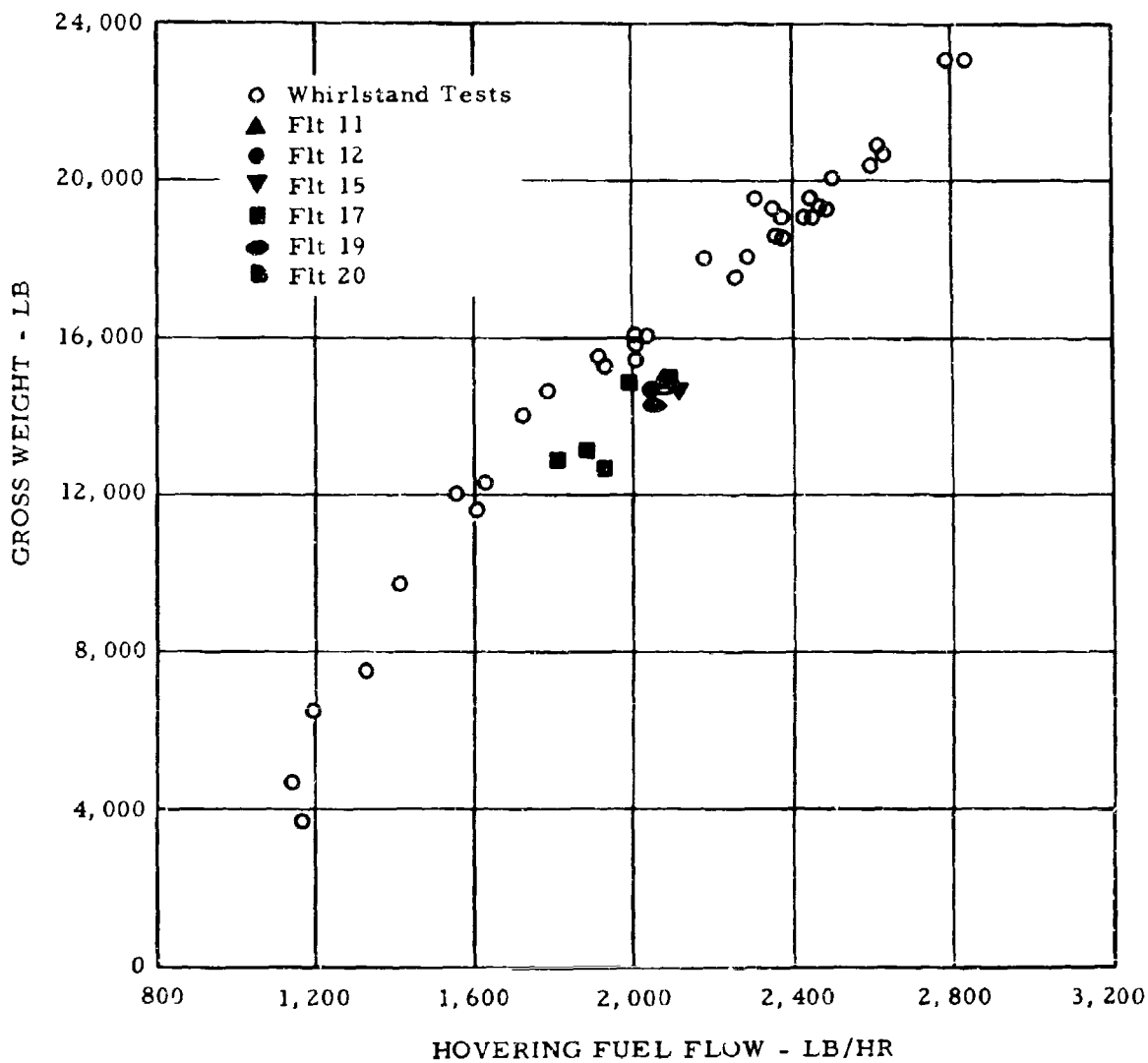
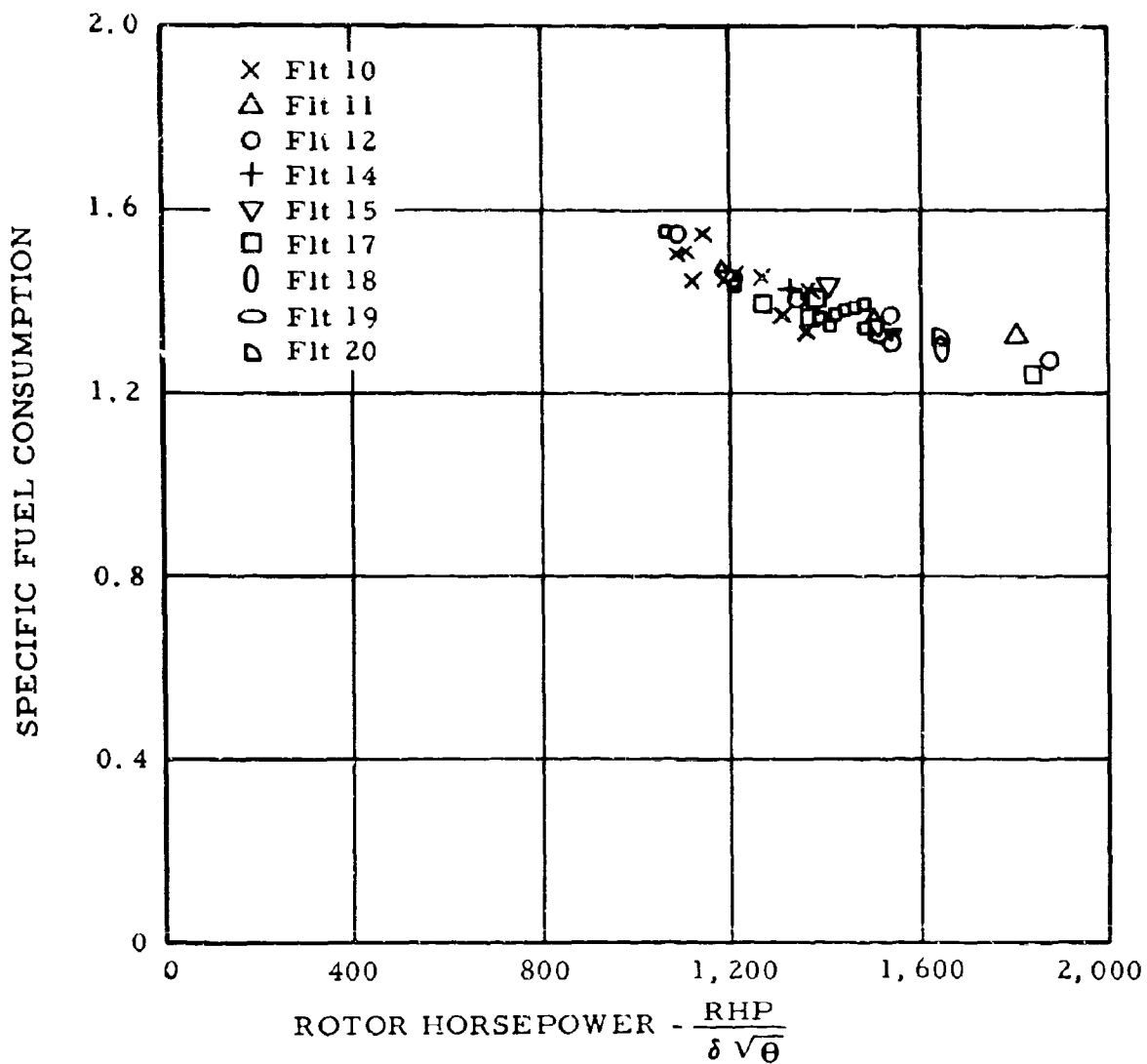


Figure 59. Observed Hovering Fuel Flow Versus Gross Weight.



preliminary (YT-64) engines used during the tests. This correction is typically approximately 8 percent for the flight tests and approximately 10 percent for the whirl tests. The magnitude of the correction used in reducing observed fuel flow for Figure 19 is displayed in Figure 22. The procedure for correcting fuel flow consists of first increasing air-flow as the inverse square root of  $T_5$ , then reducing fuel/air ratio in direct proportion to engine temperature rise ( $T_5 - T_2$ ). The final correction thus varies more than the square root of  $T_5$ , but not so much as the first power of  $T_5$ .

As an expedient, the XV-9A utilizes compressor bleed to drive an aspirator system for engine oil cooling. This system imposes an unnecessarily large fuel consumption penalty, but, to save time and money, was employed on the research vehicle. In order to reflect the inherent rotor system performance, the fuel flow attributable to this bleed extraction has been subtracted from the data as plotted. This correction was no more than 5 percent. The effect of the bleed is seen in Figure 26 as an increase of the test fuel/air ratio at a given engine temperature rise above the predelivery calibration. The correction of hovering fuel flow for compressor bleed amounts to moving the fuel/air ratio points from their observed location to the General Electric calibration lines.

#### Rotor Horsepower Versus Gas Horsepower Considerations

A tip-jet, or "Hero" turbine of fixed geometry operating at a constant tip speed produces rotor horsepower that varies linearly with the supply pressure (above choking pressure) and varies less strongly with supply temperature. This is contrary to the relationship that most engineers usually encounter, and may cause some to misinterpret the rotor power available.

An understanding of this unusual characteristic of the Hot Cycle propulsion system can best be gained by referring to the equations that follow. The final results are, of course, independent of the analytical approach taken herein (which is to show the relationship of pressure and temperature).

First consider the case of a nonrotating system, where jet thrust can be related to the supply pressure and the exit area through the following equation:

$$F_j = C_F A_e \left[ P_{t_e} \frac{P_e}{P_{t_e}} (1 + \gamma_e M_e^2) - P_0 \right]$$

For  $\gamma_e = 1.35$  and choked exit flow, this equation becomes:

$$F_j = C_F A_e (1.27 P_{t_e} - P_0)$$

Temperature enters into this equation only through  $\gamma$ , and changes of a few hundred degrees lead to negligible effects on the jet thrust.

As this system is allowed to rotate, the forces and pressures at the tip continue to be related by the previous equation; however, coriolis forces are now present in the ducting that supplies the tip-jet. The integral of the coriolis forces can be expressed as an equivalent tip drag by the following equation:

$$F_C = - \frac{W}{g} V_T,$$

and expanding the mass flow term (choked flow) leads to

$$F_C = \frac{-0.525}{g} A_e \sqrt{\frac{P_{t_e}}{T_{t_e}}} V_T$$

Net rotor power becomes:

$$RHP = \frac{F_N V_T}{550} = C_F A_e (1.27 P_{t_e} - P_0) \frac{-0.525}{g} A_e \sqrt{\frac{P_{t_e}}{T_{t_e}}} V_T$$

It is obvious that increasing gas temperature increases rotor horsepower only through a square root reduction in the coriolis acceleration term. Meanwhile, the gas horsepower input to the rotor has followed the equation:

$$GHP = \frac{778}{550} W C_P \Delta T = \frac{778 (0.525)}{550} A_e \sqrt{\frac{P_{t_e}}{T_{t_e}}} C_P f\left(\frac{P_t}{P}\right) T_{t_e}$$

Therefore, gas horsepower input varies as the square root of absolute gas temperature for constant pressure and fixed exit area.

As an example of the effect of gas temperature on rotor power at a given pressure, calculations were made using gas conditions from XV-9A flight tests. The variation of rotor horsepower with temperature was found to be approximately 60 percent of the variation of gas horsepower with temperature. Thus the Hot Cycle rotor is capable of utilizing a large portion of the available gas energy.

It should be noted that gas turbine engines can be built with only a limited spread of temperature with pressure, and best Hot Cycle performance is obtained with high-pressure engines. Recent studies have shown that the available high-pressure engines have a pressure-temperature characteristic such that payload/empty weight ratios in excess of 2.0 are attainable in Hot Cycle helicopters.

UNCLASSIFIED

Security Classification

DOCUMENT CONTROL DATA - R&D		
(Security classification of title, body of abstract and indexing annotation must be entered when the overall report is classified)		
1 ORIGINATING ACTIVITY (Corporate author) Hughes Tool Company - Aircraft Division Culver City, California		2a REPORT SECURITY CLASSIFICATION Unclassified 2b GROUP
3 REPORT TITLE GROUND AND FLIGHT TESTS, XV-9A HOT CYCLE RESEARCH AIRCRAFT		
4 DESCRIPTIVE NOTES (Type of report and inclusive dates) Summary Report, 10 August 1964 to 5 February 1965		
5 AUTHOR(S) (Last name, first name, initial) Pieper, C. W.		
6 REPORT DATE March 1966	7a TOTAL NO. OF PAGES 149	7b NO. OF PAGES 11
8a. CONTRACT OR GRANT NO. DA 44-177-AMC-877(T) b. PROJECT NO. Task 1M121401D14403 c. d.	9a. ORIGINATOR'S REPORT NUMBER(S) USAAVLABS Technical Report 65-68 9b. OTHER REPORT NO(S) (Any other numbers that may be assigned this report) HTC-AD 65-13	
10. AVAILABILITY/LIMITATION NOTICES Distribution of this document is unlimited.		
11. SUPPLEMENTARY NOTES	12. SPONSORING MILITARY ACTIVITY U. S. Army Aviation Materiel Laboratories Fort Eustis, Virginia	
13 ABSTRACT <p>Under the terms of Contract DA 44-177-AMC-877(T), Hughes Tool Company, Aircraft Division has conducted a ground and flight test program on the XV-9A Hot Cycle Research Aircraft to demonstrate the flight feasibility of the Hot Cycle Rotor System.</p> <p>During the tests, performed from 10 August 1964 through 5 February 1965, the performance, structural qualities, and feasibility of the Hot Cycle rotor and propulsion system were successfully verified for all normal helicopter flight modes. Ground tests consisted of preflight and tie-down tests, which provided a functional checkout of the aircraft systems and test instrumentation and a final checkout of the completed aircraft prior to start of flight tests. The 15 hours of flight testing included evaluation of aircraft and rotor system performance, flight loads, cooling, and flying qualities in various flight modes.</p>		

DD FORM 1 JAN 64 1473

UNCLASSIFIED  
Security Classification

**UNCLASSIFIED**  
Security Classification

14. KEY WORDS	LINK A		LINK B		LINK C	
	ROLE	WT	ROLE	WT	ROLE	WT
<p align="center"><b>Hot Cycle Rotor System VTOL Aircraft</b></p>						

**INSTRUCTIONS**

**1. ORIGINATING ACTIVITY:** Enter the name and address of the contractor, subcontractor, grantee, Department of Defense activity or other organization (*corporate author*) issuing the report.

**2a. REPORT SECURITY CLASSIFICATION:** Enter the overall security classification of the report. Indicate whether "Restricted Data" is included. Marking is to be in accordance with appropriate security regulations.

**2b. GROUP:** Automatic downgrading is specified in DoD Directive 5200.10 and Armed Forces Industrial Manual. Enter the group number. Also, when applicable, show that optional markings have been used for Group 3 and Group 4 as authorized.

**3. REPORT TITLE:** Enter the complete report title in all capital letters. Titles in all cases should be unclassified. If a meaningful title cannot be selected without classification, show title classification in all capitals in parenthesis immediately following the title.

**4. DESCRIPTIVE NOTES:** If appropriate, enter the type of report, e.g., interim, progress, summary, annual, or final. Give the inclusive dates when a specific reporting period is covered.

**5. AUTHOR(S):** Enter the name(s) of author(s) as shown on or in the report. Enter last name, first name, middle initial. If military, show rank and branch of service. The name of the principal author is an absolute minimum requirement.

**6. REPORT DATE:** Enter the date of the report as day, month, year, or month, year. If more than one date appears on the report, use date of publication.

**7a. TOTAL NUMBER OF PAGES:** The total page count should follow normal pagination procedures, i.e., enter the number of pages containing information.

**7b. NUMBER OF REFERENCES:** Enter the total number of references cited in the report.

**8a. CONTRACT OR GRANT NUMBER:** If appropriate, enter the applicable number of the contract or grant under which the report was written.

**8b, 8c, & 8d. PROJECT NUMBER:** Enter the appropriate military department identification, such as project number, subproject number, system numbers, task number, etc.

**9a. ORIGINATOR'S REPORT NUMBER(S):** Enter the official report number by which the document will be identified and controlled by the originating activity. This number must be unique to this report.

**9b. OTHER REPORT NUMBER(S):** If the report has been assigned any other report numbers (*either by the originator or by the sponsor*), also enter this number(s).

**10. AVAILABILITY/LIMITATION NOTICES:** Enter any limitations on further dissemination of the report, other than those imposed by security classification, using standard statements such as:

- (1) "Qualified requesters may obtain copies of this report from DDC."
- (2) "Foreign announcement and dissemination of this report by DDC is not authorized."
- (3) "U. S. Government agencies may obtain copies of this report directly from DDC. Other qualified DDC users shall request through \_\_\_\_\_."
- (4) "U. S. military agencies may obtain copies of this report directly from DDC. Other qualified users shall request through \_\_\_\_\_."
- (5) "All distribution of this report is controlled. Qualified DDC users shall request through \_\_\_\_\_."

If the report has been furnished to the Office of Technical Services, Department of Commerce, for sale to the public, indicate this fact and enter the price, if known.

**11. SUPPLEMENTARY NOTES:** Use for additional explanatory notes.

**12. SPONSORING MILITARY ACTIVITY:** Enter the name of the departmental project office or laboratory sponsoring (*paying for*) the research and development. Include address.

**13. ABSTRACT:** Enter an abstract giving a brief and factual summary of the document indicative of the report, even though it may also appear elsewhere in the body of the technical report. If additional space is required, a continuation sheet shall be attached.

It is highly desirable that the abstract of classified reports be unclassified. Each paragraph of the abstract shall end with an indication of the military security classification of the information in the paragraph, represented as (TS), (S), (C), or (U).

There is no limitation on the length of the abstract. However, the suggested length is from 150 to 225 words.

**14. KEY WORDS:** Key words are technically meaningful terms or short phrases that characterize a report and may be used as index entries for cataloging the report. Key words must be selected so that no security classification is required. Identifiers, such as equipment model designation, trade name, military project code name, geographic location, may be used as key words but will be followed by an indication of technical context. The assignment of links, rules, and weights is optional.

**UNCLASSIFIED**  
Security Classification